Západočeská univerzita v Plzni
Fakulta aplikovaných věd

FRAKCIONÁLNÍ MODELY FINANČNÍCH TRHŮ SE STOCHASTICKOU VOLATILITOU

Mgr. Tomáš Sobotka, M.Sc.

Disertační práce k získání akademického titulu doktor (Ph.D.) v oboru Aplikovaná matematika

Školitel: prof. RNDr. Bohdan Maslowski, DrSc.
Odborný vedoucí: Ing. Jan Pospíšil, Ph.D.

Katedra matematiky

Plzeň, 2019

University of West Bohemia
Faculty of Applied Sciences

FRACTIONAL STOCHASTIC VOLATILITY MODELS OF FINANCIAL MARKETS

Mgr. Tomáš Sobotka, M.Sc.

Dissertation thesis for qualifying to academic degree Doctor of Philosophy (Ph.D.) in specialization Applied Mathematics

Supervisor: prof. RNDr. Bohdan Maslowski, DrSc.
Technical supervisor: Ing. Jan Pospíšil, Ph.D.

Department of Mathematics

Plzeň, 2019

DECLARATION

I do hereby declare that the entire thesis is my original work and that I have used only the cited sources

Plzeň, December 20, 2019

Mgr. Tomáš Sobotka, M.Sc.

RÉSUMÉ

The main contribution of the thesis is to extend results in Merino – Pospíšil – Sobotka – Sottinen – Vives (2019) regarding αRFSV model and to summarize author's research activities based on published academic articles.

SHRNUTÍ PRÁCE

Hlavním přínosem této kvalifikační práce spočívá v rozšíření výsledků získaných v manuskriptu Merino – Pospíšil – Sobotka – Sottinen – Vives (2019) týkajících se αRFSV modelu a ve shrnutí výzkumných aktivit studenta na základě publikovaných vědeckých článků.

ZUSAMMENFASSUNG

Der Hauptbeitrag der Arbeit besteht darin, die Ergebnisse in Merino – Pospíšil – Sobotka – Sottinen – Vives (2019) in Bezug auf das αRFSV Modell zu erweitern und die Forschungsaktivitäten des Autors zusammenzufassen.

ABSTRACT

In the thesis we provide a motivation for a class of financial market models that has lately captured attention of both academics and practitioners – a class of stochastic volatility (SV) models and, even more recently, rough SV models. This is done by introducing the so called *stylized facts* - observed properties of markets which should be taken into account by a good modelling approach.

After the introduction to financial markets is drawn, we provide a comprehensive review of the literature on SV models which focuses on popular approaches including the latest fractional and rough models. We briefly discuss a set of common assumptions that all mentioned approaches utilize and we also comment on the main differences between the proposed models.

In practice, the main scope of SV models includes a management of risks coming from complex financial derivatives – contracts depending on future evolution of specific financial assets. Before being able to use SV models on these complex derivatives, however, one needs to calibrate the models to relevant market observables. Typical instruments suitable for calibration are vanilla derivatives such as forwards, European options and recently also variance swaps / forwards. Hence, we introduce a standard formulation of derivative valuation and calibration problems, alongside market standard definitions of European options and variance swaps derivative contracts in Chapter 3.

In line with recent trends in SV modelling, the main focus of this thesis is laid on αRFSV model introduced by Merino – Pospíšil – Sobotka – Sottinen – Vives (2019). In the reference above, we developed a short-time approximation to option fair value under the αRFSV model and in this thesis the result is extended to an exact semi-closed formulation of the continuous fair variance. In particular we show how to express specific conditional expectations of the variance process assumed by the model.

Due to the lack of publicly available data on fair variances for most of the financial assets, we have reviewed a connection between variance and option markets using Carr – Madan (1998) approach which became a market standard for vanilla variance swap valuation over the years. Using the Carr – Madan (1998) approach, we are able to transform option prices into fair variances and to test the newly introduced αRFSV formulation on the task of market calibration.

The novelty of the proposed calibration routine is that we use fair variance data to infer a superior initial guess of model parameters for option calibration. Although we retrieve a similar quality of the calibration fit as in Merino – Pospíšil – Sobotka – Sottinen – Vives (2019) without the fair variance data, due to having very good initial guesses we are able to increase efficiency of the calibration task. In our small numerical experiment based on the real market data, we saved approximately 46% of the computational time.

Last part of the thesis concludes on author's research activities by displaying published research articles which were co-written by the author.

Keywords: Rough volatility, fractional Brownian motion, European options, variance swaps, stylized facts, financial market models.

MSC classification: 00A69, 91G20, 91G80

GLOSSARY

TABLE OF ABBREVIATIONS AND TECHNICAL TERMS

Abbreviation	Meaning
ATM	At-the-money; denoting an option with strike close to the current spot price, i.e. intrinsic value of the option is close to zero.
$\delta(\cdot)$	Dirac's delta function
$DF(\cdot,\cdot)$	Discount factor $DF(s,t)$ from time s to t for any $0 \leqslant s < t \leqslant +\infty$.
FV	Fair value of a derivative is represented by market implied expected value of discounted future cash-flows implied by the derivative conditional on current available information, see Chapter 3.
FS	Fair variance (sometimes also called fair strike) of a variance swap derivative is a strike value which would implied zero fair value for the original variance swap.
$\Gamma(\cdot)$	Gamma function, e.g. for $\Re(z) > 0$ defined as $\Gamma(z) = \int_0^\infty x^{z-1}e^{-x}dx$
$\{\Gamma_i\}, \{\Lambda_j\}$	Parameter sets of αRFSV model where $\Gamma = \{\sigma_{t_0}, \xi, H, \rho\}$ and $\Lambda = \Gamma - \{\rho\}$
H	Hurst exponent, a parameter of a fractional Brownian motion, as defined in Chapter 2, but also a similar exponent parameter for e.g. $\alpha-$RFSV model as introduced in Chapter 4.
$N(\cdot)$	Denotes cumulative distribution function of a standard Gaussian random variable
OTC	Over-the-counter, OTC derivatives are contracts traded privately between two parties, without involving any exchange. As opposed to exchange traded contracts, OTC derivatives have trade terms negotiated between the two parties and terms might not need to be disclosed.
PDE	Partial differential equation
PnL	Profit and loss of resulting from a particular financial position
SDE	Stochastic differential equation
VSC	Variance swap curve also denoted as $\xi_s(t)$, is a curve containing fair variances for variance swap started at time s and maturing at time t, defined by (50)

ACKNOWLEDGEMENTS

"Human beings, who are almost unique in having the ability to learn from the experience of others, are also remarkable for their apparent disinclination to do so."

Douglas N. Adams

I would like to express my sincere gratitude to the supervisor of this thesis, prof. RNDr. Bohdan Maslowski, DrSc., and to the consultant specialist, Ing. Jan Pospíšil, Ph.D., whose comments helped to improve the text significantly.

This work was partially supported by the GACR Grant 14-11559S Analysis of Fractional Stochastic Volatility Models and their Grid Implementation. Computational resources were provided by the CESNET LM2015042 and the CERIT Scientific Cloud LM2015085, provided under the programme "Projects of Large Research, Development, and Innovations Infrastructures".

CONTENTS

1 INTRODUCTION

1.1 STRUCTURE OF THE THESIS

A structure of the thesis is described as follows. First of all, we provide a motivation on models which are used to manage risks coming from complex derivatives and then we describe both preliminary modelling set-up and basic definitions related to financial markets in Chapter 1. Last but not least, we introduce a set of stylised facts - typically observed properties of financial markets. These properties should be captured by a good modelling approach.

In Chapter 2 we provide a thorough review of the literature on stochastic volatility models which are the main subject of this thesis. Not only traditional well know models, but also latest rough volatility approaches are briefly introduced.

We also review two important tasks in practice in Chapter 3: valuation of derivative contracts and a calibration to option markets. The last part of the chapter is devoted to the connection between option and variance derivatives and also include reasoning why this connection can be used also for stochastic volatility models.

Main results of the thesis are provided in Chapter 4 and in Appendix B. In Chapter 4 we describe the αRFSV model studied by Merino – Pospíšil – Sobotka – Sottinen – Vives (2019) in detail. A formula under this model for a quantity called the fair variance is derived and subsequently tested on a small numerical experiment.

In Appendix B we provide published articles co-written by the thesis author. In particular, we attach the following articles:

- Pospíšil – Sobotka (2016) – We introduced a long-memory fractional stochastic volatility model and compare it to a more traditional approach on the real market data.
- Mrázek – Pospíšil – Sobotka (2016) – Various calibration techniques are studied alongside several stochastic volatility models.
- Baustian – Mrázek – Pospíšil – Sobotka (2017) – A new pricing technique for a class of jump-diffusion stochastic volatility models is derived based on a complex Fourier transformation of the partial integral differential valuation equation.
- Merino – Pospíšil – Sobotka – Vives (2018) – A short-time / low volatility of volatility pricing formula is developed for jump-diffusion stochastic volatility models.
- Pospíšil – Sobotka – Ziegler (2019) – Robustness of various stochastic volatility models is tested under data-structure uncertainty.

In Chapter 5 and Appendix A we conclude the main results of this thesis and we illustrate some of the additional market properties, respectively.

1.2 MOTIVATION

Many academics and practitioners were fascinated by financial stock markets, but it was not until 1900 when the first mathematical treatment of the stock returns and option pricing problem was introduced. It was due to the thesis called *Théorie de la Spéculation* written by Louis Bachelier (Bachelier, 1900). Bachelier derived a relation between derivative securities and the underlying financial stock. The relation was based on the assumption that stock prices evolve as a continuous-time stochastic process, today known as Wiener process[1]. Moreover, for the first time a connection between the heat equation and the newly introduced process was shown. Hence, Bachelier is by many considered as a founder of the financial mathematics (Dimand – Ben-El-Mechaiekh, 2012), but his pioneering results contributed to the theory of stochastic processes and stochastic analysis as well.

1 In fact, several mathematicians, including W. Feller and P. Lévy among others, suggested using the term Bachelier-Wiener process (Feller, 1968; Lévy, 1948).

Bachelier's thesis, however, was not widely known until 1960 when its English translation was published in Paul Cootner's *The Random Character of Stock Market Prices* (Cootner, 1964). The proposed approach later inspired Paul Samuelson who added a deterministic drift term to the assumed stock price dynamics. The main breakthrough in option pricing came in 1973 and was caused by Black – Scholes (1973) and Merton (1973) who introduced the highly regarded Black-Scholes model. The stock prices are modelled by a geometric Brownian motion (so unlike for previous approaches, stock prices cannot take negative values if combined with appropriate initial condition), but more importantly the authors have justified several techniques that were intuitively used by Bachelier. This led to a significant increase in derivative trading which resulted in the opening of the Chicago Board Options Exchange in 1973 (Sircar – Papanicolaou, 1998). However, the Black-Scholes model raised also a wave of criticism. Especially after the *flush crises* of 1987 it became apparent that the approach insufficiently describes market movements and using the model on the option pricing thus might not lead to a reasonably good approximation of a fair market price. Drawbacks of the Black-Scholes dynamics are summarized by the so called *stylized facts* which we will discuss in the following sections.

One of the direct application of any pricing model comes from over-the-counter (OTC) trading. Typically, a provider of a non-traded OTC contract calibrates a trusted model to the related market(s) and using the model assumptions alongside calibrated parameters he or she computes a fair price of the contract. The price obtained from a good model should help in answering the question what the contract is worth. According to the survey of the Bank for International Settlements (BIS, 2016), the OTC trading of derivatives (excluding commodity markets) increased in the gross market value from 5 811 billions USD in 1998 to 38 316 billions USD in 2014 while topping 55 000 billions USD in 2008 (see Figure 1). Hence, the need for an accurate and robust modelling approach for derivative valuation and risk management is obvious.

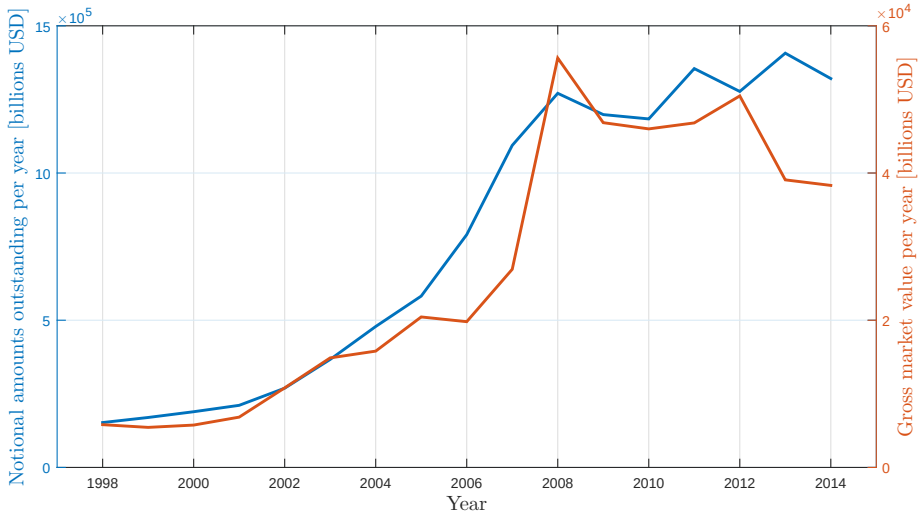

Figure 1: Notional amounts outstanding and gross market value per year for OTC derivatives excluding commodity markets depicted from 1998 to 2014. Source:BIS (2016) available at www.bis.org/statistics/derstats.htm.

1.3 PRELIMINARY SET-UP

In this section, we define our notation and a modelling set-up used throughout the thesis. The latter will be specified more thoroughly for a particular model. We assume that the reader is familiar with basic measure-theoretic concepts.

Modelling set-up

Unless explicitly stated otherwise, we assume a filtered probability space - a family $(\Omega, \mathcal{F}, (\mathcal{F}_t)_{t\geqslant 0}, \mu)$, where Ω is the sample space, $\mathcal{F}$ denotes a $\sigma-$algebra on Ω, i.e. a collection of subsets of Ω such that $\Omega \in \mathcal{F}$, $\mathcal{F}$ is closed under complements and closed under union of countably many subsets. Filtration $(\mathcal{F}_t)_{t\geqslant 0}$ is an increasing (in terms of inclusion) collection of sub $\sigma-$algebras of $\mathcal{F}$. The last object, μ, is a probability measure - a measure on $\mathcal{F}$ satisfying $\mu(\Omega) = 1$.

As a tool to describe the evolution of asset prices, we use continuous-time real-valued stochastic processes. A real-valued stochastic process $(X_t)_{t\in I}$ is a family of random variables on the probability space $(\Omega, \mathcal{F}, \mu)$ with values in a common measurable space $(\mathbb{R}, \mathcal{B})$ where $\mathcal{B}$ denotes a Borel $\sigma-$algebra on $\mathbb{R}$.

In our case, index t represents time and hence the index set I for all considered stochastic processes will be an interval, usually of a finite length. Instead of I we write either $t \geqslant 0$ or we specify a corresponding interval for t.

Moreover, we consider in this thesis processes which are adapted to the assumed filtration. A stochastic process $(X_t)_{t\geqslant 0}$ is said to be adapted to $(\mathcal{F}_t)_{t\geqslant 0}$ if X_t is $\mathcal{F}_t$-measurable for every $t \geqslant 0$. This is essential for financial applications. By filtration we model the information known at time t and hence all asset price processes are assumed to be non-anticipating - i.e. all modelled variables with respect to time t are fully determined (i.e. observed) at time t, not before.

A special case of an $\mathcal{F}_t$-adapted process would be a martingale with respect to the filtration $\mathcal{F}_t$, i.e. a process (X_t) satisfying the following conditions:

- $\mathbb{E}|X_t| < +\infty$, for any $t \geqslant 0$,
- $\mathbb{E}[X_u|\mathcal{F}_t] = X_t$, for any $u \geqslant t \geqslant 0$.

Most notorious example of a martingale process with respect to its natural filtration is a standard Wiener process. A real-valued continuous time stochastic process $(W_t)_{t\geqslant 0}$ is called standard Wiener process if

(i) $W_0 = 0$ almost surely (a.s.),

(ii) the paths $t \mapsto W_t$ are a.s. continuous,

(iii) $W_t - W_s$ is normally distributed with zero mean and variance $t - s$ for all $0 \leqslant s \leqslant t$,

(iv) for $0 < t_1 < t_2 < ... < t_n < \infty$, the increments W_{t_1}, $W_{t_2} - W_{t_1}, ..., W_{t_n} - W_{t_{n-1}}$ are independent random variables.

An important statement provided e.g. in (Øksendal, 2003, Chapter 2) ensures the existence of a process with above properties. Other examples of stochastic processes applied in financial models are Poisson process (defined e.g. in Bauer (1996), Chapter VIII, §41) and a fractional Brownian motion introduced below in Chapter 2.

In previous definitions we used a generic probability measure μ. In practice, one is often interested in two specific types of probability measures - a "historical" measure P under which the observed events occur (according to our model) and a "pricing" measure Q under which a discounted asset price process $(S_t)_{t\geqslant 0}$ (yet to be specified) is a martingale with respect to the assumed filtration. Both measures are equivalent (i.e. they agree on the null set and on Ω consequently) and hence Q is also known as the equivalent martingale measure with respect to $(S_t)_{t\geqslant 0}$. Since we are interested in pricing tasks, we mainly utilize the equivalent martingale measure Q. For instance, the notation $\mathbb{E}^Q[\cdot]$ is used to stress out that we take the expectation with respect to the corresponding measure.

To make this text compact, we also assume that the reader is familiar with definitions of (Itô) stochastic integrals and stochastic differential equations alongside necessary results of stochastic calculus. To name a few, one should be familiar with the Itô lemma and the Girsanov theorem to fully comprehend this text. The definitions and theorems can be found e.g. in Øksendal (2003) and Maslowski (2006).

1.4 FINANCIAL MARKETS

All considered models utilize a framework under which there are three investment types available:

1. Risk-free investment
   This investment typically provides the least volatile appreciation of invested funds and in practise is realised by money markets and government securities. The value of portfolio B_t with \$1 investment at $t = 0$ satisfies

$$dB_t = r(t)B_t\,dt, \tag{1}$$

$$B_0 = 1, \tag{2}$$

   where $r(t)$ in our case would be a positive constant, $r(t) = r \in \mathbb{R}^+$. The risk-free investment is necessary for no-arbitrage arguments - by no-arbitrage it is meant that one cannot make a profit without a risk and his or her own capital. This implies that if we are able to create a risk-free portfolio containing the upcoming two investments only, a yield of the portfolio[2]

2 Otherwise for the annual return higher than r one would borrow money for r and after paying back for the loan one would keep a positive profit.

must be the same as in the case of B_t. A precise formulation of arbitrage opportunities is presented e.g. in Delbaen – Schachermayer (1994).

2. Risky assets (stocks, FX pairs, commodities etc)
   Evolution of the asset market price in time is harder to foreseen, hence it is modelled as a specific stochastic process (depending on a selected model, see Chapter 2) which is set up on a filtered probability space. In our case, we review models where the asset price follows a continuous-time stochastic process and the filtration in consideration is the natural one (unless specified otherwise).
3. Financial derivatives (futures, options, etc)
   The last available investment choice is represented by derivatives on the risky asset. A derivative is a financial contract between two parties (i.e. buyer and seller) with a value derived from the performance of the risky asset. Hence, the risky asset is called *underlying* of the derivative.

In our case we focus on equity indices as risky assets and as derivatives we consider European options and variance swaps, although many of the following ideas are not limited to this choice and are applicable to different assets as well. Either Overnight Indexed Swaps (OIS) are utilized to back up a proxy of the risk-free interest rate or inter-banking rates (LIBOR, EURIBOR etc) can be used as a traditional approximation of the risk-free rate. We note that inter-banking rates are less commonly used for this purpose nowadays due to their decreasing liquidity and also due to the transition plans and regulatory reforms in favour of alternative reference rates[3].

European options

A European call (put) option is a derivative that gives the buyer a right, not an obligation, to buy (sell) a unit of the underlying risky asset for a fixed price $K > 0$ at a specific time in the future called maturity and denoted by $T > 0$. The seller grants this right in exchange for an option price / premium. K is traditionally known as the strike price and we use Greek letter τ throughout this text to denote a remaining time to the maturity of an option, i.e. $\tau = T - t$ for $0 \leqslant t \leqslant T$. At the maturity T, the buyer receives a payment depending on the current price of the risky asset S_T. For a call option this can be formalized as:

$$P^{\text{Call}}(S_T) = (S_T - K)^+ = \max(S_T - K, 0). \tag{3}$$

The pay-off function $P^{\text{Call}}(\cdot)$ takes non-negative values only, because if the asset price at maturity is lower than the strike price K, i.e. $S_T < K$, the buyer lets the option expire without exercising it and, if necessary, he or she buys the asset for its market price instead. In case of European options, the right can be only exercised at the maturity and thus $P^{\text{Call}}(S_t) = 0$ for any t from the inception time t_0 to the maturity, i.e. $t \in (t_0, T)$. Similarly, we could formalize the pay-off definition for put options.

Typically, the contracts described above are known as vanilla European options. By the key word "European" we understand a single contractual exercise date and "vanilla" means that the payoff at maturity depends on the underlying price solely by a relation provided above. Non vanilla options might have, for example, a path dependency - P^{Call} would be a function of the underlying price at several referencing dates.

To know a fair value of an option contract is of the eminent interest for market participants. For instance, if we knew option fair values we can pose some implications on the assumed dynamics of the risky asset - option fair values can be viewed as a set of constraints for asset dynamics in this context.

These constraints are posed typically by model calibration exercise which is described in Chapter 3. A mathematical definition of the fair value - which defines the connection between a model and market quoted prices - is introduced in the same chapter.

Variance swaps

A variance swap is a contract that enables its buyer to swap a future realized variance of the underlying risky asset returns for a pre-agreed fixed value, denoted as a variance strike K^2_{var}. In particular,

3 For a brief overview on the situation in the UK, i.e. SONIA vs LIBOR rates please refer to https://jwg-it.eu/sonia-and-libor-the-end-of-an-infamous-benchmark.

plain vanilla variance swaps are with respect to the daily returns and a typical contractual definition is introduced bellow:

$$\sigma_R^2(t_0, T) = \frac{A}{M} \sum_{i=1}^{M} \left(\ln \frac{S_{t_i}}{S_{t_{i-1}}} \right), \tag{4}$$

$$P_T^{VS} = 100^2 \frac{N_{vega}}{2K_{var}} \left(\sigma_R^2(t_0, T) - K_{var}^2 \right), \tag{5}$$

where

- A is an annualization factor (typically $A = 252$),
- K_{var}^2 is a contractual variance strike,
- M is a number of trading days aggregated into the realized variance calculation,
- N_{vega} is a Vega notional and is related to the standard variance notional as $N_{vega} = 2K_{var}N_{var}$,
- $\{t_1, t_2, ..., t_M\}$ is a set of M consecutive referencing dates,
- S_{t_i} is the underlying asset price at the end of trading day t_i.

The Vega notional is more frequently used than the standard variance notional, because it reflects a PnL change, when volatility changes by one percent point (rather than the same change in variance terms for standard variance notional). Unlike for European options, we can decompose the pay-off function P^{VS} into deterministic (i.e. contractual) terms and a term depending on a future performance of the underlying asset - a stochastic term. This decomposition leads to the quantity referred to as fair variance which will be introduced later in Chapter 3.

1.5 DESIRED PROPERTIES OF MARKET MODELS

In this section, we introduce typical properties of risky assets also known as *stylized facts*. A good modelling approach should take these properties into account. Regarding the stylized facts, Cont (2001) noted: "*As such, they should be viewed as constraints that a stochastic process has to verify in order to reproduce the statistical properties of returns accurately*". Firstly, we inspect directly observed properties of risky assets.

Observed properties of financial assets

- *Asymmetry of asset price distribution*
  Typically one can observe large drawdowns in asset prices, but not equally large upward movements. This observation is common for equity markets and less typical for exchange rates (Cont, 2001).
- *Heavy tailed distribution of asset returns*
  This market property is widely accepted since Mandelbrot (1963) pointed out the insufficiency of the normal distribution for modelling the asset returns distribution due to the heavy-tailed nature of returns. The Black-Scholes model assumes normally distributed logarithmic returns and hence cannot reflect this fact.
- *Leverage effect*
  The property states that realized volatility of an asset is negatively correlated to the asset returns. According to Cont (2001), it should not matter which statistical measure of realized volatility we use.
- *Non-correlated asset returns*
  Autocorrelation of asset returns is typically insignificant as was shown e.g. by Čekal (2012). However, we do not state this is the case for small time scales (due to the market microstructure) nor if we consider a non-linear dependence of returns.
- *Slow decay in autocorrelation of absolute returns*
  Sample autocorrelation function of absolute returns decays slowly as a function of time lag λ. Usually this decay is similar to the power law $\exp(-\beta\lambda)$, where β is typically ranging from $[0.2, 0.4]$, see Figure 2 and (Cont, 2001).
- *Volatility clustering*
  Statistical measures of realized volatility exhibit a significant positive autocorrelation over several days period. This accounts for a well documented observation that high volatility events tend to cluster.

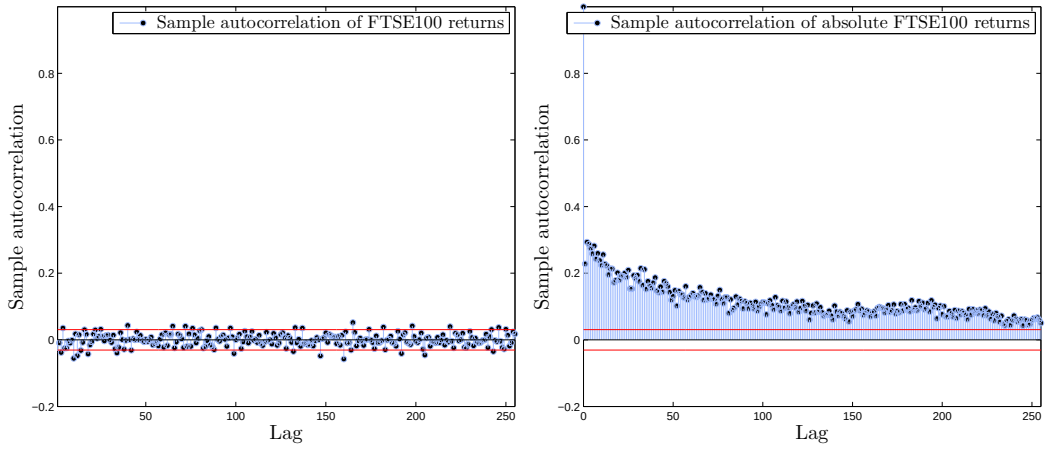

Figure 2: Sample autocorrelation of returns (on the left) and absolute returns (on the right) - FTSE 100 index (1/2000 - 2/2016).

Several other stylised facts have been observed on some markets, for a more thorough review see Bollerslev et al. (1992), Brock – De Lima (1996), Campbell et al. (1997), Gourieroux – Jasiak (2001), Pagan (1996), Shephard (1996) or a more recent study in Takayasu (2013). An overview without any particular model in focus can be found in Cont (2001). In what follows, we illustrate some of the stylized facts using time-series data sets of 5 major stock indices from January 2000 to February 2016[4].

In Figure 3 we depict a sample density of German industrial index DAX. Similarly to other available data sets (see Appendix A), we can notice a much sharper peak and heavier tails compared to the fitted normal distribution. Also an asymmetry of the returns density can be observed. Sample skewness and kurtosis of this data set reads approximately -0.1003 and 7.9647 respectively. Difference between a normal and observed distribution is well depicted by quantile-quantile plot, see Figure 4.

Autocorrelation of daily returns is typically insignificant which we show for the 5% level of significance and for the British FTSE 100 index in Figure 2. However, this is not the case for absolute returns, that are only slowly decaying - see the right half of Figure 2.

To depict the other two stylized facts, we plot closing quotes of S&P 500 index and a high frequency estimate of its realized volatility[5]. One can notice that the realized volatility reaches highest levels, when the underlying value of the index is falling (e.g. time periods 2008 - 2010 or $2000 - 2003$, Figure 5). On the other hand, when index quotes increase, lower values of the realized volatility are observed. The phenomenon of volatility clustering is also plain to see in Figure 5.

In Appendix B, similar figures are depicted for all 5 indices, namely for the German industrial average index *DAX*, American Dow Jones Index *DJIA*, British *FTSE* 100, Japanese *NIKKEI* 225 and American Standard & Poor's 500 - *S&P* 500. Equity indices are (weighted) arithmetical averages of stock prices of most capitalized or traded companies on a specific market. The equity indices are well recognised as benchmark markets for model calibration tasks - they typically comprise of exchange traded derivatives with highest liquidity and lowest ask-bid spreads. Hence, index options would make a good testing data for the task of model calibration introduced in Chapter 3.

Properties implied by derivatives

These properties of risky assets are inherited from observed prices of derivatives traded on the assets. In our case, we consider mainly properties of European option prices on equity indices. For this purpose, we define a notion of the (Black-Scholes) implied volatility. Firstly, we look at the well-known Black-Scholes pricing formula. Let $(S_t)_{t\geqslant 0}$ be a geometric Brownian motion[6] with constant volatility σ_{BS} defined on the filtered probability space $(\Omega, \mathcal{F}, (\mathcal{F}_t)_{t\geqslant 0}, \mathbb{P})$ and let Q denote the uniquely defined equivalent martingale measure to P with respect to $(S_t)_{t\geqslant 0}$ and let $(\mathcal{F}_t)_{t\geqslant 0}$ be the natural filtration of the asset price process. Let $C_{BS} : \mathbb{R}^+ \to \mathbb{R}^+$ maps from an asset dynamics

4 Index quotes alongside high frequency estimates of realized variance thereof were obtained from http://realized.oxford-man.ox.ac.uk/data

5 We took an estimate with 5-minutes re-sampling, see http://realized.oxford-man.ox.ac.uk/data.

6 For definition of a geometric Brownian motion see Shreve (2004).

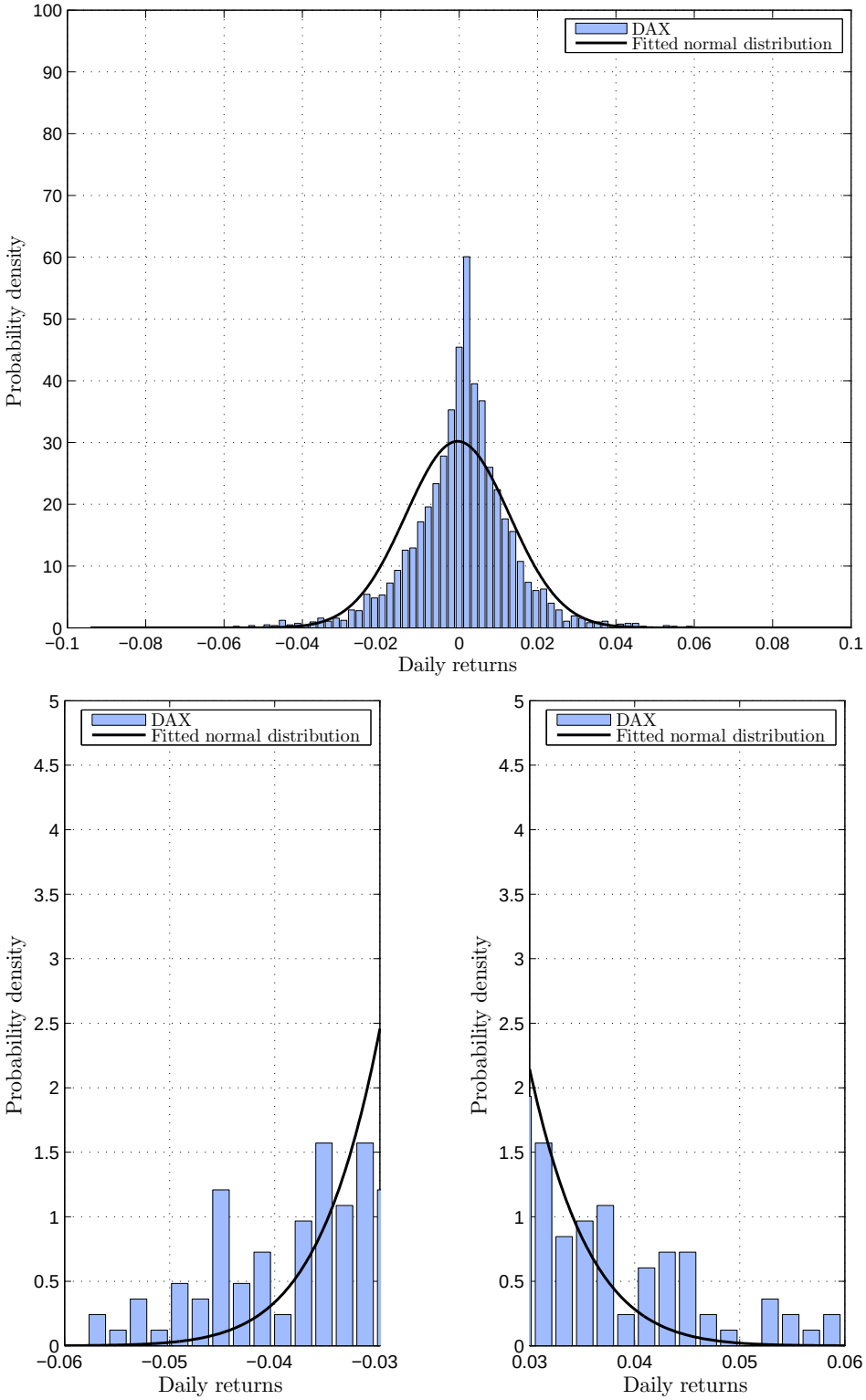

Figure 3: Empirical distribution of DAX Index (1/2000 - 2/2016) compared to the normal distribution.

parameter $\sigma_{BS} > 0$ to the fair value of a call option (which is described more thoroughly in Chapter 3),

$$\mathbb{E}^{Q}\left[e^{-r\tau}(S_T - K)^{+} | \mathcal{F}_{t_0}\right], \tag{6}$$

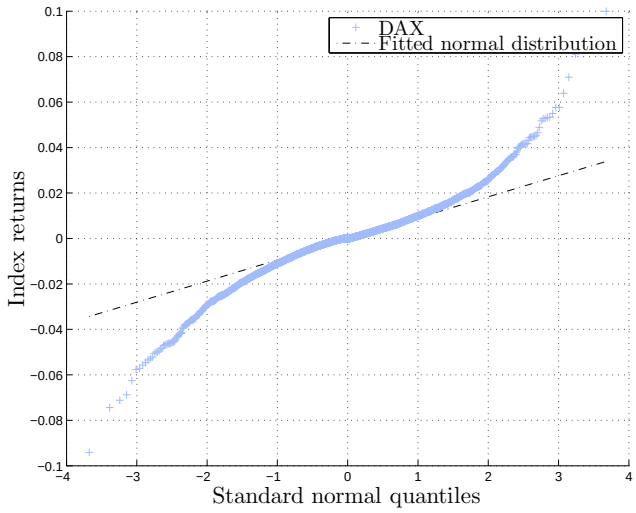

Figure 4: Quantile-quantile plot of DAX Index (1/2000 - 2/2016).

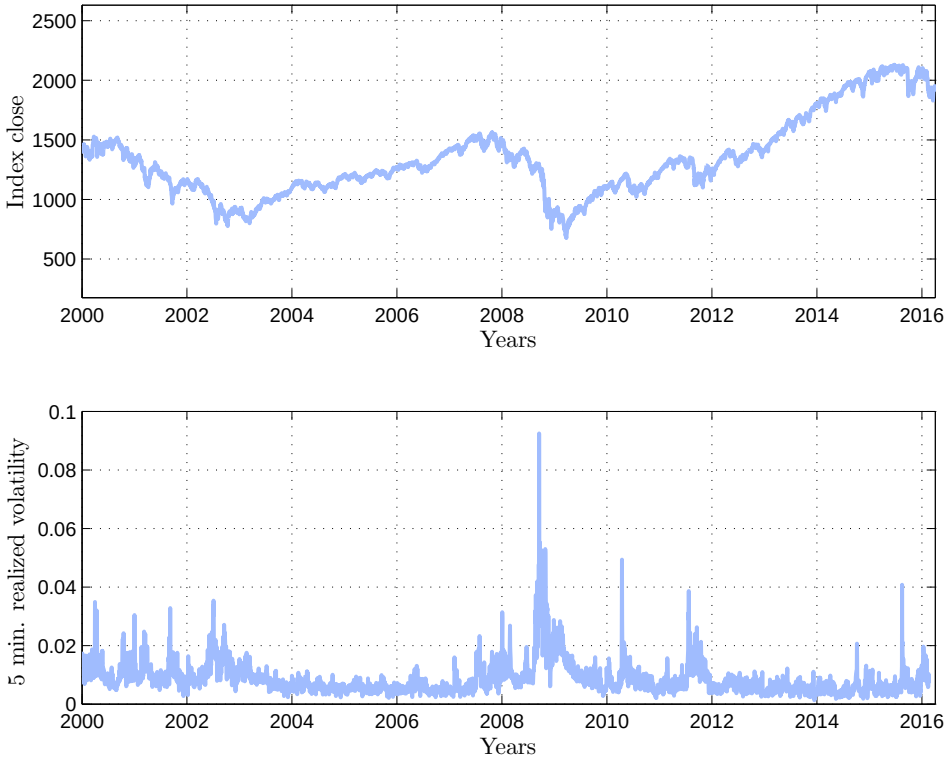

Figure 5: S&P 500 index quotes alongside 5-min. realized volatility.

with strike K and maturity T (respectively $\tau := T - t_0$, where t_0 is the corresponding inception time $0 \leqslant t_0 \leqslant T$). Then, as was derived in the original paper Black – Scholes (1973), C_{BS} takes the following form:

$$\begin{aligned} C_{BS}(\sigma) &= N(d_1)S_{t_0} - N(d_2)Ke^{-r\tau} \\ d_1 &= \frac{1}{\sigma\sqrt{\tau}}\left[\ln\left(\frac{S_{t_0}}{K}\right) + \left(r + \frac{\sigma^2}{2}\right)\tau\right], \\ d_2 &= d_1 - \sigma\sqrt{\tau}, \end{aligned} \tag{7}$$

where $N(\cdot)$ denotes the cumulative distribution function of a standard Gaussian random variable. The mapping C_{BS} is strictly increasing and for $\sigma_{BS} \to 0$ tends to $(S_{t_0} - K\exp(-r\tau))^+$ and as $\sigma_{BS} \to \infty$ it tends to S_{t_0}. These are also the natural bounds for a market option price and thus it makes sense to define the implied volatility σ_{IV} as follows.

Definition 1 (*Implied volatility*)**.** Let S_{t_0} be observed on the market and let $C > 0$ be the market observed price of a European call option with strike K, time to maturity τ quoted at time t_0, then a unique non-negative solution σ_{IV} of

$$C = C_{BS}(\sigma) \tag{8}$$

is called the implied volatility corresponding to the market option with price C.

The uniqueness and existence of the implied volatility (also for other pricing models) is discussed e.g. in Jacquier (2016). In practice, one can often observe market implied volatilities instead of option prices. They are also used to depict well known discrepancies of the Black-Scholes model, dubbed as *volatility smile* and *volatility term structure*. We will inspect these phenomena by considering a mapping[7] $K \times \tau \to \sigma_{BS}(K, \tau)$ which is known as the *volatility surface*. Observed properties of the surface can help us to choose an accurate pricing model and also, based on our volatility surface data, we can reject some of the unsuitable approaches with respect to the particular data. However, for each risky asset the surface might look differently. This can happen even for options on the same asset only quoted at different times, see Figure 7. In this text we mention typical properties of the surfaces with respect to index options, according to analyses by Cont – Da Fonseca (2002), Alòs et al. (2007) and Bayer et al. (2016).

Firstly, we start with vertical slices of the implied volatility surface. Taking a vertical slice along K for a fixed $\tau = \hat{\tau}$ we obtain a volatility smile for $\hat{\tau}$. In Figure 7 we depict volatility smiles for available times to maturity with respect to DAX index options (and specific historical dates) by red curves. In doing so, we use an interpolation technique introduced by Gatheral – Jacquier (2014). We can observe v-shaped volatility smiles that are more pronounced for shorter times and flatter for greater τ's. This property is typical for equity index surfaces, but it can be observed also for different risky assets (Cont – Da Fonseca, 2002). Unlike the Black-Scholes model, a good SV model should be able to generate a surface that well mimics observed properties.

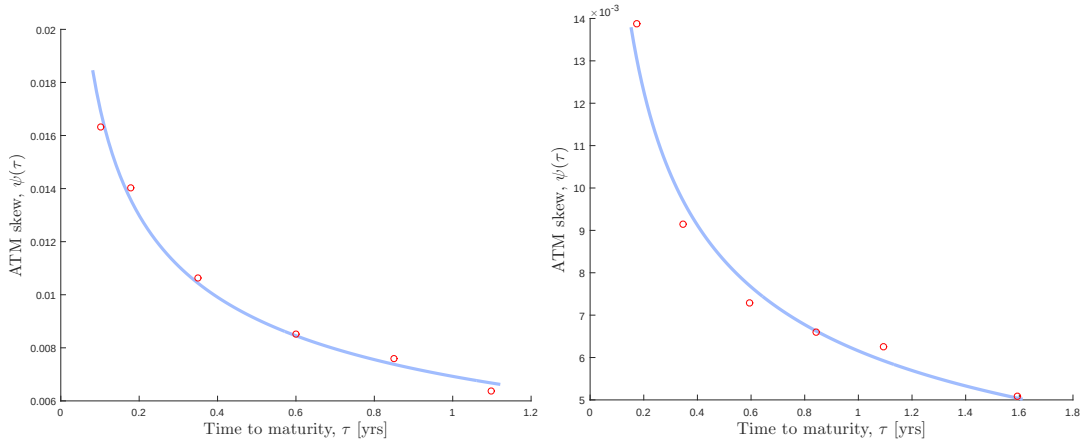

(a) ATM volatility term structure, $\alpha = 0.3909$, (13/5/2015).

(b) ATM volatility term structure, $\alpha = 0.4291$, (15/5/2015).

Figure 6: ATM volatilities are represented by red circles and the blue curve is the least-square fit of the form $\psi(\tau) = A\tau^{-\alpha}$.

A vertical slice for a fixed strike, $\hat{K}$, along τ is known as the volatility term structure or skew. According to Gatheral et al. (2018), the at-the-money volatility ($\hat{K} = S_{t_0}$) skew can be approximated by a power law function $\psi(\tau) = A\tau^{-\alpha}$ where for equity indices α should be typically less than 0.5. In Figure 6 we fitted $\psi(\tau)$ to the data for DAX index using a least-square minimization. In the case of the market data from 13/5/2015 we obtained $\alpha = 0.3909$ and $\alpha = 0.4291$ for the 15/5/2015 at-the-money volatility skew.

To create a surface by a calibrated model that fits the market data well for wide range of strikes and time to maturities is a challenging task. E.g. the Black-Scholes model always creates a flat shape (i.e. implied volatilities are assumed to be constant for all combinations of K and τ). As for the models to be introduced in Chapter 2, the SABR model can capture one volatility smile and the original Heston model can fit reasonably well two smiles at once (Gatheral et al., 2018). The

7 However, not all combinations of K and τ are typically available, in that case one has to use a suitable interpolation technique instead of solving (8).

power law decaying skew can be modelled by multi-factor Bergomi approach (Bergomi, 2008) and more naturally by a stochastic volatility model where volatility process is driven by a fractional Brownian motion with $H < 0.5$. The connection between the Hurst parameter H and the power law skew exponent α is studied in Bayer et al. (2016). Fractional Brownian motion alongside recently proposed models is introduced in Chapter 2. Although an orientation and levels of the equity index surfaces might change for different trading days, the overall shape remains similar, see Figure 7. Based on this observation, Bayer et al. (2016) suggest that the price process of a risky asset should be modelled by a time-homogeneous stochastic process and the parameters of a suitable model should be constant in time.

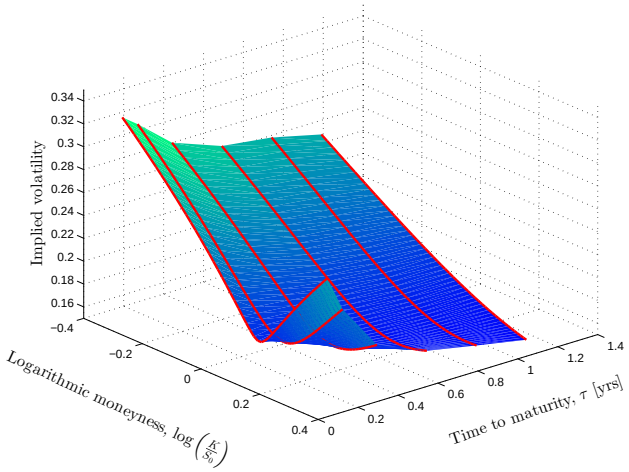

(a) Implied volatilities - 13/5/2015.

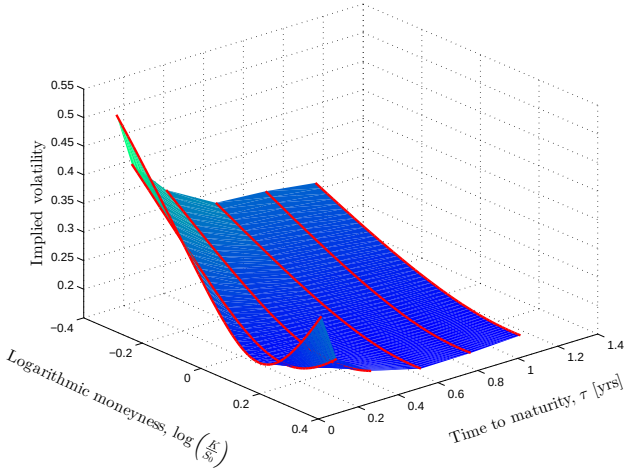

(b) Implied volatilities - 14/5/2015.

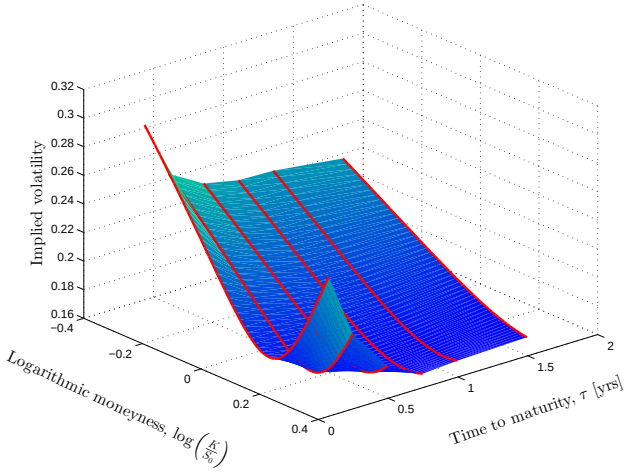

(c) Implied volatilities - 15/5/2015.

Figure 7: Implied volatilities of DAX Index options for three different trading days. Interpolation of volatility surfaces is performed using SVI parametrization described in Gatheral – Jacquier (2014).

2

STOCHASTIC VOLATILITY MODELS

In this section we review popular stochastic volatility (SV) models. Each model is set up on a filtered probability space $(\Omega, \mathcal{F}, (\mathcal{F}_t)_{t\geqslant 0}, \mathbb{Q})$ where the filtration $(\mathcal{F}_t)_{t\geqslant 0}$ is generated by all Wiener processes and fractional Brownian motions (introduced later in this Chapter) considered by a specific model. I.e. for a standard SV model with two Wiener processes $(W_t,\ W_t^\star)_{t\geqslant 0}$, the filtration $(\mathcal{F}_t)_{t\geqslant 0}$ is given by $\mathcal{F}_t = \sigma(W_u, W_u^\star; 0 \leqslant u \leqslant t)$. We also note that, unlike for the Black-Scholes case, $\mathbb{Q}$ might not be uniquely determined. Restrictions on model dynamics to ensure existence of the measure (which translates into the desired well-posedness of the pricing problem) are discussed in Delbaen – Schachermayer (2006) and Jacquier (2016). A positive risk-free rate r is determined by the unique growth rate of a risk-free investment. While in academic literature on SV models, this is for simplicity assumed to be constant over time, typically in practice a deterministic term-structure of the risk-free yield is imposed. In the following review we start by listing common assumptions of all considered models, then we describe earlier and simpler approaches. Last but not least, we describe models with fractional noise in the volatility process.

All considered models share the following *classical* assumptions (see e.g. Wilmott (2007) Part I, Chapter 5 and Part IV, Chapter 51):

SV models' assumptions

- No arbitrage opportunities occur, thus the risk-free rate r is unique. Moreover, r is constant during the life of the given option;
- There are no transaction costs for buying nor for selling, i.e. the market is frictionless;
- Any fraction of a risky asset can be bought and trading of assets and derivatives is continuous in time;
- Short selling of any asset is allowed at the considered market.

We do not consider models with dynamic risk-free rate r and we focus on models where the risky asset is assumed to be traded continuously in time. By the notion short selling, appearing in the last assumption, we mean that an investor is allowed to sell any available asset even the one he or she does not own at the current time. It that is the case, later the investor re-purchases the asset to finalize the transaction.

2.1 STANDARD SV MODELS

In the case of standard SV models, the asset dynamics is typically modelled by a system of two Itô stochastic differential equations (SDEs) accompanied by an initial value condition. A strong solution S_t of the first SDE is a price process of the risky asset, a strong solution of the second equation typically represents variance process of the asset price. We assume that at the inception time $t_0 \geqslant 0$ we can observe S_{t_0} and ν_{t_0}, hence the initial value problem is of deterministic nature, $S_{t_0} = s;\ \nu_{t_0} = \nu;\ s, \nu \in \mathbb{R}^+$.

The first acknowledged SV model was introduced by Hull – White (1987). The assumed dynamics takes the following form:

$$dS_t = rS_t\,dt + \sqrt{\nu_t}S_t\,dW_t, \tag{9}$$
$$d\nu_t = C_1\nu_t\,dt + C_2\nu_t\,dW_t^\star, \tag{10}$$

where C_1 and $C_2 \in \mathbb{R}$ are parameters of the model. Wiener processes $(W_t,\ W_t^\star)_{t\geqslant 0}$ are stochastically independent in the original model. Wiggins (1987) suggested the use of correlation coefficient ρ, such that $\mathbb{E}[dW_t\,dW_t^\star] = \rho dt$. For $\rho < 0$ processes $(S_t, \nu_t)_{t\geqslant 0}$ can reproduce the leverage effect property described in Chapter 1. Hence, the correlation of driving processes is assumed for all the later approaches. The variance process ν_t follows a geometric Brownian motion which implies that some of the interesting statistical properties of the volatility process are explicitly known to us, e.g. (Jäckel, 2004):

$$\mathbb{E}[\sqrt{\nu_t}] = \mathbb{E}[\sigma_t] = \sigma_0 \exp\left\{\frac{1}{2}C_1 t - \frac{1}{8}C_2^2 t\right\},$$
$$\mathrm{Var}[\sigma_t] = \sigma_0^2\left(1 - \exp\left\{-\frac{1}{4}C_2^2 t\right\}\right)\exp\{C_1 t\}.$$

Chin (2011) argues, using the empirical analysis of Cont (2001), that a model with variance process v_t defined by (10) cannot reflect the volatility skew observed at financial markets[1]. To deal with this shortcoming, volatility mean-reverting approaches have been developed by Scott (1987). We will review a modified version of the model introduced by Chesney – Scott (1989) defined by the system of Itô SDEs,

$$\begin{aligned} dS_t &= rS_t\,dt + e^{y_t}S_t\,dW_t, && (11)\\ dy_t &= -\kappa(y_t - \bar{y})\,dt + \sigma\,dW_t^\star. && (12) \end{aligned}$$

Unlike in most of the models, instantaneous volatility of the asset price is expressed as e^{y_t}. There are two parameters within the drift term of dy_t; κ describes a reversion rate and $\bar{y}$ denotes an average level around which process y_t fluctuates. The diffusion term is represented by a constant σ. According to Jäckel (2004), the model needs strong negative correlation to reflect observed properties of implied volatilities.

Arguably the most popular mean-reverting model is the one proposed by Heston (1993) with the assumed market dynamics given by,

$$\begin{aligned} dS_t &= rS_t\,dt + \sqrt{v_t}S_t\,dW_t, && (13)\\ dv_t &= -\kappa(v_t - \theta)\,dt + \sigma v_t\,dW_t^\star, && (14) \end{aligned}$$

where θ represents a long term variance, κ is a reversion rate and σ denotes volatility of v_t. Popularity of the model comes from its tractability and from the existence of a semi-closed solution for European option prices. Unless the *Feller's* condition is satisfied, $2\kappa\theta \geqslant \sigma^2$ (Feller, 1951), the variance process can reach negative values, which is an issue that has to be dealt with[2]. Many extensions of this model have been proposed, for instance a model where parameters v_0, κ, θ, σ, ρ are (non-constant) functions of time. The case of piece-wise constant parameters was studied in Mikhailov – Nögel (2003), a linear time dependence in Elices (2008) and a more general case was introduced by Benhamou et al. (2010). Due to the argument of Bayer et al. (2016) mentioned in Chapter 1, these models might not be consistent with implied volatility surfaces. Later in this text, we will review jump-diffusion extensions to the Heston model.

A different approach, mainly used for interpolation of a single volatility smile, has been developed by Hagan et al. (2002) and takes the form:

$$\begin{aligned} dS_t &= \sigma_t S_t^\beta\,dW_t, && (15)\\ d\sigma_t &= \alpha\sigma_t\,dW_t^\star. && (16) \end{aligned}$$

The approach is commonly known as the Stochastic Alpha, Beta, Rho or briefly SABR model. Unless we are using a version with time-dependent thereof, it is well known, that the SABR model cannot fit complex volatility surfaces (Bayer et al., 2016).

An SV model that lately caught attention of both practitioners and academics was introduced by Bergomi (2005, 2008). Instead of modelling dynamics of variance v_t, the author proposed using a *forward variance curve*, defined as $\xi_t(u) = \mathbb{E}[v_u|\mathcal{F}_t]$, instead. The most general model utilizes $n+1$ Wiener processes $(W, W^{(1)}, ..., W^{(n)})_{t\geqslant 0}$ that are correlated with each other and $\mathcal{F}_t = \sigma\{W_s, W_s^{(1)}, ..., W_s^{(n)}; 0 \leqslant s \leqslant t\}$. Model dynamics is denoted by

$$\begin{aligned} dS_t &= rS_t\,dt + \sqrt{\xi_t(t)}S_t\,dW_t, && (17)\\ d\xi_t(u) &= \omega\sum_{i=1}^{n}\lambda_i(t,u,\xi_t(u))dW_t^{(i)}, && (18) \end{aligned}$$

where ω is a common scaling factor and λ_i, for $i = 1, 2, ..., n$, depends on a forward variance curve $\xi_t(u)$ and time, but not on the underlying price S_t. Suitable choices of λ_i are discussed in Bergomi (2008). For $n \geqslant 2$ the model can reproduce the volatility skew accurately, but as notes Bayer et al. (2016), even for $n = 2$ the model is over-parametrized. We also review its modified version with a single fractional Brownian motion replacing n Wiener processes.

Another important class of SV approaches are jump-diffusion models. The first model to utilise jump-diffusion processes in finance was introduced by Merton (1976). A jump process alongside stochastic volatility has been proposed by Bates (1996) who postulated the following model dynamics:

$$\begin{aligned} d\,dS_t &= rS_t\,dt + \sqrt{v_t}S_t\,dW_t + S_{t-}\,dQ_t, && (19)\\ dv_t &= -\kappa(v_t - \theta)\,dt + \sigma\sqrt{v_t}\,dW_t^\star, && (20) \end{aligned}$$

1 see Chapter 1, especially Figures 6, 7 and the accompanied text.

2 For instance, if the Feller's condition is not satisfied, the measure Q might not be generally well defined, see Jacquier (2016) .

where Wiener processes are, as in previous cases, correlated with coefficient ρ. Under the notation S_{t-} we understand $\lim_{k\to t-} S_k$, $(Q_t)_{t\geqslant 0}$ is a compensated compound Process with jump intensity $\lambda \in \mathbb{R}^+$ and sizes of jumps are i.i.d. random variables. Bates (1996) assumed log-normally distributed jump sizes, later Yan – Hanson (2006) proposed a model with log-uniform distribution thereof. Drift and diffusion terms of dv_t are the same as in case of the Heston approach.

A model with jumps not only in the underlying price, but also in the variance process, was introduced by Duffie et al. (2000). Similarly to the previous model,

$$dS_t = rS_t\,dt + \sqrt{v_t}S_t\,dW_t + S_{t-}\,dQ_t, \tag{21}$$
$$dv_t = -\kappa(v_t-\theta)\,dt + \sigma\sqrt{v_t}\,dW_t^\star + dQ_t^\star. \tag{22}$$

There were proposed two version of the model, either with correlated or independent compound Poisson processes $(Q_t, Q_t^\star)_{t\geqslant 0}$. As empirical studies have shown (e.g. Gatheral (2006), Gleeson (2005)), this approach might suffer from over fitting. While having four more parameters, it might not provide as good market fit as the Bates model.

2.2 FRACTIONAL SV MODELS

In this section we look at fractional SV models, i.e. models where the variance process is driven by either fractional Brownian motion (fBm) or a stochastic process with a similar covariance structure.

Definition 2 (*fBm*)**.** A fractional Brownian motion $(W_t^H)_{t\geqslant 0}$ with Hurst parameter $H \in (0,1)$ is a centred continuous Gaussian process with covariance,

$$R(s,t) := \mathbb{E}\left[W_s^H W_t^H\right] = \frac{1}{2}(s^{2H} + t^{2H} - |t-s|^{2H}).$$

FBm was introduced by Kolmogorov (1940) and studied in more detail by Mandelbrot – Van Ness (1968). From the definition, one can make the following observation - for $H = 0.5$ the covariance function of fBm reads $\frac{1}{2}(s+t-|t-s|) = \min(s,t)$ which coincides with the covariance of a standard Wiener process. Increments of the process are positively correlated for $H > 0.5$ and negatively for $H < 0.5$. This also effects regularity of the sample paths, see property *ii.* in the following summary and Figure 8:

Properties of fBm (Decreusefond – Üstünel, 1999)

i. (*Stationary increments*) An increment $W_t^H - W_s^H$, for any $t > s \geqslant 0$, is a Gaussian random variable with zero mean and variance $|t-s|^{2H}$.

ii. (*Hölder continuity*) Sample paths of fBm are almost surely Hölder continuous of order $H-\epsilon$ for $\epsilon > 0$.

iii. (*Self-similarity*) The random variables $\alpha^{-H}W_{\alpha t}^H$ and W_t^H have the same distribution for any $\alpha > 0$ and $t > 0$.

iv. (*Long-range dependence*) For $H > 0.5$ a sequence of increments $(X_n)_{n=1}^{+\infty} := \left(W_n^H - W_{n-1}^H\right)_{n=1}^{+\infty}$ posses a long-range dependence, i.e. the sum of auto-covariances $\sum_{k=1}^{+\infty}\mathrm{Cov}(X_m, X_{m+k})$ for any $m \in \mathbb{N}$ diverges.

Comte – Renault (1998) pioneered the use of a fractional Brownian motion in SV models. The proposed model dynamics is a modification of the original Hull-White approach and authors assume $H > 0.5$, alongside the model dynamics:

$$d(\ln S_t) = \sigma_t\,dW_t, \tag{23}$$
$$d(\ln \sigma_t) = \kappa \ln \sigma_t + \gamma\,dW_t^H. \tag{24}$$
$$\tag{25}$$

W_t^H defined by

$$W_t^H = \int_0^t \frac{(t-s)^{H-1/2}}{\Gamma(H+1/2)}\,dW_s^\star. \tag{26}$$

which is sometimes known as the Riemann–Liouville fractional Brownian motion, because it posses similar properties to the previously discussed fBm. Standard Wiener processes $(W_t, W_t^\star)_{t\geqslant 0}$ are,

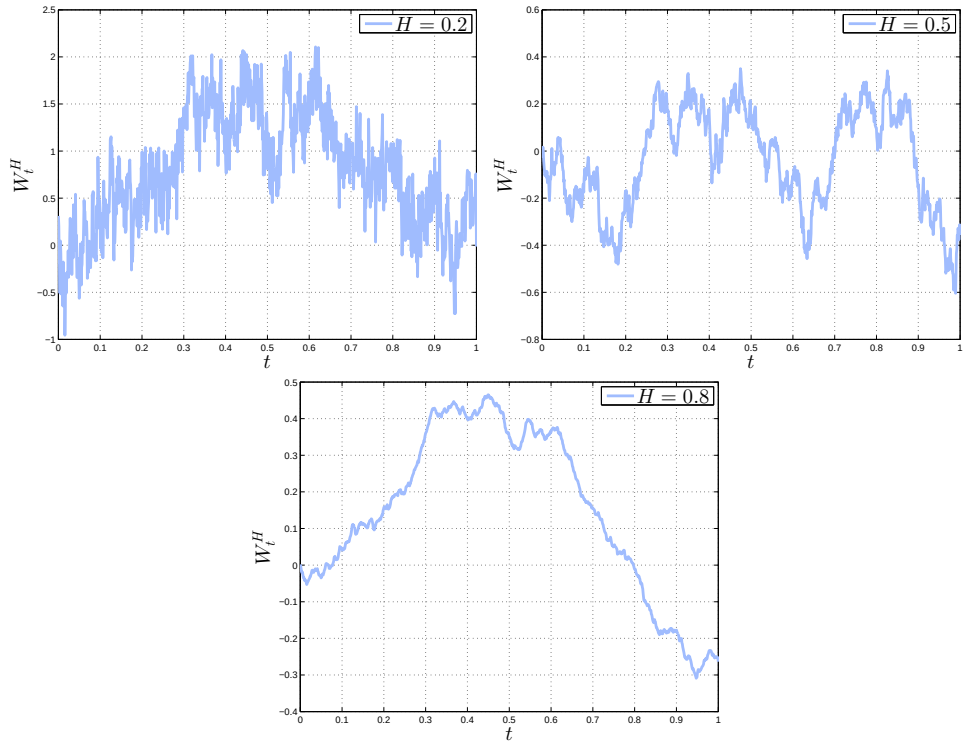

Figure 8: Sample paths of fBm for $H = 0.2$, $H = 0.5$ and $H = 0.8$

similarly to other models, instantaneously correlated with coefficient ρ, $\Gamma(x)$ denotes a gamma function of x and both $\kappa > 0$, γ are parameters of the model. The authors have recently proposed an affine fractional model with the following dynamics (Comte et al., 2012):

$$dS_t = rS_t\,dt + \sqrt{v_t}S_t\,dW_t^{(1)}, \tag{27}$$

$$dX_t = -\kappa(X_t - \theta_1)\,dt + \gamma X_t\,dW_t^{(2)}, \tag{28}$$

$$v_t = \theta_2 + X_t^H. \tag{29}$$

where κ, θ_1, θ_2, σ, ρ are model parameters and X_t^H can be formally expressed using the following relation,

$$X_t^H = \int_{-\infty}^{t} \frac{(t-s)^{H-1/2}}{\Gamma(H+1/2)} X_s\,ds. \tag{30}$$

For definition of the integral (30) see Comte et al. (2012). The model is, in fact, a fractional extension to the Heston model and the authors have proposed a simulation scheme for the stock price process S_t. Gatheral et al. (2018) have shown that the model for $H > 0.5$ is inconsistent with the considered realized variance data and Fukasawa (2011) noted that in case of $H > 0.5$ the corresponding ATM skew $\psi(\tau)$ is an increasing function of time to maturity (see Figure 6 for the DAX market ATM skew). A similar version of the model, only assuming $H < 0.5$ was introduced alongside a numerical pricing formula based on characteristic function in El Euch – Rosenbaum (2019). Many other articles considering this extension of the original model have appeared since, e.g. El Euch et al. (2018); Forde et al. (2019).

Bayer et al. (2016) introduced a *rough* Bergomi (rBergomi) model (assuming $H < 0.5$) which was motivated by findings in the highly cited preprint by Gatheral et al. (2014), that was published almost four years later as Gatheral et al. (2018).

$$dS_t = rS_t\,dt + \sqrt{v_t}S_t\,dW_t, \tag{31}$$

$$v_t = \xi_0(t)\exp\left\{\eta\widehat{W}_t^H - \frac{1}{2}\eta^2 r(t)\right\}, \tag{32}$$

where $\widehat{W}_t^H$ is defined similarly to the Riemann–Liouville fBm and up to a constant factor its covariance structure coincides with the fBm. As in case of the original Bergomi model, $\xi_u(t)$ denotes the forward variance curve and $r(t)$ is the variance of $\widehat{W}_t^H$. This model alongside correct parameter values satisfies most of stylized facts introduces in Chapter 1, but until recently only a cumbersome simulation techniques were available to obtain option prices under the model.

In Merino – Pospíšil – Sobotka – Sottinen – Vives (2019) we have introduced an approximative option pricing solution for αRFSV model. We also illustrated, that the approximation works well for short times to maturity and is more efficient than Monte-Carlo simulation techniques. Under the model, the following dynamics of the asset price process and its variance process are assumed:

$$dS_t = rS_t\,dt + \sqrt{v_t}S_t\,dW_t, \tag{33}$$

$$v_t = v_0 \exp\left\{\xi B_t - \frac{1}{2}\alpha\xi^2 r(t)\right\}, \quad t \geqslant 0, \tag{34}$$

where model parameters are later discussed in more details in Chapter 4 and the driving noise is assumed to be a Gaussian Volterra process:

$$B_t = \int_0^t K(t,s)\,dW_s^{(2)}, \tag{35}$$

with the kernel function $K(t,s,)$ such that $\int_0^t K(t,s)\,ds < \infty$ and $\mathcal{F}_t^B = \mathcal{F}_t^{W^{(2)}}$ for every $t > 0$. Examples of Volterra process considered in Merino – Pospíšil – Sobotka – Sottinen – Vives (2019) are standard fractional Brownian motion or, as previously, processes with a similar covariance structure as fBm.

Many other research articles appeared recently, tackling various issues inspired by the rBergomi model and rough volatility models alike, e.g. pricing of target volatility options under a similar model was discussed by Alòs et al. (2019),and calibration of rough models using machine learning methods Horvath et al. (2019).

3

OPTION PRICING AND MODEL CALIBRATION

In this section we formulate the task of model calibration as an optimization problem. This task should answer the question what are the parameter values for which the assumed model describes the market prices of derivatives *in the best way*. As noted by Jacquier – Jarrow (2000), choosing an appropriate formulation of the problem alongside a suitable optimization method is nearly as important as choosing the model itself.

First of all, we describe suitable pricing frameworks for SV models and we focus on a method which is obtained by using hedging arguments.

3.1 OPTION PRICING

A model option price is denoted by a function that maps from the space of specific model parameters Θ to a non-negative real number. This mapping also involves parameters of two kind - firstly a strike K and a time to maturity τ both of which define the call option contract being priced. The second kind corresponds to the observed values at the considered market, in our case it would involve a current price of the asset $s \in \mathbb{R}^+$ and a value of the risk-free rate $r \in \mathbb{R}^+$ [1]. Then the ultimate goal is to find a mapping that assigns to a given parameters $\eta \in \Theta$ and to contractual parameters a fair value of the contract as implied by the model.

If we assume that the asset price follows a stochastic process[2] $(S_t^\eta)_{t_0 \leqslant t \leqslant T}$ alongside $S_{t_0} = s$ almost surely and that a filtration $(\mathcal{F}_t)_{t_0 \leqslant t \leqslant T}$ is generated by the assumed process (as mentioned at the beginning of Chapter 2) - then we are able to express the pricing function by

$$\widehat{FV}(\eta; K, \tau) = \mathbb{E}^Q \left[e^{-r\tau} f(S_T) \middle| \mathcal{F}_{t_0} \right], \tag{36}$$

or specifically,

$$\widehat{FV}_{call}(\eta; K, \tau) = \mathbb{E}^Q \left[e^{-r\tau} \left(S_T^\eta - K \right)^+ \middle| \mathcal{F}_{t_0} \right], \tag{37}$$

for a call option with pay-off function f and maturity $T := t_0 + \tau$. Assertion (37) has a natural interpretation - the right hand side represents the present value of the expected discounted pay-off under Q, hence the name fair value of the option[3]. As mentioned by Chin – Dufresne (2012), typically the distribution of the risky asset is either unknown or is too complicated to directly evaluate right-hand side of (37) as an integral with respect to the conditional distribution of S_T^η. To find the relation between model parameters and the model option price, various authors propose methods mainly of three types:

i) By hedging and no-arbitrage arguments one obtains a partial differential equation (PDE) for the fair value time-evolution. Solving the PDE with respect to appropriate boundary conditions for market parameters S_{t_0}, τ gives us the fair value at initial time t_0.

ii) A known pricing relation of a simpler model (typically the Black-Scholes model) is perturbed in a specific way to obtain a computational form of (37). The perturbed price (or implied volatility) is usually expressed by a function series and, in practise, one uses only the first $k \in \mathcal{N}$ terms to approximate the price.

iii) An estimate of the fair price can be also obtained via a Monte Carlo simulation framework, i.e. by simulating sample paths of $(S_t)_{t \geqslant 0}$ up to time T and averaging out the option pay-offs for different realizations. By this we essentially estimate the Q-density of the option pay-off.

More thoroughly we inspect only the first method with respect to standard SV models. To show how the pricing PDE is obtained we assume the following dynamics of the asset price process $(S_t)_{t \geqslant 0}$,

$$\begin{aligned} dS_t &= rS_t dt + \sqrt{v_t} S_t dW_t, & (38) \\ dv_t &= p(v_t)dt + q(v_t)dW_t^\star, & (39) \\ \mathbb{E}\left[dW_t dW_t^\star\right] &= \rho dt, & (40) \end{aligned}$$

1 For simplicity neglecting risk-free curve term structure and stochasticity of rates.

2 Depending on a specific model, we choose the process $(S_t^\eta)_{t_0 \leqslant t \leqslant T}$ where superscript η is used to stress out the dependence on model parameters.

3 Ideally, with a fair buying price of the contract one would not earn nor loose any money on the contract in average, see Wilmott (2007).

where $p, q \in C^\infty(0,\infty)$ are general coefficient functions of the variance process as in Baustian – Mrázek – Pospíšil – Sobotka (2017), $\rho \in [-1,1]$ is the correlation of the two Wiener processes and $r \in \mathbb{R}^+$ denotes the positive risk-free rate. Differentials dW_t, $dW_t^\star$ are, similarly to the standard SV models in Chapter 2, understood in the Itô sense. For dynamics of the aforementioned structure we are able to set up a PDE for the option fair value.

Proposition 1. *Let the risky asset price follow (38) - (40) and let the standard assumptions (A1) listed in Chapter 2 be valid. Then the fair value of a European call option with strike* K *and maturity* T *as a function* $F = F(S,v,t)$ *of variables* $S_t = S$, $v_t = v$ *and time* t *satisfies*

$$\begin{aligned} -\frac{\partial F}{\partial t} = &-rF + rS\frac{\partial F}{\partial S} + \frac{1}{2}vS^2\frac{\partial^2 F}{\partial S^2} + p(v)\frac{\partial F}{\partial v} + \frac{1}{2}q^2(v)\frac{\partial^2 F}{\partial v^2} \\ &+ \rho q(v) S\sqrt{v}\frac{\partial^2 F}{\partial S \partial v} \end{aligned} \tag{41}$$

for $S, v \in (0,+\infty)$ *and* $t \in [0,T]$ *alongside the terminal condition,*

$$F(S,v,T) = (S-K)^+. \tag{42}$$

Proof. We utilize arguments of Gatheral (2006) and Wilmott (2007). Before arbitrage arguments can be applied, we need to set up a portfolio that is *hedged* for $t = [t_0, T]$ which means that the portfolio value Π_t is immune to the changes in the underlying price S_t and its variance v_t, i.e. $\frac{\partial \Pi}{\partial S}\Big|_t = \frac{\partial \Pi}{\partial v}\Big|_t = 0$ for any $t = [t_0, T]$. This can be done by setting up a portfolio with one call option on the underlying, $(-\Delta^*)$ call options on instantaneous volatility and it would also involve $(-\Delta)$ shares of the risky asset. The numbers Δ, Δ^* are about to be exploited after the following step[4]. Let $S = S_t$ be the price of the risky asset, $F = F(S,v,t)$, $F^* = F^*(S,v,t)$ be the value of an option on the asset and on the instantaneous volatility respectively. After loosing time indices, $\Pi = \Pi_t$ is defined by

$$\Pi = F - \Delta S - \Delta^* F^*.$$

The portfolio is self-financing, i.e. we cannot add nor withdraw funds and hence, assuming continuous-time trading, a change in the portfolio value can be expressed as

$$\begin{aligned} d\Pi &= dF - \Delta dS - \Delta^* dF^* \qquad (43) \\ &= \left[\frac{\partial F}{\partial t} + \frac{1}{2}vS^2\frac{\partial^2 F}{\partial S^2} + \frac{1}{2}q^2(v)\frac{\partial^2 F}{\partial v^2} + \rho\sqrt{v}q(v)S\frac{\partial^2 F}{\partial v \partial S}\right] dt \\ &- \left[\frac{\partial F^*}{\partial t} + \frac{1}{2}vS^2\frac{\partial^2 F^*}{\partial S^2} + \frac{1}{2}q^2(v)\frac{\partial^2 F^*}{\partial v^2} + \rho\sqrt{v}q(v)S\frac{\partial^2 F^*}{\partial v \partial S}\right]\Delta^* dt \\ &+ \left[\frac{\partial F}{\partial S} - \Delta^*\frac{\partial F^*}{\partial S} - \Delta\right] dS + \left[\frac{\partial F}{\partial v} - \Delta^*\frac{\partial F^*}{\partial v}\right] dv, \qquad (44) \end{aligned}$$

where differentials dF and dF^* were obtained using the Itô lemma (Maslowski, 2006, Theorem 4.17, 32 p.) and the assumed market dynamics (38)-(40). In order to hedge the portfolio we need to choose

$$\Delta = \frac{\partial F}{\partial S} - \frac{\partial F/\partial v}{\partial F^*/\partial v}\frac{\partial F^*}{\partial S} \text{ and } \Delta^* = \frac{\partial F/\partial v}{\partial F^*/\partial v}, \tag{45}$$

which cancels out dv and dS terms[5] in (44). In fact, we have build up a hedged portfolio that represents a risk-free investment and due to the uniquely defined yield of those investments it follows that

$$\begin{aligned} d\Pi &= r\Pi dt \\ &= r\left(F - \Delta S - \Delta^* F^*\right) dt. \end{aligned} \tag{46}$$

Combining (44), (45) and (46) we obtain

$$\begin{aligned} &\frac{\frac{\partial F}{\partial t} + \frac{1}{2}vS^2\frac{\partial^2 F}{\partial S^2} + \frac{1}{2}q^2(v)\frac{\partial^2 F}{\partial v^2} + \rho\sqrt{v}q(v)S\frac{\partial^2 F}{\partial v \partial S} + rS\frac{\partial F}{\partial S} - rF}{\frac{\partial F}{\partial v}} = \\ &\frac{\frac{\partial F^*}{\partial t} + \frac{1}{2}vS^2\frac{\partial^2 F^*}{\partial S^2} + \frac{1}{2}q^2(v)\frac{\partial^2 F^*}{\partial v^2} + \rho\sqrt{v}q(v)S\frac{\partial^2 F^*}{\partial v \partial S} + rS\frac{\partial F^*}{\partial S} - rF^*}{\frac{\partial F^*}{\partial v}}. \end{aligned} \tag{47}$$

4 Buying a negative amount $-\Delta$ corresponds to the short selling technique mentioned in Chapter 2.

5 We briefly remark that since $F^*(S,v,t)$ assigns the value of an option on volatility v, $\partial F^*/\partial v \neq 0$ and therefore Δ, Δ^* are well defined.

We are interested in F rather than F^* and thus we utilize an argument of (Gatheral, 2006, p. 7), that under risk-neutral dynamics each side of (47) must be equal to the drift of dv_t with a negative sign, which leads to

$$\frac{\partial F}{\partial t} + \frac{1}{2}vS^2\frac{\partial^2 F}{\partial S^2} + \frac{1}{2}q^2(v)\frac{\partial^2 F}{\partial v^2} + \rho\sqrt{v}q(v)S\frac{\partial^2 F}{\partial v \partial S} + rS\frac{\partial F}{\partial S} - rF = -p(v)\frac{\partial F}{\partial v}.$$

By rearranging terms we retrieve (41) and the terminal condition follows from the pay-off of a call option that takes place at the maturity T. □

Remark 1. *The classical solution ($F \in C^2$) of the PDE (41) at S_{t_0}, v_{t_0} and t_0 is the model assumed fair value (37). The solution is usually obtained by integral transform methods, e.g. Heston (1993) used the Fourier transform, and its evaluation typically involves numerical computation of inverse transformation integrals.*

Remark 2. *In a similar way one can set up a partial integro-differential equation for SV models with jumps in the assumed dynamics. This was shown for the first time by Bates (1996). For models with fBm, which is not semimartingale for $H \neq 0.5$, one cannot use a standard Itô lemma to derive the pricing PDE (41). So called approximative fractional SV models in Pospíšil – Sobotka (2016) and Mrázek – Pospíšil – Sobotka (2016) utilize a semimartingale approximation of fBm that was introduced by Zähle (1998) and Intarasit – Sattayatham (2011). In Pospíšil – Sobotka (2016) and Mrázek – Pospíšil – Sobotka (2016) authors show how to obtain corresponding PDE for a call option price and they show how to solve the equation with one linearised term by the Fourier and generalized complex Fourier transformation respectively. The former solution is computationally more efficient which was shown in Baustian – Mrázek – Pospíšil – Sobotka (2017).*

The pricing solution obtained by perturbation techniques was derived for the first popular SV model by Hull – White (1987). Lately this approach has become more popular and has been applied for the Bergomi and SABR models (Hagan et al., 2002; Osajima, 2007; Bergomi, 2008). Recently, several theoretical papers on asymptotic expansions of (37) with respect to fractional SV models have appeared, for instance Fukasawa (2011) who uses Yoshida's martingale expansion theory (Yoshida, 1997). The option pricing task for fractional SV models has been performed by Monte-Carlo simulation schemes only and finding a more efficient relation for the option price is a matter of an ongoing research. This fact is also mentioned by Gatheral et al. (2014) and due to the inefficiency of simulation approach, Bayer et al. (2016) were not able to use any calibration procedure to fit market option prices.

3.2 CALIBRATION TO OPTION MARKETS

Before any SV model can be used in practise, one needs to calibrate the model from market data. The model calibration task is, in fact, an inverse problem to the option pricing. During the calibration one would like to find a parameter set from Θ such that the conditional expectation (37) corresponds to observed option prices on derivative markets. A standard way to proceed with the calibration is via optimization formulation of the problem. Let $FV_1, ..., FV_N$ be prices of traded call options on the underlying priced $S_{t_0} \in \mathbb{R}^+$. For each call option we know a pair (K_i, τ_i) that represents a strike price and a time to maturity of the i-th option respectively. Corresponding to each pair (K_i, τ_i), to observed properties of markets S_{t_0}, r and to parameters η we have a model price $\widehat{FV}(\eta; K_i, \tau_i)$. Let also $m \geqslant 1$ and $w_1, ..., w_N$ be a set of weights, i.e. $\forall i = 1, ..., N : w_i > 0$, and $\sum_{i=1}^N w_i = 1$. Then the standard procedure (see e.g. Mikhailov – Nögel (2003) or Mrázek – Pospíšil – Sobotka (2016)) to obtain calibrated parameters $\eta \in \Theta$ is to minimize the following criterion,

$$\arg \inf_{\eta \in \Theta} G(\eta), \tag{48}$$

$$G(\eta) = \sum_{i=1}^{N} w_i \left(FV_i - \widehat{FV}(\eta; K_i, \tau_i)\right)^m, \tag{49}$$

where m is usually set up to 2. In that case, (49) is a weighted least square criterion. The optimization problem is typically non-convex and one needs to use a suitable optimization procedure, see Mrázek – Pospíšil – Sobotka (2016). As was shown by the authors, several SV models might also attain many local minima in their utility function (49).

Local optimizers suitable for solving the least-square minimization problem are usually based on the Newton or Levenberg–Marquardt methods described e.g. in Kienitz – Wetterau (2012). These methods and several modifications thereof, have to be initialized be providing an initial starting guess $\hat{\eta} \in \Theta$ that is preferably in the vicinity of the global minima. In that case, one also might modify the criterion (49) by adding a penalizing function, i.e. an increasing function of a distance between the initial guess and η. The local methods are time-efficient, however, one might not have such $\hat{\eta}$ at his/her disposal.

Global optimizing methods are not very sensitive to the initial guess $\hat{\eta}$ and in theory they should converge to a global minimum of (49). The global optimizing techniques are usually inspired by several natural phenomena, including genetic evolution, annealing of a metal and a swarm behaviour to name a few. Description of the methods with respect to the nonlinear least-square criterion is available in Kienitz – Wetterau (2012) and several results alongside comments on the implementation are discussed in Mrázek – Pospíšil – Sobotka (2016). These methods are computationally very expensive and in practise one has to impose a stopping criteria that terminates a specific algorithm before a global minimum is reached.

Another possibility that was inspected in Mrázek – Pospíšil – Sobotka (2014) and more thoroughly in Mrázek – Pospíšil – Sobotka (2016) is to use a global optimization technique to obtain an initial guess for a local optimizer. This two-step calibration procedure proved to be a superior optimization strategy in terms of (49) (Mrázek – Pospíšil – Sobotka, 2016), especially for more complex models with jump-diffusion dynamics.

Having a specific model in mind, several authors proposed specialized schemes where the criterion differs from (49). For instance, in case of the Heston model Alòs et al. (2015) introduced a new scheme based on properties of an approximation pricing function derived in Alòs (2012). This scheme, however, might not work for complex derivative markets that involve many mid-dated options with times to maturity $0.1 < \tau_i < 3$ - these options are not directly considered in the calibration procedure. Other schemes that differ from (49) are used for specific markets only and therefore we do not include them into our review.

Another procedure how to identify the market parameters is via Maximum likelihood estimates (MLE). The methods are based on finding maximum of the corresponding likelihood function on Θ to obtain model parameters for which the observed prices of the risky assets have the greatest probability of occurring. These methods has been applied to the task of SV model calibration e.g. by Fatone et al. (2014); Hurn et al. (2015). However, using a time-series data of the risky asset implies problems of two types. Firstly, the realized variance is not directly observable and secondly only approximations of the maximum likelihood function are available even for simpler models (e.g. for the Heston model case see Atiya – Wall (2009)). To deal with the former problem, Hurn et al. (2015) suggested using both time-series and historical option price data and the authors proposed a calibration scheme for the Heston model. Generally, MLE methods are not as convenient for option pricing - one usually deals with two probability measures P and Q. We are not going to describe MLE methods in more detail, but when using MLE one has to keep in mind that the time-series estimates might differ from the ones obtained by solving (48) which was well documented by Bakshi et al. (1997).

3.3 CONNECTION BETWEEN OPTION MARKETS AND VARIANCE SWAPS

In this section we introduce a connection between the variance swaps and option markets by utilizing replication and hedging arguments. We start with a quantity commonly referred to as the fair variance.

Fair Variance

The strike of a variance swap contract is determined (or agreed on) at its inception. On the other hand, the floating leg will be determined no sooner than at the maturity. The fair variance at any time t between the inception and maturity is a quantity that will effectively cancel out the conditional expectation[6] of the variance swap payoff – on average neither buyer nor seller is expected to make any profits. Formally, we can define the fair variance as follows.

Definition 3 (Fair variance)**.** Let σ_t^2 be instantaneous volatility of the assumed stock evolution process $(S_\cdot)$ at a reference time instance $t \geqslant 0$ and let $T > t$ be any end point time reference[7]. The fair variance of a variance swap contract starting t, expiring at T is then defined under a market given risk-neutral measure $\mathbb{Q}$ and corresponding filtration $\mathcal{F}_t$ as

$$FS := FS(t,T) = \mathbb{E}^{\mathbb{Q}}\left[\frac{1}{T-t}\int_t^T \sigma_s^2 ds \,\middle|\, \mathcal{F}_t\right] = \mathbb{E}^{\mathbb{Q}}\left[\sigma_R^2(t,T)|\mathcal{F}_t\right] \tag{50}$$

Hence, the fair variance can be interpreted as a strike of a variance swap contract such that the contract fair value equals to zero at time t under $\mathcal{F}_t$. Following the quantitative finance jargon, we will introduce a variance swap curve as observed at time t as a mapping $\xi_t(x) : \mathbb{R}^+ \mapsto \mathbb{R}^+$ where

$$\xi_t(T) := FS(t,T). \tag{51}$$

In what follows we will denote $\xi_t(T)$ if market observed quantity is meant and $FS(t,T)$ if the same quantity is calculated.

Replication arguments of Carr – Madan (1998)

The replication technique firstly introduced by Carr – Madan (1998) is the market standard approach to price vanilla variance swaps and it is also used for quoting volatility indices such as VIX[8]. The main advantages of their approach are listed below:

a) Only a static hedge of vanilla options is used (i.e. no dynamic hedging).

b) It does not need to specify the volatility process of the underlying.

Property a) is considered to be important for practitioners, wheras property b) will be of an essential importance for us – it enables us to use option market implied variance swap prices to be used for calibration of rough volatility models. However, rough volatility models are typically not consistent with the Carr-Madan approach – we will devote a separate paragraph to justify why well calibrated rough volatility models should be fairly in-line with Carr-Madan variance swap fair values. Also there are several ways how one can derive Carr – Madan (1998) replication formula – we will start by postulating local volatility assumptions which are key to this approach.

In particular we posit that asset evolves according to the following Itô SDE:

$$dS_t^l = \mu S_t^l dt + \sigma(t, S_t^l) S_t^l dW_t \tag{52}$$

$$S_0^l = S_0 \in R^+ \tag{53}$$

where we assume that (W_t) is a standard Wiener process under a market given risk neutral measure $\mathbb{Q}$ and furthermore:

- **(A1)**: μ – is a constant drift which represent risk-free interest yield, subtracts any yield dividend and borrow costs.

6 Conditioned on $\mathcal{F}_t$ under a market implied risk-neutral measure

7 Typically called fair variance tenor, i.e. maturity of an associated Variance swap contract

8 See http://www.cboe.com/vix for more details on VIX.

- **(A2)**: $\sigma(t, S_t^l)$ – is a Dupire local volatility function – a deterministic function (non-parametric) of the time t and spot price, such that the Fair Values of all observable European options at $t = 0$ on the modelled asset with underlying price S_0 are matched by the model. For all observed call options with time to maturities (τ) and strikes (K) holds:

$$FV^{\text{market}}(\tau_i, K_i) = DF(\tau)\mathbb{E}^Q[\max(S^l_{\tau_i} - K_i; 0)|\mathcal{F}_0] \tag{54}$$

  and similarly for observed put options.

- **(A3)**: Since (52) is a pure Itô diffusion process, there are no jumps assumed. In practise, jump-like evolution of the asset price might be observed due to:

  a) Cash dividends paid by the stock, corporate actions (mergers, stock splits) etc.
  b) Idiosyncratic reasons – i.e. caused by a sudden change in market expectations.

The postulate[9] **(A1)** tells us that we neglect dynamics of the yield curve, but also we neglect the current term structure of the yield curve. The second part of the postulate is introduced here only to simplify the notation. In practise, the term structure will be considered where typically, the yield-curve dynamics (i.e. stochastic rates model) is not used to model stock prices.

To specify (52) in more detail – we use Dupire original idea (Dupire, 1994): there exists a unique diffusion process which is in-line with risk neutral densities derived from market traded European options. This is given by **(A2)**.

The last postulate **(A3)** will in practise introduce errors any time:

a) market knows that there is a scheduled corporate action or cash dividend event – they are included in observed option fair values, but we would incorrectly re-adjust local volatility function σ to match the fair values;

b) market has indication that our underlying asset prices might include idiosyncratic jumps[10].

In the following section we will show how these postulates alongside standard market assumptions translate into variance swap replication formula.

Log-contract and a strip of vanilla options

Proposition 2 (Fair variance under assumptions **(A1)-(A3)**). *Let the underlying asset price process follows diffusion* (52) *(incl. assumptions **(A1)-(A3)**). Then the continuously aggregated fair variance can be expressed in terms of the fair value of a log-contract as*

$$FS(t,T) = \frac{2}{T-t}\left\{\mu(T-t) - \mathbb{E}^Q\left[\ln\left(\frac{S_T^l}{S_t^l}\right)\middle|\mathcal{F}_t\right]\right\}. \tag{55}$$

Proof. Assuming (52), we can obtain the relation for $d\ln(S_t^l)$ using Itô lemma,

$$d\ln S_t^l = \left(\mu - \frac{\sigma^2(t, S_t^l)}{2}\right)dt + \sigma^2(t, S_t^l)\, dW_t. \tag{56}$$

Subtracting (56) from (52) leads to the continuous increments aggregating to the realized variance of S_t^l,

$$\frac{dS_t^l}{S_t^l} - d\ln(S_t^l) = \frac{\sigma^2(t, S_t^l)}{2}\, dt, \tag{57}$$

which can be integrated e.g. on interval $(0, T); T > 0$, without any loss of generality.

$$\frac{1}{T}\int_0^T \sigma^2(t, S_t^l)dt = \frac{2}{T}\left(\int_0^T \frac{dS_t^l}{S_t^l} - \ln\left(\frac{S_T^l}{S_0^l}\right)\right) \tag{58}$$

9 Here we understand a postulate as an assumption which is taken to be true without being verified. Indeed, some of (A1)-(A3) do not hold, but the impact of these assumptions is typically neglected, unless it is material.

10 I.e. crash cliquet prices or other jump-sensitive derivatives are marked to higher levels for this asset.

To get the stated expression for the fair variance, we need to apply conditional expectation operator and algebraic operations.

$$\begin{aligned}
FS(0,T) &= \frac{2}{T}\mathbb{E}^Q\left[\int_0^T \frac{dS_t^l}{S_t^l} - \ln\left(\frac{S_T^l}{S_0^l}\right)\middle|\mathcal{F}_t\right] \\
&= \frac{2}{T}\left(\mathbb{E}^Q\left[\int_0^T \frac{dS_t^l}{S_t^l}\middle|\mathcal{F}_t\right] - \mathbb{E}^Q\left[\ln\left(\frac{S_T^l}{S_0^l}\right)\middle|\mathcal{F}_t\right]\right) \\
&= \frac{2}{T}\left(\mu T - \mathbb{E}^Q\left[\ln\left(\frac{S_T^l}{S_0^l}\right)\middle|\mathcal{F}_t\right]\right).
\end{aligned}$$

□

Remark 3. *The previous statement indicates that the variance swap can be replicated by a log-contract with fair values,* $\mathbb{E}^Q\left[\ln\left(\frac{S_T^l}{S_0^l}\right)\middle|\mathcal{F}_t\right]$*, which depends only on the terminal distribution of the underlying asset at time* T*.*

In fact, we switched from computing the fair variance to finding a fair value of the log contract paying $\ln(S_T^l/S_t^l)$. However, since these contracts are typically not exchange traded, we will use the following lemma to express log contracts in terms of vanilla options.

Lemma 1. *Let* $f : \mathbb{R}^+ \to \mathbb{R}$ *be a twice differentiable function and let* $S^* > 0$ *be a known constant. Then*

$$f(x) = f(S^*) + f'(S^*)(x - S^*) + \int_0^{S^*} f''(K)(K - x)\,dK + \int_{S^*}^{+\infty} f''(K)(K - x)\,dK \tag{59}$$

Proof. The above statement can be proved using a Dirac's delta function, $\delta()$, to represent $f(x)$,

$$f(x) = \int_0^{S^*} f(K)\delta(x - K)\,dK + \int_{S^*}^{+\infty} f(K)\delta(x - K)\,dK,$$

for any $S^* > 0$, and applying consecutive integration by parts of the integrals above (until we reach the statement). □

Theorem 1 (Carr – Madan (1998))**.** *Under market dynamics* (52) *and assumptions* ***A1-A3****, the valuation of a continuous fair variance,* $FS(t,T)$*, is down to a semi-closed form expression for* $0 \leqslant t < T$*:*

$$\begin{aligned}
FS(t,T) = \frac{2}{\tau}\Bigg[&\mu\tau - \left(\frac{S_t^l}{S^*}e^{\mu\tau} - 1\right) - \ln\frac{S^*}{S_t^l} + e^{-\mu\tau}\int_0^{S^*}\frac{1}{K^2}FV_{put}(\tau,K)dK \\
&+ e^{-\mu\tau}\int_{S^*}^{+\infty}\frac{1}{K^2}FV_{call}(\tau,K)dK\Bigg],
\end{aligned} \tag{60}$$

where S^* *is a positive constant - in practise typically set to the value of the forward with maturity* T*,* $\tau = T - t$ *is the time to maturity and* $FV_{call\,/\,put}$ *is the fair value of a call / put option with time to maturity* τ *and strike* K *implied from the market (and also consistent with dynamics* (52)*).*

Proof. Firstly, we apply technical Lemma 1 on $f(x) = \ln(x)$ for $x = S_T^l$, to obtain:

$$\ln S_T^l - \ln S^* = \frac{S_T^l}{S^*} - 1 - \int_0^{S^*}\frac{1}{K^2}(K - S_T^l)^+dK - \int_{S^*}^{+\infty}\frac{1}{K^2}(K - S_T^l)^+dK \tag{61}$$

Then we take into consideration that the following relations hold:

- $S_t^l = e^{-\mu\tau}\mathbb{E}\left[S_T^l|\mathcal{F}_t\right]$ (by definition of (52))
- $\ln\frac{S_T^l}{S_t^l} = \ln\frac{S_T^l}{S^*} + \ln\frac{S^*}{S_t^l}$, for arbitrary positive S^*
- $FV_{put}(\tau,K) = e^{-\mu\tau}\mathbb{E}\left[(K - S_T^l)^+|\mathcal{F}_t\right], \tau = T - t$
- $FV_{call}(\tau,K) = e^{-\mu\tau}\mathbb{E}\left[(S_T^l - K)^+|\mathcal{F}_t\right], \tau = T - t$
- $FS(t,T) = \frac{2}{T-t}\left\{\mu(T-t) - \mathbb{E}^Q\left[\ln\left(\frac{S_T^l}{S_t^l}\right)\middle|\mathcal{F}_t\right]\right\}$ (See Proposition 2)

Combining the above with (61) and integrability properties of $\frac{1}{K^2}FV_{put/call}(\tau, K)$, we retrieve the statement (60). □

Remark 4. *The famous replication formula in Theorem 1 transforms the problem of pricing unquoted log-contracts into pricing of liquid vanilla options. However, it is assumed that we have an infinite strip of call / put options, whereas in practise we have quotes for a finite number of options. Hence, in order to obtain the fair strike for a particular variance swap contract we need to interpolate volatility smile for corresponding maturity T. I.e. a well interpolated / extrapolated volatility surface is needed, but in practise, the issue is how to extrapolate for strikes $x < K_{min}$, where K_{min} is the smallest observed strike. This is due to the fact that the formula is not sensitive to changes of implied volatilities for $x > K_{max}$ where K_{max} is the highest traded strike on the valuation date.*

Application of Gyöngy's Theorem

Up to now, we have derived a known formula for the fair variance under standard market assumptions of local volatility. Nevertheless, local volatility dynamics do not mimic empirically observed properties of financial time-series which were discussed in Section 1. Even more importantly for this study, the local volatility assumption seems to be not in-line with stochastic volatility dynamics which will be used in the upcoming sections.

There is a known market wisdom - local volatility models can almost perfectly fit arbitrage-free volatility surfaces observed on various markets, but Greeks – fair value sensitivities to particular risk factors – of the model might be contradicting what we empirically observe.

To understand why capturing volatility surface - i.e. having marginal distribution implied from the market quotes - does not necessarily guarantee that we retrieve reasonable dynamical assumptions, we introduce Gyöngy (1986) theorem. Interpretation of the theorem will give us a link between local-volatility dynamics (52) and more complex stochastic volatility models.

Theorem 2 (Gyöngy (1986) theorem)**.** *Let (Z_t) be an m-dimensional standard Wiener process adapted to filtration $(\mathcal{F}_t)$ and*

$$dX_t = \alpha(t, \omega)\, dt + \beta(t, \omega)\, dZ_t \tag{62}$$

be an n-dimensional Itô stochastic differential equation with $n \times 1$ and $n \times m$ bounded $\mathcal{F}_t$—adapted processes α and β, respectively, and ω denotes a sample path of Z_t. Then, there exists an Itô stochastic differential equation,

$$dY_t = a(t, Y_t)\, dt + b(t, Y_t)\, dZ_t, \tag{63}$$

with measurable deterministic coefficient functions a, b, such that the marginal distributions of X_t and Y_t are the same. Moreover, the coefficient functions are given by:

$$a(t, y) = \mathbb{E}\left[\alpha(t, \omega) | X_t = y\right] \tag{64}$$

$$b(t, y) b^T(t, y) = \mathbb{E}\left[\beta(t, \omega)\beta^T(t, \omega) | X_t = y\right], \tag{65}$$

where by $b^T(t, y)$ we denote a transposition of the vector coefficient function b.

Proof. See Gyöngy (1986). □

Remark 5. *In our case, our local volatility function σ^l_t will be given by*

$$\sigma^l_t(t, y) = b(t, y)/y \tag{66}$$

assuming vanilla option fair values are given by a stochastic process X_t.

Remark 6. *This theorem, which has been recently generalized by several authors, is of great importance in our use case, because it implies that fair values of vanilla European options can be correctly repriced under local volatility set-up (52), although the actual dynamics of the underlying follows a much more complex process (possible with a stochastic drift and diffusion).*

On the other hand, if we manage to calibrate perfectly a stochastic volatility model to a particular volatility surface, we will retrieve the marginals of Dupire's local volatility approach (52).

Since we have used only vanilla European options and forwards to replicate variance swaps, we can conclude that fair variances should be correct under specific assumptions, even if a non-local volatility model drives the underlying asset evolution. Hence, many practitioners are using formula (60), although this is an approximation only[11].

11 In practice, one has only limited amount of traded contracts, hence one needs to interpolate / extrapolate implied volatilities. Moreover, the formula (60) is sensitive on implied volatilities for low strikes which are typically illiquid - they are obtained by a combination of expert judgement and jump-sensitive instrument marking.

4

VARIANCE SWAPS UNDER ROUGH VOLATILITY

In previous sections, we described how closely linked is the computing of variance swap fair values to computing particular fair variances. Thus, we limit ourselves on deriving the fair variance in this section and we base our derivation on a rough volatility model which we have introduced in Merino – Pospíšil – Sobotka – Sottinen – Vives (2019) - the αRFSV model. Moreover, knowing the fair variance under particular model, we can also derive fair values of several non-vanilla variance swaps as e.g. gamma and corridor variance swaps (using similar replication arguments).

4.1 ASSUMED ROUGH VOLATILITY MODEL

Let $(S_t, t \in [0,T])$ be a strictly positive asset price process under a market chosen risk neutral probability measure Q,

$$\frac{dS_t}{S_t} = \mu\, dt + \sigma_t \left(\rho\, dW_t + \sqrt{1-\rho^2}\, d\tilde{W}_t \right), \tag{67}$$

$$S_{t_0} \in \mathbb{R}^+,\ t > t_0, \tag{68}$$

where S_{t_0} is the current price, $\mu \geqslant 0$ is the risk-neutral drift of the modelled asset[1], W_t and $\tilde{W}_t$ are independent standard Wiener processes defined on a filtered probability space $(\Omega, \mathcal{F}, (\mathcal{F}_t)_{t\geqslant 0}, Q)$ and $\rho \in (-1,1)$ is a constant instantaneous correlation of the two Wiener processes. $\mathcal{F}_t^W$ and $\mathcal{F}_t^{\tilde{W}}$ are the filtrations generated by W_t and $\tilde{W}_t$, respectively. Then, we define $\mathcal{F}_t := \mathcal{F}_t^W \vee \mathcal{F}_t^{\tilde{W}}$.

The volatility process σ_t is a square-integrable process adapted to the filtration $\mathcal{F}_t^W$ with almost surely càdlàg trajectories which are strictly positive almost everywhere and is given explicitly by

$$\sigma_t = \sigma_{t_0} \exp\left\{ \xi Y_t - \alpha \frac{1}{2} \left[(t+\varepsilon)^{2H} - \varepsilon^{2H} \right] \right\}, \tag{69}$$

where $\xi > 0, \alpha \in [0,1], H \in (0; 0.5]$ are model parameters, $\varepsilon > 0$ is a positive constant and process Y_t is defined as a Volterra process,

$$Y_t = \sqrt{2H} \int_0^t (t-s+\varepsilon)^{H-\frac{1}{2}}\, dW_s. \tag{70}$$

We note that the same Wiener process W_t appears also in (67). In Merino – Pospíšil – Sobotka – Sottinen – Vives (2019), we analyzed a more general class of models where a square integrable volatility process was given by a class of functions of two variables - time and a state variable represented by a general Volterra process. Few examples of Volterra processes were also specified, e.g. a fractional Brownian motion represented by Volterra process with a Molchan – Golosov (1969) kernel.

In what follows, we denote two ordered sets of model parameters: $\Lambda = \{\sigma_{t_0}, \xi, H, \alpha\}$ and $\Gamma = \Lambda \cup \{\rho\}$.

Argumentation on why we use the process (70) in this thesis follows

- The process is a semi-martingale unlike a standard fractional Brownian motion (this was shown in Zähle (1998) and Sattayatham et al. (2007)). Tools as Itô lemma for semi-martingales can be used.
- It attains similar path-wise properties as the standard fractional Brownian motion and if we let $\varepsilon \longrightarrow 0$ then also variances of the two processes coincide for all t.
- Under the model (81) alongside Volterra process (70), we have derived a numerically tractable solution to price European option in Merino – Pospíšil – Sobotka – Sottinen – Vives (2019).
- The process (70) with $\varepsilon = 0$ appears in various recent articles, e.g. in McCrickerd – Pakkanen (2018).

1 Again, for simplicity assuming it is constant. However, derivations introduced in Merino – Pospíšil – Sobotka – Sottinen – Vives (2019) and here would hold only with minor adjustments in a deterministic, but non-constant setting.

Properties of Volterra process (70)

In order to have a pricing approximation for European options as derived in Merino – Pospíšil – Sobotka – Sottinen – Vives (2019), we need to compute the conditional mean and covariances of the process. Unsurprisingly, these quantities will prove to be useful for derivation of fair variances under the model.

To shorten our notation all following expectations will be under Q measure unless mentioned otherwise and we use a short-hand notation:

$$m_t(u) := \mathbb{E}[Y_u|\mathcal{F}_t], \tag{71}$$

for $0 \leqslant t < u$, where $m_t(u)$ is a conditional mean process and $r(u,s), r(u), r_t(u,s)$,

$$r(u,s) := \mathbb{E}\left[(Y_u - \mathbb{E}[Y_u])(Y_s - \mathbb{E}[Y_s])\right] = \mathbb{E}\left[Y_u Y_s\right] \tag{72}$$

$$r(u) := r(u,u) \tag{73}$$

$$r_t(u,s) := \mathbb{E}\left[(Y_u - m_t(u))\,(Y_s - m_t(s))\,|\mathcal{F}_t\right] \tag{74}$$

for $u, s \geqslant 0$, denote autocovariance, variance and conditional covariance process of (Y_t), respectively. We also define a kernel function[2]

$$K(t,s) = \sqrt{2H}(t-s+\varepsilon)^{H-\frac{1}{2}} \tag{75}$$

for $t, s, \geqslant 0$.

In the text below, we utilize a theorem which we introduced in Merino – Pospíšil – Sobotka – Sottinen – Vives (2019) to extend results of Sottinen – Viitasaari (2018).

Proposition 3 (Prediction law for process (70), based on general Theorem 4.1 in Merino – Pospíšil – Sobotka – Sottinen – Vives (2019))**.** *Let $(Y_t, t \geqslant 0)$ be the Gaussian Volterra process defined by (70). Then, the conditional process $(Y_u|\mathcal{F}_t, 0 \leqslant t \leqslant u)$ is also Gaussian with mean*

$$m_t(u) = \int_0^t K(u,s)\,dW_s = \sqrt{2H}\int_0^t (u-s+\varepsilon)^{H-\frac{1}{2}}\,dW_s, \tag{76}$$

and deterministic covariance function

$$r_t(u_1,u_2) = r(u_1,u_2) - \int_0^t K(u_1,s)K(u_2,s)ds \tag{77}$$

for $u, u_1, u_2 \geqslant t$. Variance function of the conditional process is expressed as

$$r_t(u) = (u-t+\varepsilon)^{2H} - \varepsilon^{2H} \tag{78}$$

Proof. Since for $t \in \mathbb{R}^+$,

$$\int_0^t K^2(t,s)\,ds < \infty, \tag{79}$$

holds and since the process Y_t is adapted to the filtration of the Wiener process in (70), $\mathcal{F}_t^W$, the proof for the statements of (76) follows directly from Theorem 4.1. and Example 4.11 in Merino – Pospíšil – Sobotka – Sottinen – Vives (2019). The variance function is then retrieve using calculations,

$$\begin{aligned} r_t(u) &= r(u) - \int_0^t K^2(u,s)\,ds \\ &= (u+\varepsilon)^{2H} - \varepsilon^{2H} - 2H\int_0^t (u-s+\varepsilon)^{2H-1}\,ds \\ &= (u+\varepsilon)^{2H} - \varepsilon^{2H} + (u-t+\varepsilon)^{2H} - (u+\varepsilon)^{2H} \\ &= (u-t+\varepsilon)^{2H} - \varepsilon^{2H}. \end{aligned}$$

□

2 This corresponds to the Volterra kernel function of (70)

4.2 FAIR VARIANCE FORMULA

Using the set-up introduced in the previous section, we would like to find a parametric expression which is tractable (not necessary analytic) for the fair variance (50) with respect to the market dynamics given by (67)-(70). As previously, instead of discrete fair variance, we use its continuous version

$$FS(t_0, T) = \mathbb{E}\left[\frac{1}{T-t_0}\int_{t_0}^{T}\sigma_u^2\,du\,\middle|\,\mathcal{F}_{t_0}\right]. \tag{80}$$

where, T denotes time to maturity of the variance swap. Using the continuously aggregated variance helps us to express the fair variance under specified market model dynamics which is also assumed to be continuous.

We note that the variance process of the αRFSV model is given by:

$$\sigma_u^2 = \sigma_{t_0}^2 \exp\left\{2\xi B_u - \alpha\xi^2 r(u)\right\}. \tag{81}$$

Theorem 3 (Fair variance under αRFSV model)**.** *Under assumptions of αRFSV model on asset dynamics* (67)-(70) *alongside Volterra kernel function* $K(t,s)$ *defined in* (70)*, we obtain the following fair variance:*

$$FS^{\alpha RFSV}(t_0, T) = \frac{1}{T-t_0}\int_{t_0}^{T}\mathbb{E}\left[\sigma_u^2|\mathcal{F}_{t_0}\right]du \tag{82}$$

where the conditional expectation of σ_u^2 *can be expressed by*

$$\mathbb{E}[\sigma_u^2|\mathcal{F}_{t_0}] = \sigma_0^2 \exp\left\{-\alpha\xi^2 r(u) + 2\xi m_{t_0}(u) + 2\xi^2 r_{t_0}(u)\right\}. \tag{83}$$

Proof. To lighten the notation, we also use here $\mathbb{E}_{t_0}[\cdot] = \mathbb{E}[\cdot|\mathcal{F}_{t_0}]$. Starting from the variance process (81) for $0 \leqslant t_0 < u$ we retrieve:

$$\mathbb{E}_{t_0}[\sigma_u^2] = \mathbb{E}_{t_0}\left[\sigma_0^2 \exp\left\{2\xi B_u - \alpha\xi^2 r(u)\right\}\right] \tag{84}$$

$$= \sigma_0^2 \exp\left\{-\alpha\xi^2 r(u)\right\}\mathbb{E}_{t_0}\left[\exp\{2\xi B_u\}\right] \tag{85}$$

Using the explicit expression for σ_{t_0} we further obtain,

$$\mathbb{E}_{t_0}[\sigma_u^2] = \sigma_{t_0}^2 \exp\left\{-\alpha\xi^2[r(u) - r(t_0)]\right\}\mathbb{E}_{t_0}\left[\exp\{2\xi(B_u - B_{t_0})\}\right] \tag{86}$$

Since B_{t_0} is $\mathcal{F}_{t_0}$-measurable and since we can divide the Volterra integral into two parts:

$$B_u = \int_0^{t_0} K(s,z)\,dW_z + \int_{t_0}^{u} K(u,z)\,dW_z, \tag{87}$$

we decompose the right-hand side of (86) into

$$\mathbb{E}_{t_0}[\sigma_u^2] = \sigma_{t_0}^2 \exp\left\{-\alpha\xi^2[r(u) - r(t_0)] + 2\xi\int_0^{t_0} K(u,z) - K(t_0,z)dW_z\right\}\cdot$$
$$\cdot\,\mathbb{E}_{t_0}\left[\exp\left\{2\xi\int_{t_0}^{u} K(u,z)dW_z\right\}\right] \tag{88}$$

Let $M_t = 2\xi\int_{t_0}^{t} K(t,z)dW_z$ for finite $t > t_0$, where thanks to the kernel K, the process M_t is an $\mathcal{F}_t$ semi-martingale. Then using Itô lemma we can express $\exp\{M_t\}$ in the following way.

$$d\left(e^{M_s}\right) = 2\xi K(u,s)e^{M_s}\,dM_s + \frac{1}{2}4\xi^2K^2(u,s)e^{M_s}\,ds$$
$$e^{M_u} - 1 = 4\xi^2\int_{t_0}^{u} K^2(u,s)e^{M_s}\,dW_s + 2\xi^2\int_{t_0}^{u} K^2(u,s)e^{M_s}\,ds$$

Moreover, if we apply the conditional expectation operator on both sides and the Fubini's theorem to exchange expectation and integration, we retrieve

$$\mathbb{E}_{t_0}\left[e^{M_u} - 1\right] = 2\xi^2\int_{t_0}^{u} K^2(u,s)\mathbb{E}_{t_0}e^{M_s}\,ds \tag{89}$$

Using a separation of variables and substituting the result into (88), we recover statement (83) of the proposition, as shown below:

$$\begin{aligned}\mathbb{E}_{t_0}[\sigma_u^2] &= \sigma_{t_0}^2 \exp\left\{-\alpha\xi^2[r(u)-r(t_0)]+2\xi\int_0^{t_0} K(u,z)-K(t_0,z)dW_z\right\}\cdot \\ &\quad\cdot\exp\left\{2\xi^2\int_{t_0}^{u} K^2(u,z)du\right\} \\ &= \sigma_0^2\exp\left\{-\alpha\xi^2 r(u)+2\xi\int_0^{t_0} K(u,z)dW_z+2\xi^2\int_{t_0}^{u} K^2(u,z)dz\right\}. \end{aligned} \tag{90}$$

Since the integral in (82) is by assumptions on the asset evolution finite (for a finite integration domain $\tau = T - t_0$) and because its integrand is strictly positive, we can use the Fubini's theorem as previously to interchange the conditional expectation and the integral. □

Remark 7. *The fair variance could be also derived under a more general setting (e.g. for standard fractional Brownian motion), however with much more technically demanding derivation. For more details, please refer to Merino – Pospíšil – Sobotka – Sottinen – Vives (2019), Lemma 4.3.*

Remark 8. *Should there be no liquid quotes on variance swap for a given financial asset, we can use Carr-Madan approach discussed in Section 3.3 to infer fair variance from liquid European options and equate them with (82). Solving this equation would lead to a model which is in-line with variance swap replication techniques.*

However, the Carr-Madan approach is based on various assumptions which typically create a gap between actual market fair strikes and replicated fair variances using option markets.

4.3 HYBRID CALIBRATION USING VARIANCE SWAPS

In this section, we will introduce a novel calibration approach with respect to the αRFSV model. The procedure can be divided into 3 steps:

Step 1 A given variance swap curve is fitted by finding optimal subset of model parameters (we can only find parameters which appear in (83)).

Step 2 All parameters are to be found by a calibration task with respect to the observed vanilla option surface. The subset of parameters obtained in the previous step are used as an initial guess for the calibration and also a regularization term is introduced for these parameters.

Step 3 Quality of the fit to the variance swap curve and option surface is checked, if it is unsatisfactory, then step 2 is repeated with a scaled regularization term or the calibration is terminated.

Below, we provide a detailed description of each step.

Step 1

In particular, step 1 is obtained by a simple least square minimization technique, where market variance curve (or approximation thereof) is fitted at all observed points by (82).

$$f(\Lambda) = \sum_{i=1}^{M}\left[\xi_t(T_i) - FS^{\alpha RFSV}(t_0,T_i|\Lambda)\right]^2 \tag{91}$$

$$\Lambda^{opt} = \arg\min_{\Lambda\in I^\Lambda} f(\Lambda), \tag{92}$$

where by $FS^{\alpha RFSV}(t_0,T_i) = FS^{\alpha RFSV}(t_0,T_i|\Lambda)$ we denote explicit dependence on model parameters Λ and $I^\Lambda \subset \mathbb{R}^4$ is a state space of admissible parameter values and M is the total number of fair variances observed.

We note that the step 1 takes the least computational time out of the three steps due to tractability of (82)-(83) which expresses $FS^{\alpha RFSV}(t_0,T_i|\Lambda)$. Only one numerical integration is necessary and hence adding this step does not worse the total computational time significantly. On the other hand, in the following text we will show how the computational time can be improved using this step.

Step 2

The step 2 involves calibration to vanilla options using information on parameters inferred from the variance swap curve (step 1). For this purpose, we use an approximation formula we introduced in Merino – Pospíšil – Sobotka – Sottinen – Vives (2019) for options with time to maturity less than $\tau < 0.5$ and MC simulation scheme in McCrickerd – Pakkanen (2018) otherwise.

Again we formulate the problem as a least-square minimization problem. This time we also use a regularization term to penalize major discrepancies from Λ^{opt}.

$$g(\Gamma) = \sum_{i=1}^{N} w_i \left[FV(T_i, K_i) - FV^{\alpha RFSV}(T_i, K_i|\Gamma) \right]^2 - \Theta \sum_{j=1}^{|\Lambda|} \left| \Lambda_j^{opt} - \Gamma_j \right| \tag{93}$$

$$\Gamma^{opt} = \arg\min_{\Gamma \in I^{\Gamma}} g(\Gamma), \tag{94}$$

where N is the total number of calibrated options, $(w_i)_1^N$ are weights associated to each option[3], $\Theta \geqslant 0$ is a scaling parameter which affects a "strength" of the regularization term and $FV^{\alpha RFSV}(T_i, K_i|\Gamma)$ is the option price under αRFSV model with model parameters Γ.

Step 3

Last but not least, we check a fit to the variance swap curve by evaluating

$$AAE_{VSC} = \frac{1}{M} \sum_{i=1}^{M} |\xi_t(T_i) - FS^{\alpha RFSV}(t_0, T_i|\Gamma^{opt})|, \tag{95}$$

and we compare it to the optimal fit obtained with parameters Λ^{opt} within step 1.

$$AAE_{VSC}^{step1} = \frac{1}{M} \sum_{i=1}^{M} |\xi_t(T_i) - FS^{\alpha RFSV}(t_0, T_i|\Lambda^{opt})|, \tag{96}$$

$$MAE_{VSC}^{step1} = \max_{i=1,..,M} |\xi_t(T_i) - FS^{\alpha RFSV}(t_0, T_i|\Lambda^{opt})|, \tag{97}$$

$$\Delta_{VSC} = AAE_{VSC} - AAE_{VSC}^{step1}. \tag{98}$$

Similar measures are also evaluated for calibration to option markets – this time we measure differences in terms of relative option FV. In particular, we are interested in

$$AAE_{FV} = \frac{1}{NS_{t_0}} \sum_{i=1}^{N} |FV(T_i, K_i) - FV^{\alpha RFSV}(T_i, K_i|\Gamma^{opt})|, \tag{99}$$

$$MAE_{FV} = \max_{i=1,..,N} |FV(T_i, K_i) - FV^{\alpha RFSV}(T_i, K_i|\Gamma^{opt})|. \tag{100}$$

Using the formulation above, two correction measures are instantly available:

- In case we are not satisfied with calibration quality to option markets we can rerun the calibration lowering Θ. If we don't have confidence in variance swap marking we can also set $\Theta = 0$.
- On the other hand, should we get further away from the optimal fit of the variance curve after calibration to option markets, we can strengthen the regularization term and rerun the option calibration (step 2).

4.3.1 *Illustration of hybrid calibration - numerical results*

In this section, we present results of few numerical experiments. The main idea is not to substantiate enough evidence that the introduced calibration scheme is superior to all alternative schemes, but rather to illustrate suitability of this approach on a selected real-market data set under few simplifying assumptions.

3 Typically, the weights are expressed as a function of liquidity of the particular contract or for simplification as a function of the bid-ask spread.

Simplifying assumptions of the numerical experiments

(S1) Market variance curve data is not at our disposal for this test, hence we use a market-standard Carr – Madan (1998) approach to get approximation thereof. For simplicity, we use a linear interpolation in variance terms of the market observed implied volatilities and we use a basic data cleaning for variance swap curve approximation, more details on this are provided below.

(S2) We assume there is no borrow / no dividend term for our underlying asset to simplify the calibration procedure.

(S3) We use option calibration (step 2) only for smiles with short time to maturity (up to approximately 1 month), to be able to use Merino – Pospíšil – Sobotka – Sottinen – Vives (2019) approximation pricing technique only – i.e. without utilizing Monte-Carlo simulations.

Detailed description of experiments

For the numerical experiments we use a set of European options on Apple Inc. stocks as observed on 15th March 2015. The data were obtained from Bloomberg L.P. alongside data sets discussed in Pospíšil – Sobotka – Ziegler (2019). Only basic data cleaning was performed – in case some of the information for a particular option were not available (e.g. missing ask / bid quotes), we got rid of the particular option. Also for the fair variance computation, we interpolated / extrapolated implied volatilities linearly in variance terms in the strike dimension from $30\%S_0$ to $500\%S_0$ and we used only time to maturities from ca 0.019 to 0.67 years not to have too sparse implied volatilities.

Due to simplification (S3), we focus on calibration to short-maturity options only, in particular to options with time to maturity ca 1 week (7 trading days) and ca 1 month (24 trading days). However, options with longer maturities are utilized in fair variance calibration (step 1) – to reconstruct approximation of the variance swap curve.

We further note that we have used the same factor $\varepsilon = 10^{-5}$ as in Merino – Pospíšil – Sobotka – Sottinen – Vives (2019) and regularization scaling constant was set to $\Theta = 0.1$. To solve constrained optimization problems in step 1 and step 2, we use a Trust-Region-Reflective optimization method implemented in Matlab's `lsqnonlin` function[4]. Equidistant weighting for option calibration was used, i.e. $w_i = 1$ for all i. This was mainly due to calibrating only to two volatility smiles, if more expiries were considered non-constant weights might prove useful. Optimization setting in Table 1 was utilized to retrieve all results:

Table 1: Optimisation parameters

Parameter	Description	Setting
`MaxFunEvals`	Maximal number of utility function evaluations	400
`MaxIter`	Maximal number of iteration steps	40
`TolX`	Tolerance in the parameter space	`1e-6`
`TolFun`	Tolerance in the utility function	`1e-6`

We note that whenever optimizer reaches Maximal number of iterations or function evaluations, it stops prematurely. This wasn't the case for our experiments, the utility function tolerance criterion was the stopping rule for all our experiments.

Obtained results

Starting from calibration to the variance swap curve, we note that we have retrieved a model variance curve which correctly captures overall shape of the fitted curve, but cannot mimic non-monotonous behaviour of the input curve. The fitting errors are described in Tables 2 and 3.

Although the calibration results on the VSC curve are far from perfect, we also back-test the calibration on option markets. In particular, in Figure 9 we display how we fitted 1W and 1M volatility smiles in terms of relative FV after VSC calibration. Here we have found a very good match between market and model prices, especially considering the fact that calibration to the variance swap curve took less then 1 sec in our case[5]. To see how a typical initial guess (prior to knowing calibrated parameters) might fit the option markets we provided illustration in Figure 10.

4 For more details please refer to `https://www.mathworks.com/help/optim/ug/lsqnonlin.html`.

5 Retrieved on a PC with i7-6500 CPU, 8 GB memory and MATLAB 2015b.

Table 2: Fitting errors - initial VSC calibration

Error measure	Result
AAE_{VSC}^{step1}	1.6pp
MAE_{VSC}^{step1}	2.0pp

Table 3: Calibrated parameters - initial VSC calibration

σ_{t_0}	ξ	H	α
0.05	1.27	0.49	0.37

We also tried to improve already a reasonably good fit to the options by solving optimization problem defined in step 2. The fit obtained using initial parameters from VSC calibration (Table 3) is illustrated in Figure 11 for 1W and 1M maturities. We also display absolute differences from reference relative FV. We note that absolute value of calibration errors below 0.1% mark is typically considered as a very good result and anything above 0.5% should be understood as a significant miss-calibration.

As for the final calibration illustrated in Figure 11, all obtained errors stayed within $\pm$0.5pp bound and most of them were lower in absolute value than 0.1pp mark. When back testing with variance swap curve, we retrieved $\Delta_{VSC} = 0.27$pp. Should we have more trust in variance swap curve marking we could potentially lower Δ_{VSC} by increasing the value of Θ to have stronger regularization term. However, this is not our case, because we used only an approximation of the VSC which is also sensitive to the least liquid options from our data set.

We also calibrated αRFSV model using initial guess as in Figure 10. We have retrieved a very similar calibration fit (same number of options outside $\pm$0.1pp bound), but there was a major difference in the computational time. E.g. for 1W time to maturity options we needed only 42 utility function evaluations starting from VSC calibrated parameters (i.e. 840 option prices computed). Compared to the situation without a good initial guess, we had to perform 78 evaluation and hence computing 1560 option prices. Due to the multiple numerical integrations needed to approximate one option price, we managed to save a significant portion of the total calibration time – approx. 46% saving.

The calibrated parameters from option market slightly differed compared to the VSC calibration parameters. The most significant change was in the Hurst parameter which decreased from 0.49 to 0.34. In our case, lower values of H enabled a good fit to short-term options with strikes close to at-the-money.

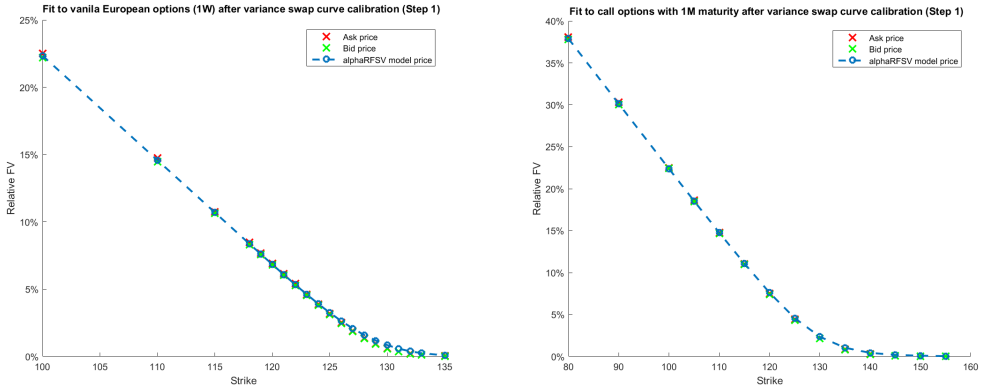

Figure 9: Fit to the option market using VSC calibration parameters and $\rho = -0.4$

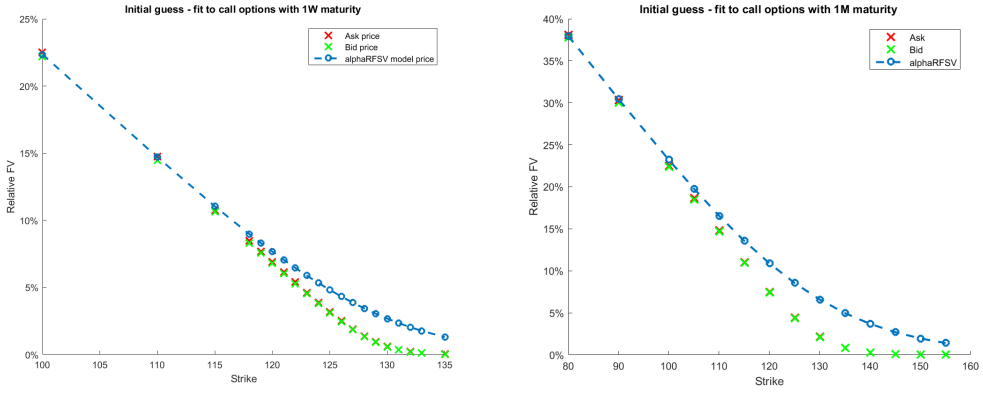

Figure 10: Fit of the initial guess, with $\sigma_{t_0} = 0.3, \xi = 0.5 \rho = -0.4, H = 0.1, \alpha = 0.5$

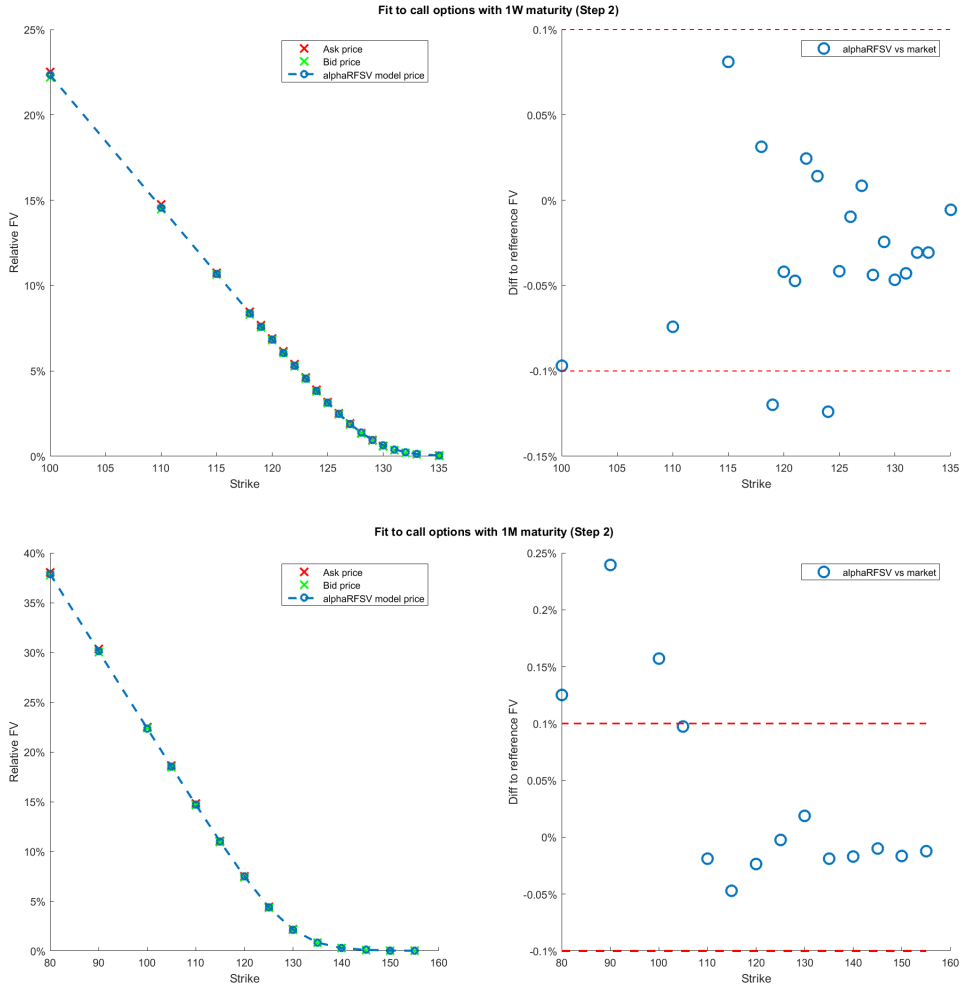

Figure 11: Final calibration to option markets, using VSC calibration parameters as a initial guess

5

CONCLUSION

Aim of the thesis is threefold. Firstly, we review author's contribution due to published articles. We also extend the latest article and we show how the extension could significantly improve the original goal of the model. Last but not least, we include a comprehensive introduction to selected financial engineering tasks, corresponding financial markets and most common modelling approaches.

One of the main challenges of a financial engineer within financial market risk areas is to be able to find a fair value of a particular derivative contract which is consistent with relevant market observables. Unless the derivative is exchange traded with observable fair value, a modelling choice has to be made and the challenge is typically divided into two tasks:

i. Calibration of the model parameters to market observables – to make sure our underlying model is as close as possible to the market implied properties;

ii. Utilizing calibrated model to retrieve a non-observed fair value and sensitivity to risk factors for the derivative contract subject to analysis.

For plain vanilla derivative contracts – i.e. contracts similar to the exchange traded derivatives – both of the tasks above typically simplify to interpolation / extrapolation of market observable values. Importance of the model calibration is fully acknowledged when non-vanilla derivatives are to be analyzed. In this case, one should find such a model that

- can be efficiently and accurately calibrated to the most relevant market[1],
- makes sense in terms of typical behaviour of markets (consistent with so called stylized facts, see Section 1) and provides intuitive interpretation of the modelling outcomes.

Having in mind derivative valuation and risk management tasks for non-vanilla derivatives, a popular class of models are stochastic volatility (SV) approaches. These models have been vastly studied since the original article by Hull – White (1987). The main common idea of the SV models is that not only the first risk factor (typically market observable price of the underlying asset) is stochastic, but also its second moment is of a random nature as well.

Formally, let $(S_t)_{t\geqslant 0}$ be a stochastic process defined on a filtered probability space $(\Omega, \mathcal{F}, (\mathcal{F}_t)_{t\geqslant 0}, Q)$ where the filtration $\mathcal{F}_t$ represents the information known at time t and Q is a market chosen risk-neutral probability measure. Then, the fair value of a derivative paying to its holder at some future time T, $f(S_T)$ for a pre-defined $T-$measurable function $f : \mathbb{R}^+ \mapsto \mathbb{R}$, is given by:

$$FV = \mathbb{E}^Q \left[DF(t_0, T) f(S_T) | \text{"model parameters"} \cup \mathcal{F}_{t_0} \right] \tag{101}$$

where $DF(t_0, T)$ is a discount factor from t_0 to T which is – for the sake of simplicity – represented by $e^{-r(T-t_0)}$ throughout the thesis. Typically, we might have market observable fair values of vanilla derivatives on our underlying asset and hence, should we have a tractable representation of (101), then we can infer model parameters (i.e. the only unknown entity) by means of

- bootstrapping – in case of a simple relation with only a few parameters (e.g. observed FV mapped to implied volatility),
- calibration – finding parameters with an optimal fit to the observable fair values.

Since the SV models tend to be more complex in terms of parametrization, bootstrapping methods are not applicable. Hence, we focus only on the calibration techniques.

For traditional SV models, both task i. and ii. are well developed in the literature. However, for a special case – rough fractional volatility models – a lack of thorough treatment for both tasks is apparent as of the date this thesis is compiled. These models, as reviewed in Section 2, add extra complexity due to its non-Markovianity[2], irregularity of paths etc. In particular, the driving noise considered in the volatility / variance process of the asset price is not a standard Wiener process, but either a fractional Brownian motion or a process with similar path-wise properties.

1 For the sake of low dimensionality and tractability, one typically calibrates only to the most relevant markets that drive the main risk factors of the selected derivative.

2 Sample realizations depend on all previous realizations.

In particular, a fractional Brownian motion $(W_t^H)_{t\geqslant 0}$ with Hurst parameter $H \in (0,1)$ is a centred continuous Gaussian process with covariance,

$$R(s,t) := \mathbb{E}\left[W_s^H W_t^H\right] = \frac{1}{2}(s^{2H} + t^{2H} - |t-s|^{2H}).$$

Most interesting, from the financial applications point of view, is the case when the process attains *rough* paths, i.e. for $H \in (0, 0.5)$, see Figure 12 and also Section 2.2 for a more detailed discussion.

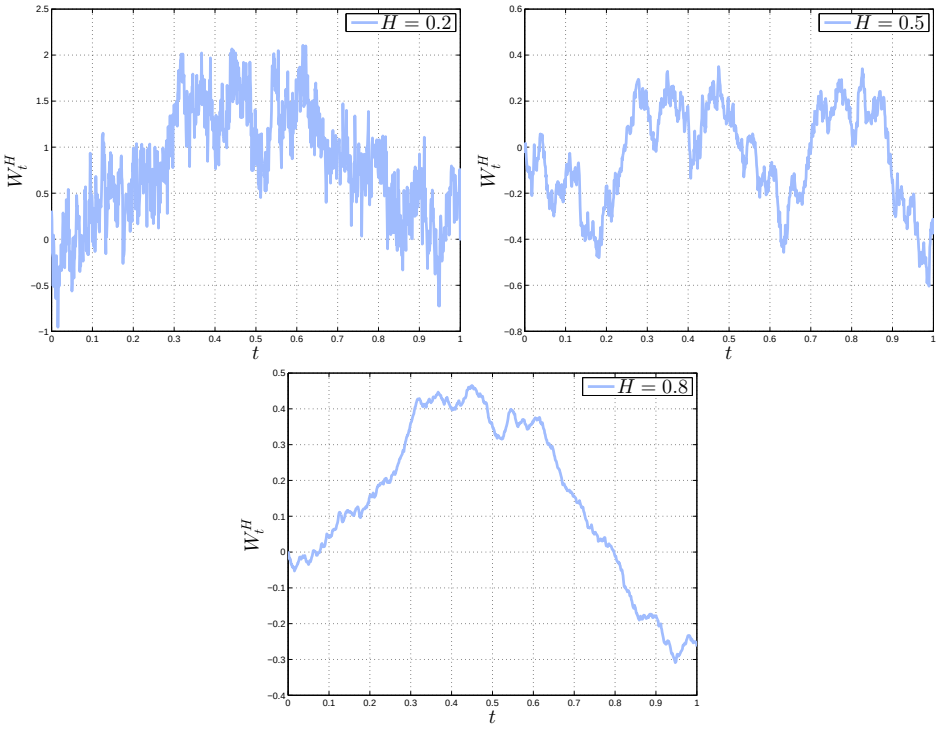

Figure 12: Sample paths of a fractional Brownian motion for $H = 0.2$ (rough paths), $H = 0.5$ (standard Wiener case) and $H = 0.8$

Recently, many articles on rough volatility models appeared, Bayer et al. (2016), Gatheral et al. (2018), El Euch et al. (2018), Alòs et al. (2019), El Euch – Rosenbaum (2019) to name a few, where authors either propose a new way to approach several financial engineering tasks or show a remarkable ability of rough models to mimic various market observables.

In our thesis we extend an approach which we introduced in Merino – Pospíšil – Sobotka – Sottinen – Vives (2019) – a short-term option price approximation technique introduced for volatility models driven by a class of Volterra processes which also include a standard fractional Brownian motion with $H < 0.5$ as a special case. Moreover, for a Volterra process which can be formally denoted as

$$Y_t = \sqrt{2H}\int_0^t (t-s+\varepsilon)^{H-\frac{1}{2}}\, dW_s \tag{102}$$

where dW_s is the standard Wiener process and $\varepsilon \geqslant 0$, we have shown that a corresponding exponential rough volatility model can be successfully calibrated using the approximation to short maturity options and via Monte-Carlo simulation techniques to medium and long maturity options in (Merino – Pospíšil – Sobotka – Sottinen – Vives, 2019).

However, although the approximation tends to be more computationally efficient than Monte-Carlo simulations, due to multiple numerical procedures to approximate one option fair value, it is still significantly slower compared to the best practises for standard SV models. This is an issue, especially for the task of model calibration, which might include numerous evaluations of option fair values.

To remediate the issue above we propose a way for a potential shortening of calibration computational time under the considered rough volatility model. The main idea is to leverage not only European options as market observables, but also variance swap contracts.

Variance swaps have become increasingly popular in the past 10 years and for several financial assets they are also considered as market observables[3]. To be able to illustrate our idea, we have

3 Either thanks to observable volatility indices or due to consensus pricing services.

reviewed a market standard approach of Carr – Madan (1998) which connects vanilla options and variance swaps, in case the latter is not observed. Although, the connection holds under certain assumptions (see Section 3.3), it enables us to build an approximation of the so called variance swap curve (VSC), defined in (51), from market observable fair values of options. Moreover, we were able to derive a tractable formula for VSC under the studied rough model (see Section 4), which helps to calibrate the model to variance swap data.

To make the calibration task significantly more efficient with respect to the main market observables – European options, we calibrate the studied model first to VSC using the newly introduced approach in Section 4. This extra step takes only few computation resources[4] and overall provides a very good initial guess for the option calibration. Having a good initial guess, typically means that our standard calibration procedure needs fewer iterations – and hence less function evaluations which are expensive – to reach the optimal solution. We illustrate this on a small numerical exercise on Apple Inc. options and on VSC constructed using Carr – Madan (1998) approach, to show that in our case we have saved approximately 46% of the total computational time, while obtaining as good fit as in Merino – Pospíšil – Sobotka – Sottinen – Vives (2019).

Last but not least, in Appendix B we attached other articles related to SV models where the author has contributed while pursuing his PhD candidature.

4 It takes less than few seconds in our numerical examples.

Alòs, E. A decomposition formula for option prices in the Heston model and applications to option pricing approximation. *Finance Stoch.* 2012, 16, 3, p. 403–422. ISSN 0949-2984. doi: 10.1007/s00780-012-0177-0.

Alòs, E. – León, J. A. – Vives, J. On the short-time behavior of the implied volatility for jump-diffusion models with stochastic volatility. *Finance Stoch.* 2007, 11, 4, p. 571–589. ISSN 0949-2984. doi: 10.1007/s00780-007-0049-1.

Alòs, E. – Santiago, R. – Vives, J. Calibration of stochastic volatility models via second-order approximation: The Heston case. *Int. J. Theor. Appl. Finance*. 2015, 18, 6, p. 1–31. ISSN 0219-0249. doi: 10.1142/S0219024915500363.

Alòs, E. et al. Target volatility option pricing in lognormal fractional SABR model. *Quant. Finance*. 2019, 19, 8, p. 1339–1356. ISSN 1469-7688. doi: 10.1080/14697688.2019.1574021.

Atiya, A. F. – Wall, S. An analytic approximation of the likelihood function for the Heston model volatility estimation problem. *Quant. Finance*. 2009, 9, 3, p. 289–296. ISSN 1469-7688. doi: 10.1080/14697680802595601.

Bachelier, L. Théorie de la Spéculation. *Ann. Sci. Ec. Norm. Super.* 1900, 3, 17, p. 21–86.

Bakshi, G. – Cao, C. – Chen, Z. Empirical performance of alternative option pricing models. *J. Finance*. 1997, 52, 5, p. 2003–2049. ISSN 1540-6261. doi: 10.1111/j.1540-6261.1997.tb02749.x.

Bates, D. S. Jumps and Stochastic Volatility: Exchange Rate Processes Implicit in Deutsche Mark Options. *Rev. Financ. Stud.* 1996, 9, 1, p. 69–107. doi: 10.1093/rfs/9.1.69.

Bauer, H. *Probability theory*. De Gruyter studies in mathematics. Bod Third Party Titles, 1996. ISBN 9783110139358.

Baustian, F. – Mrázek, M. – Pospíšil, J. – Sobotka, T. Unifying pricing formula for several stochastic volatility models with jumps. *Appl. Stoch. Models Bus. Ind.* 2017, 33, 4, p. 422–442. ISSN 1524-1904. doi: 10.1002/asmb.2248.

Bayer, C. – Friz, P. – Gatheral, J. Pricing under rough volatility. *Quant. Finance*. 2016, 16, 6, p. 887–904. ISSN 1469-7688. doi: 10.1080/14697688.2015.1099717.

Benhamou, E. – Gobet, E. – Miri, M. Time dependent Heston model. *SIAM J. Finan. Math.* 2010, 1, 1, p. 289–325. ISSN 1945-497X. doi: 10.1137/090753814.

Bergomi, L. Smile dynamics II. *Risk Magazine*. 2005, 18, 10, p. 67–73. Also available at SSRN: http://ssrn.com/abstract=1493302.

Bergomi, L. Smile dynamics III. *Risk Magazine*. 2008, 21, 10, p. 90–96. Also available at SSRN: http://ssrn.com/abstract=1493308.

BIS. Semiannual OTC derivatives statistics, 2016. Available from: <www.bis.org/statistics/derstats.htm>.

Black, F. S. – Scholes, M. S. The pricing of options and corporate liabilities. *J. Polit. Econ.* May-June 1973, 81, 3, p. 637–654. ISSN 0022-3808. doi: 10.1086/260062.

Bollerslev, T. – Chou, R. Y. – Kroner, K. F. ARCH modeling in finance: A review of the theory and empirical evidence. *J. Econometrics*. 1992, 52, 1-2, p. 5–59. ISSN 0304-4076. doi: 10.1016/0304-4076(92)90064-X.

Brock, W. A. – De Lima, P. J. F. Nonlinear time series, complexity theory, and finance. *Handbook of Statistics*. 1996, 14, p. 317–361.

Campbell, J. Y. et al. *The econometrics of financial markets*. 2. Princeton University press, Princeton, NJ, 1997. ISBN 9780691043012.

Carr, P. – Madan, D. B. Towards a theory of volatility trading. In *Volatility: New Estimation Techniques for Pricing Derivatives*, Risk Books. London: R. Jarrow, 1998. p. 417–427.

Chesney, M. – Scott, L. Pricing European currency options: A comparison of the modified Black-Scholes model and a random variance model. *J. Financ. Quant. Anal.* 1989, 24, 3, p. 267–284. ISSN 0022-1090. doi: 10.2307/2330812.

Chin, S. – Dufresne, D. A general formula for option prices in a stochastic volatility model. *Appl. Math. Finance*. 2012, 19, 4, p. 313–340. ISSN 1350-486X. doi: 10.1080/1350486X.2011.624823.

Chin, S. S. *Stochastic volatility model and option pricing*. PhD thesis, The University of Melbourne, 2011.

Comte, F. – Renault, E. M. Long memory in continuous-time stochastic volatility models. *Math. Finance*. 1998, 8, 4, p. 291–323. ISSN 0960-1627. doi: 10.1111/1467-9965.00057.

Comte, F. – Coutin, L. – Renault, E. Affine fractional stochastic volatility models. *Ann. Finance*. 2012, 8, 2–3, p. 337–378. ISSN 1614-2446. doi: 10.1007/s10436-010-0165-3.

Cont, R. Empirical properties of asset returns: stylized facts and statistical issues. *Quant. Finance*. 2001, 1, 2, p. 223–236. ISSN 1469-7688. doi: 10.1080/713665670.

Cont, R. – Da Fonseca, J. Dynamics of implied volatility surfaces. *Quant. Finance*. 2002, 2, 1, p. 45–60. ISSN 1469-7688. doi: 10.1088/1469-7688/2/1/304.

Cootner, P. H. *The random character of stock market prices*. MIT Press, 1964. ISBN 9780262030090.

Decreusefond, L. – Üstünel, A. Stochastic analysis of the fractional Brownian motion. *Potential Analysis*. 1999, 10, 2, p. 177–214. ISSN 1572-929X. doi: 10.1023/A:1008634027843.

Delbaen, F. – Schachermayer, W. *The mathematics of arbitrage*. Springer, 2006. ISBN 9783540219927.

Delbaen, F. – Schachermayer, W. A general version of the fundamental theorem of asset pricing. *Mathematische Annalen*. 1994, 300, 1, p. 463–520. ISSN 0025-5831. doi: 10.1007/bf01450498.

Dimand, R. W. – Ben-El-Mechaiekh, H. Louis Bachelier's 1938 monograph on the calculus of speculation: Mathematical finance and randomness of asset prices in Bachelier's later work. *J. Electron. Hist. Probab. Stat.* 2012. ISSN 1773-0074.

Duffie, D. – Pan, J. – Singleton, K. Transform analysis and asset pricing for affine jump-diffusions. *Econometrica*. 2000, 68, 6, p. 1343–1376. ISSN 0012-9682. doi: 10.1111/1468-0262.00164.

Dupire, B. Pricing with a Smile. *Risk Magazine*. 1994, p. 18–20.

El Euch, O. – Rosenbaum, M. The characteristic function of rough Heston models. *Math. Finance*. 2019, 29, 1, p. 3–38. ISSN 0960-1627. doi: 10.1111/mafi.12173.

El Euch, O. et al. Short-Term At-the-Money Asymptotics under Stochastic Volatility Models. *SIAM J. Finan. Math.* 2019, 10, 2, p. 491–511. ISSN 1945-497X. doi: 10.1137/18M1167565.

El Euch, O. – Gatheral, J. – Rosenbaum, M. Roughening heston. *Available at SSRN 3116887*. 2018. Available from: <https://papers.ssrn.com/sol3/papers.cfm?abstract_id=3116887>.

Elices, A. Models with time-dependent parameters using transform methods: application to Heston's model. Available at arXiv: https://arxiv.org/abs/0708.2020, 2008.

Fatone, L. et al. The calibration of some stochastic volatility models used in mathematical finance. *Open Journal of Applied Sciences*. 2014, 2014.

Feller, W. Two singular diffusion problems. *Ann. Math.* 1951, 54, 1, p. 173–182. ISSN 0003-486X. doi: 10.2307/1969318.

Feller, W. *An introduction to probability theory and its applications*. 1. Wiley, January 1968. ISBN 0471257087.

Forde, M. – Smith, B. – Viitasaari, L. Rough unbounded volatility with CGMY jumps conditioned on a finite history and the Rough Heston model-small-time Edgeworth expansions and the prediction formula for the Riemann-Liouville process. *Preprint*. 2019. Available from: <https://nms.kcl.ac.uk/martin.forde/RSVEdgeworthTwoSidedJumps.pdf>.

Fukasawa, M. Asymptotic analysis for stochastic volatility: martingale expansion. *Finance Stoch.* 2011, 15, 4, p. 635–654. ISSN 0949-2984. doi: 10.1007/s00780-010-0136-6.

Gatheral, J. *The volatility surface: A practitioner's guide*. Wiley Finance. John Wiley & Sons, 2006. ISBN 9780470068250.

Gatheral, J. – Jacquier, A. Arbitrage-free SVI volatility surfaces. *Quant. Finance*. 2014, 14, 1, p. 59–71. ISSN 1469-7688. doi: 10.1080/14697688.2013.819986.

Gatheral, J. – Jaisson, T. – Rosenbaum, M. Volatility is rough. Available at arXiv: https://arxiv.org/abs/1410.3394, 2014.

Gatheral, J. – Jaisson, T. – Rosenbaum, M. Volatility is rough. *Quant. Finance*. 2018, 18, 6, p. 933–949. ISSN 1469-7688. doi: 10.1080/14697688.2017.1393551.

Gleeson, C. Pricing and hedging S&P 500 index options : A comparison of affine jump diffusion models. Master's thesis, Banking & Finance, Australian School of Business, UNSW, 2005.

Gourieroux, C. – Jasiak, J. *Financial econometrics: Problems, models, and methods*. 1. Princeton University press, Princeton, NJ, 2001. ISBN 9780691088723.

Gyöngy, I. Mimicking the one-dimensional marginal distributions of processes having an Ito differential. *Probab. Theory Related Fields*. 1986, 71, 4, p. 501–516. ISSN 0178-8051. doi: 10.1007/BF00699039.

Hagan, P. S. et al. Managing smile risk. *Wilmott Magazine*. 2002, 2002, January, p. 84–108.

Heston, S. L. A closed-form solution for options with stochastic volatility with applications to bond and currency options. *Rev. Financ. Stud.* 1993, 6, 2, p. 327–343. ISSN 0893-9454. doi: 10.1093/rfs/6.2.327.

Horvath, B. – Muguruza, A. – Tomas, M. Deep Learning Volatility. Available at arXiv: https://arxiv.org/abs/1901.09647, 2019.

Hull, J. C. – White, A. D. The pricing of options on assets with stochastic volatilities. *J. Finance*. June 1987, 42, 2, p. 281–300. ISSN 1540-6261. doi: 10.1111/j.1540-6261.1987.tb02568.x.

Hurn, A. S. – Lindsay, K. A. – McClelland, A. J. Estimating the parameters of stochastic volatility models using option price data. *Journal of Business & Economic Statistics*. 2015, 33, 4, p. 579–594.

Intarasit, A. – Sattayatham, P. An approximate formula of European option for fractional stochastic volatility jump-diffusion model. *J. Math. Stat.* 2011, 7, 3, p. 230–238. ISSN 1549-3644. doi: 10.3844/jmssp.2011.230.238.

Jäckel, P. Stochastic volatility models: past, present and future. In *The Best of Wilmott 1: Incorporating the Quantitative Finance Review*. New Jersey: John Wiley & Sons, 2004. p. 379–390.

Jacquier, A. Advanced Methods in Derivatives Pricing, with application to Volatility Modelling, 2016. Available from: <wwwf.imperial.ac.uk/~ajacquie/IC_AMDP/IC_AMDP_Docs/AMDP.pdf>. Lecture notes.

Jacquier, E. – Jarrow, R. Bayesian analysis of contingent claim model error. *J. Econometrics*. 2000, 94, 1–2, p. 145–180. ISSN 0304-4076. doi: 10.1016/S0304-4076(99)00020-2.

Kienitz, J. – Wetterau, D. *Financial modelling: Theory, implementation and practice with MATLAB source*. The Wiley Finance Series. Wiley, 2012. ISBN 9781118413319.

Kolmogorov, A. N. Wienersche Spiralen und einige andere interessante Kurven im Hilbertschen Raum. *Dokl. Akad. Nauk SSSR*. 1940, 26, p. 115–118.

Lévy, P. *Processus stochastiques et mouvement brownien*. Gauthier-Villars, 2nd edition, 1948. 1965 reprinted edition. ISBN 9782876470910.

Mandelbrot, B. The variation of certain speculative prices. *J. Bus.* 1963, 36, 4, p. 394–419. ISSN 0021-9398.

Mandelbrot, B. – Van Ness, J. Fractional Brownian motions, fractional noises and applications. *SIAM Rev.* 1968, 10, 4, p. 422–437. doi: 10.1137/1010093.

Maslowski, B. Stochastic equations and stochastic methods in partial differential equations. In *Proceedings of seminar in differential equations*, p. 7–62, 2006.

McCrickerd, R. – Pakkanen, M. S. Turbocharging Monte Carlo pricing for the rough Bergomi model. *Quant. Finance*. 2018, 18, 11, p. 1877–1886. ISSN 1469-7688. doi: 10.1080/14697688.2018.1459812.

Merino, R. et al. Decomposition formula for jump diffusion models. *Int. J. Theor. Appl. Finance*. 2018, 21, 8, p. 1850052. ISSN 0219-0249. doi: 10.1142/S0219024918500528.

Merino, R. et al. Decomposition formula for rough Volterra stochastic volatility models. Available at arXiv: https://www.arxiv.org/abs/1906.07101., 2019.

Merton, R. C. Theory of rational option pricing. *Bell J. Econ.* 1973, 4, 1, p. 141–183. ISSN 0005-8556. doi: 10.2307/3003143.

Merton, R. C. Option pricing when underlying stock returns are discontinuous. *J. Financ. Econ.* 1976, 3, 1–2, p. 125–144. ISSN 0304-405X. doi: 10.1016/0304-405X(76)90022-2.

Mikhailov, S. – Nögel, U. Heston's stochastic volatility model - implementation, calibration and some extensions. *Wilmott magazine*. 2003, 2003, July, p. 74–79.

Molchan, G. M. – Golosov, J. I. Gaussian stationary processes with asymptotic power spectrum. *Sov. Math. Dokl.* 1969, 10, p. 134–137. ISSN 0197-6788. Translation from Dokl. Akad. Nauk SSSR 184, 546–549 (1969).

Mrázek, M. – Pospíšil, J. – Sobotka, T. On optimization techniques for calibration of stochastic volatility models. In *Applied Numerical Mathematics and Scientific Computation*, p. 34–40, Athens, Greece, 2014. Europment. ISBN 978-1-61804-253-8, AMCM 2015, November 28-30, 2014, Athens, Greece.

Mrázek, M. – Pospíšil, J. – Sobotka, T. On calibration of stochastic and fractional stochastic volatility models. *European J. Oper. Res.* 2016, 254, 3, p. 1036–1046. ISSN 0377-2217. doi: 10.1016/j.ejor.2016.04.033.

Øksendal, B. *Stochastic differential equations: An introduction with applications*. Universitext. Springer-Verlag, 2003. ISBN 3-540-04758-1.

Osajima, Y. The asymptotic expansion formula of implied volatility for dynamic SABR model and FX hybrid model. Available at SSRN: http://ssrn.com/abstract=965265, 2007.

Pagan, A. The econometrics of financial markets. *Journal of empirical finance*. 1996, 3, 1, p. 15–102.

Pospíšil, J. – Sobotka, T. Market calibration under a long memory stochastic volatility model. *Appl. Math. Finance*. 2016, 23, 5, p. 323–343. ISSN 1350-486X. doi: 10.1080/1350486X.2017.1279977.

Pospíšil, J. – Sobotka, T. – Ziegler, P. Robustness and sensitivity analyses for stochastic volatility models under uncertain data structure. *Empir. Econ.* 2019, 57, 6, p. 1935–1958. ISSN 0377-7332. doi: 10.1007/s00181-018-1535-3.

Sattayatham, P. – Intarasit, A. – Chaiyasena, A. P. A fractional Black-Scholes model with jumps. *Vietnam J. Math.* 2007, 35, 3, p. 231–245.

Scott, L. O. Option pricing when the variance changes randomly: Theory, estimation, and an application. *J. Financ. Quant. Anal.* 1987, 22, 4, p. 419–438. ISSN 0022-1090. doi: 10.2307/2330793.

Shephard, N. Statistical aspects of ARCH and stochastic volatility. *Time Series Models in Econometrics, Finance and Other Fields,(ed. by D.R. Cox, D. V. Hinkley and O. E. Barndorff-Neilsen)*. 1996, 1, p. 67.

Shreve, S. E. *Stochastic calculus for finance. II*. Springer Finance. Springer-Verlag, 2004. ISBN 978-0-387-40101-0.

Sircar, R. K. – Papanicolaou, G. General Black-Scholes models accounting for increased market volatility from hedging strategies. *Appl. Math. Finance*. 1998, 5, 1, p. 45–82. ISSN 1350-486X. doi: 10.1080/135048698334727.

Sottinen, T. – Viitasaari, L. Conditional-mean hedging under transaction costs in Gaussian models. *Int. J. Theor. Appl. Finance*. 2018, 21, 02, p. 1850015. doi: 10.1142/S0219024918500152.

TAKAYASU, H. *Empirical science of financial fluctuations: The advent of econophysics*. Springer Japan, 2013. ISBN 9784431669937.

ČEKAL, M. Blackovy-Scholesovy modely oceňování opcí. Master's thesis, MFF UK, 2012.

WIGGINS, J. B. Option values under stochastic volatility: Theory and empirical estimates. *Journal of Financial Economics*. 1987, 19, 2, p. 351–372.

WILMOTT, P. *Paul Wilmott on quantitative finance*. John Wiley & Sons, 2007. ISBN 9780470060773.

YAN, G. – HANSON, F. B. Option pricing for a stochastic-volatility jump-diffusion model with log-uniform jump-amplitude. In *Proceedings of American Control Conference*, p. 2989–2994, Piscataway, NJ, 2006. IEEE. doi: 10.1109/acc.2006.1657175.

YOSHIDA, N. Malliavin calculus and asymptotic expansion for martingales. *Probab. Theory Related Fields*. 1997, 109, 3, p. 301–342. ISSN 0178-8051. doi: 10.1007/s004400050134.

ZÄHLE, M. Integration with respect to fractal functions and stochastic calculus. I. *Probab. Theory Related Fields*. 1998, 111, 3, p. 333–374. ISSN 0178-8051. doi: 10.1007/s004400050171.

APPENDIX A

In what follows, we provide further illustration of financial market stylized facts, as introduced in Chapter 1. The illustration is based on a data comprising of historical quotes with respect to 5 equity indices from 2000 to 2016. The data were obtained from http://realized.oxford-man.ox.ac.uk/data and figures are listed in the alphabetical order.

A.1 AUTOCORRELATION PLOTS

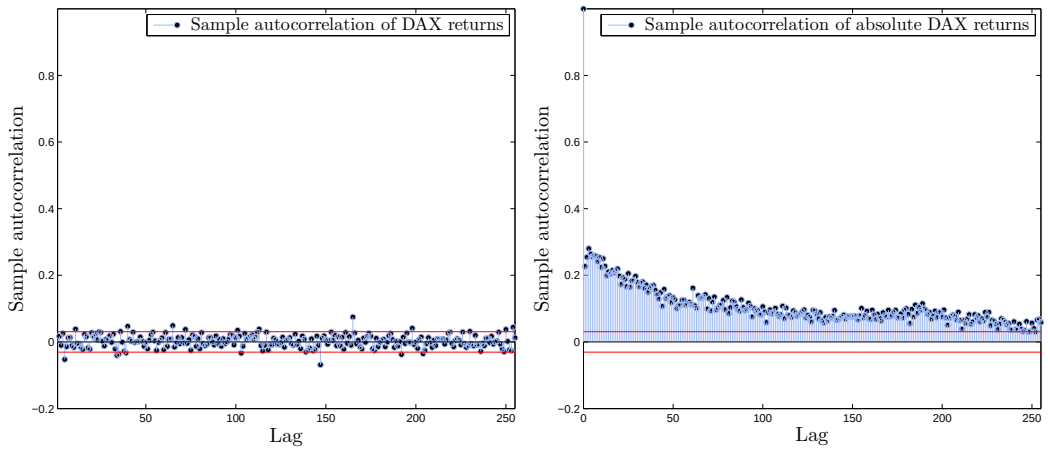

Figure 13: Sample autocorrelation of returns (on the left) and absolute returns (on the right) - DAX index (1/2000 - 2/2016).

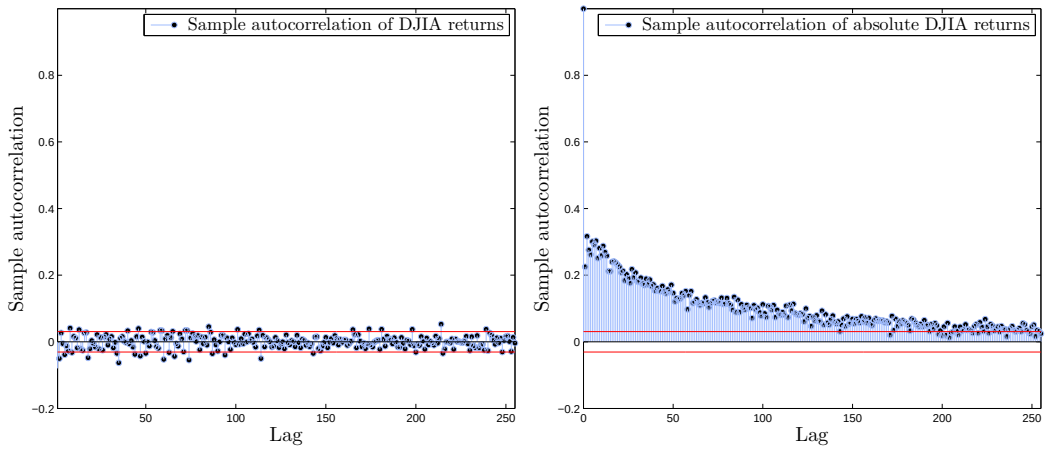

Figure 14: Sample autocorrelation of returns (on the left) and absolute returns (on the right) - DJIA index (1/2000 - 2/2016).

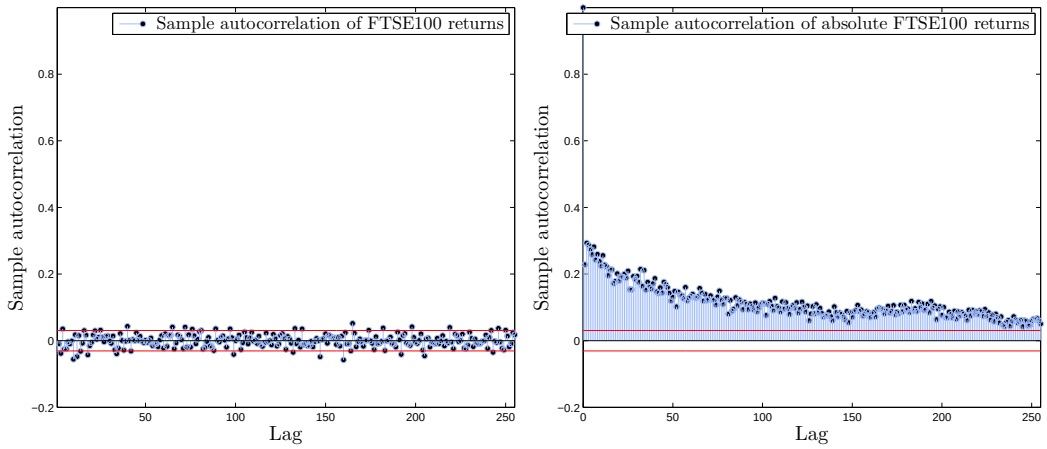

Figure 15: Sample autocorrelation of returns (on the left) and absolute returns (on the right) - FTSE 100 index (1/2000 - 2/2016).

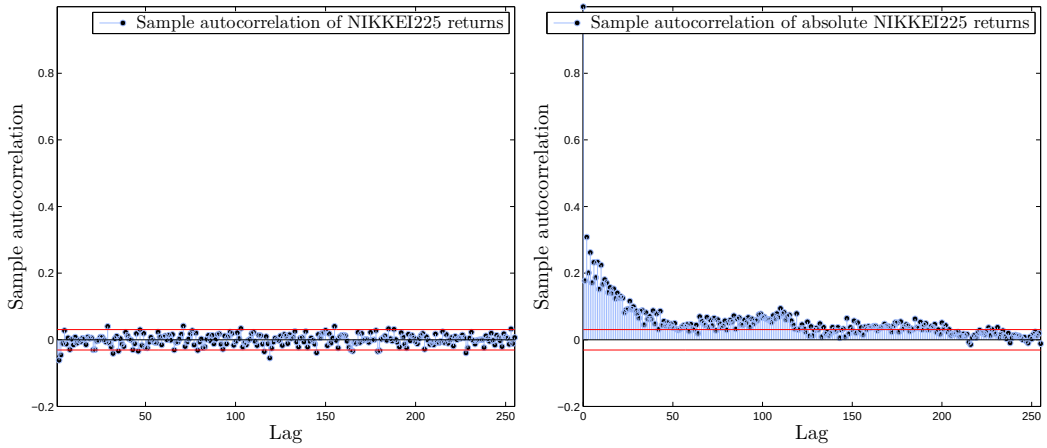

Figure 16: Sample autocorrelation of returns (on the left) and absolute returns (on the right) - NIKKEI 225 index (1/2000 - 2/2016).

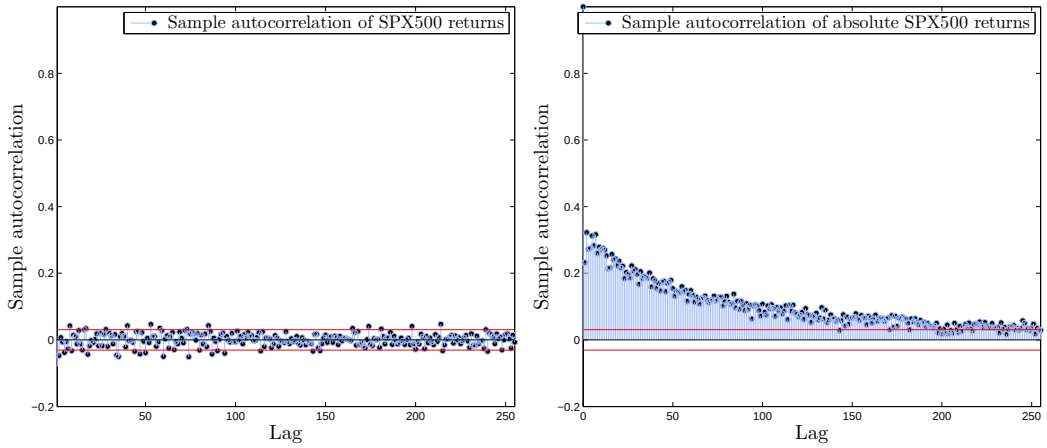

Figure 17: Sample autocorrelation of returns (on the left) and absolute returns (on the right) - SPX 500 index (1/2000 - 2/2016).

A.2 HISTOGRAMS

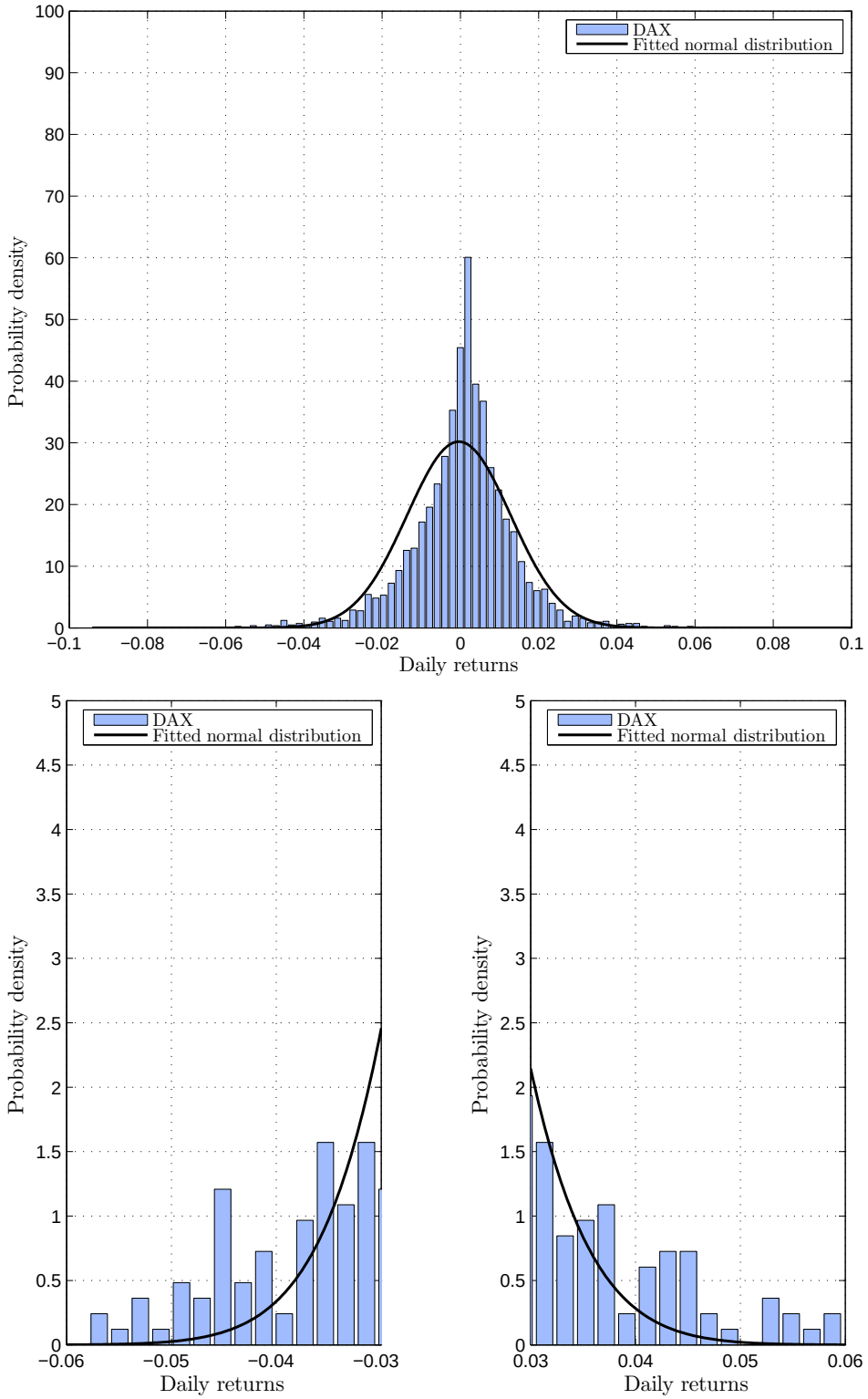

Figure 18: Empirical distribution of DAX Index (1/2000 - 2/2016) compared to the normal distribution.

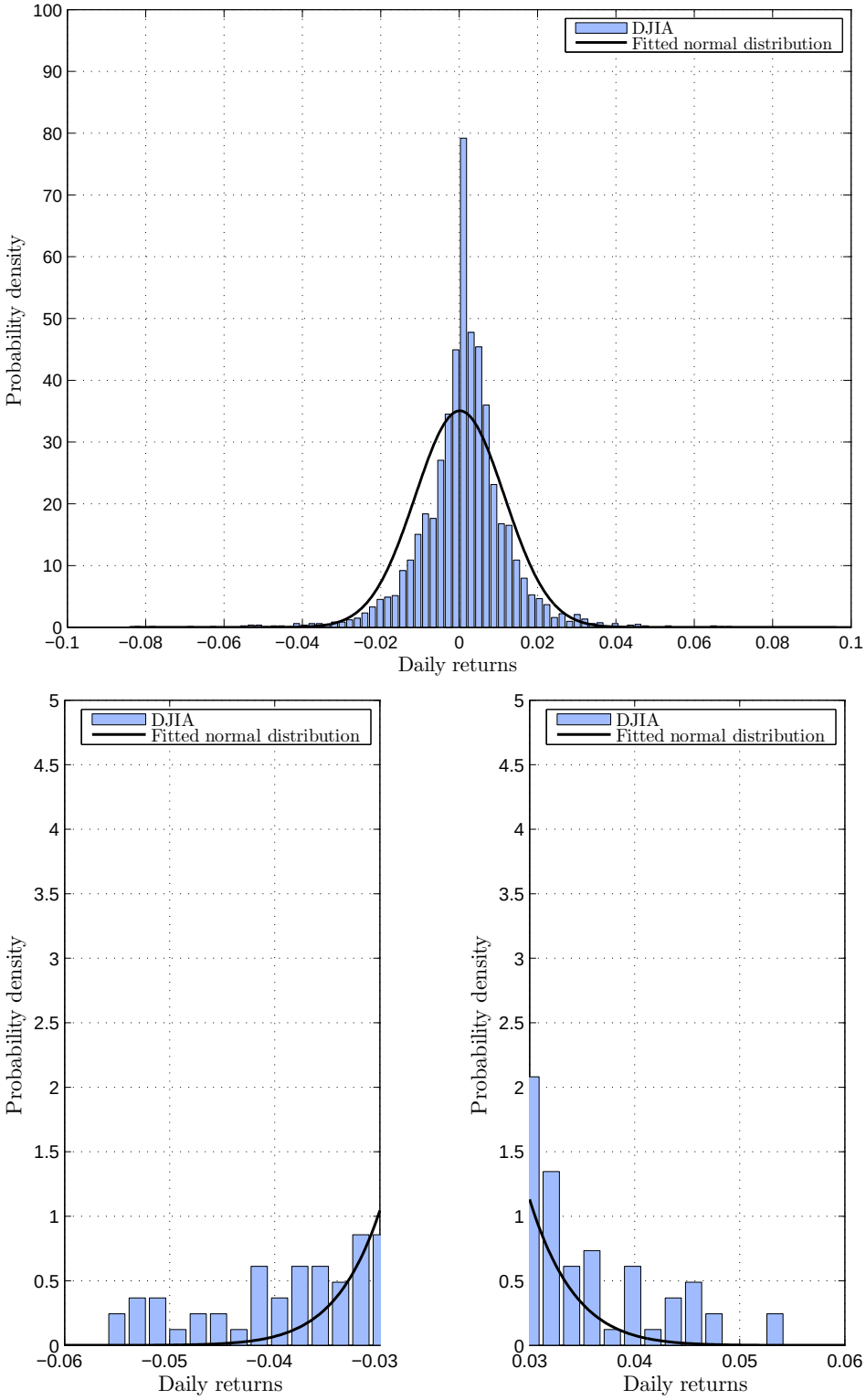

Figure 19: Empirical distribution of DJIA Index (1/2000 - 2/2016) compared to the normal distribution.

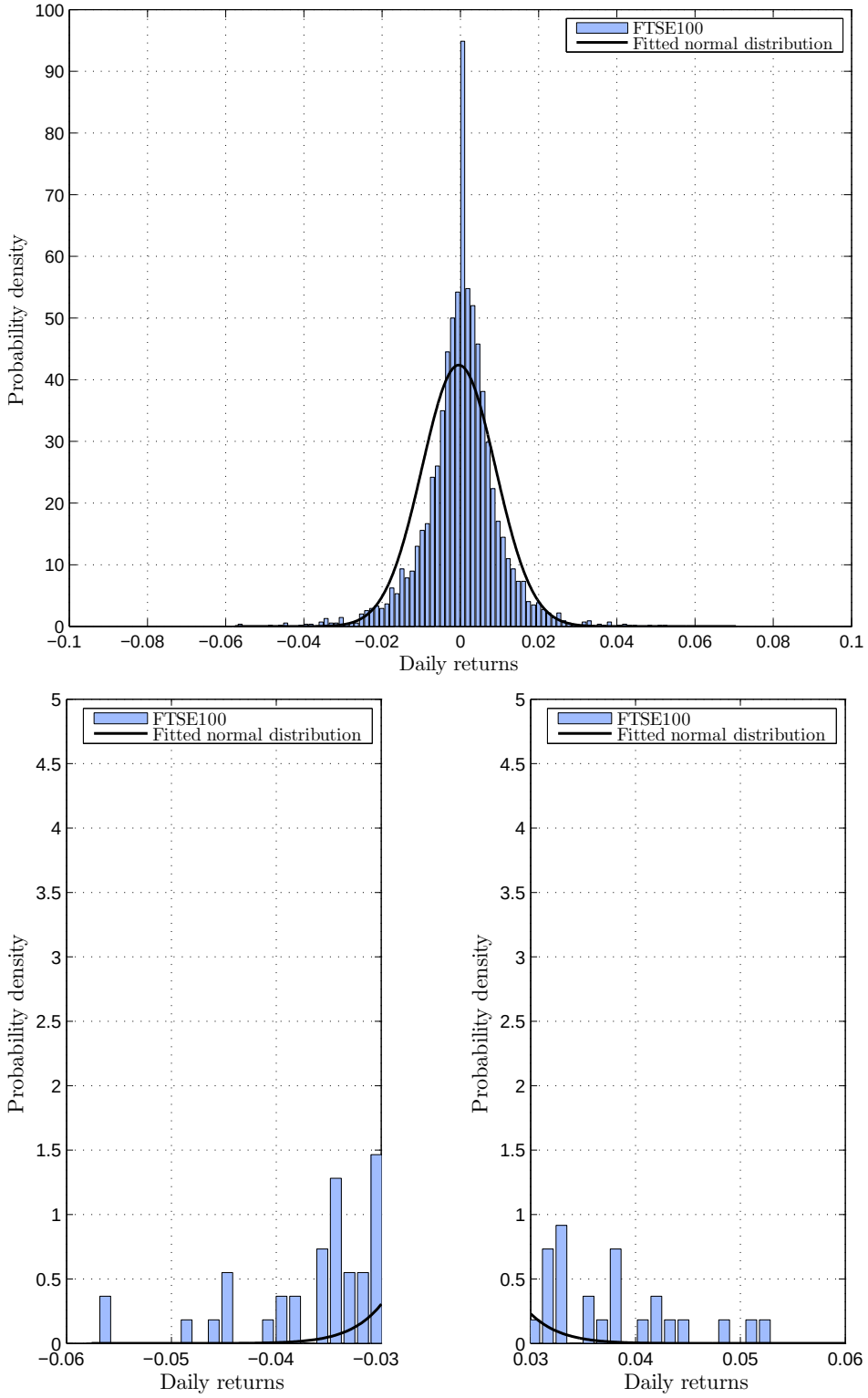

Figure 20: Empirical distribution of FTSE 100 Index (1/2000 - 2/2016) compared to the normal distribution.

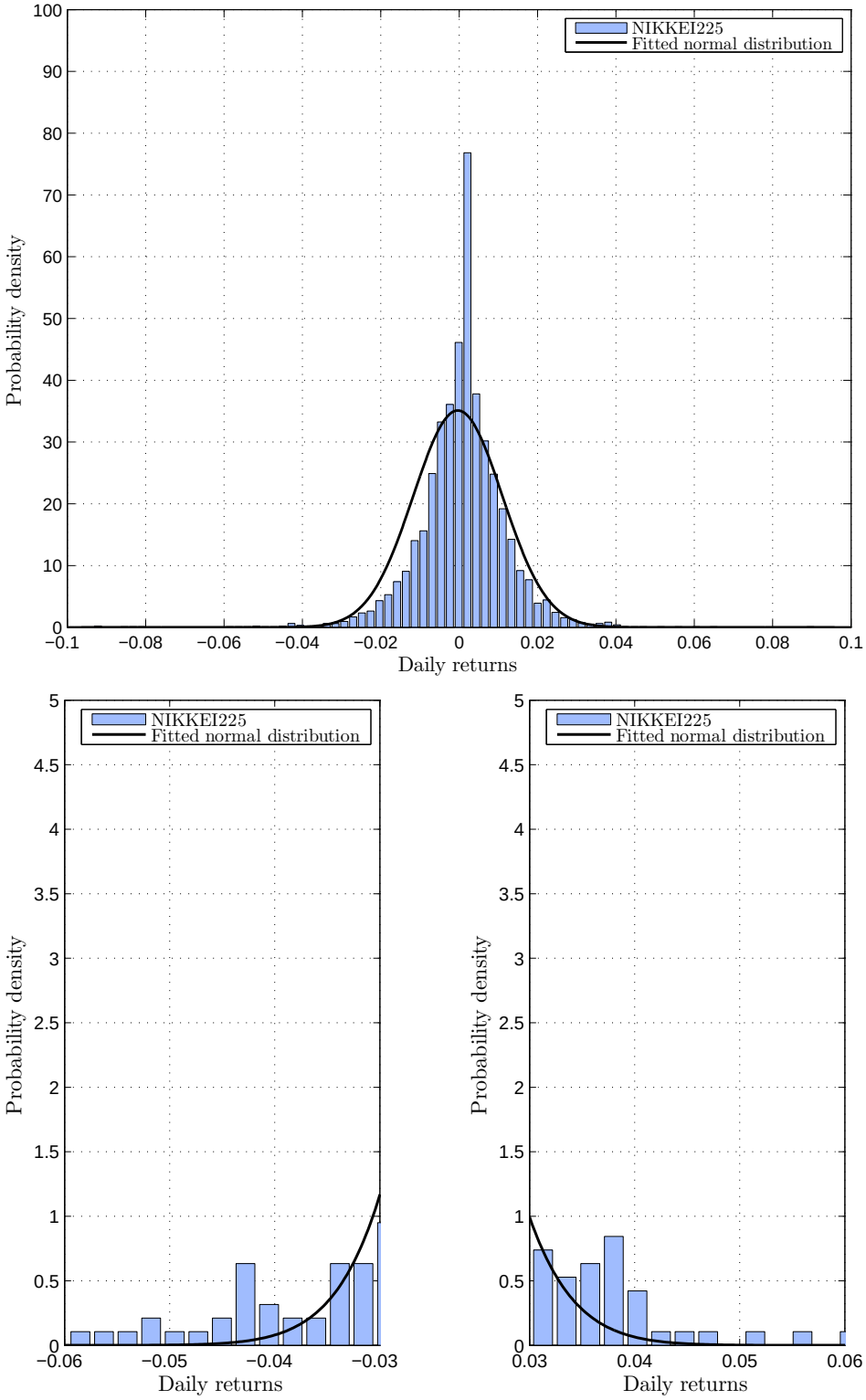

Figure 21: Empirical distribution of NIKKEI 225 Index (1/2000 - 2/2016) compared to the normal distribution.

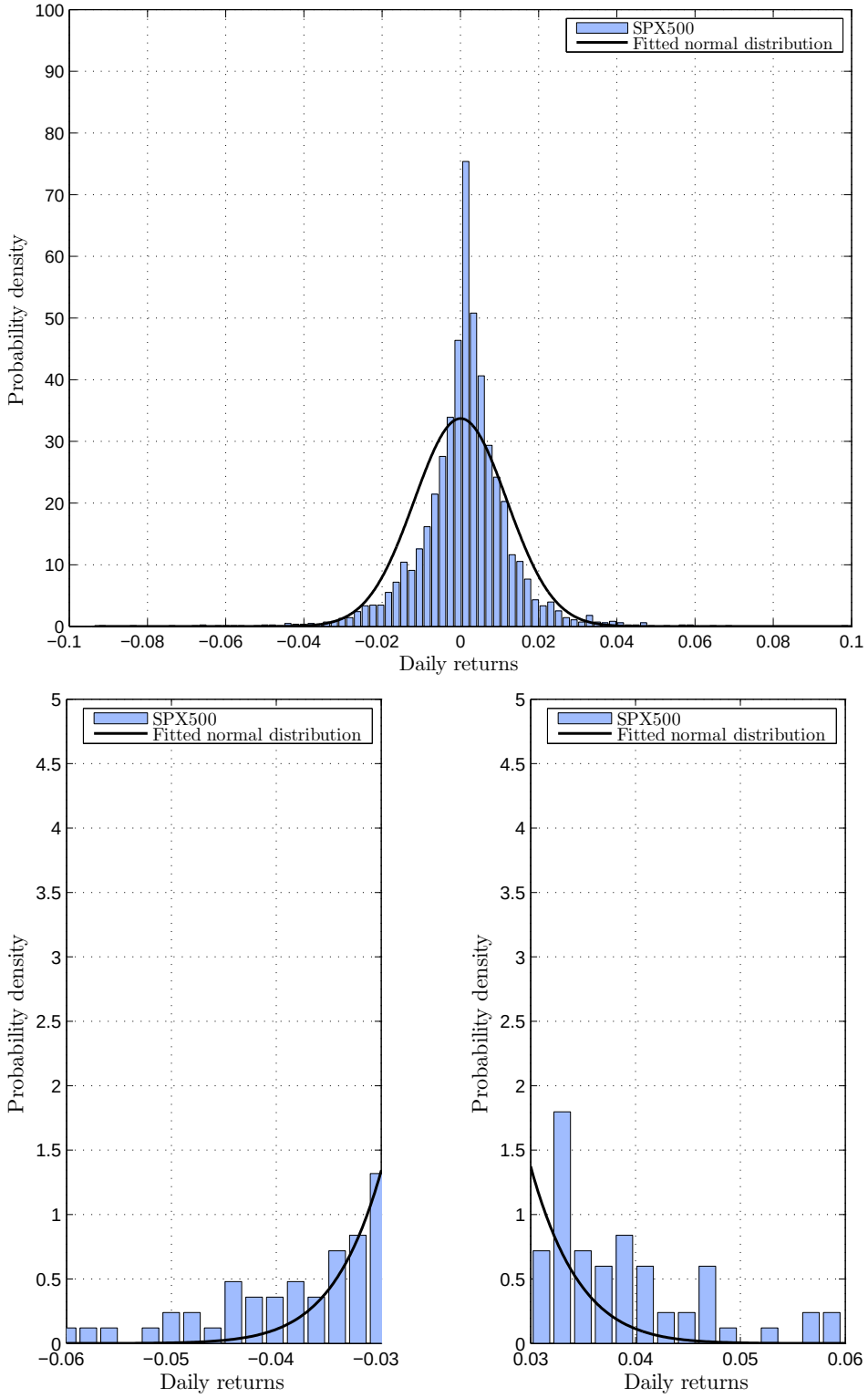

Figure 22: Empirical distribution of SPX 500 Index (1/2000 - 2/2016) compared to the normal distribution.

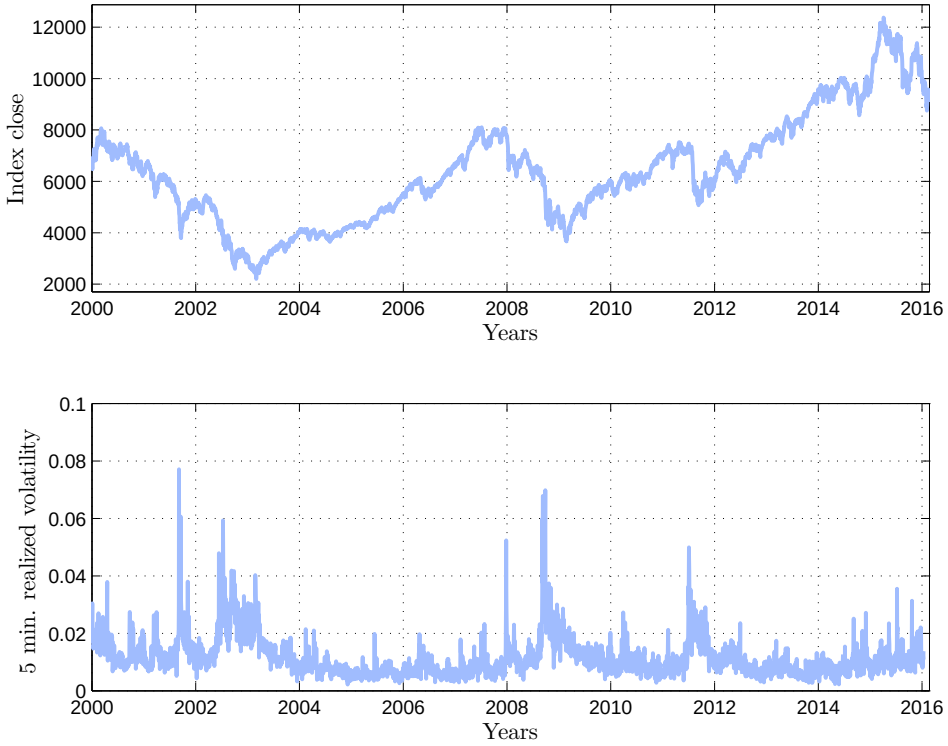

Figure 23: DAX index quotes alongside 5-min. realized volatility.

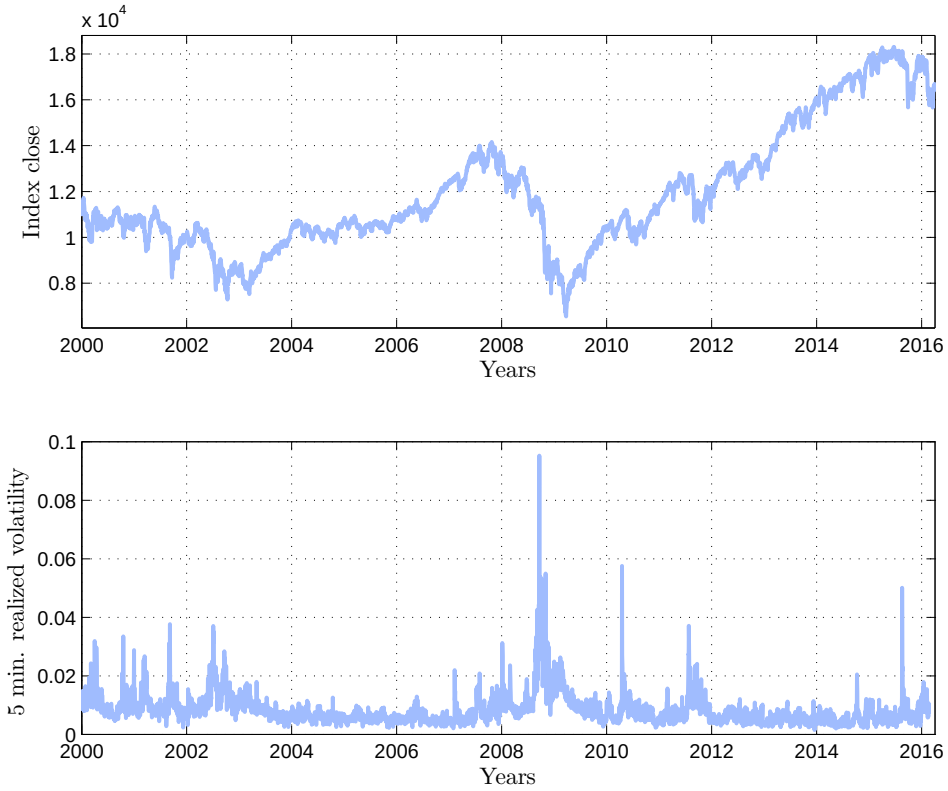

Figure 24: DJIA index quotes alongside 5-min. realized volatility.

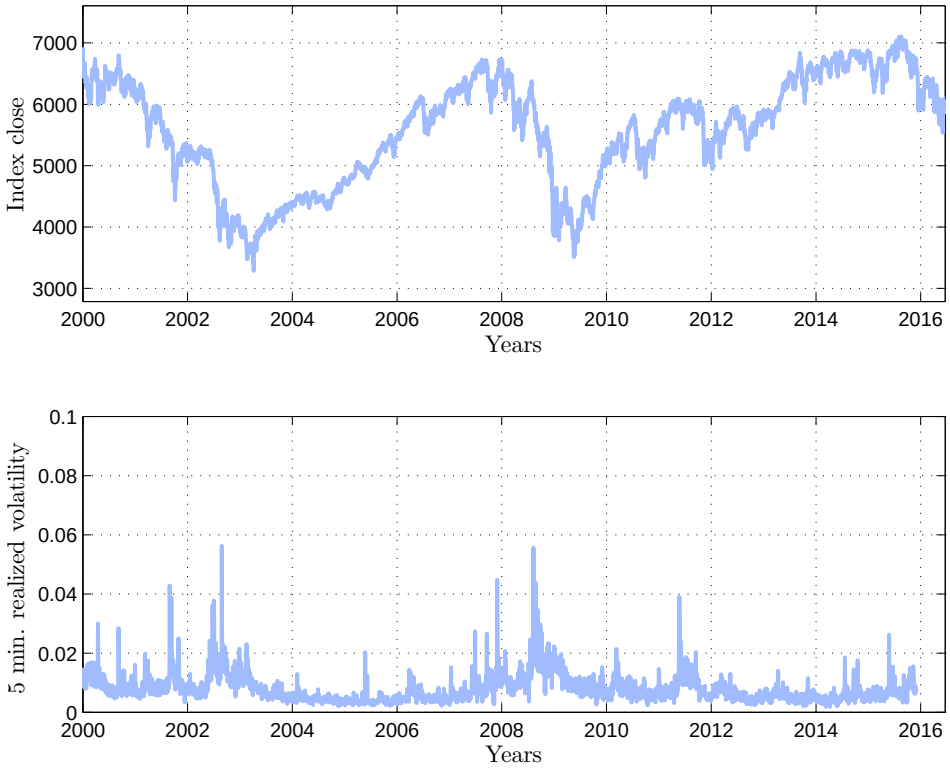

Figure 25: FTSE 100 index quotes alongside 5-min. realized volatility.

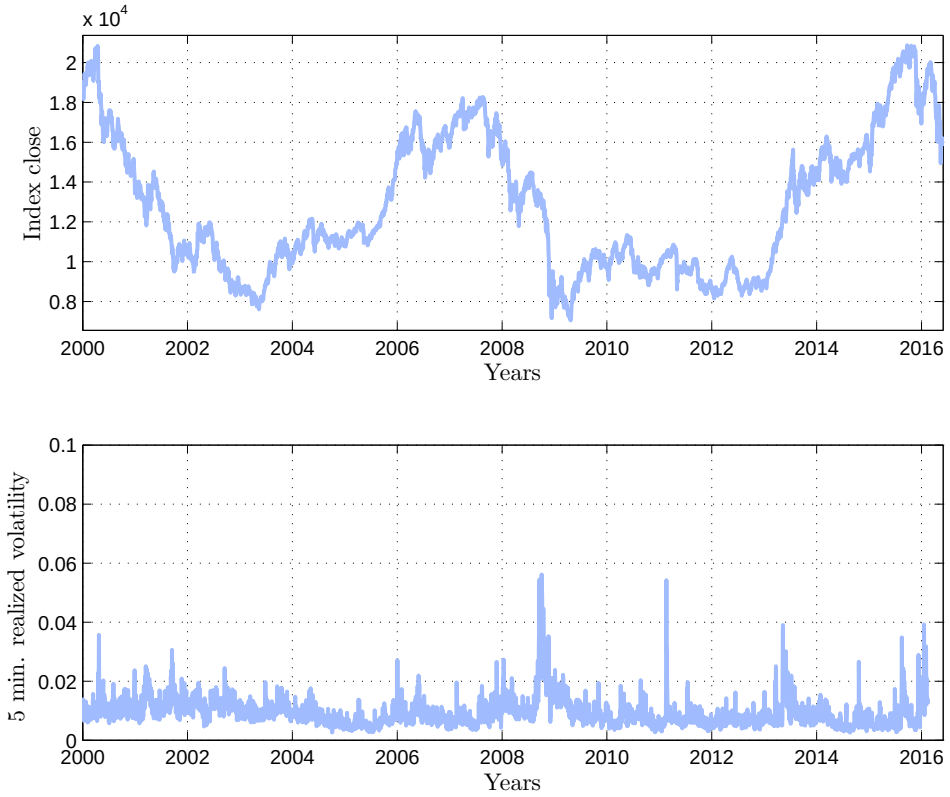

Figure 26: NIKKEI 225 index quotes alongside 5-min. realized volatility.

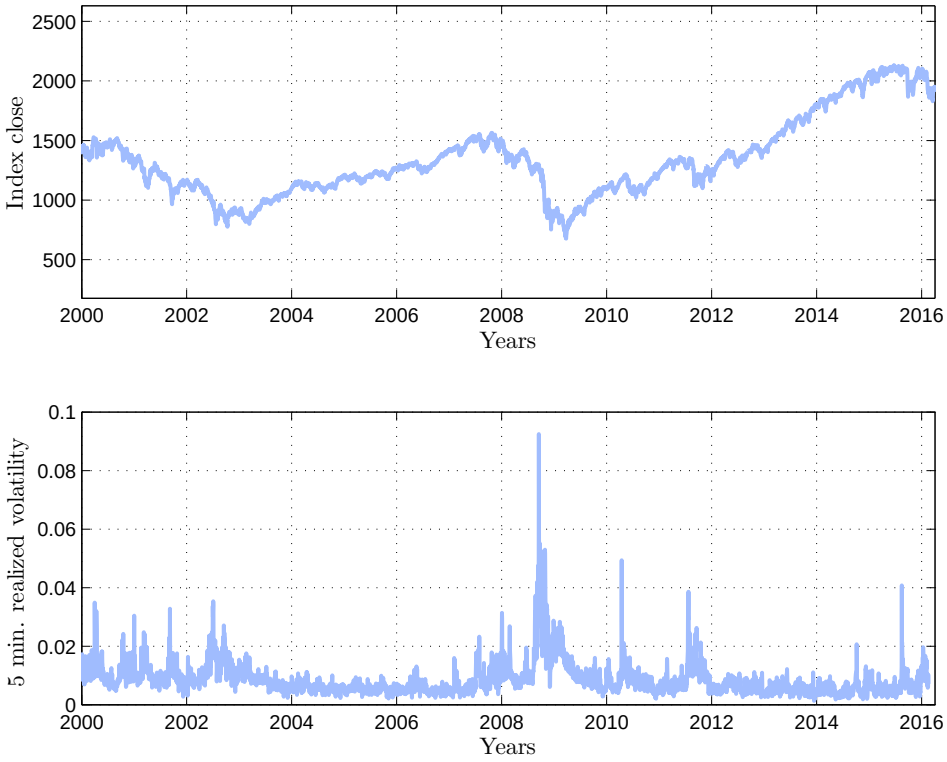

Figure 27: SPX 500 index quotes alongside 5-min. realized volatility.

A.4 QUANTILE-QUANTILE PLOTS

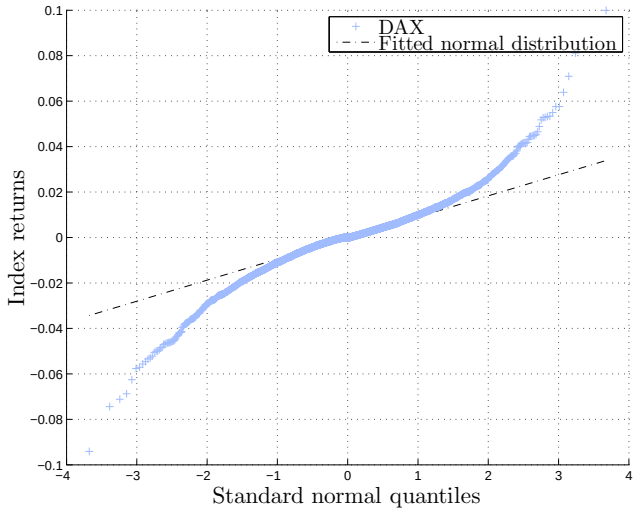

Figure 28: Quantile-quantile plot of DAX Index (1/2000 - 2/2016).

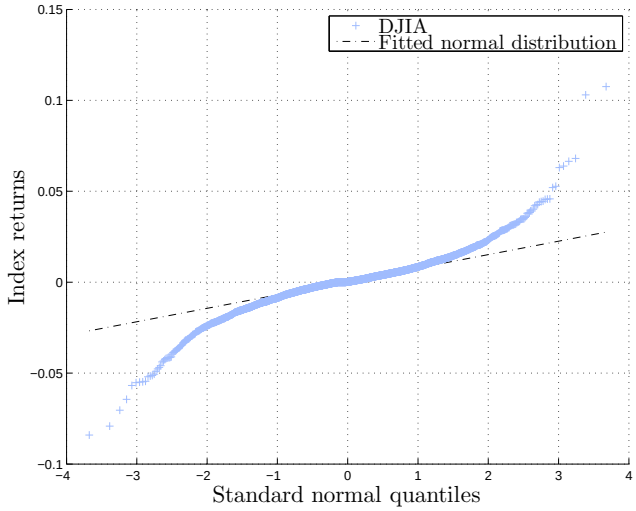

Figure 29: Quantile-quantile plot of DJIA Index (1/2000 - 2/2016).

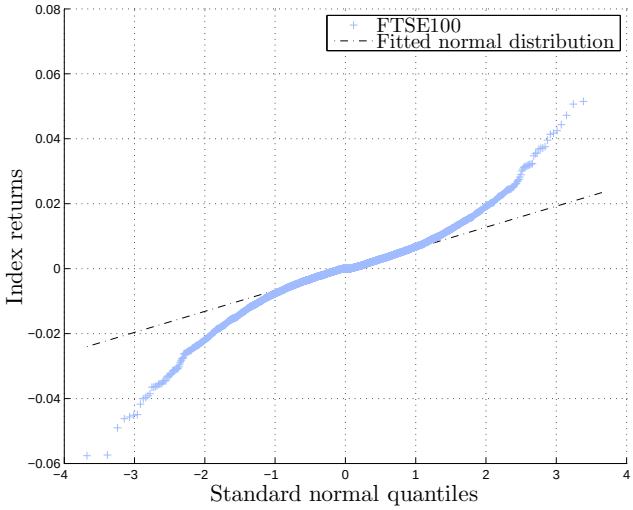

Figure 30: Quantile-quantile plot of FTSE 100 Index (1/2000 - 2/2016).

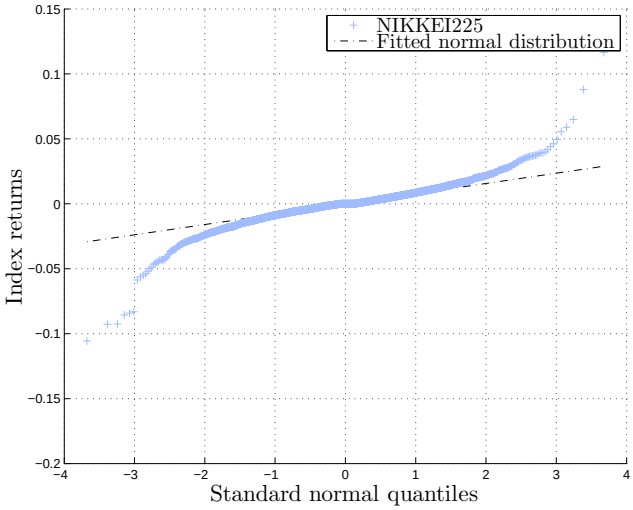

Figure 31: Quantile-quantile plot of NIKKEI 225 Index (1/2000 - 2/2016).

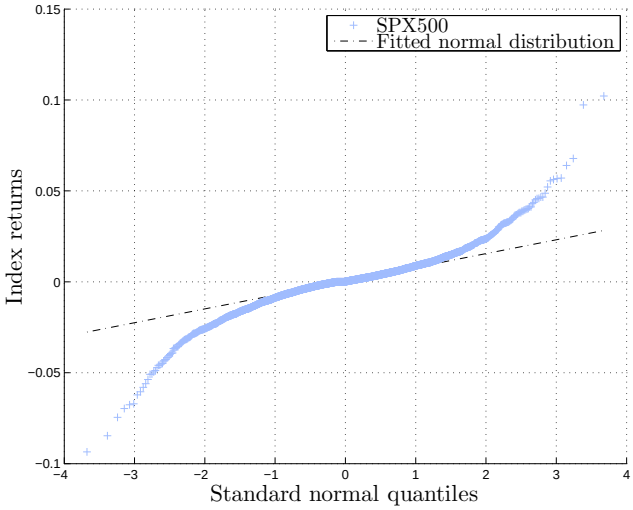

Figure 32: Quantile-quantile plot of SPX 500 Index (1/2000 - 2/2016).

B

APPENDIX B - PUBLISHED PAPERS OF THE AUTHOR

In this appendix we present published articles which were co-written by the thesis author. The references are listed in Table 4 and they are provided on the upcoming pages as they were published, i.e. without any formatting or content modification.

Table 4: List of published articles of the author

Reference	Title	Journal
Pospíšil – Sobotka (2016)	Market calibration under a long memory stochastic volatility model	Applied Mathematical Finance
Mrázek – Pospíšil – Sobotka (2016)	On calibration of stochastic and fractional stochastic volatility models	European Journal of Operational Research
Baustian – Mrázek – Pospíšil – Sobotka (2017)	Unifying approach to several stochastic volatility models with jumps	Applied Stochastic Models in Business and Industry
Merino – Pospíšil – Sobotka – Vives (2018)	Decomposition formula for jump diffusion models	International Journal of Theoretical and Applied Finance
Pospíšil – Sobotka – Ziegler (2019)	Robustness and sensitivity analyses for stochastic volatility models under uncertain data structure	Empirical Economics

The latests manuscript of the author, Merino – Pospíšil – Sobotka – Sottinen – Vives (2019), is under review and can be viewed at: https://arxiv.org/abs/1906.07101.

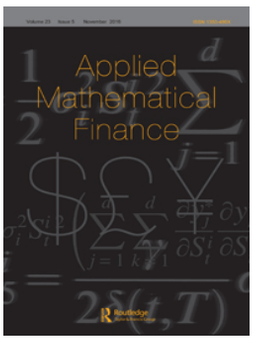

Routledge
Taylor & Francis Group

Applied Mathematical Finance

ISSN: 1350-486X (Print) 1466-4313 (Online) Journal homepage: https://www.tandfonline.com/loi/ramf20

Market calibration under a long memory stochastic volatility model

Jan Pospíšil & Tomáš Sobotka

To cite this article: Jan Pospíšil & Tomáš Sobotka (2016) Market calibration under a long memory stochastic volatility model, Applied Mathematical Finance, 23:5, 323-343, DOI: 10.1080/1350486X.2017.1279977

To link to this article: https://doi.org/10.1080/1350486X.2017.1279977

APPLIED MATHEMATICAL FINANCE, 2016
VOL. 23, NO. 5, 323–343
http://dx.doi.org/10.1080/1350486X.2017.1279977

Routledge
Taylor & Francis Group

Market calibration under a long memory stochastic volatility model

Jan Pospíšil and Tomáš Sobotka

New Technologies for the Information Society, European Centre of Excellence, University of West Bohemia, Plzeň, Czech Republic

ABSTRACT

In this article, we study a long memory stochastic volatility model (LSV), under which stock prices follow a jump-diffusion stochastic process and its stochastic volatility is driven by a continuous-time fractional process that attains a long memory. LSV model should take into account most of the observed market aspects and unlike many other approaches, the volatility clustering phenomenon is captured explicitly by the long memory parameter. Moreover, this property has been reported in realized volatility time-series across different asset classes and time periods. In the first part of the article, we derive an alternative formula for pricing European securities. The formula enables us to effectively price European options and to calibrate the model to a given option market. In the second part of the article, we provide an empirical review of the model calibration. For this purpose, a set of traded FTSE 100 index call options is used and the long memory volatility model is compared to a popular pricing approach – the Heston model. To test stability of calibrated parameters and to verify calibration results from previous data set, we utilize multiple data sets from NYSE option market on Apple Inc. stock.

ARTICLE HISTORY
Received 8 January 2015
Accepted 15 December 2016

KEYWORDS
European call option; stochastic volatility; long memory; fractional process; market calibration

1. Introduction

The purpose of this article is to revisit a jump-diffusion and fractional stochastic volatility approach proposed by Intarasit and Sattayatham (2011). Using our alternative formula for pricing European options, we present empirical calibration results and we comment on suitability of this approach.

First of all, we define a long-range dependence (LRD or equivalently a long memory) property. Let $(\Omega, \mathcal{F}, P)$ be a generic probability space that is used for all stochastic processes in this article unless explicitly stated otherwise. Let $(X_t)_{t\in\mathrm{R}^+}$ be a stationary stochastic process defined on the probability space. Then, its auto-covariance function for arbitrary real $s, t : 0 \leq s < t$ depends only on the lag $k := t - s$ and is denoted by $\gamma_X(k)$,

$$\gamma_X(k) = \mathrm{E}[(X_s - \mathrm{E}X_s)(X_{s+k} - \mathrm{E}X_{s+k})].$$

CONTACT Jan Pospíšil honik@kma.zcu.cz Univerzitní 8, 306 14 Plzeň, Czech Republic.

A stochastic process X_t is said to have a LRD if

$$\lim_{k\to+\infty} \frac{\gamma_X(k)}{Ck^{-\alpha}} = 1, \tag{1}$$

where both C and α are constants and $\alpha \in (0, 1)$. Also, the sum of auto-covariances for different lags diverges,

$$\sum_{k=1}^{+\infty} \gamma_X(k) = +\infty. \tag{2}$$

One can understand the LRD phenomenon quite intuitively. For increasing lag, the dependence might be small, but its cumulative effect is not negligible (due to (2)).

One of the first evidences of LRD in market volatility comes from Taylor (1986) and Ding, Granger and Engle (1993). In both studies, a strong evidence of autocorrelation of absolute returns is presented (even for longer lags). Authors also noticed that correlation estimates decay significantly slower for absolute returns than for the returns themselves. Breidt, Crato and De Lima (1998) used spectral tests and R/S analysis to estimate a long memory parameter for volatility of market indexes' daily returns from 1962 to 1989. To incorporate the long memory phenomenon into volatility modelling, Bollerslev and Mikkelsen (1996) suggested a modification of a well-known GARCH (Generalized Auto-Regressive Conditional Heteroskedasticity) model – fractionally integrated GARCH. The authors compare several models in terms of forecasting realized volatility and they also compare model prices of (synthetic) options. Further improvement of the ARCH-type approach to option pricing is suggested by Zumbach and Fern´Andez (2013) and Zumbach and Fern´Andez (2014). They provide an insight into construction of the risk-neutral measure and explain how to estimate the parameters, reproduce the volatility smile and the term structure of the surfaces without any calibration of the observed option prices.

Another discrete-time modelling approach that captures LRD is ARFIMA model (fractionally integrated ARMA) (Granger and Joyeux 1980). Martens, Van Dijk and De Pooter (2004) have shown, using their own study alongside similar works by various authors, that ARFIMA models can provide more satisfactory results than GARCH-type approaches. The estimates of a fractional differencing parameter for market volatility typically lie in [0.2, 0.4] which is equivalent to the Hurst exponent ranging in [0.7, 0.9]. Koopman, Jungbacker and Hol (2005) also empirically confirmed that long memory ARFIMA models seem to provide the most accurate forecasts of realized volatility. Lately, Asai, McAleer and Medeiros (2012) introduced a new correction term for the ARFIMA model with respect to volatility modelling. For an empirical comparison of ARMA and ARFIMA models, see e.g. the thesis by Čekal (2012). Beran et al. (2013), Zumbach (2013) and the references therein provide a comprehensive review of recent advances in discrete-time long memory modelling.

Many practitioners prefer continuous-time models for calibration to the whole volatility surface. Pioneering a long memory stochastic volatility (LSV), Comte and Renault (1998) introduced a modification of the Hull–White model. The stochastic

volatility process is driven by a fractional Brownian motion (fBm), i.e. a centred Gaussian process, $(B_t)_{t\in\mathbb{R}^+}$, defined via its covariance structure

$$\mathrm{E}[B_t B_s] = \frac{1}{2}\left(t^{2H} + s^{2H} - |t-s|^{2H}\right), \tag{3}$$

where H is a constant in (0,1), commonly known as the Hurst exponent. This process possesses many interesting properties, most noticeably, for $H \in (1/2, 1)$, fBm exhibits a LRD (Mandelbrot and Van Ness 1968). Comte and Renault also comment on a no-arbitrage condition which is satisfied by a market model with the suggested dynamics alongside a standard class of admissible portfolios. This differs from a situation where market dynamics is due to the fractional Black–Scholes model (i.e. stock prices follow a geometric fBm). In that case, one has to come up with a different integration theory accompanied by a different class of admissible strategies (on that matter, see e.g. Øksendal 2003). Comte, Coutin and Renault (2012) introduced a more refined model with more degrees of freedom where stochastic volatility follows a fractional CIR process. Since fBm is not a semimartingale for $H \neq 0.5$, we cannot use a well-developed Itô stochastic calculus on any of the aforementioned fractional stochastic volatility models.

Intarasit and Sattayatham (2011) came up with a new LSV model which would be subject to the main focus of this article. Authors applied theoretical results by Thao (2006) and Zähle (1998) to overcome restrictions inherited from the usage of fBm. They started with fBm in the Liouville form (Mandelbrot and Van Ness 1968),

$$B_t = \frac{1}{\Gamma(H+1/2)}\left[Z_t + \int_0^t (t-s)^{H-1/2}\mathrm{d}W_s\right],$$

where $Z_t = \int_{-\infty}^{0}\left[(t-s)^{H-1/2} - (-s)^{H-1/2}\right]\mathrm{d}W_s$ and $(W_t)_{t\in\mathbb{R}^+}$ is a standard Wiener process. The stochastic process Z_t has continuous trajectories and thus, for the sake of long memory, one can consider only the following part of B_t with the Hurst exponent $H \in (1/2, 1)$.

$$\hat{B}_t = \int_0^t (t-s)^{H-1/2}\mathrm{d}W_s. \tag{4}$$

Thao (2006) showed that one can approximate $\hat{B}_t$ by

$$\hat{B}_t^{\varepsilon} = \int_0^t (t-s+\varepsilon)^{H-1/2}\mathrm{d}W_s; \quad \hat{B}_t^{\varepsilon} \overset{L^2(\Omega)}{\to} \hat{B}_t, \tag{5}$$

as $\varepsilon \to 0^+$. Also, $\hat{B}_t^{\varepsilon}$ is a semimartingale with respect to the filtration $(\mathcal{F}_t)_{t\in\mathbb{R}^+}$ generated by the standard Wiener process W_t. Intarasit and Sattayatham (2011) proposed a jump-diffusion model with approximative fractional volatility. In this paper, we focus on similar dynamics of the stock prices that follow a system of two stochastic

differential equations which under a risk-neutral probability measure[1] take the following form,

$$\mathrm{d}S_t = rS_t\,\mathrm{d}t + \sqrt{v_t}S_t\,\mathrm{d}W_t^{(1)} + Y_tS_{t-}\,\mathrm{d}N_t, \tag{6}$$

$$\mathrm{d}v_t = -\kappa(v_t - \bar{v})\mathrm{d}t + \xi\sqrt{v_t}\,\mathrm{d}\hat{B}_t^{\varepsilon}, \tag{7}$$

where $\kappa, \bar{v}, \xi$ are model parameters such that, κ is a mean-reversion rate, $\bar{v}$ stands for an average volatility level and, finally, ξ is so-called volatility of volatility. Under the notation S_{t-}, we understand $\lim_{\tau\to t-}S_\tau$ and $(N_t)_{t\in\mathrm{R}^+}$, $\left(W_t^{(1)}\right)_{t\in\mathrm{R}^+}$ are a Poisson process and a standard Wiener process, respectively. Y_t denotes an amplitude of a jump at t (conditional on occurrence of the jump) and differential $\mathrm{d}\hat{B}_t^{\varepsilon}$ corresponds to the following integral which Thao and Nguyen (2003) defined for arbitrary stochastic process with bounded variation $(F_t)_{t\in\mathrm{R}^+}$,

$$I_t = \int_0^t F_s\mathrm{d}\hat{B}_s^{\varepsilon} := F_t\hat{B}_t^{\varepsilon} - \int_0^t \hat{B}_s^{\varepsilon}\mathrm{d}F_s - \left[F, \hat{B}^{\varepsilon}\right]_t, \tag{8}$$

provided the right-hand side integral exists in a Riemann–Stieltjes sense, while $\left[F, \hat{B}^{\varepsilon}\right]_t$ being a mixed variation of F_t and $\hat{B}_t^{\varepsilon}$.

The use of approximation $\hat{B}_t^{\varepsilon}$ instead of fBm provides several advantages. Most significantly, we are able to derive a pricing PDE using Itô calculus and standard hedging arguments. Moreover, using theoretical results of Thao and Nguyen (2003), we can transform volatility process into standard settings similarly as was shown by Intarasit and Sattayatham (2011),

$$\mathrm{d}v_t = (a\xi\varphi_t\sqrt{v_t} - \theta + \kappa v_t)\mathrm{d}t + \xi\varepsilon^a\sqrt{v_t}\,\mathrm{d}W_t^{(2)}, \tag{9}$$

where $a := H - 1/2$, $\theta := \kappa\bar{v}$ is a constant and φ_t represents an Itô integral,

$$\varphi_t = \int_0^t (t - s + \varepsilon)^{H-3/2}\mathrm{d}W_s^{(3)}, \tag{10}$$

$\left(W_t^{(2)}\right)_{t\in\mathrm{R}^+}$, $\left(W_t^{(3)}\right)_{t\in\mathrm{R}^+}$ are standard Wiener processes. To have a more realistic model of market dynamics, we also add an instantaneous correlation $\rho\colon \mathrm{E}\left[W_t^{(1)}W_t^{(2)}\right] = \rho$ to mimic the stock-volatility leverage effect. Also, we assume $W_t^{(3)}$ is stochastically independent on $W_t^{(1)}$, $W_t^{(2)}$ and the jump part $Y_tS_{t-}\,\mathrm{d}N_t$ which is yet to be defined.

2. An alternative semi-closed form solution

Up to now, we have introduced a theoretical background for the model mainly using the original research by Intarasit and Sattayatham (2011). In this section, we consider a model with dynamics (6) and (7) and we derive an alternative formula for pricing

European contracts and thereafter, we show, employing empirical data sets, that this formula can be efficiently used for applications in practise, such as a market calibration.

We utilize dynamics (6) and (7) with process N_t defined as

$$N_t = \sum_{i=1}^{P_t} Y_i, \tag{11}$$

where (Y_n) are *i.i.d.* random variables $Y_n = \exp\left\{\alpha_J + \gamma_J \psi_n\right\} - 1$, $\psi_n \sim \mathcal{N}(0,1)$ and P_t is a Poisson process with hazard rate λ.

Unlike in case of Intarasit and Sattayatham (2011), we will assume[2] that the jump part is stochastically independent on diffusion processes in market dynamics (6) and (7) which will significantly simplify the option pricing problem. Instead of solving partial integral differential equations with respect to (6) and (7), we consider the following system of market dynamics without jumps.

$$\mathrm{d}S_t = rS_t\,\mathrm{d}t + \sqrt{v_t}S_t\,\mathrm{d}W_t^{(1)}, \tag{12}$$

$$\mathrm{d}v_t = \alpha\,\mathrm{d}t + \beta\sqrt{v_t}\,\mathrm{d}W_t^{(2)}, \tag{13}$$

where the functions α and β take the following form $\alpha = \alpha(S_t, v_t, t) := \left(a\xi\varphi_t - \kappa\right)v_t + \theta$, $\beta = \beta(S_t, v_t, t) := \xi\varepsilon^a$. We will derive the valuation PDE which can be solved using the Fourier method. The price of a European option is expressed in terms of characteristic functions and to include jumps in the stock price process, it is sufficient to multiply these characteristic functions with their jump counterparts.[3] A fair price of a vanilla option V is expressed as a discounted expectation of the terminal payoff. In case of a call option, this reads

$$\begin{aligned} V_c(S_t, v_t, t) &= e^{-r\tau}\mathrm{E}\left[(S_T - K)^+\right] \\ &= S_t P_1(x_t, v_t, \tau) - e^{-r\tau}KP_2(x_t, v_t, \tau) \\ &= e^{x_t}P_1(x_t, v_t, \tau) - e^{-r\tau}KP_2(x_t, v_t, \tau), \end{aligned} \tag{14}$$

where parameters of the contract K and $\tau := T - t$ represent a strike price and time to maturity, respectively. P_1, P_2 can be interpreted as the risk-neutral probabilities that option expires in the money conditional on the value of $x_t = \ln S_t$ and finally, r is assumed to be a uniquely determined risk-free rate constant.

Applying standard hedging arguments alongside constant risk-free rate paradigm, one arrives at the initial value problem (Sobotka 2014),

$$-\frac{\partial V_c}{\partial \tau} + \frac{1}{2}v_t\frac{\partial^2 V_c}{\partial x_t^2} + \left(r - \frac{1}{2}v_t\right)\frac{\partial V_c}{\partial x_t} + \rho\beta v_t\frac{\partial^2 V_c}{\partial v_t \partial x_t} - rV_c + \frac{1}{2}v_t\beta^2\frac{\partial^2 V_c}{\partial v_t^2} + \alpha\frac{\partial V_c}{\partial v_t} = 0; \tag{15}$$

$$V_c(S_T, v_T, \tau = 0) = (S_T - K)^+. \tag{16}$$

As we would like to express probabilities P_1, P_2, we input (14) therein. Equation (15) has to be satisfied for any combination of parameters $K, r \in \mathrm{R}, \tau \in \mathrm{R}^+$ and for

any price $S_t \geq 0$. Thus, we are able to set $K = 0$, $S_t = 1$, to obtain a PDE with respect to P_1 only.

$$-\frac{\partial P_1}{\partial \tau} + \frac{1}{2}v_t \frac{\partial^2 P_1}{\partial x_t^2} + \left(r + \frac{1}{2}v_t\right)\frac{\partial P_1}{\partial x_t} + \rho\beta v_t \frac{\partial^2 P_1}{\partial v_t \partial x_t} + \frac{1}{2}v_t\beta^2 \frac{\partial^2 P_1}{\partial v_t^2} + (\alpha + \rho\beta v_t)\frac{\partial P_1}{\partial v_t} = 0. \tag{17}$$

Following similar arguments, we retrieve a PDE for P_2 only by setting $S_t = 0, K = -1$.

$$-\frac{\partial P_2}{\partial \tau} + \frac{1}{2}v_t \frac{\partial^2 P_2}{\partial x_t^2} + \left(r - \frac{1}{2}v_t\right)\frac{\partial P_2}{\partial x_t} + \rho\beta v_t \frac{\partial^2 P_2}{\partial v_t \partial x_t} + \frac{1}{2}v_t\beta^2 \frac{\partial^2 P_2}{\partial v_t^2} + \alpha\frac{\partial P_2}{\partial v_t} = 0. \tag{18}$$

Instead of solving the system of two PDEs (17) and (18) directly, we express characteristic functions $f_j = f_j(\phi, \tau)$, $j = 1, 2$. After analytical expressions for f_j are known, we can easily obtain P_j using the inverse Fourier transform,

$$P_j = \frac{1}{2} + \frac{1}{\pi}\int_0^\infty \Re\mathrm{e}\left[\frac{e^{i\phi \ln(K)} f_j}{i\phi}\right]\mathrm{d}\phi, \tag{19}$$

where $\Re\mathrm{e}(x)$ denotes a real part of a complex number x. As in the original paper by Heston (1993), we are looking for characteristic functions f_j in the form,

$$f_j = \exp\{C_j(\tau, \phi) + D_j(\tau, \phi)v_t + i\phi x\}. \tag{20}$$

As a direct consequence of the discounted version of Feynman–Kac theorem (as e.g. in Shreve 2004), f_j follows PDE (17) and (18). First, we substitute assumed expression (20) with respect to f_1.

$$\begin{aligned} -\left(\tfrac{\partial C_1}{\partial \tau} + v_t \tfrac{\partial D_1}{\partial \tau}\right)f_1 + \rho\beta v_t i\phi D_1 f_1 - \tfrac{1}{2}v_t\phi^2 f_1 + \tfrac{1}{2}v_t\beta^2 D_1^2 f_1 \\ + \left(r + \tfrac{1}{2}v_t\right)i\phi f_1 + (\alpha + \rho\beta v_t) f_1 D_1 = 0, \end{aligned} \tag{21}$$

f_1 cannot be identically equal to zero which enables us to get the following relation.

$$\begin{aligned} -\tfrac{\partial C_1}{\partial \tau} + v_t \tfrac{-\partial D_1}{\partial \tau} + \rho\beta v_t i\phi D_1 - \tfrac{1}{2}v_t\phi^2 + \tfrac{1}{2}v_t\beta^2 D_1^2 \\ + \left(r + \tfrac{1}{2}v_t\right)i\phi + (\alpha + \rho\beta v_t) D_1 = 0. \end{aligned} \tag{22}$$

Now, we are ready to substitute back for α. After rearranging terms with C_1, D_1 and factoring out v_t, we obtain the upcoming PDE,

$$v_t\left[-\frac{\partial D_1}{\partial \tau} + \rho\beta i\phi D_1 - \frac{1}{2}\phi^2 + \frac{1}{2}\beta^2 D_1^2 + \frac{1}{2}i\phi + \left(a\xi\varphi_0 - \kappa + \rho\beta\right)D_1\right] - \frac{\partial C_1}{\partial \tau} + ri\phi + \theta D_1 = 0, \tag{23}$$

where we recall that φ_t is a martingale and $\varphi_0 = \mathrm{E}\left[\varphi_t\right]$ is used. None of the terms outside brackets involves v_t; hence, we can split (23) into a system of two equations.

$$\frac{\partial D_1}{\partial \tau} = \rho\beta i\phi D_1 - \frac{1}{2}\phi^2 + \frac{1}{2}\beta^2 D_1^2 + \frac{1}{2}i\phi + \left(a\xi\varphi_0 - \kappa + \rho\beta\right)D_1; \tag{24}$$

$$\frac{\partial C_1}{\partial \tau} = ri\phi + \theta D_1, \tag{25}$$

provided $v_t > 0$ for $t : 0 \leq t \leq T$. Following the same steps, one can obtain a similar system for f_2 as well. As a result thereof, characteristic functions f_j defined by (20) have to satisfy the following system of four differential equations

$$\frac{\partial D_1}{\partial \tau} = \rho\beta i\phi D_1 - \frac{1}{2}\phi^2 + \frac{1}{2}\beta^2 D_1^2 + \frac{1}{2}i\phi + \left(a\xi\varphi_0 - \kappa + \rho\beta\right)D_1; \tag{26}$$

$$\frac{\partial D_2}{\partial \tau} = \rho\beta i\phi D_2 - \frac{1}{2}\phi^2 + \frac{1}{2}\beta^2 D_2^2 - \frac{1}{2}i\phi + \left(a\xi\varphi_0 - \kappa\right)D_2; \tag{27}$$

$$\frac{\partial C_j}{\partial \tau} = ri\phi + \theta D_j; \tag{28}$$

with respect to the initial condition

$$C_j(0, \phi) = D_j(0, \phi) = 0, \tag{29}$$

where $j = 1, 2$. The first two equations for D_j are known as the Riccati equations with constant coefficients. Once D_j are obtained, one can solve the last two ODE's by a direct integration.

First, we show how to express D_j from the Ricatti equations. For the sake of a simpler notation, we will rewrite Equations (26) and (27) using abbreviated form.

$$\frac{\partial D_j(\tau, \phi)}{\partial \tau} = A_j D_j^2 + B_j D_j + K_j, \tag{30}$$

where A_j, B_j and $K_j \in \mathrm{C}$. Let us also denote:

$$\Delta_j = \sqrt{B_j^2 - 4A_j K_j}; \quad Y_j = \frac{-B_j + \Delta_j}{2A_j}; \quad g_j = \frac{B_j - \Delta_j}{B_j + \Delta_j}.$$

Proposition 2.1: Assuming $A_j \neq 0$ for $j = 1, 2$, Ricatti equation (30) attain an analytical solution with respect to the initial condition $D_j(0, \phi) = 0$,

$$D_j(\tau, \phi) = \frac{Y_j(1 - e^{\Delta_j \tau})}{1 - g_j e^{\Delta_j \tau}}.$$

Proof: Without loss of generality, we will solve the equation for a fixed index j and for $y := D_j$, while $A := A_j, B := B_j, K := K_j$

$$y' = Ay^2 + By + K, \tag{31}$$

$$Ay' = (Ay)^2 + ABy + AK, \tag{32}$$

Since A, B and K are constant in time (or with respect to τ), we are able to substitute $v = Ay; \quad v' = Ay' + A'y = Ay'$.

$$v' = v^2 + Bv + AK, \tag{33}$$

$$-\frac{u''}{u} = -B\frac{u'}{u} + AK, \tag{34}$$

where $v = -u'/u$; $v' = -\left[u''u - (u')^2\right]/u^2 = v^2 - u''/u'$. The equation can be rewritten in the following form

$$0 = u'' - Bu' + AKu. \tag{35}$$

We are able to solve (35) explicitly.

$$\begin{aligned} u(\tau) &= I_1 \exp\left\{\frac{B - \sqrt{B^2 - 4AK}}{2}\tau\right\} + I_2 \exp\left\{\frac{B + \sqrt{B^2 - 4AK}}{2}\tau\right\} \\ &= I_1 e^{((B-\Delta)/2)\tau} + I_2 e^{((B+\Delta)/2)\tau}, \end{aligned}$$

where $I_1, I_2 \in \mathrm{R}$ are both constants can be expressed due to the initial condition:

$$\begin{aligned} u'(0) &= I_1\left(\tfrac{B-\Delta}{2}\right) + I_2\left(\tfrac{B+\Delta}{2}\right) = 0, \\ u(0) &= I_1 + I_2 = \gamma; \gamma \in \mathrm{R} - \{0\}. \end{aligned}$$

Solving the system of two linear equations, we retrieve I_1, I_2,

$$I_1 = \gamma\tfrac{B+\Delta}{2\Delta},$$

$$I_2 = -\gamma\tfrac{B-\Delta}{2\Delta},$$

and the solution $u(\tau)$,

$$u(\tau) = \gamma\left[\left(\frac{B+\Delta}{2\Delta}\right)e^{((B-\Delta)/2)\tau} - \left(\frac{B-\Delta}{2\Delta}\right)e^{((B+\Delta)/2)\tau}\right]. \tag{36}$$

To obtain $y(\tau)$, we go through steps (31)–(35) backwards. The first derivative of u takes the form

$$u' = \gamma\left[\frac{AK}{\Delta}e^{((B-\Delta)/2)\tau} - \frac{AK}{\Delta}e^{((B+\Delta)/2)\tau}\right] \tag{37}$$

and since $v = -u'/u$, v reads

$$v = \frac{-2AK\left(e^{((B-\Delta)/2)\tau} - e^{((B+\Delta)/2)\tau}\right)}{(B+\Delta)e^{((B-\Delta)/2)\tau} - (B-\Delta)e^{((B+\Delta)/2)\tau}}.$$

Using $y = v/A$, one can obtain the solution,

$$\begin{aligned} y &= \frac{-2K\left(e^{((B-\Delta)/2)\tau} - e^{((B+\Delta)/2)\tau}\right)}{(B+\Delta)e^{((B-\Delta)/2)\tau} - (B-\Delta)e^{((B+\Delta)/2)\tau}} \\ &= \frac{-2K\left(e^{((B-\Delta)/2)\tau} - e^{((B+\Delta)/2)\tau}\right)}{(B+\Delta)e^{((B-\Delta)/2)\tau}(1 - (B-\Delta)/(B+\Delta)e^{\Delta\tau})} \\ &= \frac{-2K/(B+\Delta)(1 - e^{\Delta\tau})}{1 - (B-\Delta)/(B+\Delta)e^{\Delta\tau}}. \end{aligned} \tag{38}$$

Hence, we have arrived at the expression in Proposition 2.1.

In the next step, we integrate the right-hand side of (28) for $t \in [0, \tau]$ to express C_j.

$$\begin{aligned} C_j(\tau,\phi) &= ri\phi\tau + \theta \int_0^\tau D_j(t,\phi)\mathrm{d}t \\ &= ri\phi\tau + \theta \int_0^\tau \frac{Y_j(1-e^{\Delta_j t})}{1-g_j e^{\Delta_j t}}\mathrm{d}t \\ &= ri\phi\tau + \theta Y_j \left[\tau + \int_0^\tau \frac{(g_j-1)e^{\Delta_j t}}{1-g_j e^{\Delta_j t}}\mathrm{d}t\right] \\ &= ri\phi\tau + \theta Y_j\tau - \theta Y_j \frac{g_j-1}{\Delta_j g_j}\ln\left(\frac{1-g_j e^{\Delta_j \tau}}{1-g_j}\right) \\ &= ri\phi\tau + \theta Y_j\tau - \frac{\theta}{A}\ln\left(\frac{1-g_j e^{\Delta_j \tau}}{1-g_j}\right). \end{aligned} \tag{39}$$

Characteristic functions f_j, under the original notation, take the following form

$$f_j(\tau,\phi) = \exp\Big\{C_j(\tau,\phi) + D_j(\tau,\phi)v_t + i\phi\ln(S_t) + \psi_j(\phi)\tau\Big\},$$

with

$$\begin{aligned} C_j(\tau,\phi) &= r\phi i\tau + \theta Y_j\tau - \frac{2\theta}{\beta^2}\ln\left(\frac{1-g_j e^{d_j\tau}}{1-g_j}\right), \\ D_j(\tau,\phi) &= Y_j\left(\frac{1-e^{d_j\tau}}{1-g_j e^{d_j\tau}}\right), \\ \psi_2(\phi) &= -\lambda_J i\phi\left(e^{\alpha_J+\left(\gamma_J^2/2\right)}-1\right) + \lambda_J\left(e^{i\phi\alpha_J-\left(\phi^2\gamma_J^2/2\right)}-1\right), \\ \psi_1(\phi) &= \psi_2(\phi - i), \\ Y_j &= \frac{b_j - \rho\beta\phi i + d_j}{\beta^2}, \\ g_j &= \frac{b_j - \rho\beta\phi i + d_j}{b_j - \rho\beta\phi i - d_j}, \\ d_j &= \sqrt{\left(\rho\beta\phi i - b_j\right)^2 - \beta^2\left(2u_j\phi i - \phi^2\right)}, \\ \beta &= \xi\varepsilon^{H-1/2}, \\ u_1 &= 1/2, \quad u_2 = -1/2, \quad \theta = \kappa\bar{\nu}, \quad b_1 = \kappa - (H-1/2)\xi\varphi_0 - \rho\beta, \\ b_2 &= \kappa - (H-1/2)\xi\varphi_0. \end{aligned}$$

To obtain the price of a European call, one numerically computes the integral in Equation (19). The result thereof goes into the first part of the formula, expression (14).

Table 1. Price differences for various choices of the upper integration limit in integral (19) across various parameter sets.[a]

Upper integration limit	50	100	150	200	250	300
ITM Average absolute differences	2.1×10^{-8}	2.8×10^{-8}	2.4×10^{-8}	2.5×10^{-8}	2.1×10^{-8}	2.1×10^{-8}
ITM 99-percentile differences	1.5×10^{-7}	1.6×10^{-7}	1.4×10^{-7}	1.4×10^{-7}	1.4×10^{-7}	1.4×10^{-7}
ITM Maximal absolute differences	1.1×10^{-3}	1.1×10^{-3}	1.1×10^{-3}	1.1×10^{-3}	1.1×10^{-3}	1.1×10^{-3}
ATM Average absolute differences	2.6×10^{-8}	3.3×10^{-8}	2.7×10^{-8}	2.7×10^{-8}	2.4×10^{-8}	2.3×10^{-8}
ATM 99-percentile differences	1.9×10^{-7}	2.0×10^{-7}	1.8×10^{-7}	1.9×10^{-7}	1.9×10^{-7}	1.9×10^{-7}
ATM Maximal absolute differences	1.1×10^{-3}	1.1×10^{-3}	1.1×10^{-3}	1.1×10^{-3}	1.1×10^{-3}	1.1×10^{-3}
OTM Average absolute differences	3.0×10^{-8}	3.9×10^{-8}	3.2×10^{-8}	3.2×10^{-8}	2.9×10^{-8}	2.0×10^{-8}
OTM 99-percentile differences	2.5×10^{-7}	2.6×10^{-7}	2.3×10^{-7}	2.4×10^{-7}	2.4×10^{-7}	2.5×10^{-7}
OTM Maximal absolute differences	1.5×10^{-3}	1.5×10^{-3}	1.5×10^{-3}	1.0×10^{-3}	1.0×10^{-3}	1.0×10^{-3}

[a]792,000 distinct parameter sets for each trial. The first experiment deals with in-the-money call option (ITM, moneyness 90%), second with at-the-money call (ATM) and the final one is with respect to out-of-the-money call option (OTM, moneyness 110%).
Computation using upper limit $u = 1000$ is considered as the reference price.

The main advantage of this approach lies in its tractability. In fact, only the aforementioned Fourier integral has to be dealt with by numerical procedures. Moreover, its integrand is well behaved for a wide range of model parameters (see Table 1 and Figure 1).

For numerical evaluation, one also might set a finite upper integration limit u in the integral (or apply a suitable transformation). In case of the Heston model, it has been shown that when using the alternative option pricing formula as in Gatheral (2006), even a basic choice of the upper limit, $u = 100$, can be justified. For the presented long memory model, an illustration of the price sensitivity with respect to finite values of the integration bounds is provided by Figure 1 and by Table 1. In the latter, we display average, 99% quantile and maximal absolute differences between the reference price and convenient choices of the upper limits across various model parameter sets.

The choice of the upper integration limit plays a crucial role in the task of market calibration, especially when using heuristic optimization procedures. Since all values in

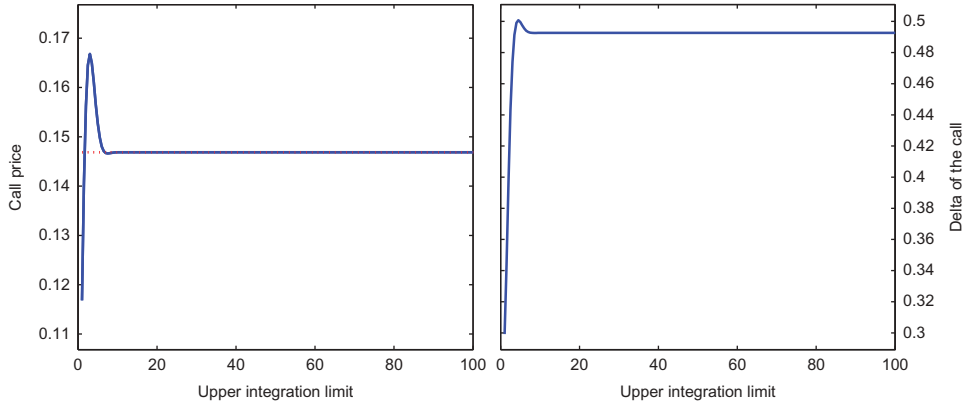

Figure 1. Numerical prices of a European call option and values of option *delta* using (19) with finite upper integration limits. Values correspond to the parameters of the contract: $S_0 = 1$, $K = 0.9$, $T = 1$, $r = 0.009$, model parameters $\kappa = 2$, $v_0 = 0.15$, $\bar{v} = 0.15$, $\xi = 0.5$, $\rho = -0.7$, $\lambda_J = 1$, $\alpha_J = -0.5$, $\gamma_J = 1$, $H = 0.7$. The computation is performed with approximating factor $\varepsilon = 10^{-5}$.

the previous experiment provided a sufficient level of precision, we focus on computational efficiency when choosing integration bounds.

3. Market calibration

In this section, we employ the previously derived formula to retrieve risk-neutral market parameters with respect to a given set of traded call options. This procedure is known as a market calibration. Another way of looking at the task can be obtained via mathematical programming. One tries to find a set of model parameters $\Theta^\star$ such that the criterion (40) is minimized.[4]

$$G(\Theta) = \sum_{i=1}^{N} w_i \left| C(S_0, K_i, T_i, r) - C^{\text{model}}(S_0, K_i, T_i, r, \Theta) \right|^p; \tag{40}$$

$$\Theta^\star = \arg \inf_{\Theta \in A} G(\Theta), \tag{41}$$

for a market that consists of N traded call contracts. We set the value of $p, p \geq 1$, and we choose appropriate weight sequence $(w_i)_{i=1,\ldots,N}$. An intuitive setting, $w_i = 1/N$ for all $i = 1, \ldots, N$ and $p = 2$, brings us to the classic least square minimization problem. Using distinct weights for each contract, we can emphasize more liquid options over the less traded contracts. For the first empirical study, we calibrate models using three choices of weights which are defined,

$$w_i^{(1)} = \frac{1}{\left| C_i^{(\text{ask})} - C_i^{(\text{bid})} \right|}, \tag{42}$$

$$w_i^{(2)} = \frac{1}{\sqrt{\left| C_i^{(\text{ask})} - C_i^{(\text{bid})} \right|}}, \tag{43}$$

$$w_i^{(3)} = \frac{1}{\left(C_i^{(\text{ask})} - C_i^{(\text{bid})} \right)^2}, \tag{44}$$

for $i = 1, \ldots, N$. $C_i^{(\text{bid})}, C_i^{(\text{ask})}$ stand for a bid price of the ith market option and ask price, respectively. Also, we assume that the price spread is strictly positive for all quoted contracts. The minimization is with respect to simple bounds (see Table 2) which are introduced to ensure that all parameters stay in their domains (e.g. we consider $H \in [0.5, 1)$).

As several authors pointed out (e.g. Mikhailov and Nögel 2003), the minimization problem (41) is typically non-convex and without a very good initial guess, it might be hard to solve using local optimization techniques only. Hence, for the task of model comparison, we utilize global procedures, a genetic algorithm (GA) and simulated annealing (SA), as well as a local trust-region method for least square problems (LSQ).

Table 2. Parameter bounds for optimization problem.

	κ	v_0	$\bar{v}$	ξ	ρ	λ_J	α_J	γ_J	H
Lower bound	0	0	0	0	−1	0	−10	0	0.5
Upper bound	50	1	1	4	1	100	5	4	0.9999

Table 3. Optimizer settings for market calibration.

	GA criterion	Value	SA criterion	Value
Evolution rules				
	Population size	60	Annealing fun	Uniform direction, temp. step length
	Elite count	20%	Initial temperature	100
	Selection distribution	Uniform	Temperature fun	Exponential
	Mutation distribution	Gaussian	Reannealing interval	100
	Crossover fun	Random binary scatter	Acceptance fun	Exp. decay[a]
Stopping rules				
	No of generations	500	Maximum iterations	–
	Time limit	–	Time limit	–
	Fitness limit	–	Fitness limit	–
	Stall generations	60	Maximum fun. evaluations	100,000
	Fun. tolerance	1e − 8	Fun. tolerance	1e − 8
	Constraint tolerance	1e − 6		
	Stall time limit	–		
	Stall test	Average change		

[a]Exponentially decaying acceptance function (acceptancesa) is defined in Matlab documentation, see also www.mathworks.com/help/gads/simulated-annealing-options.html.

Results obtained by a global heuristic optimizer may vary significantly depending on how the routine is set. Most important criteria with respect to the global optimization are of two types: evolution and stopping rules. For both GA and SA, we altered stopping rule defaults used in the Matlab's Global Optimization Toolbox. First and foremost, we did not want the solver to stop prematurely – algorithms should terminate on a Function tolerance criterion, i.e. if the value of utility function (40) declines over the successive iteration by less than a given tolerance (1e − 8). For comparison purposes, we also employed the same settings for both less complex Heston model and LSV approach. The complete evolution and stopping rules used in the upcoming experiments are listed in Table 3.

3.1. *Error measures*

In order to compare the presented long memory volatility approach with the Heston model, we evaluate these market fit criteria,

$$\mathrm{AAE}(\Theta) = \frac{1}{N}\sum_{i=1}^{N}\left|C_i - C_i^{\mathrm{model}}(\Theta)\right|; \tag{45}$$

$$\mathrm{AARE}(\Theta) = \frac{1}{N}\sum_{i=1}^{N}\frac{\left|C_i - C_i^{\mathrm{model}}(\Theta)\right|}{C_i}; \tag{46}$$

$$\mathrm{MAE}(\Theta) = \max_{i=1,2,\ldots,N}\left|C_i - C_i^{\mathrm{model}}(\Theta)\right|. \tag{47}$$

Due to varying price levels, the most interesting error measure is represented by $\mathrm{AARE}(\Theta)$ which reflects the average absolute values of relative errors. $\mathrm{ARE}(\Theta)$, on the other hand, represents the average absolute errors. We also might want to fit the calibrated surface with a preset error bound. The minimal bound that will suffice for each calibration trial is denoted by the maximal absolute error measure, $\mathrm{MAE}(\Theta)$.

3.2. *Empirical study – FTSE 100 vanilla call market*

The main data set was obtained on 8 January 2014 and consists of 82 traded call options. The underlying is FTSE 100 index, quoted at 6721.80 points. The considered prices range from 17.5 to 514.5 and the data sample includes both in-the-money (ITM), at-the-money (ATM) and out-of-the-money (OTM) calls.[5]

Using combined optimization approaches that first utilize global (heuristic) methods and then the solution is improved by a local search method, we were able to retrieve superior results for both models. For these routines, the LSV model achieved a better market fit compared to the Heston model. The lowest value of the absolute relative error was obtained for the LSV model using a GA combined with a trust region method alongside weights $w^{(3)}$. However, the results for weights $w^{(1)}, w^{(2)}$ and also for a combined SA (SA + LSQ) are almost indifferent with respect to the selected error measures.

Option premia surface, created by the Heston model with calibrated parameters, is not consistent with market prices especially for OTM calls. This is partly because of the preset weights and partly, it might be caused by a low degree of freedom of the model.

When calibrating the LSV model by using combined approaches, we retrieved values of the Hurst parameter $H \in [0.5935, 0.6654]$. This result is in line with several statistical studies on long memory estimation for realized volatility time series (e.g. Breidt, Crato, and De Lima 1998) and implied values are only slightly lower than their time-series estimates (Sobotka 2014, FTSE 100 realized volatilities, 2004–2014). All calibration errors are displayed in Table 4 and the corresponding price surfaces are depicted in Figure 2 for a combined GA and in Figure 3 for a combined SA method, respectively. We also illustrate errors retrieved only by heuristic optimization methods in Figure 4. Unlike previous calibration trials, the quality of market fit for the latter calibration is far from perfect.

3.3. *Empirical study – stability of parameters in time – AAPL call options*

We also compared the models on Apple Inc. European call options traded on NYSE MKT LLC. This time, however, we considered 21 data sets, i.e. close quotes from Apple Inc. option market for all trading days in April 2015. Each data set included at least 113

Table 4. Calibration errors for weights $w^{(1)}$, $w^{(2)}$ and $w^{(3)}$.

Weights	Model	Error measure	GA	GA + LSQ	SA	SA + LSQ
$w^{(1)}$	LSV model	AARE (%)	4.29	2.34	3.79	2.34
		AAE ()	7.33	3.27	5.52	3.27
		MAE ()	49.34	17.13	24.17	17.13
	Heston model	AARE (%)	3.72	3.36	3.67	4.43
		AAE ()	6.54	5.85	7.83	6.22
		MAE ()	30.65	30.69	32.25	29.30
$w^{(2)}$	LSV model	AARE (%)	4.61	2.34	3.01	2.34
		AAE ()	7.57	3.27	5.04	3.27
		MAE ()	35.74	17.13	25.84	17.13
	Heston model	AARE (%)	3.10	3.35	3.78	3.52
		AAE ()	6.05	5.85	6.68	5.90
		MAE ()	30.84	30.69	31.09	30.68
$w^{(3)}$	LSV model	AARE (%)	5.95	2.33	4.33	2.34
		AAE ()	12.34	3.27	9.02	3.27
		MAE ()	81.79	17.14	45.71	17.13
	Heston model	AARE (%)	5.56	5.07	6.59	4.15
		AAE ()	7.16	6.42	9.89	8.20
		MAE ()	31.07	30.83	32.49	32.30

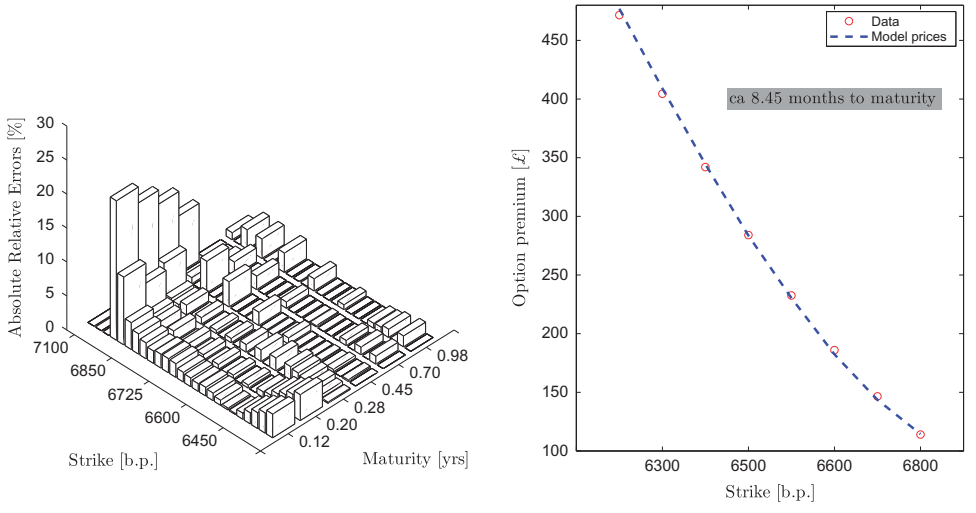

(a) Long memory SV model

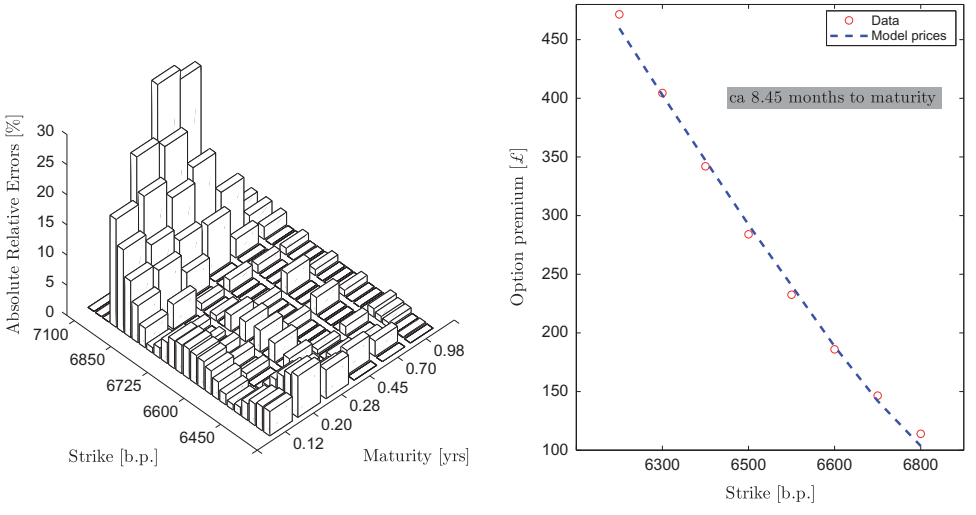

(b) Heston model

Figure 2. Calibration from FTSE 100 call option market using genetic algorithm combined with a local search method. Displayed average relative errors were obtained for weights $w_i^{(3)}$.

options (at most 212) and as in our previous experiment, we considered ITM, ATM and OTM contracts with moneyness ranging from 64.18% to 250.30% (in 30 April).[6]

Following results from previous study, we calibrated models using only GA + LSQ optimizers alongside weights $w^{(3)}$. As a main measure for model comparison, we considered weighted square errors. Namely, we compared both approaches with respect to the value of utility function $G(\Theta^\star)$ (40) where $\Theta^\star$ denotes the calibrated parameter set for a specific model.[7] Unlike in previous experiment, some data sets contained options with very low prices where both models were prone to big relative errors. Therefore, we utilized the weighted error measure rather than AARE. However, one should not compare values of

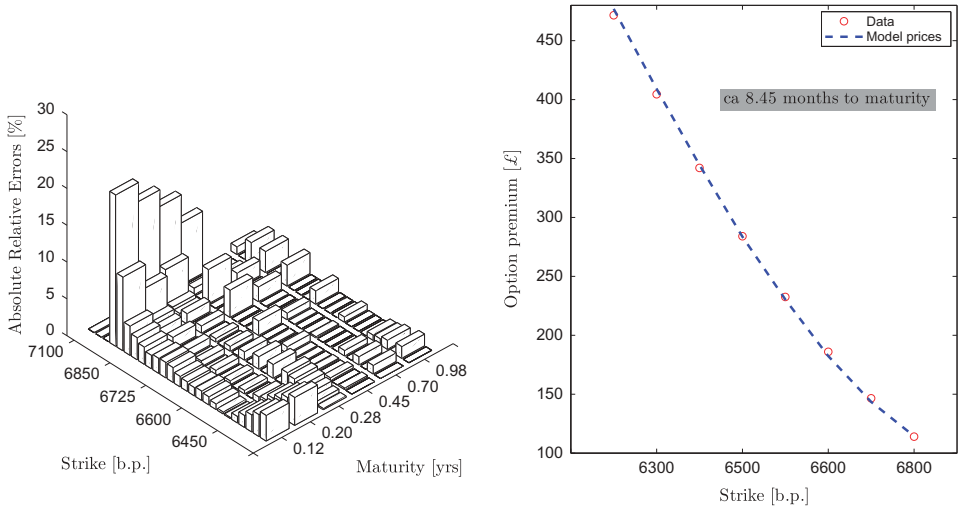

(a) Long memory SV model

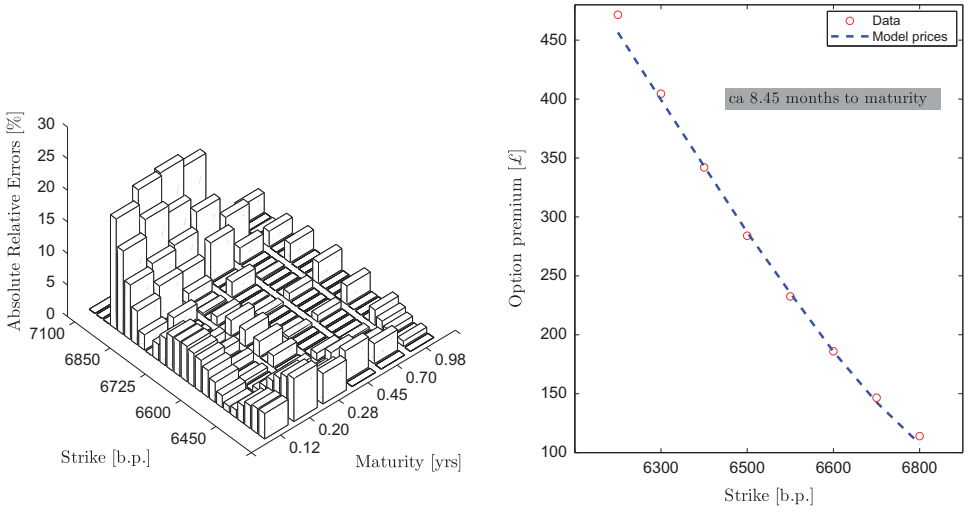

(b) Heston model

Figure 3. Calibration from FTSE 100 call option market using simulated annealing combined with a local search method. Displayed average relative errors were obtained for weights $w_i^{(1)}$.

$G(\Theta^\star)$ across different trading days – the total number of options might vary for each data set. To measure stability of the calibrated parameters over time, we employed two criteria – average absolute difference and standard deviation of parameter values.

Obtained values $G(\Theta^\star)$ ranged from 223.85 to 1711.37 and 346.61 to 1718.20 for LSV and Heston model, respectively. For 20 out of 21 data sets, Heston model was outperformed with respect to the weighted criteria – only on 29 April, we did not obtained a superior fit by LSV approach with our settings (479.51 vs. 528.85, parameters in Table 5). The lowest average absolute error (2.78%) was retrieved by LSV model on a data set from 4 April (Heston AARE – 3.37%, parameters in Table 5) and conversely,

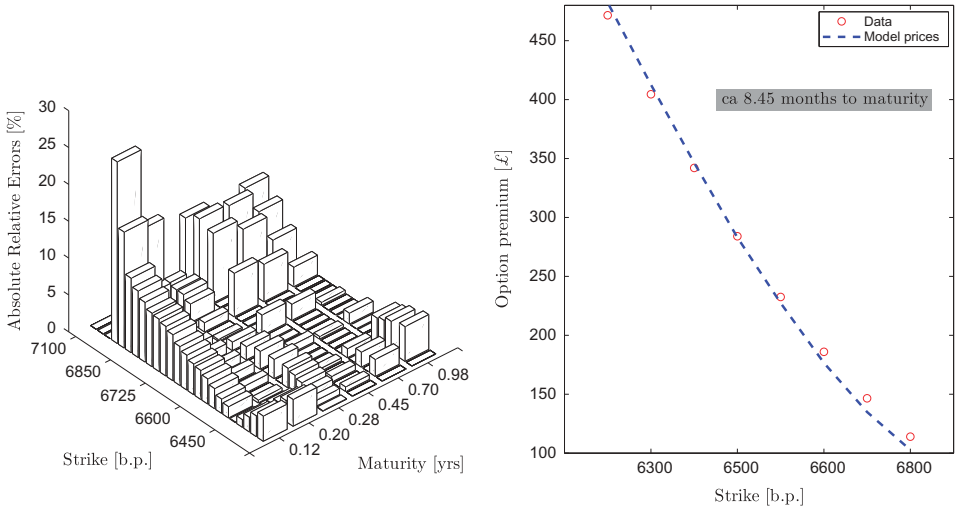

(a) Long memory SV model

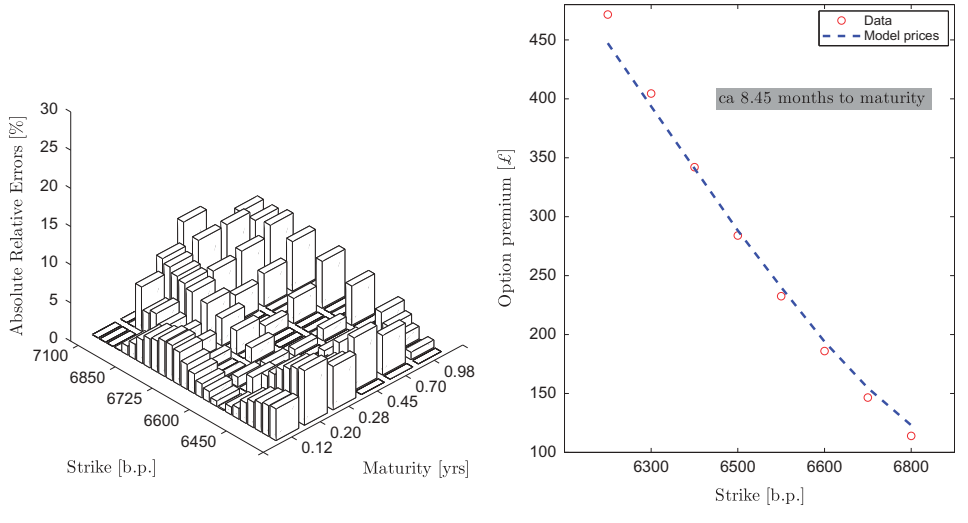

(b) Heston model

Figure 4. Calibration from FTSE 100 call option market using simulated annealing. Displayed average relative errors were obtained for weights $w_i^{(2)}$.

the worst value thereof was reached by Heston model on 20 April (5.77%). All results are conveniently listed in Table 6.

Average absolute differences alongside standard deviations of calibrated parameters are shown in Table 7. In our experiment, we managed to get similar values of the aforementioned measures for both models with respect to diffusion parameters. Evolution of v_0 and $\bar{v}$ over time is depicted by Figure 5. Calibration of LSV jump parameters, especially α_J and γ_J, provided us with more varying values compared to both diffusion parameters and the Hurst exponent. This might be due to the calibration procedure (global heuristic GA) and due to the fact that one can retrieve similar skew of

Table 5. Calibrated parameters for two trading days.

Date	κ	v_0	$\bar{v}$	ξ	ρ	λ_J	a_J	γ_J	H
	LSV model								
10 April 2015	42.5642	0.1804	0.0598	3.8964	−0.1343	0.0088	0.2545	0.1922	0.5130
29 April 2015	17.3866	0.0496	0.0611	4.0000	0.0111	0.0058	−1.0000	4.0000	0.5000
	Heston model								
10 April 2015	49.9995	0.1829	0.0632	2.3976	−0.0602				
29 April 2015	20.8354	0.0569	0.0688	2.5694	−0.1425				

Table 6. Calibration errors for weights $w^{(3)}$, Apple Inc. stock options.

	LSV model				Heston model			
Date	$G(\Theta^*)$	AARE (%)	AAE ($)	MAE ($)	$G(\Theta^*)$	AARE (%)	AAE ($)	MAE ($)
1 April 2015	**223.85**	4.16	0.32	1.42	346.61	5.49	0.34	1.50
2 April 2015	**954.71**	5.49	0.28	2.19	1368.39	4.58	0.26	1.77
6 April 2015	**441.27**	3.01	0.31	2.56	546.32	4.05	0.31	2.15
7 April 2015	**501.13**	3.42	0.31	1.28	665.78	4.33	0.35	1.81
8 April 2015	**285.26**	3.77	0.24	1.26	355.21	4.42	0.26	1.30
9 April 2015	**697.95**	3.67	0.37	1.58	715.79	4.07	0.37	1.55
10 April 2015	**313.85**	2.78	0.24	1.97	421.97	3.37	0.23	1.52
13 April 2015	**588.05**	3.15	0.24	1.25	704.98	3.31	0.26	1.27
14 April 2015	**329.33**	3.70	0.19	1.06	423.08	3.91	0.22	1.05
15 April 2015	**408.80**	3.44	0.27	1.72	542.65	3.80	0.25	1.29
16 April 2015	**363.29**	3.83	0.22	1.25	464.46	4.20	0.23	1.35
17 April 2015	**453.36**	3.06	0.20	1.14	544.60	3.20	0.21	1.08
20 April 2015	**844.47**	5.40	0.25	1.97	931.10	5.77	0.27	1.62
21 April 2015	**686.47**	5.46	0.22	1.80	856.57	4.32	0.25	1.50
22 April 2015	**1711.37**	5.03	0.42	3.15	1718.20	5.13	0.38	2.12
23 April 2015	**693.37**	3.97	0.24	1.22	700.66	3.83	0.22	1.15
24 April 2015	**998.50**	3.19	0.23	1.56	1062.61	3.21	0.22	1.37
27 April 2015	**306.37**	3.32	0.30	2.07	484.13	2.96	0.28	1.43
28 April 2015	**1043.10**	4.25	0.34	3.15	1093.86	3.76	0.35	3.60
29 April 2015	528.85	5.25	0.29	2.27	**479.51**	3.91	0.29	2.63
30 April 2015	**517.68**	3.92	0.20	1.33	527.31	3.88	0.20	1.28

Table 7. Stability of calibrated parameters.

Model	Measure	κ	v_0	$\bar{v}$	ξ	ρ	λ_J	a_J	γ_J	H
LSV	Average abs. difference	5.671	0.024	0.003	0.963	0.232	0.006	1.017	1.434	0.0596
	Standard deviation	11.110	0.049	0.003	0.976	0.294	0.006	1.331	1.459	0.084
Heston	Average abs. difference	8.744	0.0344	0.003	0.921	0.142				
	Standard deviation	10.702	0.052	0.003	0.957	0.188				

the volatility smile for different combinations of jump parameters. This shortfall can be partially improved by incorporating penalizing term in the utility function $G(\Theta)$ or by using local-search algorithm only (e.g. with initial guess from previous day calibration).

4. Summary

In the first part of the article, an alternative formula for pricing European options under a LSV model was derived. The formula is in a semi-closed form – one has to numerically evaluate a Fourier transform integral (19). For most of the observed market parameters, truncation of the upper integral bound alongside an appropriate numerical procedure leads to satisfactory results both in terms of precision (see Figure 1 and Table 1) and computational efficiency.[8]

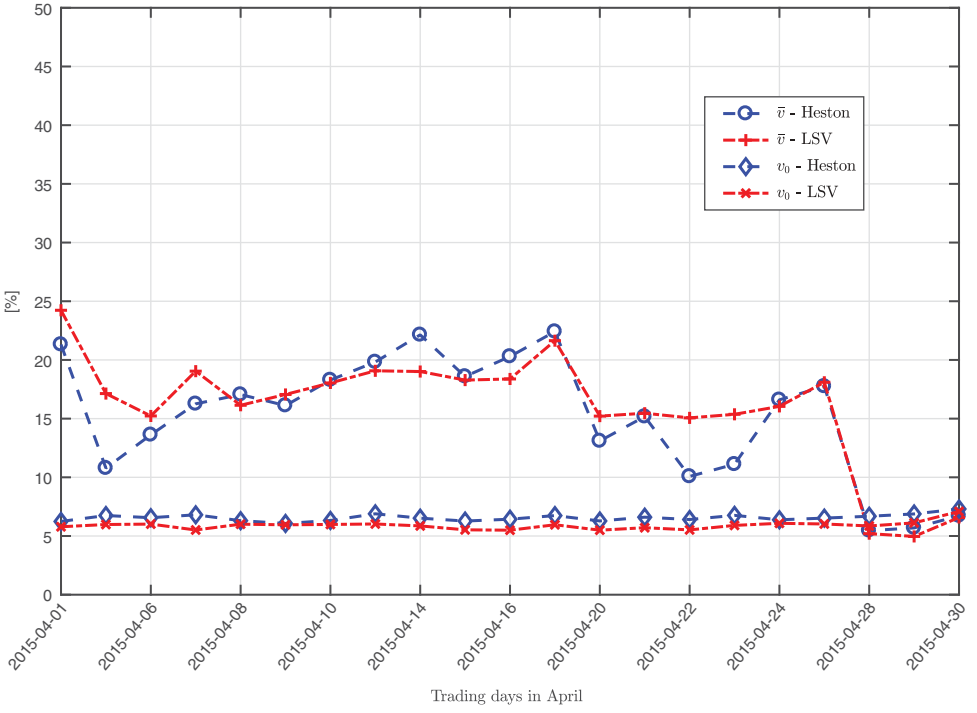

Figure 5. Evolution of calibrated parameters v_0, $\bar{v}$ for both models.

In practice, one is typically interested in a real-data performance of a particular model. To illustrate the quality of market fit, we introduced two empirical studies, both of them included a comparison with a popular approach, the Heston model. In the fist study, we utilized traded European call options on FTSE 100 index. Also, four different optimization routines and three sets of calibration weights were applied. Heuristic algorithms provided a solution that was suboptimal but (especially in case of GA) the solution represented a good initial guess for a local-search method. Since the optimization problem is non-convex, local routines, as the trust region or Levenberg–Marquardt method, need to be initialized in the vicinity of a (global) minimum.

The second study involved 21 data sets, i.e. Apple Inc. call options for all trading days in April 2015. This time, we applied GA and refined the solution by LSQ. On 20 days, LSV approach outperformed Heston model having superior (weighted) residual sum of squares as highlighted in Table 6. The inferior result on the data set from 29 April (parameters in Table 5) was obtained after GA procedure provided initial guess that for three parameters reached parameter bounds. The solution can be improved by providing better initial guess (preferably not very close to parameter bounds) or by increasing bounds. We increased an upper bound for ξ to 10 for both models,[9] Heston solution for 29 April remained the same, unlike under LSV where parameters changed to:

κ	v_0	$\bar{v}$	ξ	ρ	λ_J	α_J	γ_J	H
18.3005	0.0544	0.0649	8.3030	−0.0753	0.0046	−1.0010	0.1477	0.5000

which provided $G(\Theta) = 473.61$ and 4.15% AARE.

We managed to calibrate the LSV model using combined optimization approaches mostly with better error measures compared to the Heston model. This result was expected, since the proposed model utilizes more parameters and thus has more degrees of freedom to fit the market. However, this might not be the case of all stochastic volatility models as was shown by Duffie, Pan and Singleton (2000). The authors compare market fits of diffusion models with jumps in the underlying only to results obtained by models with jumps both in the underlying and volatility process. Although the latter approaches typically include more parameters, they might not provide a better market fit of observed option prices.

The proposed LSV model might provide better market fit compared to Heston model; however, an increased complexity of the calibration problem is the price one has to pay. To improve this issue, one might derive a pricing formula using the complex Fourier transform as suggested by Lewis (2000) for Heston model. Since calibrated parameters do change over time, one might also be interested in a time-dependent version of the LSV approach, either with piece-wise constant (Mikhailov and Nögel 2003) or functional parameters (Osajima 2007).

Another important aspect, which is out of scope of this paper, would be a comparison of the empirical and model distribution for the underlying. We commented on realized volatility time-series estimates of H which are only slightly greater than implied values obtained by calibration of the LSV approach (w.r.t. FTSE 100 index).

Notes

1. A risk-neutral probability measure for this model is not uniquely defined due to the incompleteness of the market, purely for derivatives pricing we do not need to specify it. Comments on the equivalent martingale measures for classical stochastic volatility models are available, for instance, in Sircar and Papanicolaou (1999) and references therein.
2. This assumption is taken into consideration in many jump-diffusion stock models, e.g. Bates (1996).
3. This is possible due to the stochastic independence with diffusion processes and log-normal distribution of the jumps, see Gatheral (2006).
4. In case of the presented approach, $\Theta^\star$ takes form: $\Theta^\star := \left\{\kappa^\star, v_0^\star, \bar{v}^\star, \xi^\star, \rho^\star, \lambda_J^\star, \alpha_J^\star, \gamma_J^\star, H^\star\right\}$
5. Data set obtained from OMON Screen, Bloomberg L.P. 2014.
6. Other data sets possessed slightly narrower moneyness range.
7. In fact, $G(\Theta^\star)$ represents weighted least squares of the market fit.
8. One can calibrate the model using heuristic algorithms that evaluate model prices very frequently.
9. Under Heston model, ξ represents volatility of volatility and thus, one would intuitively expect that the increased upper bound would not affect the solution. Under the LSV approach, however, vol. of vol. takes the following form, $\xi\varepsilon^{H-1/2}$ and thus, ξ might take greater values.

Acknowledgements

This work was supported by the GACR Grant 14-11559S Analysis of Fractional Stochastic Volatility Models and their Grid Implementation. Computational resources were provided by the CESNET LM2015042 and the CERIT Scientific Cloud LM2015085, provided under the programme "Projects of Large Research, Development, and Innovations Infrastructures".

Disclosure statement

No potential conflict of interest was reported by the authors.

Funding

This work was supported by the GACR Grant 14-11559S Analysis of Fractional Stochastic Volatility Models and their Grid Implementation.

References

Asai, M., M. McAleer, and M. C. Medeiros. 2012. "Modelling and Forecasting Noisy Realized Volatility." *Computation Statist Data Analysis* 56 (1): 217–230. doi:10.1016/j.csda.2011.06.024.

Bates, D. S. 1996. "Jumps and Stochastic Volatility: Exchange Rate Processes Implicit in Deutsche Mark Options." *Review of Financial Studies* 9 (1): 69–107. doi:10.1093/rfs/9.1.69.

Beran, J., Y. Feng, S. Ghosh, and R. Kulik. 2013. *Long-Memory Processes*. Heidelberg: Springer, Probabilistic properties and statistical methods.

Bollerslev, T., and O. H. Mikkelsen. 1996. "Modeling and Pricing Long Memory in Stock Market Volatility." *Journal of Econometrics* 73 (1): 151–184. doi:10.1016/0304-4076(95)01736-4.

Breidt, F. J., N. Crato, and P. De Lima. 1998. "The Detection and Estimation of Long Memory in Stochastic Volatility." *Journal of Econometrics* 83 (1–2): 325–348. doi:10.1016/S0304-4076(97)00072-9.

Čekal, M., 2012 The Effect of Long Memory Volatility on Option Pricing. Master's thesis, University of Amsterdam.

Comte, F., L. Coutin, and E. M. ´ Renault. 2012. "Affine Fractional Stochastic Volatility Models." *Annals of Finance* 8 (2–3): 337–378. doi:10.1007/s10436-010-0165-3.

Comte, F., and E. ´M. Renault. 1998. "Long Memory in Continuous-Time Stochastic Volatility Models." *Mathematical Finance* 8 (4): 291–323. doi:10.1111/mafi.1998.8.issue-4.

Cont, R. 2001. "Empirical Properties of Asset Returns: Stylized Facts and Statistical Issues." *Quantitative Finance* 1 (2): 223–236. doi:10.1080/713665670.

Ding, Z., C. W. J. Granger, and R. F. Engle. 1993. "A Long Memory Property of Stock Market Returns and A New Model." *Journal of Empirical Finance* 1 (1): 83–106. doi:10.1016/0927-5398(93)90006-D.

Duffie, D., J. Pan, and K. Singleton. 2000. "Transform Analysis and Asset Pricing for Affine Jump-Diffusions." *Econometrica* 68: 1343–1376. doi:10.1111/ecta.2000.68.issue-6.

Gatheral, J. 2006. *The Volatility Surface: A Practitioner's Guide*. Hoboken, NJ: Wiley Finance (John Wiley & Sons).

Granger, C. W. J., and R. Joyeux. 1980. "An Introduction to Long-Memory Time Series Models and Fractional Differencing." *Journal of Time Series Analysis* 1 (1): 15–29. doi:10.1111/j.1467-9892.1980.tb00297.x.

Heston, S. L. 1993. "A Closed-Form Solution for Options with Stochastic Volatility with Applications to Bond and Currency Options." *Review of Financial Studies* 6: 327–343. doi:10.1093/rfs/6.2.327.

Intarasit, A., and P. Sattayatham. 2011. "An Approximate Formula of European Option for Fractional Stochastic Volatility Jump-Diffusion Model." *Journal of Mathematics and Statistics* 7 (3): 230–238. doi:10.3844/jmssp.2011.230.238.

Koopman, S. J., B. Jungbacker, and E. Hol. 2005. "Forecasting Daily Variability of the S&P 100 Stock Index Using Historical, Realised and Implied Volatility Measurements." *Journal of Empirical Finance* 12 (3): 445–475. doi:10.1016/j.jempfin.2004.04.009.

Lewis, A. L. 2000. *Option Valuation under Stochastic Volatility, with Mathematica Code*. Newport Beach, CA: Finance Press.

Mandelbrot, B., and J. Van Ness. 1968. "Fractional Brownian Motions, Fractional Noises and Applications." *SIAM Review* 10: 422–437. doi:10.1137/1010093.

Martens, M., D. Van Dijk, and M. De Pooter, Modeling and Forecasting S&P 500 Volatility: Long Memory, Structural Breaks and Nonlinearity. (2004), Technical report TI 04–067/4, Tinbergen Institute.

Mikhailov, S., and U. Nögel (2003) Heston's Stochastic Volatility Model-Implementation, Calibration and Some Extensions., Wilmott magazine, pp. 74–79.

Øksendal, B. (2003) *Stochastic Differential Equations. An Introduction With Applications*. Sixth edition. Universitext. Springer-Verlag, Berlin. ISBN: 3-540-04758-1

Osajima, Y., The Asymptotic Expansion Formula of Implied Volatility for Dynamic SABR Model and FX Hybrid Model. (2007), Technical report, BNP Paribas Available from SSRN: http://ssrn.com/abstract=965265.

Shreve, S. E. 2004. *Stochastic Calculus for Finance. II*. New York: Springer Finance Springer-Verlag.

Sircar, K. R., and G. C. Papanicolaou. 1999. "Stochastic Volatility, Smile & Asymptotics." *Applied Mathematical Finance* 6 (2): 107–145. doi:10.1080/135048699334573.

Sobotka, T., 2014 Stochastic and fractional stochastic volatility models. Master's thesis, University of West Bohemia.

Taylor, S. 1986. *Modelling Financial Time Series*. Chichester: John Wiley & Sons.

Thao, T. H. 2006. "An Approximate Approach to Fractional Analysis for Finance." *Nonlinear Analysis: Real World Applications* 7: 124–132. doi:10.1016/j.nonrwa.2004.08.012.

Thao, T. H., and T. T. Nguyen. 2003. "Fractal Langevin Equation." *Vietnam Journal Mathematics* 30 (1): 89–96.

Zähle, M. (1998). Integration With Respect To Fractal Functions And Stochastic Calculus. I. Probability Theory Related Fields 111 (3): 333–374. doi:10.1007/s004400050171

Zumbach, G. 2013. *Discrete Time Series, Processes, and Applications in Finance*. Heidelberg: Springer Finance (Springer.

Zumbach, G., and L. Fern´Andez. 2013. "Fast and Realistic European ARCH Option Pricing and Hedging." *Quantitative Finance* 13 (5): 713–728. doi:10.1080/14697688.2012.750009.

Zumbach, G., and L. Fern´Andez. 2014. "Option Pricing with Realistic ARCH Processes." *Quantitative Finance* 14 (1): 143–170. doi:10.1080/14697688.2013.816437.

European Journal of Operational Research 254 (2016) 1036–1046

Contents lists available at ScienceDirect

European Journal of Operational Research

journal homepage: www.elsevier.com/locate/ejor

Interfaces with Other Disciplines

On calibration of stochastic and fractional stochastic volatility models

Milan Mrázek, Jan Pospíšil*, Tomáš Sobotka

NTIS – New Technologies for the Information Society, Faculty of Applied Sciences, University of West Bohemia, Univerzitní 8, Plzeň 304 14, Czech Republic

ARTICLE INFO

Article history:
Received 9 October 2015
Accepted 17 April 2016
Available online 23 April 2016

Keywords:
Fractional stochastic volatility model
Heston model
Option pricing
Calibration
Optimization

ABSTRACT

In this paper we study optimization techniques for calibration of stochastic volatility models to real market data. Several optimization techniques are compared and used in order to solve the nonlinear least squares problem arising in the minimization of the difference between the observed market prices and the model prices. To compare several approaches we use a popular stochastic volatility model firstly introduced by Heston (1993) and a more complex model with jumps in the underlying and approximative fractional volatility. Calibration procedures are performed on two main data sets that involve traded DAX index options. We show how well both models can be fitted to a given option price surface. The routines alongside models are also compared in terms of out-of-sample errors. For the calibration tasks without having a good knowledge of the market (e.g. a suitable initial model parameters) we suggest an approach of combining local and global optimizers. This way we are able to retrieve superior error measures for all considered tasks and models.

1. Introduction

In finance, stochastic volatility (SV) models are used to evaluate derivative securities, such as options. These models were developed out of a need to modify the Nobel price winning (Black & Scholes, 1973) model for option pricing, which failed to effectively take the volatility in the price of the underlying security into account. The Black Scholes model assumed that the volatility of the underlying security was constant, while SV models consider it to be a stochastic process. Among the first publications about stochastic volatility models were Hull and White (1987), Scott (1987), Stein and Stein (1991) and Heston (1993).

Later several extensions to SV models were proposed. In particular, to fit the short term prices, a model with stochastic volatility and jumps was introduced by Bates (1996), who combined approaches of Heston (1993) and Merton (1976). Furthermore, in order to capture volatility clustering phenomenon in the SV model explicitly, long memory driving process in volatility was used for example by Intarasit and Sattayatham (2011). This property is described by a long memory parameter named after hydrologist H. E. Hurst. Its value can be estimated from the realized volatility time-series as in Bollerslev and Mikkelsen (1996), Breidt, Crato, and de Lima (1998) and Martens, van Dijk, and de Pooter (2004), or it can be obtained from the calibration to the market data.

Calibration is the process of identifying the set of model parameters that are most likely given by the observed data. Heston model was the first model that allowed reasonable calibration to the market option data together with semi-closed form solution for European call/put option prices. Heston model also allows correlation between the asset price and the volatility process as opposed to Stein and Stein (1991). Although the Heston model was already introduced in 1993 and several other SV models appeared, it is nowadays still one of the most popular models for option pricing.

Many other SV models have been introduced since, including a more flexible version of the Heston model which involves time-dependent parameters. The case of piece-wise constant parameters in time is studied in Nögel and Mikhailov (2003), a linear time dependence in Elices (2008) and a more general case is introduced in Benhamou, Gobet, and Miri (2010). The later result involves only an approximation to the option price. However, Bayer, Friz, and Gatheral (2015) suggest that the general overall shape of the volatility surface does not change in time, at least to a first approximation. Hence, it is desirable to model volatility by a time-homogeneous process. Other generalizations of the Heston model with time-constant parameters include jump processes in asset price, in volatility or in both (see e.g Duffie, Pan, & Singleton, 2000).

The industry standard approach to calibration is to minimize the difference between the observed prices and the model prices. Option pricing models are calibrated to prices observed on the market in order to compute over-the-counter derivative prices or

* Corresponding author. Tel.: +420 37763 2675; fax: +420 37763 2602.
E-mail addresses: mrazekm@ntis.zcu.cz (M. Mrázek), honik@ntis.zcu.cz (J. Pospíšil), sobotkat@ntis.zcu.cz (T. Sobotka).

http://dx.doi.org/10.1016/j.ejor.2016.04.033
0377-2217/

hedge ratios. The complexity of the model calibration process increases with more realistic models and the fact that the estimation method of model parameters becomes as crucial as the model itself is mentioned by Jacquier and Jarrow (2000).

In our case, the input parameters cannot be directly observed from the market data, thus empirical estimates are of no use. It was well documented in Bakshi, Cao, and Chen (1997) that the model implied parameters differ significantly from their time-series estimated counterparts. For instance, the magnitudes of time-series correlation coefficient of the asset returns and its volatility estimated from the daily prices were much lower than their model implied counterparts.

Moreover, the information observed from market data is insufficient to exactly identify the parameters, because several sets of parameters may be performing well and provide us with model prices that are close to the prices observed on the market. This is what causes the ill-posedness of the calibration problem.

The paper is organized as follows. In Section 2 we briefly introduce the stochastic volatility models under consideration, in particular the Heston model and the approximative fractional model together with their semi-closed form solutions for vanilla options. In Section 3 we introduce the testing methodology – most importantly we disclose how we measure the model performance, how calibration tasks are formulated and we also comment in detail on the data structure. Among the considered methods there are three global optimizers, i.e. genetic algorithm (GA), simulated annealing (SA) and adaptive simulated annealing (ASA) as well as the local search method (denoted by LSQ).

In Section 4 we demonstrate how the optimization procedures can be used for the calibration problem on particular data sets. We will conclude our results in Section 5.

2. Stochastic volatility models

2.1. Heston model

Following Heston (1993) and Rouah (2013) we consider the risk-neutral stock price model:

$$dS_t = rS_t dt + \sqrt{v_t} S_t d\widetilde{W}_t^S, \tag{1}$$

$$dv_t = \kappa(\theta - v_t)dt + \sigma\sqrt{v_t} d\widetilde{W}_t^v, \tag{2}$$

$$d\widetilde{W}_t^S d\widetilde{W}_t^v = \rho\, dt, \tag{3}$$

with initial conditions $S_0 \geq 0$ and $v_0 \geq 0$, where S_t is the price of the underlying asset at time t, v_t is the instantaneous variance at time t, r is the risk-free rate, θ is the long run average price variance, κ is the rate at which v_t reverts to θ and σ is the volatility of the volatility. $(\widetilde{W}^S, \widetilde{W}^v)$ is a two-dimensional Wiener process under the risk-neutral measure $\widetilde{\mathbb{P}}$ with instantaneous correlation ρ.

Stochastic process v_t is referred to as the variance process (also known as volatility process) and it is the square-root mean reverting process, CIR process (Cox, Ingersoll, & Ross, 1985). It is strictly positive and cannot reach zero if the Feller condition $2\kappa\theta > \sigma^2$ is satisfied (Feller, 1951).

Heston SV model allows for a semi-closed form solution for vanilla option, which involves numerical computation of an integral. Several pricing formulas were added to the original one by Heston (1993) in order to overcome numerical problems that the integrand poses. The following formulation by Albrecher, Mayer, Schoutens, and Tistaert (2007) eliminates the possible discontinuities in the integrand by only simple modifications of the original formula by Heston. Let K be the strike price and $\tau = T - t$ be the time to maturity. Then the price of a European call option at time t on a non-dividend paying stock with a spot price S_t is

$$V(S, v, \tau) = SP_1 - e^{-r\tau} KP_2, \tag{4}$$

$$P_j(x, v, \tau) = \frac{1}{2} + \frac{1}{\pi}\int_0^\infty \mathrm{Re}\left[\frac{e^{-i\phi \ln(K)} f_j(x, v, \tau, \phi)}{i\phi}\right] d\phi,$$

where $x = \ln S$ and

$$f_j(x, v, \tau, \phi) = \exp\{C_j(\tau, \phi) + D_j(\tau, \phi)v + i\phi x\},$$

and where

$$C_j(\tau, \phi) = r\phi i\tau + \frac{a}{\sigma^2}\left\{(b_j - \rho\sigma\phi i - d)\tau - 2\ln\left[\frac{1 - ge^{-d\tau}}{1 - g}\right]\right\},$$

$$D_j(\tau, \phi) = \frac{b_j - \rho\sigma\phi i - d}{\sigma^2}\left[\frac{1 - e^{-d\tau}}{1 - ge^{-d\tau}}\right],$$

$$g = \frac{b_j - \rho\sigma\phi i - d}{b_j - \rho\sigma\phi i + d},$$

$$d = \sqrt{(\rho\sigma\phi i - b_j)^2 - \sigma^2(2u_j\phi i - \phi^2)},$$

for both $j = 1, 2$, where the parameters u_j, a and b_j are defined as follows:

$$u_1 = \frac{1}{2}, u_2 = -\frac{1}{2}, a = \kappa\theta, b_1 = \kappa - \rho\sigma, b_2 = \kappa.$$

Different approaches are taken in e.g. Kahl and Jäckel (2005), Lewis (2000) or Zhylyevskyy (2012). We will use here the formula by Lewis (2000), which is well-behaved and compared to the formulation by Albrecher et al. (2007) requires the numerical computation of only one integral for each call option price.

$$V(S, v, \tau) = S - Ke^{-r\tau}\frac{1}{\pi}\int_{0+i/2}^{\infty+i/2} e^{-ikX}\frac{\hat{F}(k, v, \tau)}{k^2 - ik} dk, \tag{5}$$

where $X = \ln(S/K) + r\tau$ and

$$\hat{F}(k, v, \tau) = \exp\left(\frac{2\kappa\theta}{\sigma^2}\left[qg - \ln\left(\frac{1 - he^{-\xi q}}{1 - h}\right)\right] + vg\left(\frac{1 - e^{-\xi q}}{1 - he^{-\xi q}}\right)\right),$$

where

$$g = \frac{b - \xi}{2}, \quad h = \frac{b - \xi}{b + \xi}, \quad q = \frac{\sigma^2\tau}{2},$$

$$\xi = \sqrt{b^2 + \frac{4(k^2 - ik)}{\sigma^2}},$$

$$b = \frac{2}{\sigma^2}\left(ik\rho\sigma + \kappa\right).$$

The Lewis formula (5) uses the (inverse) complex Fourier transform of the so called fundamental transform $\hat{F}(k, v, \tau)$, where k is complex-valued. Given the fundamental transform (of the corresponding pricing partial differential equation) one can obtain an option price for different particular payoff functions, not only the European call. Equivalence of the Lewis and Heston (and hence Albrecher) formulas can be found for example in Baustian, Mrázek, Pospíšil, and Sobotka (2016).

2.2. Model with approximative fractional stochastic volatility

We also consider a model with approximative fractional stochastic volatility that was motivated by Intarasit and Sattayatham (2011) and firstly introduced by Pospíšil and Sobotka (2015). Under a risk-neutral measure, the model dynamics takes the following form:

$$dS_t = (r - \lambda\beta)S_t\, dt + \sqrt{v_t} S_t\, d\widetilde{W}_t^S + S_{t-}\, dQ_t, \tag{6}$$

$$dv_t = \kappa(\theta - v_t)\, dt + \sigma\sqrt{v_t}\, d\widetilde{B}_t^{\varepsilon, H}, \tag{7}$$

where κ, θ, σ are model parameters, such that, κ is a mean-reversion rate, θ stands for an average volatility level and finally, σ is so-called volatility of volatility. Under the notation S_{t-} we understand $\lim_{k\to t-} S_k$. $(W_t^S)_{t\geq 0}$ is a standard Wiener process and $(Q_t)_{t\geq 0}$ is a compound Process with $\mathbb{E}[Q_t] = \lambda\beta t$, i.e. jumps occur with intensity λ and jump sizes are i.i.d. random variables with common mean β. Similarly to the Bates (1996) model, we will consider log-normally distributed jump sizes with mean μ_J, variance σ_J and hence with

$$\beta = \exp\left\{\mu_J + \frac{1}{2}\sigma_J^2\right\} - 1. \tag{8}$$

.

A stochastic process $(B_t^{\varepsilon,H})_{t\geq 0}$ can be formally defined as

$$B_t^{\varepsilon,H} = \int_0^t (t-s+\varepsilon)^{H-1/2} dW_s, \tag{9}$$

where H is a long-memory parameter, ε is a non-negative approximation factor (Pospíšil & Sobotka, 2015) and, as previously, $(W_t)_{t\geq 0}$ represents a standard Wiener process. Thao (2006) showed that for $\varepsilon \to 0$, $(B_t^{\varepsilon,H})_\varepsilon$ converges uniformly to a non-Markov process and H in that case coincides with the well-known Hurst parameter ranging in [0, 1]. For financial applications we are interested in a long-range dependence of volatility, therefore we consider $H \in (0.5, 1]$. Moreover, if $\varepsilon > 0$ then $B_t^{\varepsilon,H}$ is a semi-martingale (Zähle, 1998). Hence, the Itô stochastic calculus can be used when deriving an explicit model price for European options. Stochastic integral with respect to $B_t^{\varepsilon,H}$ is defined for arbitrary stochastic process with bounded variation $(G_t)_{t\geq 0}$ as (Thao & Nguyen, 2002)

$$\int_0^t G_s\, dB_s^{\varepsilon,H} := G_t B_t^{\varepsilon,H} - \int_0^t B_s^{\varepsilon,H}\, dG_s - \left[G, B^{\varepsilon,H}\right]_t, \tag{10}$$

provided the right-hand side integral exists in a Riemann–Stieltjes sense, while $[G, B^{\varepsilon,H}]_t$ being a quadratic variation of $G_t B_t^{\varepsilon,H}$.

According to Thao (2006) (Lemma 2.1) we can write the approximative fractional Brownian motion $\widetilde{B}_t^{\varepsilon,H}$ as

$$d\widetilde{B}_t^{\varepsilon,H} = (H-1/2)\psi_t dt + \varepsilon^{H-1/2} d\widetilde{W}_t^v \tag{11}$$

where $H > 1/2$ and ψ_t is a stochastic process defined by the Itô integral

$$\psi_t = \int_0^t (t-s+\varepsilon)^{H-3/2} dW_s^\psi.$$

We substitute (11) into (7) to get the market dynamics in the form,

$$dS_t = (r-\lambda\beta)S_t dt + \sqrt{v_t} S_t d\widetilde{W}_t^S + S_{t-} dQ_t, \tag{12}$$

$$dv_t = \left[(H-1/2)\psi_t\sigma\sqrt{v_t} + \kappa(\theta - v_t)\right]dt + \varepsilon^{H-1/2}\sigma\sqrt{v_t} d\widetilde{W}_t^v. \tag{13}$$

To mimic the stock-volatility leverage effect, we will also assume that both Wiener processes $\widetilde{W}_t^S$ and $\widetilde{W}_t^v$ are instantaneously correlated, i.e.

$$d\widetilde{W}_t^S d\widetilde{W}_t^v = \rho\, dt. \tag{14}$$

The above described setting is referred to as the FSV model throughout this text. In the calibration problem for the FSV model, the vector of parameters to be optimized will be $\Theta = (v_0, \kappa, \theta, \sigma, \rho, \lambda, \mu_J, \sigma_J, H)$. Their meaning is summarized in Table 1.

Pospíšil and Sobotka (2015) showed that the semi-closed formula for the European call option price V expiring at time T with pay-off $(S_T - K)^+$, where K is a strike price of the contract, has the form

$$\begin{aligned} V(S, v, \tau) &= e^{-r\tau}\mathbb{E}\left[(S_T - K)^+\right] \\ &= SP_1(S, v, \tau) - e^{-r\tau} K P_2(S, v, \tau), \end{aligned}$$

Table 1
List of FSV model parameters.

v_0	κ	θ
Initial volatility	Mean reversion rate	Average volatility
σ	ρ	λ
Volatility of volatility	Correlation coef.	Poisson intensity
μ_J	σ_J	H
Expected jump size	Variance of jump sizes	Hurst parameter

where $\tau = T - t$ is time to maturity and P_1, P_2 are risk-neutral probabilities that option expires in the money conditional on the value of S and finally r is assumed to be a uniquely determined risk-free rate constant. Pospíšil and Sobotka (2015) derived P_1, P_2 in terms of characteristic functions. Recently, a new approach to SVJD models was proposed by Baustian et al. (2016). It uses a similar techniques as Lewis used for the Heston model.

The problem of pricing an option in a model with jumps corresponds to a partial integro-differential equation (PIDE), see Hanson (2007, Theorem 7.7). Denoting $x = \ln S$ we get the PIDE for $f(x, v, \tau) = V(e^x, v, \tau)$

$$\begin{aligned} f_\tau = &-rf + (r - \lambda\beta - \frac{1}{2}v) f_x + [(H-1/2)\psi\sigma\sqrt{v} + \kappa(\theta - v)] f_v \\ &+ \frac{1}{2} v f_{xx} + \frac{1}{2}\varepsilon^{2H-1}\sigma^2 v f_{vv} + \varepsilon^{H-1/2}\rho\sigma v f_{xv} \\ &+ \lambda\int_{-\infty}^{\infty} [f(x+y, v, t) - f(x, v, t)]\varphi(y) dy, \end{aligned} \tag{15}$$

where

$$\varphi(y) = \frac{1}{\sigma_J\sqrt{2\pi}} \exp\left\{-\frac{(y-\mu_J)^2}{2\sigma_J^2}\right\},$$

$\psi = \psi_t$ and subindices denote corresponding partial derivatives, e.g. $f_{xv} = \frac{\partial^2 f}{\partial x \partial v}$, etc.

We want to apply the complex Fourier transform like in Lewis (2000, chap. 2),

$$\mathcal{F}[f] = \hat{f}(k, v, \tau) = \int_{-\infty}^{\infty} e^{ikx} f(x, v, \tau) dx$$

with the inverse transform

$$\mathcal{F}^{-1}[\hat{f}] = f(x, v, \tau) = \frac{1}{2\pi}\int_{-\infty+ik_i}^{\infty+ik_i} e^{-ikx}\hat{f}(k, v, \tau) dk,$$

where k_i is some real number such that the line $(-\infty + ik_i, \infty + ik_i)$ is in some strip of regularity depending on the restrictions given by the payoff (Baustian et al., 2016; Lewis, 2000). After the Fourier transform, PIDE (15) becomes

$$\begin{aligned} \hat{f}_\tau = &[-r - ik(r - \lambda\beta)]\hat{f} - c(k) v \hat{f} \\ &+ [(H-1/2)\psi\sigma\sqrt{v} + \kappa(\theta - v) - ik\rho\sigma v]\hat{f}_v \\ &+ \frac{1}{2}\varepsilon^{2H-1}\sigma^2 v \hat{f}_{vv} + \lambda\hat{f}[\hat{\varphi}(-k) - 1], \end{aligned} \tag{16}$$

where

$$\hat{\varphi}(k) = \exp\left\{i\mu_J k - \frac{1}{2}\sigma_J^2 k^2\right\} \tag{17}$$

and

$$c(k) = \frac{1}{2}(k^2 - ik). \tag{18}$$

Let

$$\begin{aligned} \hat{F}(k, v, \tau) = &\exp\left(-[-r - ik(r - \lambda\beta) + \lambda(\hat{\varphi}(-k) - 1)]\tau\right) \\ &\times \hat{f}(k, v, \tau). \end{aligned}$$

Then from (16) we get

$$\hat{F}_\tau = \frac{1}{2}\varepsilon^{2H-1}\sigma^2 v\hat{F}_{vv} + \left[(H-1/2)\psi_t\sigma\sqrt{v} + \kappa(\theta - v) - ik\rho\varepsilon^{H-1/2}\sigma v\right]\hat{F}_v + c(k)v\hat{F}.$$

Solution to this equation with initial condition $\hat{F}(k, v, 0) = 1$ is referred to as the fundamental solution. We are looking for the solution in the form

$$\hat{F}(k, v, \tau) = \exp(C(k, \tau) + D(k, \tau)v),$$

where C and D do not depend on v. After substitution we get

$$C_\tau + D_\tau v = \frac{1}{2}\varepsilon^{2H-1}\sigma^2 v D^2 + \left[(H-1/2)\psi\sigma\sqrt{v} + \kappa(\theta - v) - ik\rho\varepsilon^{H-1/2}\sigma v\right]D + c(k)v,$$

with initial values $C(k, 0) = D(k, 0) = 0$. We recall that $\psi = \psi_t$ is a martingale and $\psi_0 = \mathbb{E}[\psi_t] = 0$. Hence

$$v\left[-D_\tau + \frac{1}{2}\varepsilon^{2H-1}\sigma^2 D^2 - \left(\kappa + ik\rho\varepsilon^{H-1/2}\sigma\right)D - c(k)\right] - C_\tau + \kappa\theta D = 0. \tag{19}$$

Since (19) must hold for all v we can split it into a system of two equations

$$D_\tau = \frac{1}{2}\varepsilon^{2H-1}\sigma^2 D^2 - \left(\kappa + ik\rho\varepsilon^{H-1/2}\sigma\right)D - c(k), \tag{20}$$

$$C_\tau = \kappa\theta D. \tag{21}$$

Eq. (20) is a Ricatti equation and can be solved explicitly, see for example Pospíšil and Sobotka (2015, Proposition 2.1), and then we get C by integrating (21). Pricing formula for the FSV model is

$$V(S, v, \tau) = S - Ke^{-r\tau}\frac{1}{2\pi}\int_{-\infty+i/2}^{\infty+i/2} e^{-ikX}\frac{\hat{F}(k, v, \tau)}{k^2 - ik}\phi(-k)dk, \tag{22}$$

with

$$X = \ln\frac{S}{K} + r\tau,$$

$$\hat{F}(k, v, \tau) = \exp(C(k, \tau) + D(k, \tau)v),$$

$$C(k, \tau) = \kappa\theta Y\tau - \frac{2\kappa\theta}{B^2}\ln\left(\frac{1 - ge^{-d\tau}}{1 - g}\right),$$

$$D(k, \tau) = Y\frac{1 - e^{-d\tau}}{1 - ge^{-d\tau}},$$

$$Y = -\frac{k^2 - ik}{b + d},$$

$$g = \frac{b - d}{b + d},$$

$$d = \sqrt{b^2 + B^2(k^2 - ik)},$$

$$b = \kappa + ik\rho B,$$

$$B = \varepsilon^{H-1/2}\sigma,$$

$$\phi(k) = \exp\left\{-i\lambda\beta k\tau + \lambda\tau\left[\hat{\varphi}(k) - 1\right]\right\}.$$

and β is given in (8) and $\hat{\varphi}(k)$ in (17). We will use this formula in our calibration tasks below.

3. Methodology and optimization techniques

The model calibration is formulated as an optimization problem. The aim is to minimize the pricing errors between the model prices and the market prices for a set of traded options. A common approach to measure these errors is to use the squared differences between market prices and prices returned by the model, this approach leads to the nonlinear least square method

$$\inf_\Theta G(\Theta),$$

$$G(\Theta) = \sum_{i=1}^{N} w_i|v_i^\Theta(\tau_i, K_i) - v_i^*(\tau_i, K_i)|^2, \tag{23}$$

where N denotes the number of observed option prices, w_i is a weight, $v_i^*(\tau_i, K_i)$ is the observed market price of the call option and $v^\Theta(\tau_i, K_i)$ denotes the model price computed using (4), (5) or (22) and the vector of model parameters Θ.

The function G is an objective function of the optimization problem (23) and it is neither convex nor of any particular structure. It may have more than one global minimum and it is not possible to tell whether a unique minimum can be reached by gradient based algorithm. When searching for the global minimum, a set of linear constraints must be also added to the problem, because of the parameters values. For example in Heston SV model, ρ represents correlation coefficient and thus ρ needs to only attain values within the interval $[-1, 1]$.

Local deterministic algorithms can be used to solve the calibration problem, but there is significantly high risk for them to end up in a local minimum, also initial guess needs to be provided for them, which appears to affect the performance of local optimizers severely.

Different take on the calibration is represented by the regularization method. Penalization function, e.g., $f(\Theta)$ such that

$$\inf_\Theta G(\Theta) + \alpha f(\Theta)$$

is convex, is added to the objective function (23), which enables the usage of gradient based optimizing procedures. This method yields another parameter to be estimated α, which is called regularization parameter. More details on this approach can be seen in Cont and Hamida (2005).

3.1. Considered algorithms

Facing the calibration problem (23), we consider both global and local optimizers for the calibration of models to the real market data. Global optimizers are represented by genetic algorithm (GA), simulated annealing (SA) and adaptive simulated annealing (ASA). GA and SA are available in MATLAB's Global Optimization Toolbox,[1] for ASA there exists a MATLAB gateway routine[2] to Lester Ingber's ASA software.[3]

Genetic algorithm is inspired by the natural selection, the process that drives biological evolution. GA repeatedly modifies a population of individual solutions to the minimization problem. At each iteration individuals are selected at random from the current population to become parents and uses them to produce their children, the next generation. The same individual can appear more than once in the population. Populations in successive generations then lead down to an optimal solution – a global minimum. Based on empirical trials, we chose the size of the population to be 100 and the number of generations to be 500. In Heston case, number of variables in the fitness (objective) function (23) is 5, i.e. the population is represented by a 100-by-5 matrix. In FSV case it is 100-by-9 matrix.

To create a new generation from the current population, GA uses three types of rules. In our case we used a stochastic uniform *selection*, heuristic *crossover* (positive preference of the parent with higher fitness) and a Gaussian distribution for *mutations*.

[1] mathworks.com/help/gads, functions `ga()` and `simulannealbnd()`.
[2] ssakata.sdf.org/software, function `asamin()`.
[3] ingber.com/#ASA.

The algorithm stops when one of the stopping criteria is met, either the maximum number of generations is reached or if the average relative change in the best fitness function value is less than a specified tolerance, we used the order of `1e-12`.

Simulated annealing, first introduced by Metropolis, Rosenbluth, Rosenbluth, Teller, and Teller (1953), is a an optimization method inspired by the physical process of cooling down a hot metallic material. This process is called annealing and during the slow process of cooling a minimum energy structure is reached. At each iteration of the SA algorithm, a new point is randomly generated. The distance of the new point is based on a given probability distribution with a step-size proportional to the a parameter called "temperature". SA accepts both new points that lower the objective function, as well as points that raise the objective function (to avoid a possible trap in local minima). An annealing schedule is selected to decrease the temperature at each iteration step. Similarly to the physical real process of annealing, the chances of finding an optimal solution are higher when the rate of temperature decrease is slower. Price paid is the longer annealing time, and hence the computational cost.

Adaptive simulated annealing introduces an annealing schedule for temperature that is decreasing exponentially. The proposed re-annealing Ingber (1989) also permits adaptation to changing sensitivities in the multi-dimensional parameter-space. According to Ingber, re-annealing with adaptation is faster than fast Cauchy annealing and much faster than Boltzmann annealing. ASA software has over 100 options to provide robust tuning of our optimization problem. Their complete description goes beyond the scope of this article. Only slight modifications to the default option values lead to good optimization results mentioned below.

Although global optimizers can give us a reasonably good minimum, the value of the objective function can be further reduced by applying a local minimizer. This approach – a combination of global and local minimizers – approved to be the most efficient optimization strategy. Local optimizers can perform very well on their own when looking for the local minima, but a choice of initial starting point is crucial and obtained results can be very sensitive to this choice.

Local search method (denoted by LSQ) for nonlinear least squares problems is available in MATLAB's Optimization Toolbox[4] as function `lsqnonlin()` that implements the Gauss–Newton trust-region-reflective method with the possibility of choosing the Levenberg–Marquardt algorithm. Next to MATLAB, it is also possible to use the MS Excel's solver that implements generalized reduced gradient method. Although it has been shown that MS Excel's solver can perform calibration tasks well for the Heston model (Mrázek, Pospıšil, & Sobotka, 2014), we excluded it from our tests due to computational inefficiency. Recently we also performed the optimization using the variable metric methods for nonlinear least squares as they are introduced in Lukšan and Spedicato (2000), but we abandoned the results here since for large values of the utility function this method behaved badly and for the values that were close to the minima (for example those obtained from the global optimizers) the performance was comparable to the Gauss–Newton method.

3.2. Measured errors

As a criterion for the performance evaluation of the optimizing methods we were recording the following errors:

$$\mathrm{AARE}(\Theta) = \frac{1}{N}\sum_{i=1}^{N}\frac{|v_i^{\Theta} - v_i^*|}{v_i^*}; \tag{24}$$

$$\mathrm{MARE}(\Theta) = \max_i \frac{|v_i^{\Theta} - v_i^*|}{v_i^*} \tag{25}$$

for $i = 1, \ldots, N$. MARE denotes maximum absolute value of relative error and AARE is the average of the absolute relative error across all strikes and maturities.

3.3. Considered weights

Weights in (23) are denoted by w_i. It makes sense to put the most weight where the most liquid quotes are on the market, which is usually around ATM. We employed the bid ask spreads $\delta_i > 0$ with our market data and aimed to have the model prices close to the mid prices, that are considered as the market prices V_i^*. Another approach might be to set weight function according to the Black–Scholes Vega Greek. The main idea behind this approach lies in the interpretation of obtained residuals – one can consider them as a first order approximation to implied volatility errors, see Christoffersen, Heston, and Jacobs (2009). We decided not to limit ourselves with just one choice for the weight function, but to test more of these and explore any influence on the results caused by the particular choice of the weight function. The weights are denoted by capital letters A, B, C, D and we also compare the results for the uniform weights E.

$$\text{weight A:} \quad w_i = \frac{|\delta_i|^{-1}}{\sum_{j=1}^{N}|\delta_j|^{-1}}, \tag{26}$$

$$\text{weight B:} \quad w_i = \frac{\delta_i^{-2}}{\sum_{j=1}^{N}\delta_j^{-2}}, \tag{27}$$

$$\text{weight C:} \quad w_i = \frac{\delta_i^{-1/2}}{\sum_{j=1}^{N}\delta_j^{-1/2}}, \tag{28}$$

$$\text{weight D:} \quad w_i = \frac{\mathrm{Vega}_i^2}{\sum_{j=1}^{N}\mathrm{Vega}_i^2}, \tag{29}$$

$$\text{weight E:} \quad w_i = \frac{1}{N}. \tag{30}$$

For weights A–C the following holds: the bigger the spread the less weight is put on the particular difference between the model price and the market price (mid price) during the calibration process. The weights are also normalized, which does not effect obtained results, however one can easily compare values of the utility function (23) for different weights. Weights of each contract are available as a supplementary material of Pospíšil and Sobotka (2016).

3.4. In-sample vs. Out-sample data

Two market data set were used for empirical comparison of the models and algorithms:

- 97 ODAX calls traded on March 18, 2013 ranging from 86.5 percent to 112.0 percent moneyness across 5 maturities from ca. 13.5 weeks to 1.76 years;
- 107 ODAX calls traded on March 19, 2013 ranging from 88.5 percent to 112.2 percent moneyness across 6 maturities from ca. 13.4 weeks to 1.75 years.

Both data sets were obtained using Bloomberg's Option Monitor and they comprise of call contracts on the Deutsche Boerse AG German Stock Index (DAX). A systematic illustration of the data structure is conveniently shown in Fig. 1. As the risk-free rate we took the corresponding EURIBOR rate. The primary data set was used only to compare the in-sample calibration errors defined by (24) and (25) respectively. The larger data set was used for

i. out-of-sample comparison,
ii. computation of prediction errors.

[4] mathworks.com/help/optim.

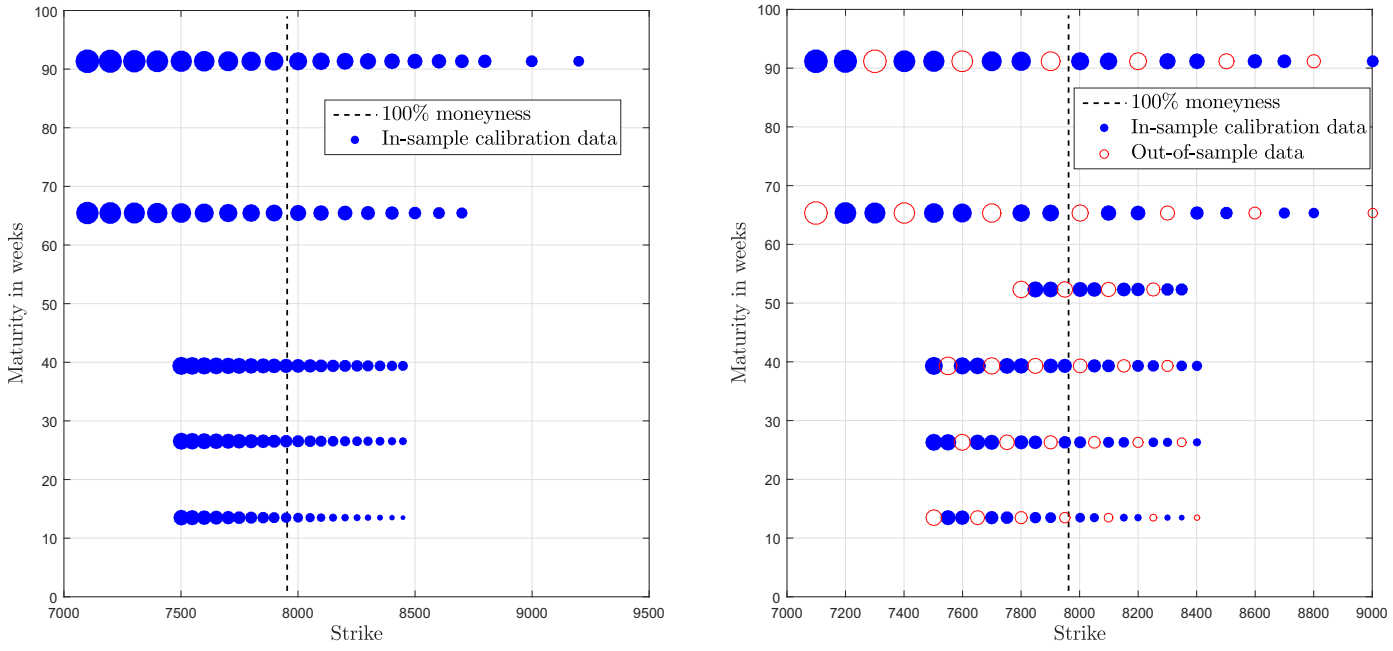

Fig. 1. Option price structure in the strike/maturity plane for the primary data set (18/3/2013) on the left and for the secondary set (19/3/2013) on the right side of the figure respectively. The center of each circle corresponds to the strike/maturity parameters of the traded contract, circle diameter is proportionate to the option premium. Data source: Bloomberg Finance L.P.

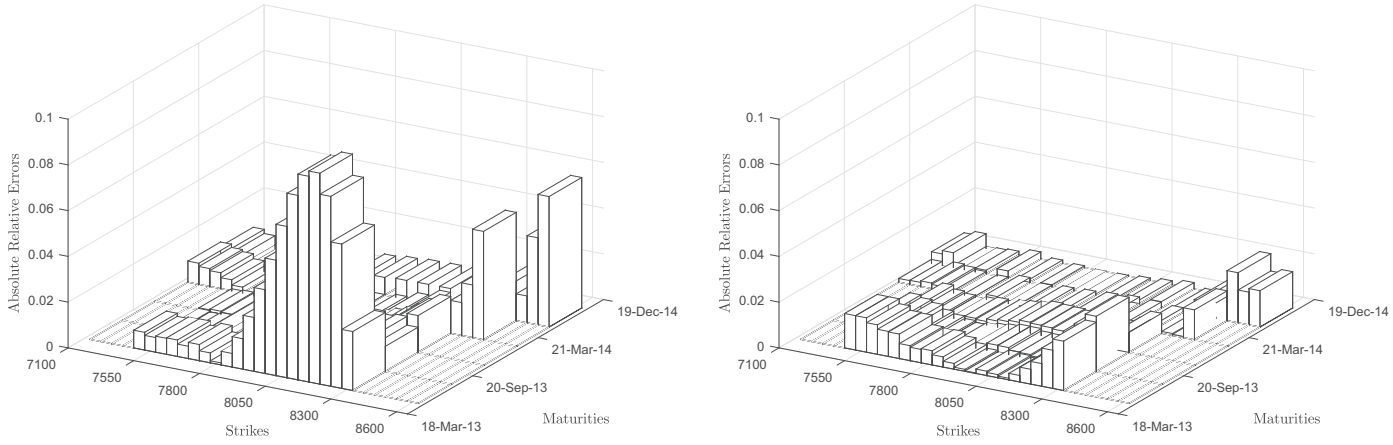

Fig. 2. Calibration results for the FSV model using SA (left figure) and SA combined with LSQ.

The first task was performed for both models and all combined approaches by dividing the set into two – we separated 71 options for calibration task and the rest (36 options) was included in the out-of-sample set. This provided us with error measures of two types, we evaluated (24) and (25) for both out-of-sample and calibration set.

The second task was motivated by the assumption of time-constant parameters employed by both models. Each model was calibrated on the primary data set (close prices of March 18, 2013) and then the introduced errors were evaluated on data from the consequent trading day. The structure of both sets is similar, however the second out-of-sample set is larger and involves one more time to maturity. Hence, we do not expect as good results, but we would like to find out whether the calibration procedures introduced with respect to the models are robust enough to provide a reasonable market fit for the next trading day.

A complex robust and uncertainty analyses of SV models based on equity option markets can be found in Pospíšil, Sobotka, and Ziegler (2016).

4. Empirical results

4.1. Primary data set: in-sample calibration results

For the task of model calibration we chose to adopt the approach of combining the global and local optimizers. We would start with a global optimizer (GA, SA, ASA) and provide the result as an initial guess to a local optimizer (LSQ). The global optimizers were quite often unable to provide competitive results for both models on their own (see Table 4, 5 and Fig. 2). Using only a local optimizer without a good initial guess, on the other hand, one might struggle to obtain calibrated parameters that correspond to a reasonably good market fit. Combining the routines, however, were able to retrieve significantly better error measure values for both models and all sets of weights.

GA and SA algorithms provided us with calibrated parameters of the Heston model that translated into average relative errors well over 1 percent and maximal relative errors topping 47.24 percent (SA, weights A). For the FSV model the situation was quite

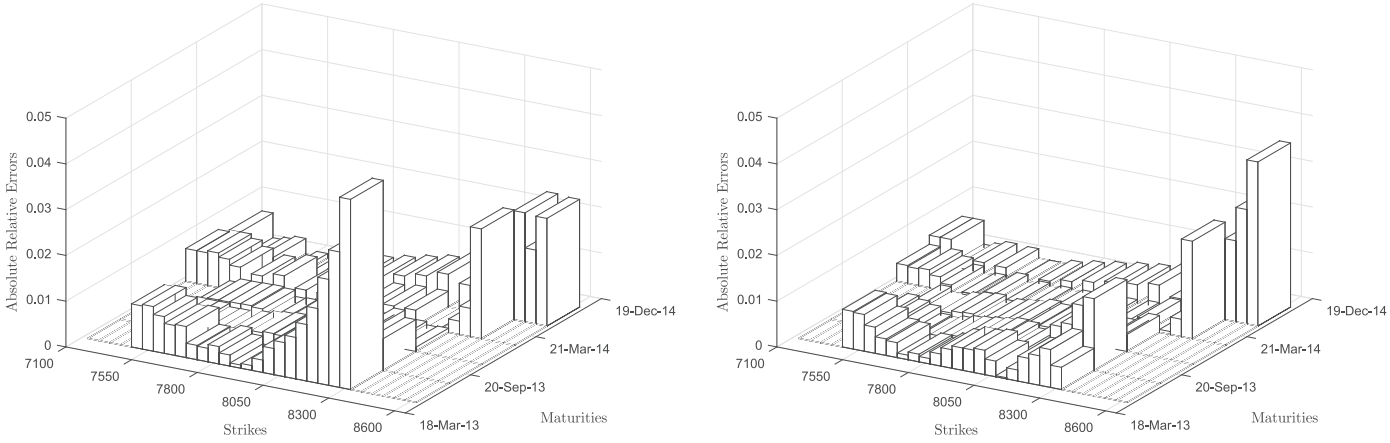

Fig. 3. Results of calibration for pair GA and LSQ for weights C – Heston model on the left and FSV model on the right.

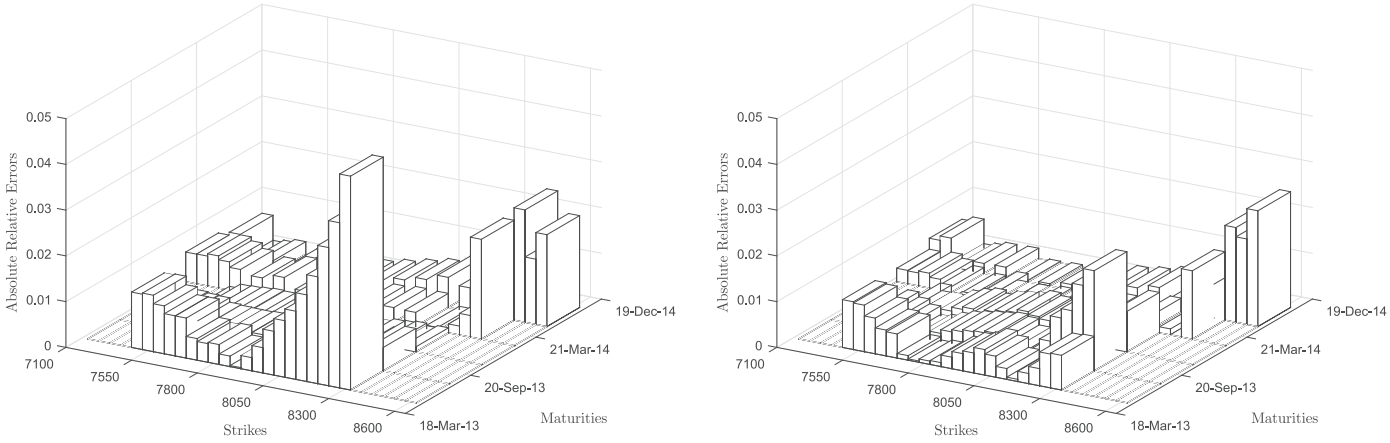

Fig. 4. Results of calibration for pair SA and LSQ for weights E – Heston model on the left and FSV model on the right.

similar, only with better values of measured errors, that never exceeded maximal error of 37.74 percent. Adaptive simulated annealing was the only global approach that got close to 1 percent AARE for the Heston model and reached 0.59 percent AARE for the FSV model. One can argue that the results are effected by algorithm settings, but in our case when increasing the number of total generations (GA) or the number of re-annealings (SA, ASA) we did not get significantly better results in a reasonable time-frame.

Combination of global and local optimizers provided us with superior results. The best market fit with respect to the Heston model was retrieved for weights B, reading 0.50 percent AARE and 2.81 percent MARE. In this case we also managed to show that all global routines served the local optimizer with a suitable initial guess. The FSV model calibrated using SA+LSQ reached even better market fit, in terms of AARE we obtained 0.39 percent and 0.38 percent for weights B and A respectively. However, we did not manage to get as good results for weights B and combined GA approach and similarly ASA failed to provide a good initial guess for the local optimizer – we ended up with a result comparable to the Heston model, despite using an approach with more degrees of freedom. Nevertheless, the FSV model calibrated using combined approaches was much more consistent with the shortest maturity call options (see Figs. 3 and 4).

To justify a combination of global and local optimizers one also has to take into consideration the time consumed by the calibration trial. Computational times were measured on a reference PC equipped with 16 gigabytes RAM and Intel i7-4770K CPU. Codes were run on MATLAB R2015a and MS Windows (x64) platform. Calibration times for global optimizers exceeded significantly those obtained by the LSQ routine itself. ASA took the most time by far, but this was mainly due to the overhead that was caused by calling the asamin wrapper. A calibration of the FSV model consumed similar amount of time as in case of the Heston model with pricing formula (4). However, one integral formula proposed by Lewis (2000) fastened the calibration process which we have shown in Table 4.

Calibration trials with Black–Scholes Vega weights (weights D) were typically outperformed by trials with different weights in the utility function, which became especially significant for combined approaches and the Heston model. All in-sample results are conveniently shown in Table 4 and 5 for the Heston and FSV model respectively and are also visually depicted in supplementary materials of Pospíšil and Sobotka (2016).

4.2. Secondary data set: out-of-sample and prediction errors

On the secondary data set, as was expected, we managed to get better in-sample errors out of the FSV model. Average relative calibration errors ranged from 0.45 percent to 0.61 percent for the FSV model and from 0.63 percent to 0.79 percent for the Heston model respectively. In terms of maximal errors, the difference between the two considered models is similar. More importantly, we were able to show that the out-of-sample errors were of the same order as the calibration ones and also that the option prices surface generated by the FSV model remained consistent with our out-of-sample data set. Hence, in this case we were also able to retrieve better fit compared to the simpler Heston model. As previously, we also noticed that weights D were least suitable for the calibration task with respect to the non-weighted errors, see Table 2.

Table 2
Results for the secondary data set – out-of-sample errors.

			In-sample errors			Out-of-sample errors	
Model	Algorithm	Weights	$G(\Theta)$	AARE (percent)	MARE (percent)	AARE (percent)	MARE (percent)
FSV	GA+LSQ	A	0.063	0.45	1.89	0.46	1.65
	GA+LSQ	B	0.100	0.61	2.52	0.70	5.06
	GA+LSQ	C	0.079	0.45	1.71	0.46	1.71
	GA+LSQ	D	0.124	0.53	3.51	0.63	5.96
	GA+LSQ	E	0.101	0.48	2.40	0.49	2.27
	SA+LSQ	A	0.063	0.45	1.89	0.46	1.65
	SA+LSQ	B	0.042	0.47	2.39	0.54	3.31
	SA+LSQ	C	0.022	0.45	1.71	0.46	1.71
	SA+LSQ	D	0.124	0.53	3.51	0.63	5.96
	SA+LSQ	E	0.101	0.47	2.41	0.50	2.29
Heston	GA+LSQ	A	0.117	0.65	2.42	0.69	2.67
	GA+LSQ	B	0.081	0.63	1.77	0.66	2.08
	GA+LSQ	C	0.137	0.67	3.66	0.73	4.07
	GA+LSQ	D	0.160	0.79	7.45	0.90	8.20
	GA+LSQ	E	0.160	0.72	5.01	0.80	5.58
	SA+LSQ	A	0.117	0.65	2.42	0.69	2.67
	SA+LSQ	B	0.081	0.63	1.77	0.66	2.08
	SA+LSQ	C	0.137	0.67	3.66	0.73	4.07
	SA+LSQ	D	0.160	0.79	7.45	0.90	8.20
	SA+LSQ	E	0.160	0.72	5.01	0.80	5.58

Table 3
Results for the secondary data set – prediction errors.

			Prediction errors	
Model	Algorithm	Weights	AARE (percent)	MARE (percent)
FSV	GA+LSQ	A	2.12	8.04
	GA+LSQ	B	2.15	9.18
	GA+LSQ	C	2.06	7.33
	GA+LSQ	D	2.10	7.92
	GA+LSQ	E	2.02	7.51
	SA+LSQ	A	2.12	8.04
	SA+LSQ	B	2.17	8.30
	SA+LSQ	C	2.06	7.33
	SA+LSQ	D	1.87	6.47
	SA+LSQ	E	2.02	7.49
Heston	GA+LSQ	A	2.18	10.58
	GA+LSQ	B	2.13	9.21
	GA+LSQ	C	2.19	11.36
	GA+LSQ	D	2.23	11.14
	GA+LSQ	E	2.21	12.08
	SA+LSQ	A	2.18	10.58
	SA+LSQ	B	2.13	9.21
	SA+LSQ	C	2.19	11.36
	SA+LSQ	D	2.23	11.14
	SA+LSQ	E	2.21	12.08

Prediction results comprised of much greater average errors (Table 3) – this observation could be partly caused by a slight difference in the March 19 data structure. As previously, the FSV approach provided a bit more robust results. For instance, the maximal errors never exceeded 10 percent unlike in case of the Heston model. The overall results, however, were not as good as we observed before and average error measures are of the similar magnitude for both models.

On the other hand, calibrated parameters from the previous day appeared to be good choices of initial parameters for the local search method. Using these parameters we were able to retrieve similar calibration errors as for the combined approaches used on the 19 March data set.

5. Conclusion

In this paper, we compared several optimization approaches to the problem of option market calibration. For the empirical study we chose a popular SV model, firstly introduced by Heston (1993), and a more up to date approximative fractional jump-diffusion model (FSV) alongside DAX index call options. The primary data set involved contracts traded on 18 March 2013, the secondary set used also for an out-of-sample comparison comprised of market data from 19 March 2013.

The corresponding optimization problem is non-convex and may contain many local minima, hence any local search method without a good initial guess may lead to unsatisfactory results. We have shown that the global optimizers on their own were unable to provide a very good market fit in a reasonable time frame. The calibrated parameters thereby obtained, however, appeared to be (in most cases) an appealing choice of initial guess for the local search method LSQ. This method further helped to improve all measured errors significantly, reaching 0.50 percent average absolute relative error (AARE) and 2.81 percent maximal absolute relative error (MARE) for weights B and the Heston model while also preserving time efficiency. The FSV model with one integral formula introduced in Section 2 was able to fit the market with 0.38 percent AARE for weights A and with initial guess provided by simulated annealing method (SA).

In case of the simpler Heston model, all global routines provided a sub-optimal solution in the neighborhood of the same local minima. Hence using any suggested combined approach we were able to get a satisfying result with respect to a particular weight function. For a more complex model, this might not be the case, which we illustrated on the FSV model. Best results (in terms of stability and absolute errors) were obtained for SA combined with LSQ, followed by genetic algorithm (GA) with the local refinement. Although adaptive simulated annealing (ASA) provided best results of all global optimizers alone, we conclude those parameters were typically the worst initial guesses for the local optimizer and thus this is not favorable routine for combined approaches, especially in case of the FSV model.

Another important aspect of calibration routines is the computational efficiency. We measured the amount of time it took to get the calibrated parameters. The greatest amount of time was consumed by global methods, especially by ASA which also included a costly overhead at each function evaluation.[5] In comparison, the refinement by LSQ is swift, especially for the Heston model. For

[5] This is however an implementation issue that might be cured by writing all codes in C.

the FSV model LSQ took slightly more time – it does $N+1$ function evaluations at each step, where N is the number of model parameters. However, despite having more degrees of freedom, the time of FSV calibration is similar (and typically shorter) to the calibration of Heston model using solution (4). We have also shown, on the other hand, that the Heston model calibration could be fastened by employing Lewis (2000) pricing formula. For the FSV model, the best overall approach for our data sets, taking also the computational time into consideration, turned out to be a combination of SA + LSQ alongside weights that take into account ask-bid spreads (weights A–C).

Investigation of optimization techniques for calibration of stochastic volatility models is an ongoing research. The presence of the numerical integral with several parameters affects the speed of calibration, which is crucial for practical use of the models. This is pointed out by Date and Islyaev (2015), who suggest a new random volatility model, which is computationally significantly less demanding to calibrate due to the use of Taylor series expansion of the option price. Their numerical experiments show for example that their high order moment-based stochastic volatility model can keep up with Heston model in terms of accuracy despite the easy pricing formula.

Possible performance and accuracy improvements of Gauss–Newton methods used in our case involve precalculation of gradients or Hessian matrix of objective functions which is rather complicated task even under the Heston model dynamics. Another possibility is to use the variable metric methods for nonlinear least squares as they are introduced in Lukšan and Spedicato (2000).

Complexity of the FSV model then opens space for fine tuning the global optimizers whose implementation in parallel and distributed computing environments is a further issue.

Acknowledgment

This work was partially supported by the GACR Grant 14-11559S Analysis of Fractional Stochastic Volatility Models and their Grid Implementation. Computational resources were provided by the MetaCentrum under the program LM2010005 and the CERIT-SC under the program Centre CERIT Scientific Cloud, part of the Operational Program Research and Development for Innovations, Reg. no. CZ.1.05/3.2.00/08.0144.

Appendix A. Calibration results in detail

Table 4
Calibration results for March 18, 2013 – Heston model.

Algorithm	Weight	AARE (percent)	MARE (percent)	Time (seconds)[a]	v_0	κ	θ	σ	ρ
GA	A	2.33	9.76	180 (305)	0.02756	14.15620	0.03927	1.88249	−0.71580
GA	B	1.34	6.76	179 (308)	0.04550	9.19613	0.04531	2.50198	−0.59138
GA	C	2.15	9.02	182 (308)	0.03638	18.96873	0.04221	3.49958	−0.65120
GA	D	2.65	13.41	254 (339)	0.02489	31.13232	0.03901	3.99901	−0.70506
GA	E	2.62	17.92	195 (327)	0.03175	19.62524	0.04436	3.98662	−0.67873
SA	A	4.08	47.24	38 (99)	0.03956	1.17994	0.10314	1.73777	−0.33177
SA	B	4.35	14.90	91 (248)	0.01332	11.08051	0.03625	0.92149	−0.48677
SA	C	3.15	23.27	64 (84)	0.01474	14.25742	0.04043	1.65886	−0.80250
SA	D	2.97	29.44	107 (289)	0.03910	19.28854	0.04099	2.87547	−0.82827
SA	E	2.96	11.36	151 (200)	0.01812	14.74490	0.03961	1.81461	−0.61193
ASA	A	1.05	7.70	319 (553)	0.03269	2.93130	0.05617	1.22382	−0.57411
ASA	B	1.38	7.61	326 (558)	0.04868	11.30381	0.04606	3.16684	−0.57539
ASA	C	1.55	13.87	343 (538)	0.04877	8.43288	0.05322	3.39390	−0.53460
ASA	D	1.34	6.23	420 (838)	0.02978	2.81918	0.05719	1.14524	−0.60785
ASA	E	1.37	8.78	310 (534)	0.03817	5.17080	0.05457	2.11144	−0.55358
GA+LSQ	A	0.55	3.44	183 (307)	0.02747	1.09713	0.06823	0.57392	−0.65061
GA+LSQ	B	0.50	2.81	181 (312)	0.02757	1.27690	0.06406	0.59618	−0.66211
GA+LSQ	C	0.58	4.16	184 (311)	0.02728	0.96942	0.07129	0.54100	−0.65341
GA+LSQ	D	0.74	6.22	257 (342)	0.02608	0.53968	0.08948	0.39121	−0.69779
GA+LSQ	E	0.61	4.68	197 (330)	0.02696	0.83390	0.07497	0.49443	−0.66541
SA+LSQ	A	0.55	3.44	40 (102)	0.02747	1.09714	0.06823	0.57392	−0.65061
SA+LSQ	B	0.50	2.81	93 (251)	0.02757	1.27680	0.06406	0.59614	−0.66212
SA+LSQ	C	0.58	4.16	66 (88)	0.02728	0.96943	0.07129	0.54101	−0.65341
SA+LSQ	D	0.74	6.22	110 (292)	0.02608	0.53968	0.08948	0.39121	−0.69779
SA+LSQ	E	0.61	4.68	153 (204)	0.02696	0.83390	0.07497	0.49442	−0.66541
ASA+LSQ	A	0.55	3.44	321 (555)	0.02747	1.09710	0.06824	0.57390	−0.65061
ASA+LSQ	B	0.50	2.81	327 (560)	0.02757	1.27684	0.06406	0.59615	−0.66212
ASA+LSQ	C	0.58	4.16	345 (540)	0.02728	0.96946	0.07129	0.54102	−0.65341
ASA+LSQ	D	0.74	6.22	424 (842)	0.02608	0.53968	0.08948	0.39121	−0.69779
ASA+LSQ	E	0.61	4.68	311 (537)	0.02696	0.83389	0.07497	0.49442	−0.66541

[a] Times in brackets are with respect to formula (4). Due to implementation issues, computational times for ASA are significantly greater than times of other approaches.

Table 5
Calibration results for March 18, 2013 – FSV model.

Algorithm	Weight	AARE (percent)	MARE (percent)	Time (seconds)[a]	v_0	κ	θ	σ	ρ	λ	μ_J	σ_J	H
GA	A	2.88	37.74	262	0.05649	1.03334	0.17120	3.24594	−0.50095	0.25879	−0.07312	0.01975	0.50599
GA	B	1.20	4.94	280	0.02833	4.70411	0.04184	1.76938	−0.73438	9.13326	0.01486	0.00172	0.58135
GA	C	1.43	6.89	251	0.02900	7.47922	0.04577	3.52082	−0.69418	2.71330	−0.04831	0.00051	0.53266
GA	D	1.71	19.32	265	0.03126	0.26349	0.19881	3.48131	−0.53215	0.03496	−0.06160	0.03224	0.72626
GA	E	1.58	20.40	255	0.02409	2.79933	0.02564	3.95672	−0.28680	0.19449	−0.24111	0.26883	0.71469
SA	A	1.44	11.70	114	0.01975	0.11422	0.10905	2.17402	−0.47231	0.06968	−0.53671	0.57367	0.81586
SA	B	3.26	22.85	118	0.01659	0.00001	0.91156	3.70953	0.24377	0.06427	−1.58758	1.06552	0.94404
SA	C	1.85	6.69	218	0.01430	0.52089	0.04028	0.55556	−0.74846	0.58599	−0.09014	0.15352	0.63296
SA	D	1.27	9.22	324	0.01856	0.07224	0.86217	2.91177	−0.82467	3.53808	−0.01874	0.06127	0.61067
SA	E	1.76	6.53	143	0.01294	0.61823	0.01421	0.36563	−0.59360	0.37251	−0.18013	0.23885	0.64913
ASA	A	1.22	10.72	2057	0.05878	37.86172	0.00592	3.63032	−0.99683	0.50964	−0.14148	0.24882	0.79761
ASA	B	0.59	4.92	1110	0.04473	28.14749	0.01820	1.42396	−0.93989	0.03537	−2.75358	1.83538	0.55999
ASA	C	1.48	15.65	2108	0.06159	38.12146	0.00384	3.25668	−0.98626	0.63093	−0.12056	0.23056	0.82485
ASA	D	1.32	4.64	2515	0.01541	2.44759	0.05235	1.27624	−0.96370	91.39088	−0.00216	0.01003	0.53431
ASA	E	0.83	5.00	2433	0.02922	2.06203	0.06318	2.41231	−0.61083	4.48047	−0.01685	0.02019	0.59395
GA+LSQ	A	0.38	4.48	315	0.02129	0.03810	0.81284	1.79257	−0.68287	0.97132	−0.03874	0.07766	0.69122
GA+LSQ	B	0.50	2.82	291	0.02745	1.35446	0.06262	1.57285	−0.66422	9.60768	−0.00369	0.00307	0.63601
GA+LSQ	C	0.40	3.59	295	0.02139	0.03398	0.88442	2.07893	−0.68495	0.86469	−0.04684	0.07617	0.72068
GA+LSQ	D	0.41	4.30	282	0.02115	0.06007	0.53217	3.09903	−0.69327	1.06276	−0.03421	0.07811	0.76501
GA+LSQ	E	0.43	2.54	309	0.02274	0.05443	0.54405	3.36746	−0.65814	0.19942	−0.15725	0.00001	0.80476
SA+LSQ	A	0.38	4.48	144	0.02130	0.03839	0.80688	2.83447	−0.68285	0.97116	−0.03875	0.07765	0.75754
SA+LSQ	B	0.39	5.65	127	0.02168	0.04738	0.66651	3.50401	−0.64226	0.84248	−0.04908	0.07711	0.78297
SA+LSQ	C	0.40	3.59	250	0.02140	0.03544	0.84959	1.05783	−0.68476	0.86333	−0.04691	0.07611	0.62280
SA+LSQ	D	0.49	2.46	356	0.02213	0.02830	0.96763	1.84331	−0.69190	0.18476	−0.16373	0.00001	0.73523
SA+LSQ	E	0.43	2.53	179	0.02278	0.06496	0.46199	0.49208	−0.65853	0.19864	−0.15681	0.00001	0.52580
ASA+LSQ	A	0.56	6.35	2071	0.02479	7.45043	0.01882	3.01923	−0.99999	0.04307	−1.43493	1.30931	0.80627
ASA+LSQ	B	0.56	8.44	1122	0.02433	5.52366	0.02039	1.00157	−0.95866	0.02326	−8.61302	3.93487	0.64411
ASA+LSQ	C	0.60	5.38	2120	0.02467	7.98466	0.01902	2.96471	−1.00000	0.04575	−1.28603	1.18172	0.80209
ASA+LSQ	D	0.68	5.10	2586	0.02577	0.61171	0.08384	0.63047	−0.70591	29.43525	−0.00022	0.00295	0.56424
ASA+LSQ	E	0.46	2.52	2468	0.02158	0.03345	0.86750	1.70842	−0.68363	0.62598	−0.07292	0.06868	0.70317

[a] Due to implementation issues, computational times for ASA are significantly greater than times of other approaches.

References

Albrecher, H., Mayer, P., Schoutens, W., & Tistaert, J. (2007). The little Heston trap. *Wilmott Magazine*, (Jan/Feb), 83–92.

Bakshi, G., Cao, C., & Chen, Z. (1997). Empirical performance of alternative option pricing models. *The Journal of Finance, 52*(5), 2003–2049.

Bates, D. S. (1996). Jumps and stochastic volatility: Exchange rate processes implicit in deutsche mark options. *Review of Financial Studies, 9*(1), 69–107.

Baustian, F., Mrázek, M., Pospíšil, J., & Sobotka, T. (2016). Unifying approach to several stochastic volatility models with jumps. In review.

Bayer, C., Friz, P., & Gatheral, J. (2015). Pricing under rough volatility. *Quantitative Finance*, 1–18.

Benhamou, E., Gobet, E., & Miri, M. (2010). Time dependent Heston model. *SIAM Journal on Financial Mathematics, 1*(1), 289–325.

Black, F., & Scholes, M. S. (1973). The pricing of options and corporate liabilities. *Journal of Political Economy, 81*(3), 637–654.

Bollerslev, T., & Mikkelsen, O. H. (1996). Modeling and pricing long memory in stock market volatility. *Journal of Econometrics, 73*(1), 151–184.

Breidt, F. J., Crato, N., & de Lima, P. (1998). The detection and estimation of long memory in stochastic volatility. *Journal of Econometrics, 83*(1–2), 325–348.

Christoffersen, P., Heston, S., & Jacobs, K. (2009). The shape and term structure of the index option smirk: Why multifactor stochastic volatility models work so well. *Management Science, 55*(12), 1914–1932.

Cont, R., & Hamida, S. B. (2005). Recovering volatility from option prices by evolutionary optimization. *Journal of Computional Finance, 8*(4), 43–76.

Cox, J. C., Ingersoll, J. E., & Ross, S. A. (1985). A theory of the term structure of interest rates. *Econometrica, 53*(2), 385–407.

Date, P., & Islyaev, S. (2015). A fast calibrating volatility model for option pricing. *European Journal of Operational Research, 243*(2), 599–606. http://dx.doi.org/10.1016/j.ejor.2014.12.031.

Duffie, D., Pan, J., & Singleton, K. (2000). Transform analysis and asset pricing for affine jump-diffusions. *Econometrica, 68*(6), 1343–1376.

Elices, A. (2008). Models with time-dependent parameters using transform methods: application to Heston's model. In *Proceedings of the 2008 International Conference CMMSE: vol. 1* (pp. 237–259). La Manga, Spain.

Feller, W. (1951). Two singular diffusion problems. *The Annals of Mathematics, 54*(1), 173–182.

Hanson, F. B. (2007). Applied stochastic processes and control for jump-diffusions: Modeling, analysis, and computation. *Volume 13 of Advances in design and control*. Philadelphia, PA: Society for Industrial and Applied Mathematics (SIAM).

Heston, S. L. (1993). A closed-form solution for options with stochastic volatility with applications to bond and currency options. *Review of Financial Studies, 6*(2), 327–343.

Hull, J. C., & White, A. D. (1987). The pricing of options on assets with stochastic volatilities. *Journal of Finance, 42*(2), 281–300.

Ingber, L. (1989). Very fast simulated re-annealing. *Mathematical and Computer Modelling, 12*(8), 967–973. doi:10.1016/0895-7177(89)90202-1.

Intarasit, A., & Sattayatham, P. (2011). An approximate formula of European option for fractional stochastic volatility jump-diffusion model. *Journal of Mathematics and Statistics, 7*(3), 230–238.

Jacquier, E., & Jarrow, R. (2000). Bayesian analysis of contingent claim model error. *Journal of Econometrics, 94*(1–2), 145–180.

Kahl, C., & Jäckel, P. (2005). Not-so-complex logarithms in the Heston model. *Wilmott Magazine*, 94–103.

Lewis, A. L. (2000). *Option valuation under stochastic volatility, with Mathematica code*. Newport Beach, CA: Finance Press.

Lukšan, L., & Spedicato, E. (2000). Variable metric methods for unconstrained optimization and nonlinear least squares. *Journal of Computational and Applied Mathematics, 124*(1–2), 61–95 Numerical analysis 2000. Vol. IV: Optimization and nonlinear equations. doi:10.1016/S0377-0427(00)00420-9.

Martens, M., van Dijk, D., & de Pooter, M. (2004). *Modeling and forecasting s&p 500 volatility: Long memory, structural breaks and nonlinearity. Technical Report. TI 04-067/4, TI.*

Merton, R. C. (1976). Option pricing when underlying stock returns are discontinuous. *Journal of Financial Economics, 3*(1–2), 125–144. http://dx.doi.org/10.1016/0304-405X(76)90022-2.

Metropolis, N., Rosenbluth, A. W., Rosenbluth, M. N., Teller, A. H., & Teller, E. (1953). Equation of state calculations by fast computing machines. *Journal of Chemical Physics, 21*(6), 1087–1092. doi:10.1063/1.1699114.

Mrázek, M., Pospıšil, J., & Sobotka, T. (2014). On optimization techniques for calibration of stochastic volatility models. In *Proceedings of international conference on applied numerical mathematics and scientific computation, Athens* (pp. 34–40).

Nögel, U., & Mikhailov, S. (2003). Heston's stochastic volatility model. Implementation, calibration and some extensions. *Wilmott Magazine*, 74–79.

Pospíšil, J., & Sobotka, T. (2015). Market calibration under a long memory stochastic volatility model. In review.

Pospíšil, J., & Sobotka, T. (2016). Test data sets for calibration of stochastic and fractional stochastic volatility models. Submitted for publication.

Pospíšil, J., Sobotka, T., & Ziegler, P. (2016). Empirical study of robustness and sensitivity for stochastic volatility models. In review.

Rouah, F. D. (2013). The Heston model and its extensions in Matlab and C#, + Website. *Wiley finance series*. Wiley.

Scott, L. O. (1987). Option pricing when the variance changes randomly: Theory, estimation, and an application. *The Journal of Financial and Quantitative Analysis, 22*(4), 419–438.

Stein, J., & Stein, E. (1991). Stock price distributions with stochastic volatility: An analytic approach. *Review of Financial Studies, 4*(4), 727–752.

Thao, T. H. (2006). An approximate approach to fractional analysis for finance. *Nonlinear Analysis: Real world Applications, 7*, 124–132.

Thao, T. H., & Nguyen, T. T. (2002). Fractal Langevin equation. *Vietnam Journal Mathematics, 30*(1), 89–96.

Zähle, M. (1998). Integration with respect to fractal functions and stochastic calculus. I. *Probability Theory and Related Fields, 111*(3), 333–374. doi:10.1007/s004400050171.

Zhylyevskyy, O. (2012). Efficient pricing of European-style options under Heston's stochastic volatility model. *Theoretical Economics Letters, 2*(1), 16–20.

Applied Stochastic Models in Business and Industry

Research Article

Received 11 April 2016, Revised 14 November 2016, Accepted 24 February 2017 Published online 4 April 2017 in Wiley Online Library

(wileyonlinelibrary.com) DOI: 10.1002/asmb.2248

Unifying pricing formula for several stochastic volatility models with jumps

Falko Baustian[a], Milan Mrázek[b], Jan Pospíšil[b*†] and Tomáš Sobotka[b]

In this paper, we introduce a unifying approach to option pricing under continuous-time stochastic volatility models with jumps. For European style options, a new semi-closed pricing formula is derived using the generalized complex Fourier transform of the corresponding partial integro-differential equation. This approach is successfully applied to models with different volatility diffusion and jump processes. We also discuss how to price options with different payoff functions in a similar way.
In particular, we focus on a log-normal and a log-uniform jump diffusion stochastic volatility model, originally introduced by Bates and Yan and Hanson, respectively. The comparison of existing and newly proposed option pricing formulas with respect to time efficiency and precision is discussed. We also derive a representation of an option price under a new approximative fractional jump diffusion model that differs from the aforementioned models, especially for the out-of-the money contracts. Copyright © 2017 John Wiley & Sons, Ltd.

Keywords: stochastic volatility models; option pricing; fundamental transform; PIDE; fractional volatility
JEL Classification C58; C63
Mathematics Subject Classification (2010) 60H10; 91G20

1. Introduction

Financial market models play a crucial part in many financial engineering tasks. Since the Nobel-prize[‡] winning Black and Scholes [1] model, both practitioners and academics try to come up with models of the same type that ideally would

– include much more realistic assumptions about the modelled market compared with the Black–Scholes model and
– remain tractable and time efficient for all practical tasks.

Improving one of the aforementioned criteria usually leads to worsening of the other. In this paper, we focus on a class of stochastic volatility jump-diffusion (SVJD) models that can be considered as a modern and more realistic ancestor of the Black–Scholes approach, and we provide a more efficient solution to the option pricing task. Moreover, the proposed approach is not restricted to just one particular model – it can be successfully applied to a wide range of SVJD models. This is demonstrated on several models in the latter part of the paper.

The main criticism of the Black–Scholes model involved the constant volatility assumption. Stochastic volatility (SV) models relax this assumption by adding a diffusion process thereof. From the derivative pricing point of view, a good model should also mimic the observed volatility surfaces. To provide better fit to the real volatility surfaces, especially for the short-term maturities, adding jumps to the stock price process was considered among the possible modifications of the SV models later on. This led to a whole new class of models with jumps in the stock price (SVJD models). Besides providing a good fit to market data, an analytical formula for the price of the European option is a desired feature of the models. Computational efficiency is critical when using the models in practice, particularly in the model calibration process.

Among the first SV models were the ones by Hull and White [2], Stein and Stein [3] and Heston [4]. The latter article introduces a well-known Heston model alongside a semi-closed formula for pricing European options. This approach

[a] *Department of Mathematics, University of Rostock, Ulmenstraße 69, 18057 Rostock, Germany*
[b] *NTIS – New Technologies for the Information Society, Faculty of Applied Sciences, University of West Bohemia, Univerzitní 8, 306 14 Plzeň, Czech Republic*
**Correspondence to: Jan Pospíšil, Department of Mathematics, University of West Bohemia, Univerzitní 8, 306 14 Plzeň, Czech Republic*
[†] *E-mail: honik@ntis.zcu.cz*
[‡] *Merton and Scholes received the Nobel Memorial Prize in Economic Sciences in 1997 for their work on the model.*

allows to have correlated increments of the asset price and the volatility process (as opposed to Stein and Stein [3]), which can mimic a volatility leverage effect observed on many financial markets. However, the model lacks the ability to fit reasonably well-complex option price surfaces [5, 6], especially the ones that involve both short-dated and long-dated contracts.

To deal with the drawbacks of the first SV models, many modifications have been introduced since, including a dynamic Heston model that involves time-dependent parameters. The case of piece-wise constant parameters in time is studied in Mikhailov and Nğel [7], a linear time dependence in Elices [8] and a more general case is analysed in Benhamou *et al.* [9]. The latter result introduces only an approximation of the option price. However, Bayer *et al.* [5] suggest that the general overall shape of the volatility surface does not change in time, at least to a first approximation given by stochastic volatility inspired (SVI) models. Hence, it is desirable to model volatility as a time-homogeneous process. Other generalizations of the Heston model with time-constant parameters include jump processes in asset price, in volatility or in both (e.g. Duffie *et al.* [10]). As Gatheral [11] notes (and supports by empirical analyses of several authors), a model with jumps in both underlying and volatility, although having more parameter and degrees of freedom, might not provide significantly better market fit than its counterpart with jumps in underlying only. The first SVJD model introduced in [12] adds a log-normally distributed jumps to the diffusion dynamics of the Heston model. Several different jump-diffusion settings were proposed, for example, models postulated by Scott [13] and Yan and Hanson [14] among others.

Another possibility to modify standard diffusion SV models is to use a Lévy subordinator as a driving noise of the volatility process. This idea was firstly developed by Barndorff–Nielsen and Shephard [15] where both volatility and asset price processes exhibit simultaneous jumps. There exists an empirical evidence that jumps might not be simultaneous [16], and to improve this aspect of the original model, several modifications have lately appeared, for example, results by Nicolato and Venardos [17], Deelstra and Petkovic [18], Bannör and Scherer [19], Mai *et al.* [20] and Sengupta [21] to name few.

Models inspired by Barndorff-Nielsen and Shephard [15] usually assume short-range dependence in the volatility process. Long-range dependence, however, has been observed on several financial markets. For instance, Breidt *et al.* [22] have shown an evidence of long memory using both semi-parametric and non-parametric detection tests. Gatheral *et al*. [23] and Bayer *et al*. [5] argue about the presence of long memory, but the authors agree with Breidt *et al*. [22] that volatility should be driven by a process similar to a fractional Brownian motion – a process originally studied by Mandelbrot and Van Ness [24]. Comte *et al*. [25] introduce an affine fractional SV model, sometimes dubbed as a fractional Heston model. This model alongside the ones considered by Gatheral *et al*. [23] can explain many observed properties of financial markets; however, only inefficient numerical schemes are available for option pricing tasks at the current time [5]. This motivates results of Pospíšil and Sobotka [26] who introduce a long-memory SVJD model. The volatility process is driven by a fractional noise that can be viewed as an semimartingale approximation of a fractional Brownian motion. The authors have also deduced a semi-closed form representation for vanilla option prices under this model.

Not only myriads of SV models have been proposed, but also several different approaches to price financial derivatives under a specific model were introduced. Starting with the Heston model, many formulas for pricing vanilla options were studied over the more than 20-year history of the model. The semi-closed formula given by Heston [4] in the original paper involves two numerical integrals on the half-open integration domain $[0, \infty)$. Moreover, it also requires evaluation of logarithms with complex arguments, which leads to numerical instabilities for some parameters. To avoid this so-called Heston trap, an alternative formula as described, for example, in Albrecher *et al*. [27] has soon been adopted by practitioners. A different approach to address the very same numerical instabilities was taken by Kahl and Jäckel [28], who also made use of a transformation to the integration domain $[0, 1]$. However, both of these approaches still involve evaluation of two numerical integrals. Reducing these integrals into one can lead to faster computation and possibly greater accuracy, which is of great help in calibration of the model and empirical studies.

Lewis [29] shows how the call price for the Heston model can be written in terms of the fundamental transform. Similar to Lewis [29], several alternate formulas for the Heston call price are presented, for example, by Lipton [30] or Attari [31]. All of these formulas involve single numerical integration, but Attari's representation also quickens the rate at which the integrand decays. To reach a similar effect of a faster decaying single integral, Carr and Madan [32] use fast Fourier transform of a call price modified by a damping factor.

Of all the aforementioned approaches, we favour the one by Lewis, which also has become an industrial standard to option pricing under Heston model[§]. In this paper, we extend this approach to the class of SVJD models. Starting with Bates [12] model, a semi-closed formula for price of European option was already available in the original paper. However, alike the original formula for its older SV companion – Heston model – it involves two numerical integrals and possible numerical instabilities. This would be not an issue anymore when using fundamental transform techniques, while also

[§] *See, for instance, NAG Numerical Library,* http://www.nag.co.uk/numeric/cl/nagdoc_cl25/pdf/s/s30nac.pdf.

significantly reducing the computational time. Furthermore, we present a framework under which any type of jumps can be incorporated into SVJD model provided that we know the characteristic function of the jump process. We demonstrate that by presenting a new formula for SVJD model with log-uniform jumps introduced by Yan and Hanson [14], which compared with the original formula reduces the integrals to a single one and thus speeds up the computation, while the numerical stability is preserved.

Even though studied models belong to the class of affine jump-diffusion models, we do not strictly rely on the techniques of Duffie *et al*. [10], but rather generalize the approach of Lewis [29,33] and intuitively apply the results not only to existing SVJD models [12, 14] but also to a newly proposed approximative fractional SV model [26]. Lately, both academics and practitioners have been interested in fractional SV models that utilize a fractional driving noise in the volatility process. We show that prices of various contracts can be expressed under the approximative fractional model by the fundamental transform techniques, which underscores the versatility of the approach.

The structure of the paper is as follows. In Section 2, we compare two pricing formulas for Heston model, the original formula by Heston [4] and a formula by Lewis [29]. Both formulas are derived by a different approach to solve the pricing partial differential equation using two different Fourier transform methods, and so far, it has not been clear, how both formulas relate to each other. This section is included especially for methodological purposes. Heston derived his formula using the assumption that the call option price can be found in the form (4) similar to the Black–Scholes formula that led to the formula with two inverse Fourier transform integrals. On the other hand, Lewis solved the same pricing partial differential equation directly with complex Fourier transform that led to a formula (5) with only one inverse Fourier transform integral. One of the advantages of the Lewis formula is therefore evident.

In Section 3, we extend the previous comparison by adding jumps to the model; in particular, we add jumps with log-normal distributed sizes to the stock price process following Bates [12]. Because the original Bates pricing formula extends the formula by Heston, our next step is to follow the steps from Section 2 and derive a Lewis-like formula (18) for the Bates model. We also comment on the important relation to the Lévy–Khintchine representation of the characteristic function for a Lévy process.

The main results of this paper are covered in Section 4. At first, we introduce a general unifying SVJD model that covers different SV models with possibly different jumps. A special attention is paid to jumps with log-normal or log-uniform distribution of the jumps sizes. The unifying pricing formulas (31) and (33) are stated for the European call options, but we also discuss how the solutions for different payoffs can be obtained. Apart from the new formulas for the Bates model derived in Section 3, we provide here two additional examples. Namely, in Section 4.1, we show how the unifying approach applies to the Yan and Hanson [14] model with log-uniform jumps, and in Section 4.2, we apply the results to the new approximative fractional SV model with log-normal jumps.

In Section 5, we numerically compare the efficiency of newly proposed formulas, in particular the new representation for Bates and Yan Hanson model. We also compare the European call option prices under all studied models including the new fractional SVJD model. We conclude all obtained results in Section 6.

2. Comparing two pricing formulas for Heston model

Before we consider SV models with jumps, we want to take a closer look at the classical Heston model established by Heston [4]. The risk-neutral stock price S_t price is modelled by

$$dS_t = rS_t dt + \sqrt{v_t} S_t d\widetilde{W}_t^S, \tag{1}$$

$$dv_t = \kappa(\theta - v_t)dt + \sigma\sqrt{v_t} d\widetilde{W}_t^v, \tag{2}$$

$$d\widetilde{W}_t^S d\widetilde{W}_t^v = \rho\, dt, \tag{3}$$

with initial conditions $S_0 \geqslant 0$ and $v_0 \geqslant 0$, where r is the risk-free rate and the instantaneous volatility v_t at time t is driven by a mean reverting process. The stochastic process (2) (called variance process or volatility process) reverts with rate κ to the long-run average price variance θ, and σ is the volatility of the volatility. If the Feller condition $2\kappa\theta > \sigma^2$ is satisfied [34], this square-root mean reverting process, CIR process [35], is strictly positive and cannot reach zero. $(\widetilde{W}^S, \widetilde{W}^v)$ is a two-dimensional Wiener process under the risk-neutral measure $\widetilde{\mathbb{P}}$ with instantaneous correlation ρ. The popularity of the Heston SV model results from its semi-closed form solution for vanilla options, which involves numerical computation of two integrals. There exist several different formulations and modifications of the original formula [4] to handle numerical problems that are connected with the integral term. We use the formulation by Albrecher *et al*. [27], which is only a slightly modification of the original one and eliminates the possible discontinuities of the integrand. Let K be the strike price and $\tau = T - t$ be the time to maturity. Then, the price of a European call option at time t on a non-dividend paying stock with a spot price S_t is

$$V(S,v,\tau) = SP_1 - e^{-r\tau}KP_2, \tag{4}$$

$$P_j(x,v,\tau) = \frac{1}{2} + \frac{1}{\pi}\int_0^{+\infty} \mathrm{Re}\left[\frac{e^{-i\phi\ln(K)}f_j(x,v,\tau,u)}{iu}\right]du,$$

where $x = \ln S$ and

$$f_j(x,v,\tau,u) = \exp\{C_j(\tau,u) + D_j(\tau,u)v + iux\},$$

with

$$C_j(\tau,u) = rui\tau + \frac{a}{\sigma^2}\left\{(b_j - \rho\sigma ui - d)\tau - 2\ln\left[\frac{1-ge^{-d\tau}}{1-g}\right]\right\},$$
$$D_j(\tau,u) = \frac{b_j - \rho\sigma ui - d}{\sigma^2}\left[\frac{1-e^{-d\tau}}{1-ge^{-d\tau}}\right],$$
$$g = \frac{b_j - \rho\sigma ui - d}{b_j - \rho\sigma ui + d},$$
$$d = \sqrt{(\rho\sigma ui - b_j)^2 - \sigma^2(2u_j ui - u^2)},$$

for both $j = 1, 2$, where the parameters u_j, a and b_j are defined as follows:

$$u_1 = \frac{1}{2}, u_2 = -\frac{1}{2}, a = \kappa\theta, b_1 = \kappa - \rho\sigma, b_2 = \kappa.$$

As mentioned before, there exist many different formulas, for example, by Kahl and Jäckel [28], Lewis[29] or Zhylyevskyy [36]. We will use the approach by Lewis [29] because it is well suited for more complex models with jumps. It is also well behaved compared with the formula by Albrecher *et al*. [27] but has the numerical advantage that we only have to calculate one integral for each call option price.

$$V(S,v,\tau) = S - Ke^{-r\tau}\frac{1}{2\pi}\int_{-\infty+i/2}^{+\infty+i/2} e^{-ikX}\frac{\hat{H}(k,v,\tau)}{k^2 - ik}dk, \tag{5}$$

where $X = \ln(S/K) + r\tau$ and

$$\hat{H}(k,v,\tau) = \exp\left(\frac{2\kappa\theta}{\sigma^2}\left[q\,g - \ln\left(\frac{1-he^{-\xi q}}{1-h}\right)\right] + \right.$$
$$\left. + vg\left(\frac{1-e^{-\xi q}}{1-he^{-\xi q}}\right)\right),$$

where

$$g = \frac{b-\xi}{2}, \quad h = \frac{b-\xi}{b+\xi}, \quad q = \frac{\sigma^2\tau}{2},$$
$$\xi = \sqrt{b^2 + \frac{4(k^2 - ik)}{\sigma^2}},$$
$$b = \frac{2}{\sigma^2}\Big(ik\rho\sigma + \kappa\Big).$$

The Lewis formula (5) is derived by applying the complex Fourier transform on the partial differential equation corresponding with the pricing process. The solution is the inverse complex Fourier transform of the so-called fundamental transform $\hat{H}(k,v,\tau)$, where k is complex valued. Knowing $\hat{H}(k,v,\tau)$, it is possible to obtain the option price for different particular payoff functions, not only the European call. We want to show that the Lewis and Heston (and hence Albrecher) formulas are equivalent representations of the same solution. We begin by splitting the integral in the Lewis formula (5).

$$
\begin{aligned}
V(S,v,\tau) &= S - Ke^{-r\tau}\frac{1}{2\pi}\int_{-\infty+i/2}^{+\infty+i/2} e^{-ikX}\frac{\hat{H}(k,v,\tau)}{k^2-ik}dk \\
&= S - Ke^{-r\tau}\frac{1}{2\pi}\int_{-\infty+i/2}^{+\infty+i/2} e^{-ikX}\left(\frac{\hat{H}(k,v,\tau)}{ik+1} - \frac{\hat{H}(k,v,\tau)}{ik}\right)dk \\
&= S - Ke^{-r\tau}\frac{1}{2\pi}\int_{-\infty+i/2}^{+\infty+i/2} e^{-ikX}\frac{\hat{H}(k,v,\tau)}{ik+1}dk \\
&\quad + Ke^{-r\tau}\frac{1}{2\pi}\int_{-\infty+i/2}^{+\infty+i/2} e^{-ikX}\frac{\hat{H}(k,v,\tau)}{ik}dk.
\end{aligned}
$$

We reformulate the first integral by a substitution and then apply the residue theorem.

$$
\begin{aligned}
\int_{-\infty+i/2}^{+\infty+i/2} e^{-ikX}\frac{\hat{H}(k,v,\tau)}{ik+1}dk &= e^{X}\int_{-\infty-i/2}^{+\infty-i/2} e^{-ikX}\frac{\hat{H}(k+i,v,\tau)}{ik}dk \\
&= e^{X}\left(\int_{-\infty+i/2}^{+\infty+i/2} e^{-ikX}\frac{\hat{H}(k+i,v,\tau)}{ik}dk + 2\pi\right);
\end{aligned}
$$

here the second integral results from the residue at the singularity $k = 0$ where $\hat{H}(i,v,\tau) = 1$. We define

$$
I_1 = \int_{-\infty+i/2}^{+\infty+i/2} e^{-ikX}\frac{\hat{H}(k+i,v,\tau)}{ik}dk, \tag{6}
$$

$$
I_2 = \int_{-\infty+i/2}^{+\infty+i/2} e^{-ikX}\frac{\hat{H}(k,v,\tau)}{ik}dk \tag{7}
$$

and obtain

$$
V(S,v,\tau) = S - Ke^{-r\tau+X}\frac{1}{2\pi}(I_1+2\pi) + Ke^{-r\tau}\frac{1}{2\pi}I_2 = -\frac{S}{2\pi}I_1 + e^{-r\tau}\frac{K}{2\pi}I_2. \tag{8}
$$

If $P_j = -\frac{1}{2\pi}I_j$ for $j = 1,2$ holds, the identity of (4) and (5) follows directly from (8). Both models have a big set of parameters, namely, $g, d, u_1, u_2, a, b_1, b_2$ for the Albrecher formula (4), and for the Lewis formula (5), we have h, q, ξ, b and again g. In the following comparisons, we will mark the parameters of (4) with a tilde like $\tilde{g}$ for g to avoid any confusions. We restart with Lewis formulation of the solution (5). For a question of notation, we use '$\cong$' to express that two terms from the two models are in *bona fide* equal but use different parameters.

$$
\begin{aligned}
b(k) &= \frac{2}{\sigma^2}\Big(ik\rho\sigma + \kappa\Big), \\
\xi(k) &= \sqrt{b(k)^2 + \frac{4}{\sigma^2}\Big(k^2 - ik\Big)}, \\
\xi(k)\frac{\sigma^2}{2} &= \sqrt{(ik\rho\sigma+\kappa)^2 + \sigma^2 k(k-i)}, \\
\xi(-k)\frac{\sigma^2}{2} &= \sqrt{(-ik\rho\sigma+\kappa)^2 + \sigma^2(-k)(-k-i)} = \sqrt{(ik\rho\sigma-\kappa)^2 + \sigma^2 k(k+i)} \\
&\cong \sqrt{(\rho\sigma ui - \tilde{b}_2)^2 + \sigma^2 u(u+i)} = \tilde{d}_2(u).
\end{aligned}
$$

We can show by similar calculations that $\xi(-k+i)\frac{\sigma^2}{2} = \tilde{d}_1(u)$. We continue with the parameters h and g.

$$h(k) = \frac{b(k)-\xi(k)}{b(k)+\xi(k)} \cdot \frac{\frac{\sigma^2}{2}}{\frac{\sigma^2}{2}} = \frac{\left(ik\rho\sigma+\kappa\right) - \xi(k)\frac{\sigma^2}{2}}{\left(ik\rho\sigma+\kappa\right) + \xi(k)\frac{\sigma^2}{2}},$$

$$h(-k) = \frac{\left(\kappa - ik\rho\sigma\right) - \xi(-k)\frac{\sigma^2}{2}}{\left(\kappa - ik\rho\sigma\right) + \xi(-k)\frac{\sigma^2}{2}}$$

$$\cong \frac{\left(\tilde{b}_2 - \rho\sigma ui\right) - \tilde{d}_2(u)}{\left(\tilde{b}_2 - \rho\sigma ui\right) + \tilde{d}_2(u)} = \tilde{g}_2(u),$$

$$g(k) = \frac{b(k)-\xi(k)}{2} = \frac{1}{\sigma^2}\left(ik\rho\sigma+\kappa\right) - \frac{\xi(k)}{2},$$

$$g(-k) = \frac{1}{\sigma^2}\left(\kappa - ik\rho\sigma\right) - \frac{\xi(-k)}{2}$$

$$\cong \frac{\tilde{b}_2 - \rho\sigma ui - \tilde{d}_2(u)}{\sigma^2},$$

which appears in C_2 and D_2 in the Heston formula. Similarly, for $h(-k+i)$ and $g(-k+i)$, we obtain

$$h(-k+i) = \tilde{g}_1(u),$$

$$g(-k+i) = \frac{\tilde{b}_1 - \rho\sigma ui - \tilde{d}_1(u)}{\sigma^2}.$$

As a next step, we prove $\hat{H}(-k,v,\tau) \cong f_2(x,v,\tau,u)e^{-iu(x+r\tau)}$.

$$\hat{H}(-k,v,\tau) = \exp\left(\frac{2\kappa\theta}{\sigma^2}\left[q\,g(-k) - \ln\left(\frac{1-h(-k)e^{-\xi(-k)q}}{1-h(-k)}\right)\right] + vg(-k)\left(\frac{1-e^{-\xi(-k)q}}{1-h(-k)e^{-\xi(-k)q}}\right)\right)$$

$$= \exp\left(\frac{2\kappa\theta}{\sigma^2}\left[\frac{\sigma^2\tau}{2}g(-k) - \ln\left(\frac{1-h(-k)e^{-\xi(-k)\frac{\sigma^2\tau}{2}}}{1-h(-k)}\right)\right] + vg(-k)\left(\frac{1-e^{-\xi(-k)\frac{\sigma^2\tau}{2}}}{1-h(-k)e^{-\xi(-k)\frac{\sigma^2\tau}{2}}}\right)\right)$$

$$\cong \exp\Bigg(\underbrace{\frac{2\tilde{a}}{\sigma^2}\left[\tau\frac{\tilde{b}_2 - \rho\sigma ui - \tilde{d}_2(u)}{2} - \ln\left(\frac{1-\tilde{g}_2(u)e^{-\tilde{d}_2(u)\frac{\sigma^2\tau}{2}}}{1-\tilde{g}_2(u)}\right)\right]}_{=C_2(\tau,u)-ru i\tau}$$

$$+ \underbrace{v\frac{\tilde{b}_2 - \rho\sigma ui - \tilde{d}_2(u)}{\sigma^2}\left(\frac{1-e^{-\tilde{d}_2(u)\frac{\sigma^2\tau}{2}}}{1-\tilde{g}_2(u)e^{-\tilde{d}_2(u)\frac{\sigma^2\tau}{2}}}\right)}_{=D_2(\tau,u)}\Bigg)$$

$$= \exp\{C_2(\tau,u) - ru i\tau + D_2(\tau,u)v + iux - iux\} = f_2(x,v,\tau,u)e^{-iu(x+r\tau)}.$$

The proof for $\hat{H}(-k+i,v,\tau) \cong f_1(x,v,\tau,u)e^{-iu(x+r\tau)}$ works analogously. We now reconsider the integral (6).

$$I_1 = \int_{-\infty+i/2}^{+\infty+i/2} e^{-ikX}\frac{\hat{H}(k+i,v,\tau)}{ik}dk = -\int_{-\infty-i/2}^{+\infty-i/2} e^{ikX}\frac{\hat{H}(-k+i,v,\tau)}{ik}dk$$

$$\cong -\int_{-\infty-i/2}^{+\infty-i/2} e^{-iu\ln K}\frac{f_1(x,v,\tau,u)}{iu}du,$$

where we used $\exp(i\phi X - i\phi x - i\phi r\tau) = \exp(i\phi \ln \frac{S}{K} + i\phi r\tau - i\phi \ln S - i\phi r\tau) = \exp(-i\phi \ln K)$. With the help of the residue theorem (for example, Ahlfors [37], section 4.5), we translate the integral to the real axis. We must pay attention to the fact that there is a singularity on the real line. The integral becomes a principal value integral, and we calculate with one-half of the residue as mentioned in Ahlfors [37], section 4.5.3.

$$\begin{aligned} -I_1 &= \int_{-\infty - i/2}^{+\infty - i/2} e^{-iu \ln K} \frac{f_1(x, v, \tau, u)}{iu} du = \int_{-\infty}^{+\infty} e^{-iu \ln K} \frac{f_1(x, v, \tau, u)}{iu} du + \pi \\ &= 2 \int_0^{+\infty} e^{-iu \ln K} \frac{f_1(x, v, \tau, u)}{iu} du + \pi, \end{aligned}$$

which leads us to $P_1 = -\frac{1}{2\pi} I_1$ and we obtain $P_2 = -\frac{1}{2\pi} I_2$ by a similar calculation from (7). Hence, we have shown that the Lewis and Heston formulas are equivalent.

We conclude this section by mentioning some of the aforementioned results for later use:

$$\hat{H}(-k) \cong f_2(u) e^{-iu(x + r\tau)}, \tag{9}$$

$$f_1(u) = \frac{f_2(u - i)}{f_2(-i)}, \tag{10}$$

$$f_2(-i) = e^{x + r\tau} = S e^{r\tau}. \tag{11}$$

3. Adding jumps: Bates SVJD model

In his article, Bates [12] considers a model similar to Heston [4] but adds a compound Poisson process Q_t with log normal distributed jump sizes to the stock price process S_t

$$dS_t = (r - \lambda\beta) S_t dt + \sqrt{v_t} S_t d\widetilde{W}_t^S + S_{t-} dQ_t, \tag{12}$$

$$dv_t = \kappa(\theta - v_t) dt + \sigma \sqrt{v_t} d\widetilde{W}_t^v, \tag{13}$$

$$d\widetilde{W}_t^S d\widetilde{W}_t^v = \rho \, dt, \tag{14}$$

with initial conditions $S_0 \geqslant 0$ and $v_0 \geqslant 0$, where $Q_t = \sum_{i=1}^{N_t} Y_i$ is a compound Poisson process and S_{t-} denotes the left limit of S at t. $Y_1, Y_2, \ldots$ are pairwise independent random variables with identically distributed jump sizes, that is, $\beta = \mathbb{E}[Y_i]$ for all $i \in \mathbb{N}$. N_t is a standard Poisson process with intensity λ also independent from the Y_i. The changed drift of the stock price process (12) guarantees that the model remains risk neutral.

In this model, jump sizes Y_i have log normal distribution, in particular $\ln(1 + Y_i) \sim \mathcal{N}(\mu_J, \sigma_J^2)$, that is,

$$\beta = \mathbb{E}[Y_i] = \exp\{\mu_J + \frac{1}{2}\sigma_J^2\} - 1.$$

In this model, the pricing formula for European call option prices follows (4), where P_1 and P_2 are defined by:

$$P_j(x, v, \tau) = \frac{1}{2} + \frac{1}{\pi} \int_0^{+\infty} \mathrm{Re}\left[\frac{e^{-iu \ln(K)}}{iu} f_j(u) \phi_j^J(u) \right] du, \quad j = 1, 2, \tag{15}$$

where $f_j(u) = f_j(x, v, \tau, u)$ is the same f_j as in the original Heston/Albrecher model satisfying (10) and the integrands are multiplied (jumps are additive in the model) by the jump characteristic functions

$$\phi^J(u) = \phi_2^J(u) = \exp\left\{ -i\lambda\beta u\tau + \lambda\tau \left[(1 + \beta)^{iu} \exp\left\{ -\frac{1}{2}\sigma_J^2 u(i + u) \right\} - 1 \right] \right\}, \tag{16}$$

$$\phi_1^J(u) = \frac{\phi_2^J(u-i)}{\phi_2^J(-i)} = \phi_2^J(u-i). \tag{17}$$

We can derive the Lewis-like formula from (15) by reversing the calculation steps used in Section 2.

$$\begin{aligned} V(S,v,\tau) &= SP_1 - e^{-r\tau}KP_2, \\ &= S\left\{\frac{1}{2} + \frac{1}{\pi}\int_0^{+\infty} \mathrm{Re}\left[\frac{e^{-iu\ln(K)}}{iu} f_1(u)\phi_1^J(u)\right] du\right\} \\ &\quad - e^{-r\tau}K\left\{\frac{1}{2} + \frac{1}{\pi}\int_0^{+\infty} \mathrm{Re}\left[\frac{e^{-iu\ln(K)}}{iu} f_2(u)\phi_2^J(u)\right] du\right\} \end{aligned}$$

omitting Re, using formula (10) for f_1 and (17) for ϕ_1

$$\begin{aligned} &= \frac{1}{2}(S - e^{-r\tau}K) \\ &\quad + S\frac{1}{\pi}\int_0^{+\infty} \frac{e^{-iu\ln(K)}}{iu}\frac{f_2(u-i)}{f_2(-i)}\phi_2^J(u-i)du \\ &\quad - e^{-r\tau}K\frac{1}{\pi}\int_0^{+\infty} \frac{e^{-iu\ln(K)}}{iu} f_2(u)\phi_2^J(u)du \end{aligned}$$

by formula (11) for $f_2(-i)$, substituting in the first integral $k = u - i$ and $k = u$ in the second integral, we obtain

$$\begin{aligned} &= \frac{1}{2}(S - e^{-r\tau}K) \\ &\quad + e^{\ln(K)}e^{-r\tau}\frac{1}{\pi}\int_{0-i}^{+\infty-i} \frac{e^{-ik\ln(K)}}{ik-1} f_2(k)\phi_2^J(k)dk \\ &\quad - e^{-r\tau}K\frac{1}{\pi}\int_0^{+\infty} \frac{e^{-ik\ln(K)}}{ik} f_2(k)\phi_2^J(k)dk \end{aligned}$$

with the symmetry property of the integrants we change the integration range

$$\begin{aligned} &= \frac{1}{2}(S - e^{-r\tau}K) \\ &\quad + e^{-r\tau}K\frac{1}{2\pi}\int_{-\infty-i}^{+\infty-i} \frac{e^{-ik\ln(K)}}{ik-1} f_2(k)\phi_2^J(k)dk \\ &\quad - e^{-r\tau}K\frac{1}{2\pi}\int_{-\infty}^{+\infty} \frac{e^{-ik\ln(K)}}{ik} f_2(k)\phi_2^J(k)dk \end{aligned}$$

using the residue theorem, where for practical reasons, we want $k = k_r + ik_i$ to be such that $0 < k_i < 1$

$$\begin{aligned} &= \frac{1}{2}(S - e^{-r\tau}K) \\ &\quad + e^{-r\tau}K\frac{1}{2\pi}\left(\int_{-\infty-ik_i}^{+\infty-ik_i} \frac{e^{-ik\ln(K)}}{ik-1} f_2(k)\phi_2^J(k)dk + \pi e^{-\ln(K)} f_2(-i)\right) \\ &\quad - e^{-r\tau}K\frac{1}{2\pi}\left(\int_{-\infty-ik_i}^{+\infty-ik_i} \frac{e^{-ik\ln(K)}}{ik} f_2(k)\phi_2^J(k)dk - \pi\right) \end{aligned}$$

from (9), we have $e^{-ik\ln(K)}f_2(k) = e^{ikX}\hat{H}(-k,v,\tau)$, where $X = \ln\frac{S}{K} + r\tau$, and by (11), we obtain

$$\begin{aligned} &= S + e^{-r\tau}K\frac{1}{2\pi}\int_{-\infty-ik_i}^{+\infty-ik_i} \frac{e^{ikX}}{ik-1}\hat{H}(-k,v,\tau)\phi_2^J(k)dk \\ &\quad - e^{-r\tau}K\frac{1}{2\pi}\int_{-\infty-ik_i}^{+\infty-ik_i} \frac{e^{ikX}}{ik}\hat{H}(-k,v,\tau)\phi_2^J(k)dk \end{aligned}$$

we change sign of the integration variable by substitution

$$\begin{aligned}
&= S - e^{-r\tau}K\frac{1}{2\pi}\int_{-\infty+ik_i}^{+\infty+ik_i}\frac{e^{-ikX}}{ik+1}\hat{H}(k,v,\tau)\phi_2^J(-k)dk \\
&\quad + e^{-r\tau}K\frac{1}{2\pi}\int_{-\infty+ik_i}^{+\infty+ik_i}\frac{e^{-ikX}}{ik}\hat{H}(k,v,\tau)\phi_2^J(-k)dk \\
&= S - e^{-r\tau}K\frac{1}{2\pi}\int_{-\infty+ik_i}^{+\infty+ik_i}e^{-ikX}\left(\frac{\hat{H}(k,v,\tau)}{ik+1} - \frac{\hat{H}(k,v,\tau)}{ik}\right)\phi_2^J(-k)dk \\
&= S - Ke^{-r\tau}\frac{1}{2\pi}\int_{-\infty+ik_i}^{+\infty+ik_i}e^{-ikX}\frac{\hat{H}(k,v,\tau)}{k^2-ik}\phi_2^J(-k)dk,
\end{aligned} \tag{18}$$

which is the Lewis-like formula for the Bates model. We can also rewrite (18) in terms of $\hat{\varphi}$ as

$$V(S,v,\tau) = S - Ke^{-r\tau}\frac{1}{2\pi}\int_{-\infty+ik_i}^{+\infty+ik_i}e^{-ik\tilde{X}}\frac{\hat{H}(k,v,\tau)}{k^2-ik}\exp\{\lambda(\hat{\varphi}(-k)-1)\tau\}dk,$$

where $\tilde{X} = \ln\frac{S}{K} + (r-\lambda\beta)\tau$ with $\beta = \exp\left\{\mu_J + \frac{1}{2}\sigma_J^2\right\} - 1$ and $\hat{\varphi}(u) = \exp\left\{i\mu_J u - \frac{1}{2}\sigma_J^2 u^2\right\}$.

Remark 1

The jump characteristic function as it is presented in (16) is not in the form of the Lévy–Khintchine formula, because

$$\phi^J(k) = \exp\left\{-i\lambda\beta k\tau + \lambda\tau\left[(1+\beta)^{ik}\exp\left\{-\frac{1}{2}\sigma_J^2 k(i+k))\right\} - 1\right]\right\}.$$

$$= \exp\left\{-i\lambda\beta k\tau + \lambda\tau\underbrace{\left[\exp\left\{\overbrace{(\ln(1+\beta) - \frac{1}{2}\sigma_J^2)}^{\mu_J}ik - \frac{1}{2}\sigma_J^2 k^2\right\}}_{\hat{\varphi}(k)} - 1\right]\right\},$$

where $\hat{\varphi}(k)$ is the characteristic function of a normal random variable $\mathcal{N}(\mu_J, \sigma_J^2)$ with

$$\mu_J = \ln(1+\beta) - \frac{1}{2}\sigma_J^2$$

or in other words if

$$\beta = \exp\left\{\mu_J + \frac{1}{2}\sigma_J^2\right\} - 1.$$

This corresponds to Lévy–Khintchine formula where we obtain (for Lévy process with drift $-\lambda\beta$)

$$\phi^J(k) = \exp\left\{-i\lambda\beta k\tau + \lambda\tau\left[\hat{\varphi}(k) - 1\right]\right\},$$

where the term in square brackets comes from the integration in the Lévy–Khintchine formula:

$$\int_{-\infty}^{+\infty}[e^{iky} - 1]\varphi(y)dy = \hat{\varphi}(k) - 1,$$

where we used the fact that φ is the density and it integrates to one.

4. Main result: a general unifying SVJD model

In this section, we introduce a general model that allows several kinds of SV processes and also different types of jumps.

Let N_t be a standard Poisson process with intensity λ. Let $Y_1, Y_2, \dots$ be random variables representing the jump sizes that are identically distributed with common mean $\beta = \mathbb{E}[Y_i]$ for all $i \in \mathbb{N}$. Also, assume that all Y_i are independent of one another and independent of the Poisson process $N(t)$. Let

$$Q_t = \sum_{i=1}^{N_t} Y_i$$

be a compound Poisson process. Then, $\mathbb{E}[Q_t] = \lambda\beta t$, and it can be shown that Q_t is not a martingale. Hence, we define

$$J_t = Q_t - \lambda\beta t, \tag{19}$$

which is a compensated compound Poisson process. Then, $\mathbb{E}[J_t] = 0$ and J_t is a martingale. We now consider the risk-neutral general jump-diffusion model

$$dS_t = rS_t dt + \sqrt{v_t} S_t d\widetilde{W}_t^S + S_{t-} dJ_t, \tag{20}$$

$$dv_t = p(v_t)dt + q(v_t)d\widetilde{W}_t^v, \tag{21}$$

$$d\widetilde{W}_t^S d\widetilde{W}_t^v = \rho\, dt, \tag{22}$$

where $p, q \in C^{+\infty}(0, \infty)$ are general coefficient functions for the volatility process and ρ is the correlation between standard Wiener processes $\widetilde{W}_t^S$ and $\widetilde{W}_t^v$. Models (20)–(22) cover several different models, in particular the Heston and the 3/2 model (cf. Lewis [29]). Table I gives typical examples of the volatility drift p and the volatility of volatility q for some of these models.

The FSVJD model that we will introduce in Section 4.2 uses a stochastic process ψ_t in the drift term. Additionally, we assume the presence of jumps in the stock price process. From definition (19), we deduce that

$$dJ_t = -\lambda\beta dt + dQ_t,$$

and (20) then becomes

$$dS_t = (r - \lambda\beta)S_t dt + \sqrt{v_t} S_t d\widetilde{W}_t^S + S_{t-} dQ_t.$$

We will give two examples for possible types of jumps.

Example 1
For a normally distributed random variable X, that is, for density

$$\varphi(y) = \frac{1}{\sigma_J\sqrt{2\pi}} \exp\left\{-\frac{(y-\mu_J)^2}{2\sigma_J^2}\right\},$$

we have that

$$\mathbb{E}[e^{ikX}] = \hat{\varphi}(k) = \int_{-\infty}^{+\infty} e^{iky}\varphi(y)dy = \exp\left\{i\mu_J k - \frac{1}{2}\sigma_J^2 k^2\right\},$$

and in particular, we obtain $\hat{\varphi}(-i) = \exp\{\mu_J + \frac{1}{2}\sigma_J^2\}$.

Table I. Different stochastic volatility models.

Model	$p(v)$	$q(v)$	Constants
Heston/Bates	$\kappa(\theta - v)$	$\sigma\sqrt{v}$	κ, θ, σ
3/2 model†	$\omega v - \tilde{\theta} v^2$	$\xi v^{\frac{3}{2}}$	$\omega, \theta, \xi, \gamma$
Geometric BM	αv	ξv	α, ξ
Fractional SVJD	$(H - 1/2)\psi_t\sigma\sqrt{v} + \kappa(\theta - v)$	$\varepsilon^{H-1/2}\sigma\sqrt{v}$	$H, \sigma, \kappa, \theta, \varepsilon$

†$\tilde{\theta} = -\frac{1}{2}\xi^2 + (1-\gamma)\rho\xi + \sqrt{(\theta + \frac{1}{2}\xi^2)^2 - \gamma(1-\gamma)\xi^2}$. SVJD, stochastic volatility jump-diffusion.

For Bates model, where jumps Y_i are log-normal, $\ln(1+Y_i) \sim \mathcal{N}(\mu_J, \sigma_J^2)$, we have that

$$\beta = \mathbb{E}[Y_i] = \exp\{\mu_J + \frac{1}{2}\sigma_J^2\} - 1 = \hat{\varphi}(-i) - 1.$$

Example 2
For a uniformly distributed random variable X, that is, for density

$$\varphi(y) = \begin{cases} \frac{1}{b-a} & a \leqslant y \leqslant b, \\ 0 & \text{otherwise}, \end{cases}$$

we have that

$$\mathbb{E}[e^{ikX}] = \hat{\varphi}(k) = \frac{1}{b-a}\int_a^b e^{iky}dy = \frac{e^{ikb} - e^{ika}}{(b-a)ik}, \tag{23}$$

and in particular $\hat{\varphi}(-i) = \frac{e^b - e^a}{b-a}$. For Yan and Hanson [14] model, see also section 4.1 below, jumps Y_i are log-uniform $\ln(1+Y_i) \sim \mathcal{U}(a,b)$ and we have that

$$\beta = \mathbb{E}[Y_i] = \frac{e^b - e^a}{b-a} - 1 = \hat{\varphi}(-i) - 1.$$

The problem of pricing an option in a model with jumps corresponds to a partial integro-differential equation (PIDE) (Hanson [38], Theorem 7.7). After substituting $x = \ln S$, we obtain the PIDE for $f(x,v,t) = V(e^x, v, t)$

$$\begin{aligned} -f_t = -rf + (r - \lambda\beta - \frac{1}{2}v)f_x + \frac{1}{2}vf_{xx} + pf_v + \frac{1}{2}q^2 f_{vv} + \rho q\sqrt{v}f_{xv} \\ + \lambda\int_{-\infty}^{+\infty}\left[f(x+y,v,t) - f(x,v,t)\right]\varphi(y)dy. \end{aligned} \tag{24}$$

We want to apply the complex Fourier transform like in Lewis [29], chapter 2,

$$\mathcal{F}\left[f\right] = \hat{f}(k,v,t) = \int_{-\infty}^{+\infty} e^{ikx} f(x,v,t)dx$$

with the inverse transform

$$f(x,v,t) = \frac{1}{2\pi}\int_{-\infty+ik_i}^{+\infty+ik_i} e^{-ikx}\hat{f}(k,v,t)dk,$$

where k_i is some real number such that the line $(-\infty+ik_i, \infty+ik_i)$ is in some strip of regularity depending on the restrictions given by the payoff (Table II). Under the Fourier transform, PIDE (24) becomes

Table II. Different payoff functions.

Financial claim	Payoff function $w(x)$	Payoff transform $\hat{w}(k)$	k-plane restrictions
Call option	$\max(e^x - K, 0)$	$-\frac{K^{ik+1}}{k^2-ik}$	Im $k > 1$
Put option	$\max(K - e^x, 0)$	$-\frac{K^{ik+1}}{k^2-ik}$	Im $k < 0$
Bull spread option	0 ..... for $0 \leqslant e^x \leqslant K_1$ $e^x - K_1$ for $K_1 < e^x \leqslant K_2$ $K_2 - K_1$ .... for $K_2 < e^x$	$\frac{K_2^{ik+1} - K_1^{ik+1}}{k^2-ik}$	Im $k > 0$
Bear spread option	$K_2 - K_1$ for $0 \leqslant e^x \leqslant K_1$ $K_2 - e^x$ for $K_1 < e^x \leqslant K_2$ 0 ..... for $K_2 < e^x$	$\frac{K_1^{ik+1} - K_2^{ik+1}}{k^2-ik}$	Im $k < 0$
Butterfly spread option†	0 ..... for $0 < e^x \leqslant K_1$ $e^x - K_1$ for $K_1 < e^x \leqslant K_2$ $K_3 - e^x$ for $K_2 < e^x \leqslant K_3$ 0 ..... for $K_3 < e^x$	$\frac{2K_2^{ik+1} - K_1^{ik+1} - K_3^{ik+1}}{k^2-ik}$	None

†where $K_2 = \frac{K_1+K_3}{2}$.

$$-\hat{f}_t = [-r - ik(r - \lambda\beta)]\hat{f} - \frac{1}{2}v(k^2 - ik)\hat{f} + (p - ik\rho q\sqrt{v})\hat{f}_v + \frac{1}{2}q^2\hat{f}_{vv} + \lambda\mathcal{F}\left[\int_{-\infty}^{+\infty}\left[f(x+y,v,t) - f(x,v,t)\right]\varphi(y)dy\right]. \tag{25}$$

It remains to derive the Fourier transform of the integral.

$$\begin{aligned}
&\mathcal{F}\left[\int_{-\infty}^{+\infty}\left[f(x+y,v,t) - f(x,v,t)\right]\varphi(y)dy\right] \\
&= \int_{-\infty}^{+\infty} e^{ikx}\left(\int_{-\infty}^{+\infty}\left[f(x+y,v,t) - f(x,v,t)\right]\varphi(y)dy\right)dx \\
&= \int_{-\infty}^{+\infty}\varphi(y)\left(\int_{-\infty}^{+\infty} e^{ikx}\left[f(x+y,v,t) - f(x,v,t)\right]dx\right)dy \\
&= \hat{f}(k,v,t)\int_{-\infty}^{+\infty}(e^{-iky} - 1)\varphi(y)dy = \hat{f}(k,v,t)(\hat{\varphi}(-k) - 1),
\end{aligned}$$

where we used the Fubini's theorem (the integrand is measurable and integrable) and the fact that $\int_{\mathbb{R}}\varphi(y)dy = 1$. We substitute $\tau = T - t$ and define $\hat{h}(k,v,t)$ by

$$\hat{h}(k,v,t) = \exp\left(-\left[-r - ik(r - \lambda\beta) + \lambda(\hat{\varphi}(-k) - 1)\right]\tau\right)\hat{f}(k,v,\tau)$$

to obtain from (25) the following equation for $\hat{h}$:

$$\hat{h}_\tau = \frac{1}{2}q^2(v)\hat{h}_{vv} + \left[p(v) - ik\rho(v)q(v)\sqrt{v}\right]\hat{h}_v - \frac{k^2 - ik}{2}v\hat{h}, \tag{26}$$

which is equal to equation (2.7) on p. 38 in Lewis [29] and has a fundamental solution $\hat{F}$ with initial value $\hat{F}(k,v,0) = 1$ (in Lewis [29], it is called fundamental transform). It is regular as a function of $k = k_r + ik_i$ within a strip $k_1 < k_i < k_2$. From this fundamental solution, we can derive the explicit formula for the option price

$$\begin{aligned}
f(x,v,t) &= \frac{1}{2\pi}\int_{-\infty+ik_i}^{+\infty+ik_i} e^{-ikx}\hat{f}(k,v,t)dk, \\
&= \frac{1}{2\pi}\int_{-\infty+ik_i}^{+\infty+ik_i} e^{-ikx}\exp\left(\left[-r - ik(r - \lambda\beta) + \lambda(\hat{\varphi}(-k) - 1)\right]\tau\right)\hat{w}(k)\hat{F}(k,v,\tau)dk,
\end{aligned} \tag{27}$$

where for call option, we have $\hat{w}(k) = \frac{-K^{ik+1}}{k^2 - ik}$ (Table II) and $1 < k_i < k_2$,

$$\begin{aligned}
&= -\frac{e^{-r\tau}}{2\pi}\int_{-\infty+ik_i}^{+\infty+ik_i} e^{-ikx}\exp\left(\left[-ik(r - \lambda\beta) + \lambda(\hat{\varphi}(-k) - 1)\right]\tau\right)\frac{K^{ik+1}}{k^2 - ik}\hat{F}(k,v,\tau)dk, \\
&= -K\frac{e^{-r\tau}}{2\pi}\int_{-\infty+ik_i}^{+\infty+ik_i} e^{-ik\tilde{X}}\exp\left\{\lambda(\hat{\varphi}(-k) - 1)\tau\right\}\frac{\hat{F}(k,v,\tau)}{k^2 - ik}dk, \quad 1 < k_i < k_2,
\end{aligned}$$

where $\tilde{X} = x - \ln K + (r - \lambda\beta)\tau = \ln(S/K) + (r - \lambda\beta)\tau$. We want to integrate over some line with $0 < k_i < 1$ where $\hat{F}$ is often free of singularities (Lewis [29]). For $\max(k_1, 0) < k_i < \min(1, k_2)$ by using the residue theorem, we obtain

$$V(s,v,\tau) = -K\frac{e^{-r\tau}}{2\pi}\left\{-2\pi i\frac{e^{\tilde{X}}}{i}\exp\{\lambda(\hat{\varphi}(-i) - 1)\tau\} + \int_{-\infty+ik_i}^{+\infty+ik_i} e^{-ik\tilde{X}}\exp\{\lambda(\hat{\varphi}(-k) - 1)\tau\}\frac{\hat{F}(k,v,\tau)}{k^2 - ik}dk\right\}, \tag{28}$$

$$= K\exp\{\tilde{X} - r\tau + \lambda(\hat{\varphi}(-i) - 1)\tau$$
$$- K\frac{e^{-r\tau}}{2\pi}\int_{-\infty+ik_i}^{+\infty+ik_i} e^{-ik\tilde{X}}\exp\{\lambda(\hat{\varphi}(-k) - 1)\tau\}\frac{\hat{F}(k,v,\tau)}{k^2 - ik}dk, \tag{29}$$

$$= Se^{\lambda(\hat{\varphi}(-i)-1-\beta)\tau} - K\frac{e^{-r\tau}}{2\pi}\int_{-\infty+ik_i}^{+\infty+ik_i} e^{-ik\tilde{X}}\exp\{\lambda(\hat{\varphi}(-k) - 1)\tau\}\frac{\hat{F}(k,v,\tau)}{k^2 - ik}dk, \tag{30}$$

where $\hat{\varphi}(-i) - 1 - \beta = 0$ (provided that jumps are log-normally or log-uniformly distributed as seen in the previous examples) and therefore

$$V(S,v,\tau) = S - Ke^{-r\tau}\frac{1}{2\pi}\int_{-\infty+ik_i}^{+\infty+ik_i} e^{-ik\tilde{X}}\exp\{\lambda(\hat{\varphi}(-k) - 1)\tau\}\frac{\hat{F}(k,v,\tau)}{k^2 - ik}dk, \tag{31}$$
$$\max(k_1, 0) < k_i < \min(1, k_2).$$

We can also rewrite (31) in terms of

$$\phi(k) = \exp\left\{-i\lambda\beta k\tau + \lambda\tau\left[\hat{\varphi}(k) - 1\right]\right\} \tag{32}$$

as

$$V(S,v,\tau) = S - Ke^{-r\tau}\frac{1}{2\pi}\int_{-\infty+ik_i}^{+\infty+ik_i} e^{-ikX}\frac{\hat{F}(k,v,\tau)}{k^2 - ik}\phi(-k)dk, \tag{33}$$

where again $X = \ln\frac{S}{K} + r\tau$.

To price other option types, we need to replace $\hat{w}$ in (27) by the Fourier transform of the payoff function (see Table II for some common examples). When calculating the final formula, one has to consider the k-plane restriction of the payoff and use the residue theorem accordingly.

4.1. Example: Yan Hanson SVJD model

In the model by Yan and Hanson [14], the drift p and the diffusion q of the volatility process are the same as in the Heston and Bates model, namely,

$$p(v) = \kappa(\theta - v), \quad q(v) = \sigma\sqrt{v},$$

where κ, θ and σ are real constants. The jump sizes are log-uniform (Example 2).

The original pricing formula from Yan and Hanson [14] is the following

$$V = S_0P_1 - Ke^{-r\tau}P_2;$$

for $j = 1, 2$:

$$P_j(\log[S_0], v, \tau; \ln[K]) = \frac{1}{2} + \frac{1}{\pi}\int_0^{+\infty}\mathrm{Re}\left[\frac{e^{-iy\log[K]}f_j(\log[S_0], v; y, \tau)}{iy}\right]dy,$$

where

$$f_j(\log[S_0], v; y, \tau) = \exp\{g_j + h_jv + iy\log[S_0] + \beta_j\},$$
$$\beta_j = r\tau\delta_{j,2}$$
$$h_j = \frac{(\eta_j^2 - \Delta_j^2)(e^{\Delta_j\tau} - 1)}{\sigma^2(\eta_j + \Delta_j - (\eta_j - \Delta)e^{\Delta_j\tau})}$$
$$g_j = \left((r - \lambda\beta)iy - \lambda J\delta_{j,1} - r\delta_{j,2}\right)\tau +$$
$$+ \lambda\tau\int_{-\infty}^{+\infty}(e^{(iy+\delta_{j,1})q} - 1)\phi_Q(q)dq -$$

$$- \frac{\kappa\theta}{\sigma^2}\left[2\log\left(1 - \frac{(\Delta_j + \eta_j)(1 - e^{-\Delta_j\tau})}{2\Delta_j}\right) + (\Delta_j + \eta_j)\tau\right],$$

$$\beta = \frac{e^b - e^a}{b - a} - 1$$

$$\eta_j = \rho\sigma(iy + \delta_{j,1}) - \kappa$$

$$\int_{-\infty}^{+\infty} (e^{(iy+\delta_{j,1})q} - 1)\phi_Q(q)dql = \frac{e^{(iy+\delta_{j,1})b} - e^{(iy+\delta_{j,1})a}}{(b - a)(iy + \delta_{j,1})} - 1.$$

For $j = 1$, we have

$$\delta_{1,1} = 1, \delta_{1,2} = 0 \text{ and } \Delta_1 = \sqrt{\eta_j^2 - \sigma^2 iy(iy + 1)};$$

for $j = 2$, we have

$$\delta_{2,1} = 0, \delta_{2,2} = 1 \text{ and } \Delta_2 = \sqrt{\eta_j^2 - \sigma^2 iy(iy - 1)}.$$

New pricing formula for the Yan Hanson model is (31) with $\hat{\phi}(k)$ defined in (23), or (33) in terms of $\phi(k)$.

4.2. Example: a new fractional SVJD model

We want to modify the Bates model from Section 3 by using an approximate fractional Brownian motion in the volatility process. This process has a long memory for Hurst parameter $H > 0.5$, and for $H = 0.5$, it turns into a standard Wiener process. Thao [39] defined approximative fractional process as an Itô integral,

$$\tilde{B}_t^\varepsilon = \int_0^t (t - s + \varepsilon)^{H-1/2} dW_s,$$

where ε represents an approximative factor that should take values close to 0. However, for any $\varepsilon > 0$, $\tilde{B}_t^\varepsilon$ is a semimartingale. The market dynamics under the square root approximative fractional SVJD model, that will be of our main interest further on, would be the following:

$$dS_t = (r - \lambda\beta)S_t dt + \sqrt{v_t}S_t d\widetilde{W}_t^S + S_{t-}dQ_t, \tag{34}$$

$$dv_t = \kappa(\theta - v_t)dt + \sigma\sqrt{v_t}d\tilde{B}_t^\varepsilon, \tag{35}$$

where the jumps are log-normal as in the Example 1. According to Thao [39] (Lemma 2.1), we can write the approximate fractional Brownian motion $\tilde{B}_t^\varepsilon$ as

$$d\tilde{B}^\varepsilon = (H - 1/2)\psi_t dt + \varepsilon^{H-1/2} d\widetilde{W}_t^v, \tag{36}$$

where $H > 1/2$ and ψ_t is a stochastic process defined by the Itô integral

$$\psi_t = \int_0^t (t - s + \varepsilon)^{H-3/2} dW_s^\psi.$$

We substitute (36) into (35) to obtain the market dynamics in the form,

$$dS_t = (r - \lambda\beta)S_t dt + \sqrt{v_t}S_t d\widetilde{W}_t^S + S_{t-}dQ_t, \tag{37}$$

$$dv_t = \left[(H - 1/2)\psi_t\sigma\sqrt{v_t} + \kappa(\theta - v_t)\right]dt + \varepsilon^{H-1/2}\sigma\sqrt{v_t}d\widetilde{W}_t^v, \tag{38}$$

which gives us

$$p(v) = \left[(H - 1/2)\psi_t\sigma\sqrt{v} + \kappa(\theta - v_t)\right], \quad q(v) = \varepsilon^{H-1/2}\sigma\sqrt{v}.$$

We can also assume that the both Wiener processes $\widetilde{W}_t^S$ and $\widetilde{W}_t^v$ are instantaneously correlated, that is,

$$d\widetilde{W}_t^S d\widetilde{W}_t^v = \rho\, dt. \tag{39}$$

To obtain option pricing formula, we need to derive the fundamental solution $\hat{F}_F(k, v, \tau)$ of Equation (26), in particular

$$\frac{\partial \hat{F}_F}{\partial \tau} = \frac{1}{2}\varepsilon^{2(H-1/2)}\sigma^2 v \frac{\partial^2 \hat{F}_F}{\partial v^2} + \left[(H-1/2)\psi_t\sigma\sqrt{v} + \kappa(\theta - v) - ik\rho\varepsilon^{H-1/2}\sigma v\right]\frac{\partial \hat{F}_F}{\partial v} + c(k)v\hat{F}_F,$$

with $c(k) = (k^2 - ik)/2$ and initial value $\hat{F}_F(k, v, 0) = 1$. We are looking for a solution of the form

$$\hat{F}_F(k, v, \tau) = \exp(C_F(k, \tau) + D_F(k, \tau)v),$$

where C_F and D_F do not depend on v. After cancelling $\hat{F}_F \neq 0$, we obtain

$$\frac{\partial C_F}{\partial \tau} + \frac{\partial D_F}{\partial \tau}v = \frac{1}{2}\varepsilon^{2(H-1/2)}\sigma^2 v D_F^2 + \left[(H-1/2)\psi_t\sigma\sqrt{v} + \kappa(\theta - v) - ik\rho\varepsilon^{H-1/2}\sigma v\right]D_F + c(k)v$$

with initial values $C_F(k, 0) = D_F(k, 0) = 0$. We recall that ψ_t is a martingale and $\psi_0 = \mathbb{E}\left[\psi_t\right] = 0$.

$$v\left[-\frac{\partial D_F}{\partial \tau} + \frac{1}{2}\varepsilon^{2(H-1/2)}\sigma^2 D_F^2 - \left(\kappa + ik\rho\varepsilon^{H-1/2}\sigma\right)D_F - c(k)\right] - \frac{\partial C_F}{\partial \tau} + \kappa\theta D_F = 0. \tag{40}$$

Because (40) must hold for all v, we can split it into a system of two equations

$$\frac{\partial D_F}{\partial \tau} = \frac{1}{2}\varepsilon^{2(H-1/2)}\sigma^2 D_F^2 - \left(\kappa + ik\rho\varepsilon^{H-1/2}\sigma\right)D_F - c(k), \tag{41}$$

$$\frac{\partial C_F}{\partial \tau} = \kappa\theta D_F. \tag{42}$$

Equation (41) is a Ricatti equation and can be solved explicitly (for example, Pospíšil and Sobotka [26], Proposition 2.1), and then we obtain C_F by integrating (42). The formula (33) for this model with approximate fractional Brownian motion is

$$V(S, v, \tau) = S - Ke^{-r\tau}\frac{1}{2\pi}\int_{-\infty+i/2}^{+\infty+i/2} e^{-ikX}\frac{\hat{F}_F(k, v, \tau)}{k^2 - ik}\phi(-k)dk, \tag{43}$$

with

$$\begin{aligned}
\hat{F}_F(k, v, \tau) &= \exp(C_F(k, \tau) + D_F(k, \tau)v)\\
C_F(k, \tau) &= \kappa\theta Y\tau - \frac{2\kappa\theta}{B^2}\ln\left(\frac{1 - ge^{-d\tau}}{1 - g}\right)\\
D_F(k, \tau) &= Y\frac{1 - e^{-d\tau}}{1 - ge^{-d\tau}}\\
Y &= -\frac{k^2 - ik}{b + d}\\
g &= \frac{b - d}{b + d}\\
d &= \sqrt{b^2 + B^2(k^2 - ik)}\\
b &= \kappa + ik\rho B\\
B &= \varepsilon^{H-\frac{1}{2}}\sigma,
\end{aligned}$$

and $\phi(k)$ is defined in (32) with $\hat{\varphi}(k)$ as in Example 1. Similarly, we could use the formula (31).

Table III. Efficiency of the Bates SVJD pricing formulas.

Pricing approach	Task	Time† (s)	Speed-up factor
Original	#1	38.01	—
	#2	407.16	—
	#3	3396.74	—
Newly proposed	#1	9.37	4.06×
	#2	80.98	5.03×
	#3	926.10	3.67×

†The results were obtained on a PC with 2× Intel Xeon E5-2630 CPU and 12-GB RAM. SVJD, stochastic volatility jump-diffusion.

5. Numerical comparison of formulas

In this section, we present a comparison of pricing formulas with respect to the previously introduced jump diffusion models.

First and foremost, the computational efficiency of our solution for Bates [12] and Yan and Hanson [14] model is assessed. We compare computational times needed to perform a selected pricing task with respect to the original and newly proposed formulas. Three pricing tasks are considered for this purpose, all of which include 100 European call options with different times to maturity and strike prices¶. To judge performance of the formulas with respect to a wide range of financial markets, parameter sets used in the computation are randomly (uniformly) generated among the parameter bounds. The first pricing task consists of 100 parameter sets. It mimics a market calibration trial with a very good initial guess. For the second task, the pricing formulas are applied for 1000 generated parameter sets. The computation time, in this case, should be similar to an average calibration from 100 market contracts using local search methods (e.g. Pospíšil and Sobotka [26]). As was shown, for instance, by Mrázek *et al*. [40], a calibration of SV models might attain more local minima, and thus, a more complex global optimization procedure can prove useful. Therefore, the last pricing task includes 10 000 randomly generated parameter sets and should be more time consuming than a calibration with local search methods.

To numerically evaluate the inverse Fourier transform integral, different numerical quadratures can be considered, typically Gauss–Laguerre or Gauss–Hermitte for infinite domain integration, or Gauss–Legendre, Gauss–Lobatto or Gauss–Kronrod for suitable finite upper integration bound. Although Newton–Cotes quadratures (trapezoidal or Simpson's rules) are simple to implement, their error usually cannot compete with the aforementioned quadratures. Nevertheless, some authors [41,42] favour the simplified trapezoidal rule for its speed. Because a proper comparison of numerical quadratures (cf. with Rouah [43], Chapter 5) is ongoing research and it goes beyond the scope of this paper, in our numerical experiments in the succeeding discussion, we used only the Gauss–Kronrod (7,15) quadrature that is implemented in the MATLAB's function `integral`.

5.1. Bates SVJD model

As the reference formula for Bates [12] model we take the one suggested by Gatheral [11]. Unlike the original one by Bates [12], it does not suffer from the well-known *Heston trap* issue.

Using the fundamental transform formula, we are able to obtain call prices in a significantly shorter time. In fact, the newly proposed formula can be evaluated three to five times faster than the reference formula with two integrals. The results can be found in Table III. The precision of the computation can however differ depending on parameters, contract setting and also on the numerical procedure used to evaluate integrals. In our setting, an absolute difference between the formulas remains typically well beyond `1e-8` (Figure 1).

5.2. Yan Hanson SVJD model

We also compare the computation efficiency of the fundamental transform solution with respect to the Yan Hanson SVJD model. As in the previous case, we are able to achieve better results compared with the original formula. The performance improvement, however, is not as remarkable as for the Bates model. Computations using the proposed formula consume 13.7–25.7% less time. The speed-up factors alongside computational times are displayed in Table IV.

¶*All combination of short, medium, longer terms (2 years) and OTM, ATM and ITM contracts are considered.*

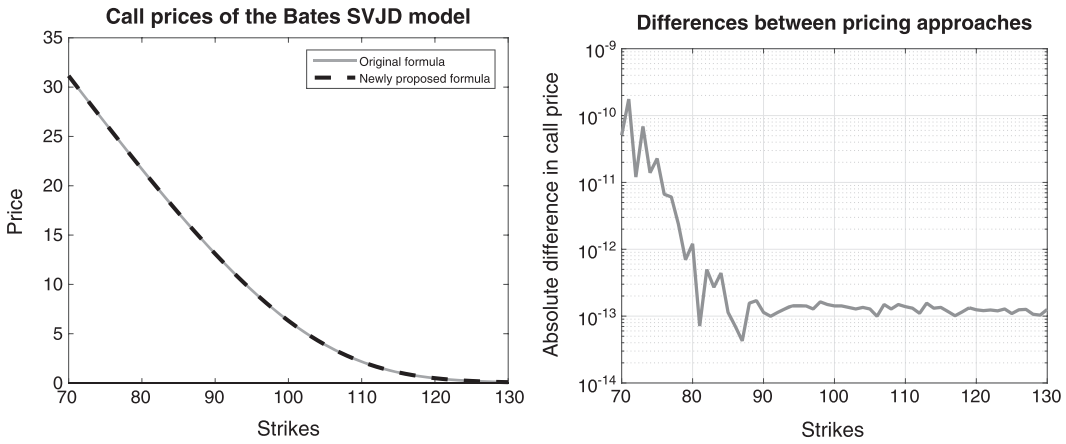

Figure 1. Comparison of the pricing formulas for the Bates SVJD model. Absolute differences between the formulas are depicted in the right part of the figure. Parameters used are as follows: $v_0 = 0.025$; $\kappa = 0.98$; $\theta = 0.07$; $\sigma = 0.25$; $\rho = -0.65$; $\lambda = 0.5$; $\mu_J = -0.05$; $\sigma_J = 0.1$; and for $S_0 = 100$, $\tau = 0.5$, $r = 0.03$. SVJD, stochastic volatility jump-diffusion.

Table IV. Efficiency of the Yan Hanson SVJD pricing formulas.

Pricing approach	Task	Time (s)	Speed-up factor
Original	#1	25.33	—
	#2	300.83	—
	#3	3011.77	—
Newly proposed	#1	21.86	1.16×
	#2	223.54	1.35×
	#3	2530.45	1.19×

†The results were obtained on a PC with 2× Intel Xeon E5-2630 CPU and 12-GB RAM. SVJD, stochastic volatility jump-diffusion.

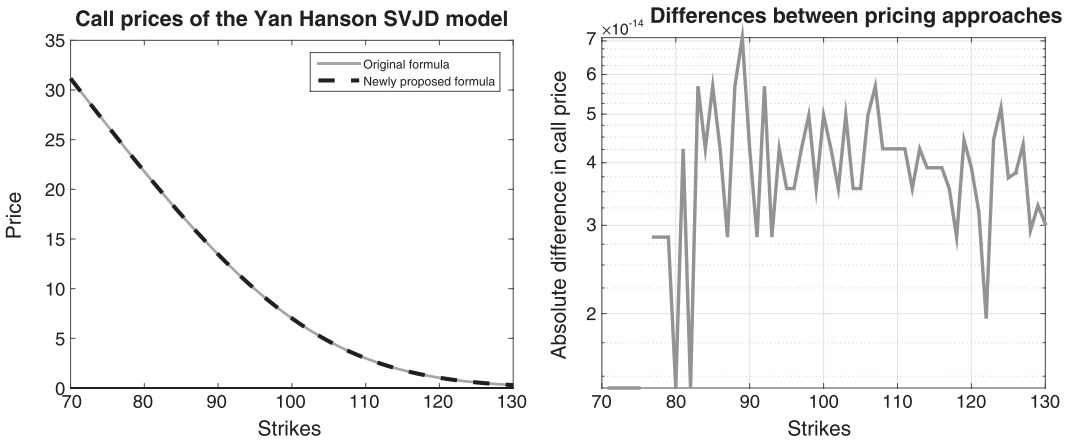

Figure 2. Comparison of the pricing formulas for the Yan Hanson SVJD model. Absolute differences between the formulas are depicted in the right part of the figure. Parameters used are as follows: $v_0 = 0.025$; $\kappa = 0.98$; $\theta = 0.07$; $\sigma = 0.25$; $\rho = -0.65$; $\lambda = 64$; $a = -0.028$; $b = 0.026$; and for $S_0 = 100$, $\tau = 0.5$, $r = 0.03$. SVJD, stochastic volatility jump-diffusion.

The prices obtained by the formulas are very much alike – the absolute differences in prices are typically of the order `1e-13` to `1e-14` (Figure 2). Again, the result depends on the numerical procedure used. The contract prices, however, are usually quoted within two or three decimal digits, and hence, the numerical differences in both formulas are negligible.

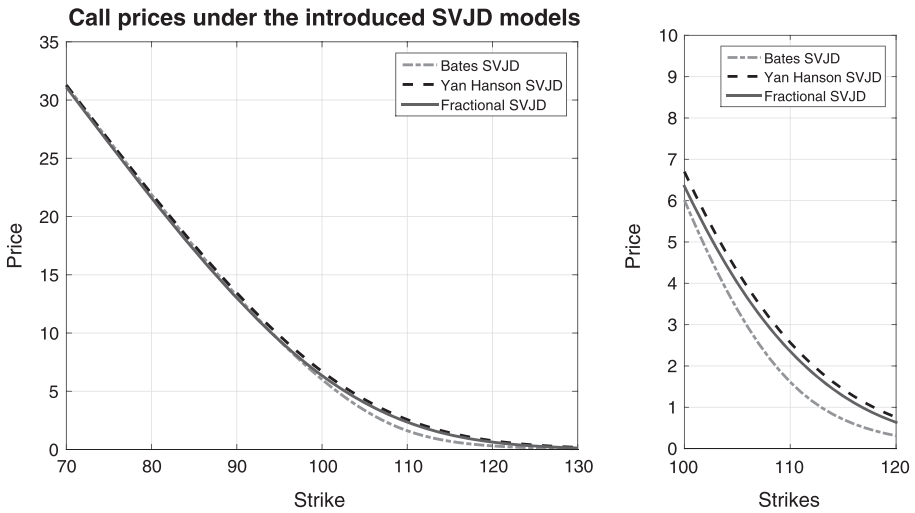

Figure 3. Option price as a function of the strike price for a call option with maturity 0.5 years and $S_0 = 100$, $r = 0.03$. SVJD, stochastic volatility jump-diffusion.

5.3. Fractional SVJD model

To judge the model performance with respect to the market calibration (for that, see [6]) or hedging is out of scope of this paper. Nonetheless, we provide a visual comparison for all the aforementioned models. In Figure 3, we depict option price smiles for SVJD models with log-normal and log-uniform jumps alongside the approximative fractional SVJD model with log-normal jumps. A significant difference in the call option prices is typically observed for out-of-the-money contracts. Counter-intuitively, the smile generated by fractional model with $H = 0.7$ is closer to the one created by Yan Hanson model with log-uniform jumps. For $H = 0.5$, we obtain the same results as for the Bates SVJD model.

6. Conclusion

The aim of this paper was to introduce a unifying approach to option pricing under continuous-time SV models with jumps. We generalized the approach by Lewis [29] to the class of SV models with jumps in the underlying stock process. We derived a new unifying formula using the complex Fourier transform of the corresponding PIDE. The unifying pricing formulas (31) and (33) are stated for the European call options, but we have also discussed how the solutions for different payoffs can be obtained. We provided also several illustrative examples. Namely, we have shown how the unifying approach applies to the Bates [12] and Yan and Hanson [14] models with log-normal and log-uniform jumps, respectively. Moreover, we applied the results to the new approximative fractional SV model.

Although the unifying approach covers various interesting SVJD models, there are other models that do not fit into the general structure described in Section 4. For these models, such as Barndorff–Nielsen and Shephard [15] model, we still might be able to derive a one integral option pricing formula, see Appendix A.

Numerical comparison of the efficiency of the new proposed formulas shows that for the Bates model, our solution is up to five times faster than the original one. As for the Yan Hanson model, the computational time also improves by approximately 14–26%. Last but not least, we compared the call prices under these models with the fractional SVJD model. The main difference was observed, especially for the out-of-the money contracts. The newly derived formulas are ready to be used out of the box for any practical task that involves option pricing. The obtained improvement in the efficiency may become crucial in model calibration to complex option surfaces.

Appendix A. The unifying formula for BNS model

Although the Barndorff–Nielsen and Shephard [15] (BNS) model with dynamics (A1) and (A2) does not fit into the general model structure described in Section 4, we are able to deduce an option pricing formula that involves only one numerical integration. This is performed by following the steps introduced in Section 3.

We will consider the 'classical' version of the model ([19] Table I) with a leverage effect originally proposed by Nicolato and Venardos [17]. Under the model, evolution of the logarithmic stock price $X_t = \ln(S_t)$ is described by risk-neutral

dynamics:

$$dX_t = (\mu + \lambda\rho - v_t/2)dt + \sqrt{v_t}dW_t + \rho dZ_t, \tag{A1}$$

$$dv_t = -\lambda v_t dt + dZ_t, \tag{A2}$$

where $(W_t)_{t\geqslant 0}$ is a standard Wiener process, $\rho < 0$, $\lambda, v_0 \geqslant 0$ and $(Z_t)_{t\geqslant 0}$ is a Lévy subordinator (independent on W_t)[‖]. The model price of a call option with strike K can be retrieved using a standard Fourier transform [17].

$$V(S, v, \tau) = SP_1 - e^{-r\tau}KP_2; \tag{A3}$$

$$P_1(S, v, \tau = \frac{1}{2} + \frac{1}{2\pi}\int_{-\infty}^{+\infty} \mathrm{Re}\left[\frac{e^{-i\phi\ln(K)}f(S, v, \tau, u - i)}{iuf(S, v, \tau, -i)}\right]du, \tag{A4}$$

$$P_2(S, v, \tau) = \frac{1}{2} + \frac{1}{2\pi}\int_{-\infty}^{+\infty} \mathrm{Re}\left[\frac{e^{-i\phi\ln(K)}f(S, v, \tau, u)}{iu}\right]du, \tag{A5}$$

$$\begin{aligned}
f(S, v, \tau, u) &= e^{A(u,\tau)+B(u,\tau)}e^{iu\ln S + iur\tau},\\
A(u, \tau) &= -\frac{v}{2\lambda}(u^2 + iu)(1 - e^{-\lambda\tau}) - \frac{iua\lambda\rho}{b - \rho}\tau,\\
B(u, \tau) &= \frac{a}{b - h_2}\left(b\ln\left(\frac{b - h_1}{b - iu\rho}\right) + h_2\lambda\tau\right),\\
h_1(u) &= iu\rho - \frac{1}{2\lambda}(u^2 + iu)(1 - e^{-\lambda\tau}), \quad h_2(u) = iu\rho - \frac{1}{2\lambda}(u^2 + iu).
\end{aligned}$$

Option price (A3) can be rewritten using the notation $C(u) = C(u, \tau) = \exp\{A(u, \tau) + B(u, \tau)\}$. Also, note that $C(-i) = 1$ for any positive τ.

$$\begin{aligned}
V(S, v, \tau) =& \frac{1}{2}(S - e^{-r\tau}K) + S\frac{1}{2\pi}\int_{-\infty}^{+\infty}\frac{e^{iuX}}{iu}\frac{C(u - i)}{C(-i)}du\\
&- e^{-r\tau}K\frac{1}{2\pi}\int_{-\infty}^{+\infty}\frac{e^{iuX}}{iu}C(u)du.
\end{aligned} \tag{A6}$$

By substituting $k = u - i$ and $k = u$, respectively, we obtain

$$= \frac{1}{2}(S - e^{-r\tau}K) + e^{-r\tau}K\frac{1}{2\pi}\left(\int_{-\infty-i}^{+\infty-i}\frac{e^{ikX}}{ik - 1}C(k)dk - \int_{-\infty}^{+\infty}\frac{e^{ikX}}{ik}C(k)dk\right). \tag{A7}$$

In order to retrieve a one integral formula that would correspond to the complex Fourier transform with $k_i = i/2$, we use the residue theorem.

$$\begin{aligned}
&= S + e^{-r\tau}K\frac{1}{2\pi}\left(\int_{-\infty-i/2}^{+\infty-i/2}\frac{e^{ikX}}{ik - 1}C(k)dk - \int_{-\infty-i/2}^{+\infty-i/2}\frac{e^{ikX}}{ik}C(k)dk\right)\\
&= S - e^{-r\tau}K\frac{1}{2\pi}\left(\int_{-\infty+i/2}^{+\infty+i/2}\frac{e^{-ikX}}{ik + 1}C(-k)dk - \int_{-\infty+i/2}^{+\infty+i/2}\frac{e^{-ikX}}{ik}C(-k)dk\right).\\
&= S - e^{-r\tau}K\frac{1}{2\pi}\int_{-\infty+i/2}^{+\infty+i/2}e^{-ikX}\frac{C(-k)}{k^2 - ik}dk
\end{aligned} \tag{A8}$$

Remark 2

The formula given by (A8) takes the same form as (33), where $C(k)$ represents a fundamental transform with respect to the BNS model.

[‖] *Lévy subordinator is a positive Lévy process which is almost surely increasing.*

Table AI. Efficiency of the BNS pricing formulas.

Pricing approach	Task	Time† (s)	Speed-up factor
Original	#1	4.14	—
	#2	46.84	—
	#3	445.98	—
Newly proposed	#1	3.37	1.23×
	#2	33.22	1.41×
	#3	332.34	1.34×

†The results were obtained on a PC with 2× Intel Xeon E5-2630 CPU and 12-GB RAM. BNS, Barndorff–Nielsen and Shephard.

As for other models, the formula (A8) is more time efficient than the original one (A3). This is illustrated in Table AI, the speed-up factor in case of the BNS model ranged between 1.23 and 1.41.

Acknowledgements

Falko Baustian was partially supported by a joint exchange programme between the Czech Republic and Germany: MSMT MOBILITY grant no. 7AMB14DE005 and DAAD PPP grant no. 57063847. The remaining authors were supported by the GACR grant 14-11559S Analysis of Fractional Stochastic Volatility Models and their Grid Implementaton. Computational resources were provided by the CESNET LM2015042 and the CERIT Scientific Cloud LM2015085, provided under the programme 'Projects of Large Research, Development, and Innovations Infrastructures'.

Conflict of Interest

The authors declare that they have no conflict of interest.

References

1. Black F, Scholes MS. The pricing of options and corporate liabilities. *Journal of Political Economy* 1973; **81**(3):637–654.
2. Hull JC, White AD. The pricing of options on assets with stochastic volatilities. *Journal of Finance* 1987; **42**(2):281–300.
3. Stein J, Stein E. Stock price distributions with stochastic volatility: an analytic approach. *Review of Financial Studies* 1991; **4**(4):727–752.
4. Heston SL. A closed-form solution for options with stochastic volatility with applications to bond and currency options. *Review of Financial Studies* 1993; **6**(2):327–343.
5. Bayer C, Friz P, Gatheral J. Pricing under rough volatility. *Quantitative Finance* 2016; **16**(6):887–904.
6. Mrázek M, Pospíšil J, Sobotka T. On calibration of stochastic and fractional stochastic volatility models. *European Journal of Operational Research* 2016; **254**(3):1036–1046.
7. Mikhailov S., Nögel U. Heston's stochastic volatility model – implementation, calibration and some extensions. *Wilmott Magazine* 2003; **2003**(July):74–79.
8. Elices A. Models with time-dependent parameters using transform methods: application to Heston's model, 2008. arXiv: 0708.2020v2.
9. Benhamou E, Gobet E, Miri M. Time dependent Heston model. *SIAM Journal on Financial Mathematics* 2010; **1**(1):289–325.
10. Duffie D., Pan J., Singleton K. Transform analysis and asset pricing for affine jump-diffusions. *Econometrica Journal of the Econometric Society* 2000; **68**(6):1343–1376.
11. Gatheral J. *The Volatility Surface: A Practitioner's Guide*, Wiley Finance. John Wiley & Sons: Hoboken, New Jersey, 2006.
12. Bates DS. Jumps and stochastic volatility: exchange rate processes implicit in Deutsche mark options. *Review of Financial Studies* 1996; **9**(1): 69–107.
13. Scott LO. Pricing stock options in a jump-diffusion model with stochastic volatility and interest rates: applications of Fourier inversion methods. *Mathematical Finance* 1997; **7**(4):413–426.
14. Yan G, Hanson FB. Option pricing for a stochastic-volatility jump-diffusion model with log-uniform jump-amplitude. In *Proceedings of American Control Conference*: IEEE: Piscataway, NJ, 2006; 2989–2994.
15. Barndorff-Nielsen OE, Shephard N. Non-Gaussian Ornstein–Uhlenbeck-based models and some of their uses in financial economics. *Journal of the Royal Statistical Society: Series B (Statistical Methodology)* 2001; **63**(2):167–241.
16. Jacod J, Todorov V. Do price and volatility jump together? *The Annals of Applied Probability* 2010; **20**(4):1425–1469.
17. Nicolato E, Venardos E. Option pricing in stochastic volatility models of the Ornstein–Uhlenbeck type. *Mathematical Finance* 2003; **13**(4): 445–466.
18. Deelstra G, Petkovic A. How they can jump together: multivariate Lévy processes and option pricing. *Belgian Actuarial Bulletin* 2010; **9**:29–42.
19. Bannör KF, Scherer M. A BNS-type stochastic volatility model with two-sided jumps with applications to FX options pricing. *Wilmott* 2013; **2013**(65):58–69.
20. Mai J-F, Scherer M, Schulz T. Sequential modeling of dependent jump processes. *Wilmott* 2014; **2014**(70):54–63.

21. Sengupta I. Generalized BNS stochastic volatility model for option pricing. *International Journal of Theoretical and Applied Finance* 2016; **19**(02):1650014.
22. Breidt FJ, Crato N, de Lima P. The detection and estimation of long memory in stochastic volatility. *Journal of Econometrics* 1998; **83**(1–2): 325–348.
23. Gatheral J, Jaisson T, Rosenbaum M. *Volatility is rough*, 2014. DOI: 10.2139/ssrn.2509457. Available at SSRN: http://ssrn.com/abstract=2509457 [11 April 2016].
24. Mandelbrot B, Van Ness J. Fractional Brownian motions, fractional noises and applications. *SIAM Review* 1968; **10**(4):422–437.
25. Comte F, Coutin L, Renault E. Affine fractional stochastic volatility models. *Annals of Finance* 2012; **8**(2–3):337–378.
26. Pospíšil J, Sobotka T. Market calibration under a long memory stochastic volatility model. *Applied Mathematical Finance* 2016; **23**(5):323–343.
27. Albrecher H, Mayer P, Schoutens W, Tistaert J. The little Heston trap. *Wilmott Magazine* 2007; **2007**(January/February):83–92.
28. Kahl C, Jäckel P. Not-so-complex logarithms in the Heston model. *Wilmott Magazine* 2005; **2005**(September):94–103.
29. Lewis AL. *Option Valuation under Stochastic Volatility, with Mathematica Code*. Finance Press: Newport Beach, CA, 2000.
30. Lipton A. The vol smile problem. *Risk* 2002; **15**(2):61–66.
31. Attari M. *Option pricing using Fourier transforms: a numerically efficient simplification*, 2004. Available at SSRN: http://ssrn.com/abstract=520042 [11 April 2016].
32. Carr P, Madan DB. Option valuation using the fast Fourier transform. *Journal of Computational Finance* 1999; **2**(4):61–73.
33. Lewis AL. A simple option formula for general jump-diffusion and other exponential Lévy processes. *Envision Financial Systems and OptionCitynet* 2001:1–24. Available at http://optioncity.net/pubs/ExpLevy.pdf [11 April 2016].
34. Feller W. Two singular diffusion problems. *Annals of Mathematics* 1951; **54**(1):173–182.
35. Cox JC, Ingersoll JE, Ross SA. A theory of the term structure of interest rates. *Econometrica Journal of the Econometric Society* 1985; **53**(2): 385–407.
36. Zhylyevskyy O. Efficient pricing of European-style options under Heston's stochastic volatility model. *Theoretical Economics Letters* 2012; **2**(1):16–20.
37. Ahlfors LV. *Complex Analysis* Third. McGraw-Hill Book Co.: New York, 1978.
38. Hanson FB. *Applied Stochastic Processes and Control for Jump-diffusions*, Advances in Design and Control, vol. 13. SIAM: Philadelphia, PA, 2007.
39. Thao TH. An approximate approach to fractional analysis for finance. *Nonlinear Analysis: Real world Applications* 2006; **7**(1):124–132.
40. Mrázek M, Pospíšil J, Sobotka T. On optimization techniques for calibration of stochastic volatility models. In *Applied numerical mathematics and scientific computation*. Euroment: Athens, Greece, 2014; 34–40.
41. Levendorskii S. Efficient pricing and reliable calibration in the Heston model. *International Journal of Theoretical and Applied Finance* 2012; **15**(7):1–44.
42. Boyarchenko S, Levendorskii S. Efficient variations of the Fourier transform in applications to option pricing. *Journal of Computational Finance* 2014; **18**(2):57–90.
43. Rouah FD. *The Heston Model and Its Extensions in Matlab and C#, + Website*, Wiley Finance Series. John Wiley & Sons: Hoboken, NJ, 2013.

International Journal of Theoretical and Applied Finance
Vol. 21, No. 8 (2018) 1850052 (36 pages)

DOI: 10.1142/S0219024918500528

World Scientific
www.worldscientific.com

DECOMPOSITION FORMULA FOR JUMP DIFFUSION MODELS

R. MERINO*,‡, J. POSPÍŠIL†, T. SOBOTKA† and J. VIVES*,§

*Facultat de Matemàtiques, Universitat de Barcelona
Gran Via 585, 08007 Barcelona, Spain

†Faculty of Applied Sciences, University of West Bohemia
NTIS – New Technologies for the Information Society
Univerzitní 8, 306 14 Plzeň, Czech Republic

‡VidaCaixa S.A., Investment Risk Management Department
C/Juan Gris, 2-8, 08014 Barcelona, Spain
§josep.vives@ub.edu

Received 2 March 2018
Revised 28 September 2018
Accepted 1 October 2018
Published 2 November 2018

In this paper, we derive a generic decomposition of the option pricing formula for models with finite activity jumps in the underlying asset price process (SVJ models). This is an extension of the well-known result by Alòs [(2012) A decomposition formula for option prices in the Heston model and applications to option pricing approximation, *Finance and Stochastics* **16** (3), 403–422, doi:10.1007/s00780-012-0177-0] for Heston [(1993) A closed-form solution for options with stochastic volatility with applications to bond and currency options, *The Review of Financial Studies* **6** (2), 327–343, doi:10.1093/rfs/6.2.327] SV model. Moreover, explicit approximation formulas for option prices are introduced for a popular class of SVJ models — models utilizing a variance process postulated by Heston [(1993) A closed-form solution for options with stochastic volatility with applications to bond and currency options, *The Review of Financial Studies* **6** (2), 327–343, doi:10.1093/rfs/6.2.327]. In particular, we inspect in detail the approximation formula for the Bates [(1996), Jumps and stochastic volatility: Exchange rate processes implicit in Deutsche mark options, *The Review of Financial Studies* **9** (1), 69–107, doi:10.1093/rfs/9.1.69] model with log-normal jump sizes and we provide a numerical comparison with the industry standard — Fourier transform pricing methodology. For this model, we also reformulate the approximation formula in terms of implied volatilities. The main advantages of the introduced pricing approximations are twofold. Firstly, we are able to significantly improve computation efficiency (while preserving reasonable approximation errors) and secondly, the formula can provide an intuition on the volatility smile behavior under a specific SVJ model.

Keywords: Option pricing; stochastic volatility models; jump diffusion models; implied volatility.

§Corresponding author.

1. Introduction

The main problem of the Black–Scholes option pricing model is a constant volatility assumption for underlying stock price process. In practice, this model is used as a marking model to quote implied volatilities instead of traded option prices. Contrary to the model assumptions, the implied volatilities observed in the vanilla option markets are not flat — they typically exhibit a nonzero skew and a convex smile-like shape in the moneyness dimension. To correctly capture the shape of implied volatility surfaces, various stochastic volatility (SV) models were developed. These models assume that not only the spot prices are stochastic, but also their volatility is driven by a suitable stochastic process. Another way how to deal with drawbacks of the Black–Scholes model is to add a jump term to the stock price process. This leads into jump diffusion settings originally studied by Merton (1976). In this paper, we build an option price approximation framework for a popular class of financial models that utilize both of the aforementioned ideas. Hence, the main objects of our study are stochastic volatility jump (SVJ) diffusion models.

The first SVJ model is credited to Bates (1996) who incorporated a stochastic variance process postulated by Heston (1993) alongside Merton (1976) — style jumps. The variance of stock prices follows a CIR process (Cox *et al.* 1985) and the stock prices themselves are assumed to be of a jump diffusion type with log-normal jump sizes. In particular, this model should improve the market fit for short-term maturity options, while the original Heston (1993) approach would often need unrealistically high volatility of variance parameter to fit reasonably well the short-term smile (Bayer *et al.* 2016, Mrázek *et al.* 2016). An SVJ model with a non-constant interest rate was introduced by Scott (1997). Several other authors studied SVJ models that have a different distribution for jump sizes, e.g. Yan & Hanson (2006) utilized log-uniform jump amplitudes.

Naturally, one can extend SVJ models by adding jumps into the variance process (e.g. a model introduced by Duffie *et al.* (2000)). However, based on several empirical studies, these models tend to overfit market prices and despite having more parameters than the original Bates (1996) model they might not provide better calibration quality measures (see e.g. Gatheral (2006)). Another way to improve standard SV models might be to introduce time-dependent model parameters. The Heston (1993) model with time-dependent parameters was studied by Mikhailov & Nögel (2003) for piece-wise constant parameters, by Elices (2008) for a linear dependence and a more general modification was introduced by Benhamou *et al.* (2010). These approaches involve several additional parameters and might also suffer from overfitting. Moreover, Bayer *et al.* (2016) mentioned that these models do not fully comply with properties of observable market data — a general overall shape of the volatility surface typically does not change in time and hence the option prices should be modelled by a time-homogeneous stochastic process.

The valuation of derivatives under these more complex models is, of course, a more elaborate task compared to the standard Black–Scholes model. Many authors

have introduced semi-closed form formulas using various transformation techniques of the pricing partial (integro) differential equations, to name a few: Heston (1993), Bates (1996), Scott (1997), Lewis (2000), Albrecher *et al.* (2007), Baustian *et al.* (2017) and many others. Although transform pricing methods are typically efficient tools to evaluate non-path dependent derivatives, they do not provide any intuition on the smile behavior. Moreover, calibration routines utilizing these methods lead typically to nonconvex optimization problems (see e.g. Mrázek *et al.* (2016)).

Other authors considered approximation techniques that were pioneered by Hull & White (1987). In the last years, the Hull & White (1987) pricing formula was reinvented using techniques of the Malliavin calculus, because a future average volatility that is used in the formula is a nonadapted stochastic process. In Alòs (2006), Alòs *et al.* (2007), Alòs *et al.* (2008), a general jump diffusion model with no prescribed volatility process is analyzed. There have been several extensions thereof, e.g. by assuming Lévy processes in Jafari & Vives (2013), see also the survey in Vives (2016).

In Alòs (2012), a new approach of dealing with the Hull and White formula and the Heston model has been proposed. The main idea of this approach is to use an adapted projection for the future volatility. The formula provides a valuable intuition on the behavior of smiles and term structures under the Heston model. This is not a purely theoretical result — it can significantly fasten/improve the calibration process by providing a good initial guess by analytical calibration or by specifying a region where calibrated parameters should lie in as it is done in Alòs *et al.* (2015). In Merino & Vives (2015), the idea of Alòs (2012) has been used to find a general decomposition formula for any stochastic volatility process satisfying basic integrability conditions.

In the present paper, we apply the same set of ideas and we extend them to the domain of SVJ models with finite activity jumps. This should serve not only to find a more efficient way to price vanilla options compared to transform pricing methods (see Sec. 5), but as a side product we come up with an intuition of the smile behavior for the studied SVJ model. In contrast to Alòs *et al.* (2007), Alòs *et al.* (2008) where a Hull–White formula is obtained to study the short-time behavior of the implied volatility, this paper focuses on obtaining a Hull–White formula that can be numerically efficient and that can infer a parametric approximation of the implied volatility surface.

In particular, we start by finding a generic decomposition formula for a vanilla call option price and an approximation for both the price and implied volatility under a specific SVJ model. Explicit pricing formulas are provided for one of the most popular SVJ models — Heston (1993) type models with compound Poisson process in the stock price evolution. To assess the accuracy and efficiency of the newly derived solution, we perform a numerical comparison for the Bates (1996) model (i.e. log-normal jump sizes) alongside its Fourier transform pricing formula introduced by Baustian *et al.* (2017).

The structure of the paper is as follows. In Sec. 2, we give basic preliminaries and our notation related to SVJ models. This notation will be used throughout the paper without being repeated in particular theorems, unless we find useful to do so in order to guide the reader through the results. In Secs. 3 and 4, we derive decomposition formulas for SV and SVJ models, respectively, generalizing the decomposition formula obtained by Alòs (2012). Newly obtained decomposition is rather versatile since it does not need to specify the underlying volatility process. Particular approximation formulas for several SVJ models are presented in Sec. 5 alongside the numerical comparison for the Bates (1996) model. The decomposition result in terms of implied volatilities is introduced in Sec. 6. A discussion of the results is provided in Sec. 7 and technical error estimates are presented in Appendix A.

2. Preliminaries and Notation

Let $S = \{S_t, t \in [0,T]\}$ be a strictly positive price process under a market chosen risk neutral probability that follows the model:

$$dS_t = rS_t dt + \sigma_t S_t(\rho dW_t + \sqrt{1-\rho^2} d\tilde{W}_t) + S_{t-} dZ_t, \tag{2.1}$$

where S_0 is the current price, W and $\tilde{W}$ are independent Brownian motions, r is the interest rate including dividends and borrow rates, $\rho \in (-1,1)$ is the correlation between the two Brownian motions and

$$Z_t = \int_0^t \int_{\mathbb{R}} (e^y - 1)\tilde{N}(ds, dy), \tag{2.2}$$

where N and $\tilde{N}$ denote the Poisson measure and the compensated Poisson measure, respectively. We can associate to measure N a compound Poisson process J, independent of W and $\tilde{W}$, with intensity $\lambda \geq 0$ and jump amplitudes given by random variables Y_i — independent copies of a random variable Y with law given by Q. Recall that this compound Poisson process can be written as

$$J_t := \int_0^t \int_{\mathbb{R}} yN(ds, dy) = \sum_{i=1}^{n_t} Y_i, \tag{2.3}$$

where n_t is a λ-Poisson process. We will denote $k := \mathbb{E}_Q(e^Y - 1)$.

Without any loss of generality, it will be convenient in the following sections, to use as the underlying asset price process, the log-price process $X_t = \log S_t, t \in [0,T]$, that satisfies

$$dX_t = \left(r - \lambda k - \frac{1}{2}\sigma_t^2\right) dt + \sigma_t(\rho dW_t + \sqrt{1-\rho^2} d\tilde{W}_t) + dJ_t. \tag{2.4}$$

We introduce also the corresponding continuous process,

$$d\tilde{X}_t = \left(r - \lambda k - \frac{1}{2}\sigma_t^2\right) dt + \sigma_t(\rho dW_t + \sqrt{1-\rho^2} d\tilde{W}_t). \tag{2.5}$$

The volatility process σ is a square-integrable process assumed to be adapted to the filtration generated by W and J and its trajectories are assumed to be a.s. square integrable, càdlàg and strictly positive a.e.

Remark 2.1. Observe that this is a very general stochastic volatility model. We can consider the following particular cases:

(i) If σ is constant and we have finite activity jumps, we have a generic jump-diffusion model as for example the Merton model. In the particular case of $\sigma = 0$ we have an exponential Lévy model.
(ii) If we assume no jumps, that is $\lambda = 0$, we have a generic stochastic volatility diffusion model. This is the case treated in Merino & Vives (2015).
(iii) If in addition $\rho = 0$ we have a generalization of different non correlated stochastic volatility diffusion models as Hull & White (1987), Scott (1987), Stein & Stein (1991) or Ball & Roma (1994).
(iv) If we assume no correlation but presence of jumps we cover for example the Heston–Kou model (e.g. see Gulisashvili & Vives (2012)), or any uncorrelated model with the addition of finite activity Lévy jumps on the price process.
(v) Finally, if we have no jumps and σ is constant, we have the classical Osborne–Samuelson–Black–Scholes model.

The following notation will be used throughout the paper:

(i) We denote by $\mathcal{F}^W$, $\mathcal{F}^{\tilde{W}}$ and $\mathcal{F}^N$ the filtrations generated by the independent processes W, $\tilde{W}$ and J, respectively. Moreover, we define $\mathcal{F} := \mathcal{F}^W \vee \mathcal{F}^{\tilde{W}} \vee \mathcal{F}^N$.
(ii) We will denote by $\mathrm{BS}(t, x, y)$ the price of a plain vanilla European call option under the classical Black–Scholes model with constant volatility y, current log stock price x, time to maturity $\tau = T - t$, strike price K and interest rate r. In this case,

$$\mathrm{BS}(t, x, y) = e^x \Phi(d_+) - K e^{-r\tau} \Phi(d_-), \tag{2.6}$$

where $\Phi(\cdot)$ denotes the cumulative distribution function of the standard normal law and

$$d_\pm = \frac{x - \ln K + \left(r \pm \dfrac{y^2}{2}\right)\tau}{y\sqrt{\tau}}. \tag{2.7}$$

(iii) In our setting, the call option price is given by

$$V_t = e^{-r\tau} \mathbb{E}_t[(e^{X_T} - K)^+]. \tag{2.8}$$

(iv) Recall that from the Feynman–Kac formula for the model (2.5), the operator

$$\mathcal{L}_\sigma := \partial_t + \frac{1}{2}\sigma_t^2 \partial_x^2 + \left(r - \lambda k - \frac{1}{2}\sigma_t^2\right)\partial_x - r \tag{2.9}$$

satisfies $\mathcal{L}_\sigma \mathrm{BS}(t, \tilde{X}_t, \sigma_t) = 0$.

(v) We define the operators $\Lambda := \partial_x$, $\Gamma := (\partial_x^2 - \partial_x)$ and $\Gamma^2 = \Gamma \circ \Gamma$. In particular, for the Black–Scholes formula we obtain:

$$\Gamma\mathrm{BS}(t,x,y) := \frac{e^x}{y\sqrt{2\pi\tau}} \exp\left(-\frac{d_+^2(y)}{2}\right), \tag{2.10}$$

$$\Lambda\Gamma\mathrm{BS}(t,x,y) := \frac{e^x}{y\sqrt{2\pi\tau}} \exp\left(-\frac{d_+^2(y)}{2}\right)\left(1 - \frac{d_+(y)}{y\sqrt{\tau}}\right), \tag{2.11}$$

$$\Gamma^2\mathrm{BS}(t,x,y) := \frac{e^x}{y\sqrt{2\pi\tau}} \exp\left(-\frac{d_+^2(y)}{2}\right)\frac{d_+^2(y) - y d_+(y)\sqrt{\tau} - 1}{y^2\tau}. \tag{2.12}$$

(vi) We define $p_n(\lambda T)$ as the Poisson probability mass function with intensity λT, i.e. p_n takes the following form:

$$p_n(\lambda T) := \frac{e^{-\lambda T}(\lambda T)^n}{n!}. \tag{2.13}$$

3. A Generic SV Decomposition Formula

In this section, following the ideas of Alòs (2012), see also Merino & Vives (2015), we extend the decomposition formula to a generic stochastic volatility model. We recall that the formula is valid without having to specify the underlying volatility process explicitly, which enables us to obtain a very flexible decomposition formula. The formula proved in Alòs (2012) is the particular case for the Heston model.

It is well known that if the stochastic volatility process is independent of the price process, then the pricing formula of a plain vanilla European call is given by

$$V_t = \mathbb{E}_t[\mathrm{BS}(t, S_t, \bar{\sigma}_t)], \tag{3.1}$$

where $\bar{\sigma}_t^2$ is the so-called average future variance and it is defined by

$$\bar{\sigma}_t^2 := \frac{1}{T-t}\int_t^T \sigma_s^2 ds. \tag{3.2}$$

Naturally, $\bar{\sigma}_t$ is called the average future volatility, see Fouque *et al.* (2000, p. 51).

The idea used in Alòs (2012) consists of using an adapted projection of the average future variance

$$v_t^2 := \mathbb{E}_t(\bar{\sigma}_t^2) = \frac{1}{T-t}\int_t^T \mathbb{E}_t[\sigma_s^2] ds \tag{3.3}$$

to obtain a decomposition of V_t in terms of v_t. This idea switches an anticipative problem related with the anticipative process $\bar{\sigma}_t$ into a nonanticipative one related to the adapted process v_t.

We define

$$M_t = \int_0^T \mathbb{E}_t[\sigma_s^2] ds, \tag{3.4}$$

and hence

$$dv_t^2 = \frac{1}{T-t}[dM_t + (v_t^2 - \sigma_t^2)dt]. \tag{3.5}$$

Recall that M is a martingale with respect the filtration generated by W and J. The following processes will play an important role in a generic decomposition formula that will be introduced in this section. Let

$$R_t = \frac{1}{8}\mathbb{E}_t\left[\int_t^T d[M,M]_u\right] \tag{3.6}$$

and

$$U_t = \frac{\rho}{2}\mathbb{E}_t\left[\int_t^T \sigma_u d[W,M]_u\right], \tag{3.7}$$

where $[\cdot,\cdot]$ denotes the quadratic covariation process. Now we prove a generic version of Theorem 2.2 in Alòs (2012) which will be useful for our problem.

Theorem 3.1 (Generic decomposition formula). *Let B_t be a continuous semimartingale with respect to the filtration $\mathcal{F}_t$, let $A(t,x,y)$ be a $C_b^{1,2,2}([0,T]\times[0,\infty)\times[0,\infty))$ function and let v_t^2, M_t be defined as above. Then we are able to formulate the expectation of $e^{-rT}A(T,\tilde{X}_T,v_T^2)B_T$ in the following way*:

$$\begin{aligned}
&\mathbb{E}[e^{-rT}A(T,\tilde{X}_T,v_T^2)B_T]\\
&\quad= A(0,\tilde{X}_0,v_0^2)B_0 + \mathbb{E}\left[\int_0^T e^{-ru}\partial_y A(u,\tilde{X}_u,v_u^2)B_u\frac{1}{T-u}(v_u^2-\sigma_u^2)du\right]\\
&\qquad+\mathbb{E}\left[\int_0^T e^{-ru}A(u,\tilde{X}_u,v_u^2)dB_u\right]\\
&\qquad+\frac{1}{2}\mathbb{E}\left[\int_0^T e^{-ru}(\partial_x^2-\partial_x)A(u,\tilde{X}_u,v_u^2)B_u(\sigma_u^2-v_u^2)du\right]\\
&\qquad+\frac{1}{2}\mathbb{E}\left[\int_0^T e^{-ru}\partial_y^2 A(u,\tilde{X}_u,v_u^2)B_u\frac{1}{(T-u)^2}d[M,M]_u\right]\\
&\qquad+\rho\mathbb{E}\left[\int_0^T e^{-ru}\partial_{x,y}^2 A(u,\tilde{X}_u,v_u^2)B_u\frac{\sigma_u}{T-u}d[W,M]_u\right]\\
&\qquad+\sqrt{1-\rho^2}\mathbb{E}\left[\int_0^T e^{-ru}\partial_{x,y}^2 A(u,\tilde{X}_u,v_u^2)B_u\frac{\sigma_u}{T-u}d[\tilde{W},M]_u\right]\\
&\qquad+\rho\mathbb{E}\left[\int_0^T e^{-ru}\partial_x A(u,\tilde{X}_u,v_u^2)\sigma_u d[W,B]_u\right]
\end{aligned}$$

$$+\sqrt{1-\rho^2}\mathbb{E}\left[\int_0^T e^{-ru}\partial_x A(u,\tilde{X}_u,v_u^2)\sigma_u d[\tilde{W},B]_u\right]$$
$$+\mathbb{E}\left[\int_0^T e^{-ru}\partial_y A(u,\tilde{X}_u,v_u^2)\frac{1}{T-u}d[M,B]_u\right]. \tag{3.8}$$

Proof. Applying the Itô formula to the process $e^{-rt}A(t,\tilde{X}_t,v_t^2)B_t$, we obtain:

$$\begin{aligned}
&e^{-rT}A(T,\tilde{X}_T,v_T^2)B_T\\
&\quad= A(0,\tilde{X}_0,v_0^2)B_0 - r\int_0^T e^{-ru}A(u,\tilde{X}_u,v_u^2)B_u du\\
&\qquad+\int_0^T e^{-ru}\partial_t A(u,\tilde{X}_u,v_u^2)B_u du + \int_0^T e^{-ru}\partial_x A(u,\tilde{X}_u,v_u^2)B_u d\tilde{X}_u\\
&\qquad+\int_0^T e^{-ru}\partial_y A(u,\tilde{X}_u,v_u^2)B_u dv_u^2 + \int_0^T e^{-ru}A(u,\tilde{X}_u,v_u^2)dB_u\\
&\qquad+\frac{1}{2}\int_0^T e^{-ru}\partial_x^2 A(u,\tilde{X}_u,v_u^2)B_u d[\tilde{X},\tilde{X}]_u\\
&\qquad+\frac{1}{2}\int_0^T e^{-ru}\partial_y^2 A(u,\tilde{X}_u,v_u^2)B_u d[v^2,v^2]_u\\
&\qquad+\int_0^T e^{-ru}\partial_{x,y}^2 A(u,\tilde{X}_u,v_u^2)B_u d[\tilde{X},v^2]_u\\
&\qquad+\int_0^T e^{-ru}\partial_x A(u,\tilde{X}_u,v_u^2)d[\tilde{X},B]_u\\
&\qquad+\int_0^T e^{-ru}\partial_y A(u,\tilde{X}_u,v_u^2)d[v^2,B]_u.
\end{aligned} \tag{3.9}$$

In the next step, we apply the Feynman–Kac operator with volatility v_t, alongside the definition of M_t. After algebraic operations, we retrieve

$$\begin{aligned}
&e^{-rT}A(T,\tilde{X}_t,v_T^2)B_T\\
&\quad= A(0,\tilde{X}_0,v_0^2)B_0 + \frac{1}{2}\int_0^T e^{-ru}\partial_x A(u,\tilde{X}_u,v_u^2)B_u(v_u^2-\sigma_u^2)du\\
&\qquad+\int_0^T e^{-ru}\partial_x A(u,\tilde{X}_u,v_u^2)B_u\sigma_u(\rho dW_u+\sqrt{1-\rho^2}d\tilde{W}_u)\\
&\qquad+\int_0^T e^{-ru}\partial_y A(u,\tilde{X}_u,v_u^2)B_u\frac{1}{T-u}dM_u
\end{aligned}$$

$$
\begin{aligned}
&+\int_0^T e^{-ru}\partial_y A(u,\tilde{X}_u,v_u^2)B_u\frac{1}{T-u}(v_u^2-\sigma_u^2)du\\
&+\int_0^T e^{-ru}A(u,\tilde{X}_u,v_u^2)dB_u+\frac{1}{2}\int_0^T e^{-ru}\partial_x^2 A(u,\tilde{X}_u,v_u^2)B_u(\sigma_u^2-v_u^2)du\\
&+\frac{1}{2}\int_0^T e^{-ru}\partial_y^2 A(u,\tilde{X}_u,v_u^2)B_u\frac{1}{(T-u)^2}d[M,M]_u\\
&+\rho\int_0^T e^{-ru}\partial_{x,y}^2 A(u,\tilde{X}_u,v_u^2)B_u\frac{\sigma_u}{T-u}d[W,M]_u\\
&+\sqrt{1-\rho^2}\int_0^T e^{-ru}\partial_{x,y}^2 A(u,\tilde{X}_u,v_u^2)B_u\frac{\sigma_u}{T-u}d[\tilde{W},M]_u\\
&+\rho\int_0^T e^{-ru}\partial_x A(u,\tilde{X}_u,v_u^2)\sigma_u d[W,B]_u\\
&+\sqrt{1-\rho^2}\int_0^T e^{-ru}\partial_x A(u,\tilde{X}_u,v_u^2)\sigma_u d[\tilde{W},B]_u\\
&+\int_0^T e^{-ru}\partial_y A(u,\tilde{X}_u,v_u^2)\frac{1}{T-u}d[M,B]_u. \qquad (3.10)
\end{aligned}
$$

After applying expectations on both sides of the equation, we end up with the statement of the theorem. □

4. A Decomposition Formula for SVJ Models

In the previous section, we have given a general decomposition formula that can be used for stochastic volatility models with continuous sample paths. In this section, we are going to extend the previous decomposition to the case of a general jump diffusion model with finite activity jumps.

The main idea, like the one used in Merino & Vives (2017), is to adapt the pricing process in a way to be able to apply the decomposition technique effectively. In our case, this would translate into conditioning on the finite number of jumps n_T. If we denote $J_n=\sum_{i=0}^n Y_i$, using the integrability of Black–Scholes function, we can obtain the following conditioning formula for European options with payoff at maturity $T:\mathrm{BS}(T,X_T,v_T)$.

$$
\begin{aligned}
V_0 &= e^{-rT}\mathbb{E}[\mathrm{BS}(T,X_T,v_T)]\\
&= e^{-rT}\sum_{n=0}^{+\infty}p_n(\lambda T)\mathbb{E}\left[\mathrm{BS}\left(T,\tilde{X}_T+\sum_{i=0}^{n_T}Y_i,v_T\right)\,\middle|\, n_T=n\right]\\
&= e^{-rT}\sum_{n=0}^{+\infty}p_n(\lambda T)\mathbb{E}[\mathrm{BS}(T,\tilde{X}_T+J_n,v_T)]
\end{aligned}
$$

$$
\begin{aligned}
&= e^{-rT} \sum_{n=0}^{\infty} p_n(\lambda T) \mathbb{E}[\mathbb{E}_{J_n}[\mathrm{BS}(T, \tilde{X}_T + J_n, v_T)]] \\
&= e^{-rT} \sum_{n=0}^{\infty} p_n(\lambda T) \mathbb{E}[G_n(T, \tilde{X}_T, v_T)],
\end{aligned}
\tag{4.1}
$$

where

$$
G_n(T, \tilde{X}_T, v_T) := \mathbb{E}_{J_n}[\mathrm{BS}(T, \tilde{X}_T + J_n, v_T)]. \tag{4.2}
$$

We have switched our problem from a jump diffusion model with stochastic volatility to another one with no jumps.

Combining the generic SV decomposition formula (from Theorem 3.1) and conditioning on the number of jumps we obtain a corner-stone for our approximation.

Corollary 4.1 (SVJ decomposition formula). *Let X_t be a log-price process* (2.4), *G_n be the previously defined function. Then we can express the call option fair value V_0 using the Poisson mass function p_n and a martingale process M_t (defined by* (3.4)*). In particular,*

$$
\begin{aligned}
V_0 = &\sum_{n=0}^{\infty} p_n(\lambda T) G_n(0, \tilde{X}_0, v_0) \\
&+ \frac{1}{8} \sum_{n=0}^{\infty} p_n(\lambda T) \mathbb{E}\left[\int_0^T e^{-ru} \Gamma^2 G_n(u, \tilde{X}_u, v_u) d[M, M]_u \right] \\
&+ \frac{\rho}{2} \sum_{n=0}^{\infty} p_n(\lambda T) \mathbb{E}\left[\int_0^T e^{-ru} \Lambda \Gamma G_n(u, \tilde{X}_u, v_u) \sigma_u d[W, M]_u \right].
\end{aligned}
\tag{4.3}
$$

Proof. We apply Theorem 3.1 to $A(t, \tilde{X}_t, v_t^2) := G_n(t, \tilde{X}_t, v_t)$ and $B_t \equiv 1$. Note that

$$
\partial_{\sigma^2} \mathrm{BS}(t, x, \sigma) = \frac{(T-t)}{2} (\partial_x^2 - \partial_x) \mathrm{BS}(t, x, \sigma) \tag{4.4}
$$

and

$$
\partial_{\sigma^2}^2 \mathrm{BS}(t, x, \sigma) = \frac{(T-t)^2}{4} (\partial_x^2 - \partial_x)^2 \mathrm{BS}(t, x, \sigma). \tag{4.5}
$$

Then, the corollary follows immediately. Note that in order to apply the Itô formula to function G_n we need to use a mollifier argument as it is done in Merino & Vives (2015). □

Remark 4.1. For clarity, in the following we will refer to terms of the previous decomposition as

$$
V_0 = \sum_{n=0}^{\infty} p_n(\lambda T) G_n(0, \tilde{X}_0, v_0) + \sum_{n=0}^{\infty} p_n(\lambda T)[(I_n) + (II_n)]. \tag{4.6}
$$

Note that if $\rho = 0$, we have

$$V_0 = \sum_{n=0}^{\infty} p_n(\lambda T) G_n(0, \tilde{X}_0, v_0) + \sum_{n=0}^{\infty} p_n(\lambda T)(I_n). \tag{4.7}$$

The term (II_n) is the correction due to the dependence between the stock and volatility processes meanwhile (I_n) is the correction of the vol–vol of the volatility model.

To compute the above expression can be cumbersome. The main idea is to find an alternative formula such that the main terms are easier to be computed while paying the price by having more terms in the formula. Fortunately, in many cases these new terms can be neglected as an approximation error. The size of the error depends on the model and whether we are focusing on short or long-time dynamics.

The following lemma is proved in Alòs (2012, p. 406); and will help us to derive bounds on the error terms that appear in the main result of this paper — a computationally suitable decomposition formula for generic finite activity SVJ models.

Lemma 4.1. *Let $0 \leq t \leq s \leq T$ and $\mathcal{G}_t := \mathcal{F}_t \vee \mathcal{F}_T^W$. For every $n \geq 0$, there exists $C = C(n)$ such that*

$$|\mathbb{E}(\Lambda^n \Gamma \mathrm{BS}(s, \tilde{X}_s, v_s)|\mathcal{G}_t)| \leq C \left(\int_s^T E_s(\sigma_\theta^2) d\theta \right)^{-\frac{1}{2}(n+1)}. \tag{4.8}$$

Theorem 4.1 (Computationally suitable SVJ decomposition). *Let X_t be a log-price process* (2.4) *and G_n be the previously defined function. Then we can express the call option fair value V_0 using the Poisson probability mass function p_n and processes R_t, U_t defined by* (3.6) *and* (3.7)*, respectively. In particular,*

$$\begin{aligned} V_0 = &\sum_{n=0}^{\infty} p_n(\lambda T) G_n(0, \tilde{X}_0, v_0) + \sum_{n=0}^{\infty} p_n(\lambda T) \Gamma^2 G_n(0, \tilde{X}_0, v_0) R_0 \\ &+ \sum_{n=0}^{\infty} p_n(\lambda T) \Lambda \Gamma G_n(0, \tilde{X}_0, v_0) U_0 + \sum_{n=0}^{\infty} p_n(\lambda T) \Omega_n, \end{aligned} \tag{4.9}$$

where Ω_n are error terms fully derived in Appendix A.1*.*

Proof. We use Theorem 3.1 iteratively for the following choices of $A(t, X_t, v_t^2)$:

(I)

$$A(t, X_t, v_t^2) := \Gamma^2 G_n(t, \tilde{X}_t, v_t) \tag{4.10}$$

and

$$B_t := R_t = \frac{1}{8} \mathbb{E}_t \left[\int_t^T d[M, M]_u \right]. \tag{4.11}$$

(II)

$$A(t, X_t, v_t^2) := \Lambda\Gamma G_n(t, \tilde{X}_t, v_t) \tag{4.12}$$

and

$$B_t := U_t = \frac{\rho}{2}\mathbb{E}_t\left[\int_t^T \sigma_u d[W, M]_u\right], \tag{4.13}$$

and then the statement follows immediately. See also the terms in Appendix A.1. □

As we will illustrate in the upcoming sections for Heston-type SVJ models - this formula can be efficiently evaluated, while the neglected error terms do not significantly limit a practical use of the formula. The main ingredients, to get SVJ approximate pricing formula, are expressions for R_0, U_0 and $G_n(0, \tilde{X}_0, v_0)$. Now we provide some insight how the latter term can be expressed under various jump-diffusion settings.

Remark 4.2. In particular, we have a closed formula for a log-normal jump diffusion model (e.g. Bates (1996) SVJ model):

$$G_n(0, \tilde{X}_0, v_0) = \mathrm{BS}\left(0, \tilde{X}_0, \sqrt{v_0^2 + n\frac{\sigma_J^2}{T}}\right), \tag{4.14}$$

where we modified the risk-free rate used in the Black–Scholes formula to

$$r^* = r - \lambda(e^{\mu_J + \frac{1}{2}\sigma_J^2} - 1) + n\frac{\mu_J + \frac{1}{2}\sigma_J^2}{T}. \tag{4.15}$$

A very similar formula for the Merton case is deduced by Hanson (2007). More details will follow in the next sections. Under general (finite-activity) jump diffusion settings, we will need to solve

$$\int_{\mathbb{R}} \mathrm{BS}(0, \tilde{X}_0 + y, v_0) f_{J_n}(y) dy, \tag{4.16}$$

where $f_{J_n} = (f_Y^{*n})(y)$ is the convolution of the law of n jumps.

Here, we provide a list of known results for various popular models.

(i) Kou (2002) double exponential model:

$$\begin{aligned} f^{*(n)}(u) = {} & e^{-\eta_1 u}\sum_{k=1}^{n} P_{n,k}\eta_1^k \frac{1}{(k-1)!}u^{k-1}\mathbf{1}_{\{u\geq 0\}} \\ & + e^{-\eta_2 u}\sum_{k=1}^{n} Q_{n,k}\eta_2^k \frac{1}{(k-1)!}(-u)^{k-1}\mathbf{1}_{\{u<0\}}, \end{aligned} \tag{4.17}$$

where

$$P_{n,k} = \sum_{i=k}^{n-1}\binom{n-k-1}{i-k}\binom{n}{i}\left(\frac{\eta_1}{\eta_1+\eta_2}\right)^{i-k}\left(\frac{\eta_2}{\eta_1+\eta_2}\right)^{n-i} p^i q^{n-i}, \tag{4.18}$$

for all $1 \leq k \leq n-1$, and

$$Q_{n,k} = \sum_{i=k}^{n-1} \binom{n-k-1}{i-k} \binom{n}{i} \left(\frac{\eta_1}{\eta_1+\eta_2}\right)^{n-i} \left(\frac{\eta_2}{\eta_1+\eta_2}\right)^{i-k} p^{n-i}q^i, \quad (4.19)$$

for all $1 \leq k \leq n-1$. In addition, $P_{n,n} = p^n$ and $Q_{n,n} = q^n$.

(ii) Yan & Hanson (2006) model uses log-uniform jump sizes and hence the density is of the form (Killmann & von Collani 2001)

$$f^{*(n)}(u) = \begin{cases} \dfrac{\sum_{i=0}^{\tilde{n}(n,u)} (-1)^i \binom{n}{i} (u - na - i(b-a))^{n-1}}{(n-1)!(b-a)^n}, & \text{if } na \leq u \leq nb, \\ 0, & \text{otherwise,} \end{cases} \quad (4.20)$$

where $\tilde{n}(n,u) := [\frac{u-na}{b-a}]$ is the largest integer less than $\frac{u-na}{b-a}$.

5. SVJ Models of the Heston Type

In this section, we apply the previous generic results to derive a pricing formula for SVJ models with the Heston variance process. The aim is not to provide pricing solution for all known/studied models, but rather to detail the derivation for a selected model and comment on possible extension to different models, i.e. we focus on models with dynamics satisfying the following stochastic differential equations:

$$dX_t = \left(r - \lambda k - \frac{1}{2}\sigma_t^2\right) dt + \sigma_t(\rho dW_t + \sqrt{1-\rho^2} d\tilde{W}_t) + dJ_t, \quad (5.1)$$

$$d\sigma_t^2 = \kappa(\theta - \sigma_t^2)dt + \nu\sqrt{\sigma_t^2} dW_t, \quad (5.2)$$

where σ_0, κ, θ, ν are positive constants satisfying the Feller condition $2\kappa\theta \geq \nu^2$. The process σ_t^2 represents an instantaneous variance of the price at time t, θ is a long run average level of the variance, κ is a rate at which σ_t reverts to θ and, last but not least, ν is a volatility of volatility parameter. We will distinguish between the two cases: either jump amplitudes follow a Gaussian process (Bates (1996) model) or they are driven by other models, e.g. a log-uniform process (Yan & Hanson (2006) model).

5.1. *Approximation of the SVJ models of the Heston type*

For a standard Heston model, we recall some results from Alòs *et al.* (2015). Define

$$\varphi(t) := \int_t^T e^{-\kappa(z-t)} dz. \quad (5.3)$$

Lemma 5.1. *We have the following results*:

(i) *For $s \geq t$, we have*

$$E_t(\sigma_s^2) = \theta + (\sigma_t^2 - \theta)e^{-\kappa(s-t)} = \sigma_t^2 e^{-\kappa(s-t)} + \theta(1 - e^{-\kappa(s-t)}),$$

so, in particular, this quantity is bounded below by $\sigma_t^2 \wedge \theta$ and above by $\sigma_t^2 \vee \theta$.

(ii) $E_t\left(\int_t^T \sigma_s^2 ds\right) = \theta(T-t) + \dfrac{\sigma_t^2 - \theta}{\kappa}(1 - e^{-\kappa(T-t)})$.

(iii) $dM_t = \nu\sigma_t\left(\int_t^T e^{-\kappa(u-t)}du\right)dW_t = \dfrac{\nu}{\kappa}\sigma_t(1 - e^{-\kappa(T-t)})dW_t$.

(iv) $U_t := \dfrac{\rho}{2}E_t\left(\int_t^T \sigma_s d\langle M, W\rangle_s\right) = \dfrac{\rho}{2}\nu\int_t^T E_t(\sigma_s^2)\left(\int_s^T e^{-\kappa(u-s)}du\right)ds$

$$= \frac{\rho\nu}{2\kappa^2}\{\theta\kappa(T-t) - 2\theta + \sigma_t^2 + e^{-\kappa(T-t)}(2\theta - \sigma_t^2) - \kappa(T-t)e^{-\kappa(T-t)}(\sigma_t^2 - \theta)\}.$$

(v) $R_t := \dfrac{1}{8}E_t\left(\int_t^T d\langle M, M\rangle_s\right) = \dfrac{1}{8}\nu^2\int_t^T E_t(\sigma_s^2)\left(\int_s^T e^{-\kappa(u-s)}du\right)^2 ds$

$$\begin{aligned} &= \frac{\nu^2}{8\kappa^2}\left\{\theta(T-t) + \frac{(\sigma_t^2 - \theta)}{\kappa}(1 - e^{-\kappa(T-t)}) - \frac{2\theta}{\kappa}(1 - e^{-\kappa(T-t)})\right. \\ &\quad - 2(\sigma_t^2 - \theta)(T-t)e^{-\kappa(T-t)} + \frac{\theta}{2\kappa}(1 - e^{-2\kappa(T-t)}) \\ &\quad \left. + \frac{(\sigma_t^2 - \theta)}{\kappa}(e^{-\kappa(T-t)} - e^{-2\kappa(T-t)})\right\}. \end{aligned}$$

(vi) $dU_t = \dfrac{\rho\nu^2}{2}\left(\int_t^T e^{-\kappa(z-t)}\varphi(z)dz\right)\sigma_t dW_t - \dfrac{\rho\nu}{2}\varphi(t)\sigma_t^2 dt$.

(vii) $dR_t = \dfrac{\nu^3}{8}\left(\int_t^T e^{-\kappa(z-t)}\varphi(z)^2 dz\right)\sigma_t dW_t - \dfrac{\nu^2}{8}\varphi(t)^2\sigma_t^2 dt$.

Furthermore, the following lemma is proved in Alòs *et al.* (2015).

Lemma 5.2. *Let all the objects be well defined as above, then for a standard Heston model we have that*

(i) $\int_s^T E_s(\sigma_u^2)du \geq \frac{\theta\kappa}{2}(\int_s^T e^{-\kappa(u-s)}du)^2$.

(ii) $\int_s^T E_s(\sigma_u^2)du \geq \sigma_s^2(\int_s^T e^{-\kappa(u-s)}du)$.

Remark 5.1. We can utilize these equalities to get analogue results for Theorem 4.1. The Ω_n terms can be founded in Appendix A.2.

Now we have all the tools needed to introduce the main practical result — the pricing formula.

Corollary 5.1 (Heston-type SVJ pricing formula). *Let $G_n(0, \tilde{X}_0, v_0)$ takes the expression as in Remark* 4.2 *for a particular jump-type setting, let*

$$R_0 = \frac{\nu^2}{8\kappa^2}\Bigg\{\theta T + \frac{(\sigma_0^2-\theta)}{\kappa}(1-e^{-\kappa T}) - \frac{2\theta}{\kappa}(1-e^{-\kappa T}) - 2(\sigma_0^2-\theta)Te^{-\kappa T} + \frac{\theta}{2\kappa}(1-e^{-2\kappa T}) + \frac{(\sigma_0^2-\theta)}{\kappa}(e^{-\kappa T}-e^{-2\kappa T})\Bigg\} \tag{5.4}$$

and let

$$U_0 = \frac{\rho\nu}{2\kappa^2}\{\theta\kappa T - 2\theta + \sigma_0^2 + e^{-\kappa T}(2\theta - \sigma_0^2) - \kappa T e^{-\kappa T}(\sigma_0^2 - \theta)\}. \tag{5.5}$$

Then the European option fair value is expressed as

$$V_0 = \sum_{n=0}^{\infty} p_n(\lambda T) G_n(0, \tilde{X}_0, v_0) + \sum_{n=0}^{\infty} p_n(\lambda T)\Gamma^2 G_n(0, \tilde{X}_0, v_0) R_0 + \sum_{n=0}^{\infty} p_n(\lambda T)\Lambda\Gamma G_n(0, \tilde{X}_0, v_0) U_0 + \sum_{n=0}^{\infty} p_n(\lambda T)\Omega_n, \tag{5.6}$$

where Ω_n are error terms detailed in Appendix A.2. *The upper bound for any Ω_n is given by*

$$\Omega_n \leq \nu^2(|\rho| + \nu)^2 \left(\frac{1}{r} \wedge (T-t)\right) \Pi(\kappa, \theta), \tag{5.7}$$

where $\Pi(\kappa, \theta)$ is a positive function. Therefore, the total error

$$\Omega = \sum_{n=0}^{\infty} p_n(\lambda T)\Omega_n \tag{5.8}$$

is bounded by the same constant.

Proof. We plug-in the Heston volatility model dynamics into Theorem 4.1. Using the integrability of the Black–Scholes function, Fubini Theorem and the fact that the upper bound of Lemma 4.1 does not depend on the log spot price, the upper bound can be used for every G_n function. Using Lemmas 5.1 and 5.2, we prove the corollary. The whole proof is in Appendix A.3. □

Remark 5.2 (Approximate fractional SVJ model). For the model introduced by Pospíšil & Sobotka (2016), one can derive a very similar decomposition as in Corollary 5.1. In fact, only the terms R_0 and U_0 have to be changed while the other terms remain the same.

5.2. *Numerical analysis of the SVJ models of the Heston type*

In this section, we compare the newly obtained approximation formula for option prices under Bates (1996) model (i.e. log-normal jump sizes alongside Heston

model's instantaneous variance) with the market standard approach for pricing European options under SVJ models — the Fourier-transform based pricing formula. The comparison is performed with two important aspects in mind: the practical precision of the pricing formula when neglecting the total error term Ω and the efficiency of the formula expressed in terms of the computational time needed for particular pricing tasks.

In particular, we utilize a semi-closed form solution with one numerical integration as a reference price (Baustian *et al.* 2017) alongside a classical solution derived by Bates (1996).[a] The numerical integration errors according to Baustian *et al.* (2017) should be typically well beyond 10^{-10}, hence we can take the numerically computed prices as the reference prices for the comparison.

Due to the theoretical properties of the total error term Ω, we illustrate the approximation quality for several values of ρ and ν while keeping other parameters fixed.[b]

In Fig. 1, we inspect a mode of low volatility of the spot variance ν and low absolute value of the instantaneous correlation ρ between the two Brownian motions. The

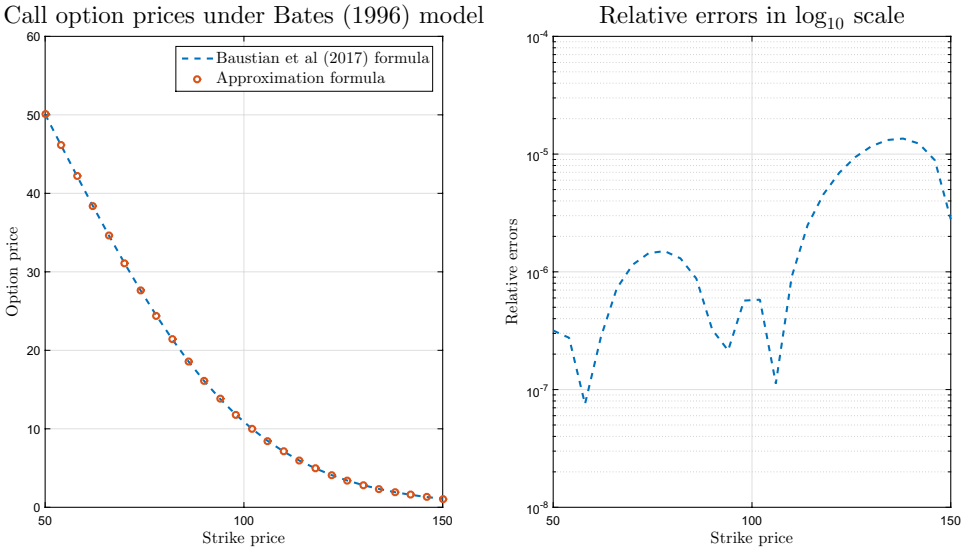

Fig. 1. On the left plot, there is a comparison of approximation and reference prices. The x- and y-axes represent the option prices and the option strikes, respectively. On the right plot, there is the relative error of the model. The x- and y-axes represent the relative error and the option strikes, respectively. The parameters are $\rho = -0.2$, $\nu = 5\%$, $\tau = 0.3$, $S_0 = 100$; $r = 0.001$; $\tau = 0.3$; $v_0 = 0.25$; $\kappa = 1.5$; $\theta = 0.2$; $\lambda = 0.05$; $\mu_J = -0.05$; and $\sigma_J = 0.5$.

[a]With a slight modification mentioned in Gatheral (2006) to not suffer from "Heston trap" issues.
[b]The considered model and market parameters take the following values: $S_0 = 100$; $r = 0.001$; $\tau = 0.3$; $v_0 = 0.25$; $\kappa = 1.5$; $\theta = 0.2$; $\lambda = 0.05$; $\mu_J = -0.05$; and $\sigma_J = 0.5$.

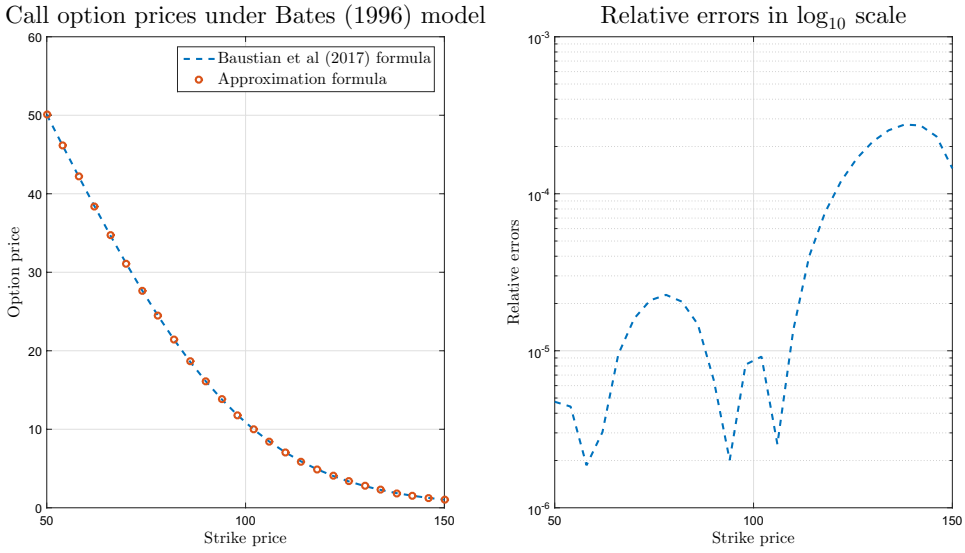

Fig. 2. On the left plot, there is a comparison of approximation and reference prices. The x- and y-axes represent the option prices and the option strikes, respectively. On the right plot, there is the relative error of the model. The x- and y-axes represent the relative error and the option strikes, respectively. The parameters are $\rho = -0.8$, $\nu = 5\%$, $\tau = 0.3$, $S_0 = 100$; $r = 0.001$; $\tau = 0.3$; $v_0 = 0.25$; $\kappa = 1.5$; $\theta = 0.2$; $\lambda = 0.05$; $\mu_J = -0.05$; and $\sigma_J = 0.5$.

errors for an option price smile that corresponds to $\tau = 0.3$ are within 10^{-4}–10^{-6} range, while slightly better absolute errors were obtained at-the-money. Increasing either the absolute value of ρ or volatility ν should, in theory, worsen the computed error measures. However, if only one of the values is increased we are still able to keep the errors below 10^{-3} in most of the cases, see Fig. 2.

Last but not least, we illustrate the approximation quality for parameters that are not well suited for the approximation. This is done by setting $\nu = 50\%$, correlation $\rho = -0.8$ and a smile with respect to $\tau = 3$. The obtained errors are depicted by Fig. 3. Despite the values of parameters, the shape of the option price curve remains fairly similar to the one obtained by a more precise semi-closed formula.

Main advantage of the proposed pricing approximation lies in its computational efficiency — which might be advantageous for many tasks in quantitative finance that need fast evaluation of derivative prices. To inspect the time consumption we set up three pricing tasks. We use a batch of 100 call options with different strikes and times to maturities that involves all types of options.[c] In the first task, we evaluate prices for the batch with respect to 100 (uniformly) randomly sampled parameter sets. This should encompass a similar number of price evaluations as

[c]It includes OTM, ATM, ITM options with short-, mid- and long-term times to maturities.

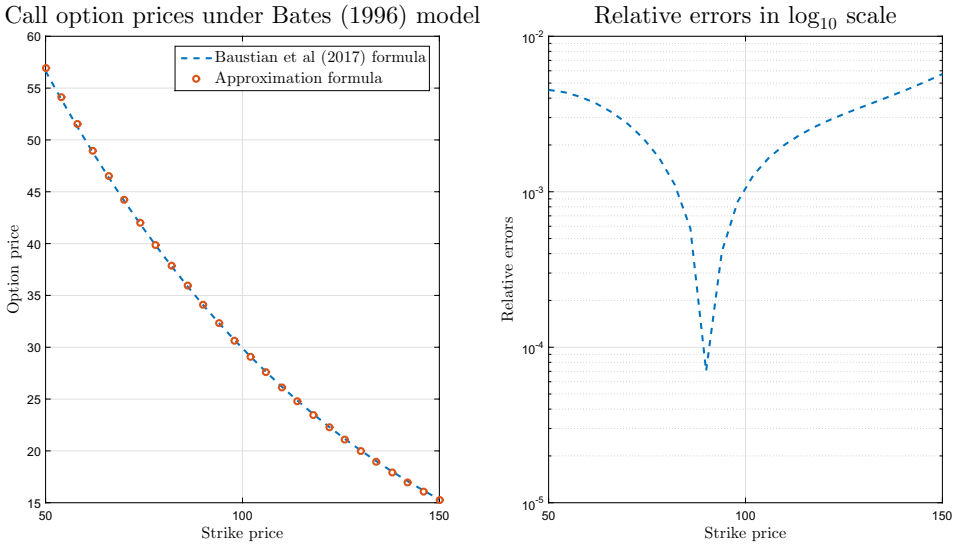

Fig. 3. On the left plot, there is a comparison of approximation and reference prices. The x- and y-axes represent the option prices and the option strikes, respectively. On the right plot, there is the relative error of the model. The x- and y-axes represent the relative error and the option strikes, respectively. The parameters are $\rho = -0.8$, $\nu = 50\%$, $\tau = 3$, $S_0 = 100$; $r = 0.001$; $\tau = 0.3$; $v_0 = 0.25$; $\kappa = 1.5$; $\theta = 0.2$; $\lambda = 0.05$; $\mu_J = -0.05$; and $\sigma_J = 0.5$.

a market calibration task with a very good initial guess. Further on, we repeat the same trials only for 1000 and 10000 parameter sets, to mimic the number of evaluations for a typical local-search calibration and a global-search calibration respectively, for more information about calibration tasks see e.g. Mikhailov & Nögel (2003) and Mrázek *et al.* (2016).

The obtained computational times are listed in Table 1. Unlike the formulas with numerical integration, the proposed approximation has almost linear dependency of

Table 1. Efficiency of the Bates SVJ pricing formulas.

Pricing approach	Task	Time[a] [sec]	Speed-up factor
Approximation formula	#1	0.97	3.23×
	#2	10.03	2.94×
	#3	99.67	2.83×
Baustian *et al.* (2017)	#1	2.09	1.52×
	#2	17.28	1.71×
	#3	135.95	2.01×
Gatheral (2006)	#1	3.18	—
	#2	29.48	—
	#3	281.72	—

[a]The results were obtained on a PC with Intel Core i7-6500U CPU and 8 GB RAM.

computational time on the number of evaluated prices. Also the results vary based on the randomly generated parameter values for numerical schemes much more than for the approximation — this is caused by adaptivity of numerical quadratures that were used.[d] The newly proposed approximation is typically 3× faster compared to the classical two integral pricing formula and the computational time consumption does not depend on the model- nor market-parameters.

6. The Approximated Implied Volatility Surface for SVJ Models of the Heston Type

In the above section, we have computed a bound for the error between the exact price and the approximated pricing formula for the SVJ models of the Heston type. Now, we are going to derive an approximation of the implied volatility surface alongside the corresponding ATM implied volatility profiles. These approximations can help us to understand the volatility dynamics of studied models in a better way.

6.1. *Derivation of implied volatility approximations for models of the Heston type*

The price of an European call option with strike K and maturity T is an observable quantity which will be referred to as $P_0^{\text{obs}} = P^{\text{obs}}(K,T)$. Recall that the *implied volatility* is defined as the value $I(T,K)$ that satisfies

$$\text{BS}(0,S_0,I(T,K)) = P_0^{\text{obs}}. \tag{6.1}$$

Define $\hat{v}_0$ such that

$$\text{BS}(0,S_0,\hat{v}_0) := \sum_{n=0}^{\infty} p_n(\lambda T)\mathbb{E}_{J_n}[\text{BS}(0,x+J_n,v_0)]. \tag{6.2}$$

Using the results from the previous section, we are going to derive an approximation to the implied volatility as in Fouque *et al.* (2003), using the idea to expand the implied volatility function $I(T,K)$ with respect to two scales $\{\delta^k\}_{k=0}^{\infty}$ and $\{\epsilon^k\}_{k=0}^{\infty}$ converging to 0. See also Alòs *et al.* (2015).

Let $\epsilon = \rho\nu$ and $\delta = \nu^2$. Then, we expand $I(T,K)$ with respect to these two scales and $\hat{v}_0$ as

$$I(T,K) = \hat{v}_0 + \rho\nu I_1(T,K) + \nu^2 I_2(T,K) + O((\rho\nu+\nu^2)). \tag{6.3}$$

We will denote by $\hat{I}(T,K) = \hat{v}_0 + \rho\nu I_1(T,K) + \nu^2 I_2(T,K)$ the approximation to the implied volatility and by $\hat{V}(0,x,v_0)$ the approximation to the option price

[d]For both Baustian *et al.* (2017) and Gatheral (2006) formulas we use an adaptive Gauss-Kronrod $(7,15)$ quadrature.

obtained in Corollary 5.1. We know that according to Corollary 5.1:

$$\begin{aligned}\hat{V}(0,x,v_0) = &\sum_{n=0}^{\infty} p_n(\lambda T)\mathbb{E}_{J_n}[\mathrm{BS}(0,x+J_n,v_0)] \\ &+ \sum_{n=0}^{\infty} p_n(\lambda T)\mathbb{E}_{J_n}[\Gamma^2\mathrm{BS}(0,x+J_n,v_0)]R_0 \\ &+ \sum_{n=0}^{\infty} p_n(\lambda T)\mathbb{E}_{J_n}[\Lambda\Gamma\mathrm{BS}(0,x+J_n,v_0)]U_0. \end{aligned} \tag{6.4}$$

To simplify the notation, we define

$$\gamma_n := \frac{d_+^2(x,r,\sigma) - d_+^2(x+J_n,r,\sigma)}{2} \tag{6.5}$$

and

$$D_1(x,J_n,\sigma,T) := \mathbb{E}_{J_n}\left[\frac{e^{J_n+\gamma_n}}{\sigma T}\left(1 - \frac{d_+(x+J_n,r,\sigma)}{\sigma\sqrt{T}}\right)\right], \tag{6.6}$$

$$D_2(x,J_n,\sigma,T) := \mathbb{E}_{J_n}\left[\frac{e^{J_n+\gamma_n}}{\sigma^3T^2}(d_+^2(x+J_n,r,\sigma) - \sigma d_+(x+J_n,r,\sigma)\sqrt{T} - 1)\right]. \tag{6.7}$$

Using the fact that

$$\partial_\sigma \mathrm{BS}(t,x,\sigma) = \frac{e^x e^{-d_+^2(\sigma)/2}\sqrt{T-t}}{\sqrt{2\pi}}, \tag{6.8}$$

we can re-write the approximated price as

$$\begin{aligned}\hat{V}(0,x,v_0) = &\sum_{n=0}^{\infty} p_n(\lambda T)\mathbb{E}_{J_n}[\mathrm{BS}(0,x+J_n,v_0)] \\ &+ \partial_\sigma\mathrm{BS}(v_0)\sum_{n=0}^{\infty} p_n(\lambda T)D_1(x,J_n,\sigma,T)U_0 \\ &+ \partial_\sigma\mathrm{BS}(v_0)\sum_{n=0}^{\infty} p_n(\lambda T)D_2(x,J_n,v_0,T)R_0. \end{aligned} \tag{6.9}$$

We write $\mathrm{BS}(v_0)$ as a shorthand for $\mathrm{BS}(0,x,v_0)$. Note that the pricing formula approximation, $\hat{V}(0,x,v_0)$, has volatility v_0, meanwhile $I(T,K)$ depends on $\hat{v}_0$. In order to conciliate one with the other, we consider the Taylor expansion of $\mathrm{BS}(0,x,I(T,K))$ around v_0:

$$\begin{aligned}\mathrm{BS}(0,x,I(T,K)) = &\mathrm{BS}(v_0) + \partial_\sigma B(v_0)(\hat{v}_0 - v_0 + \rho\nu I_1(T,K) + \nu^2 I_2(T,K) + \cdots) \\ &+ \frac{1}{2}\partial_\sigma^2\mathrm{BS}(v_0)(\hat{v}_0 - v_0 + \rho\nu I_1(T,K) + \nu^2 I_2(T,K) + \cdots)^2 + \cdots \end{aligned}$$

$$= \mathrm{BS}(v_0) + \rho\nu\partial_\sigma \mathrm{BS}(v_0) I_1(T,K) + \nu^2 \partial_\sigma \mathrm{BS}(v_0) I_2(T,K) + \sum_{n=1}^{\infty} \frac{1}{n!} \partial_\sigma \mathrm{BS}(v_0)(\hat{v}_0 - v_0)^n + \cdots. \tag{6.10}$$

Noticing that

$$\mathrm{BS}(\hat{v}_0) = \mathrm{BS}(v_0) + \sum_{n=1}^{\infty} \frac{1}{n!} \partial_\sigma \mathrm{BS}(v_0)(\hat{v}_0 - v_0)^n \tag{6.11}$$

and equating

$$\hat{V}(0,x,v_0) = \mathrm{BS}(0,x,\hat{I}(T,K)), \tag{6.12}$$

we obtain

$$\hat{I}_1(T,K) := \rho\nu I_1(T,K) = U_0 \sum_{n=0}^{\infty} p_n(\lambda T) D_1(x, J_n, v_0, T), \tag{6.13}$$

$$\hat{I}_2(T,K) := \nu^2 I_2(T,K) = R_0 \sum_{n=0}^{\infty} p_n(\lambda T) D_2(x, J_n, v_0, T). \tag{6.14}$$

Hence, we have the following approximation of implied volatility:

$$\hat{I}(T,K) = \hat{v}_0 + U_0 \sum_{n=0}^{\infty} p_n(\lambda T) D_1(x, J_n, v_0, T) + R_0 \sum_{n=0}^{\infty} p_n(\lambda T) D_2(x, J_n, v_0, T). \tag{6.15}$$

In particular, when we look at the ATM curve, we have that

$$\hat{I}^{\mathrm{ATM}}(T) = \hat{v}_0 + U_0 \sum_{n=0}^{\infty} p_n(\lambda T) \mathbb{E}_{J_n}\left[\frac{e^{J_n+\gamma_n}}{v_0 T}\left(\frac{1}{2} - \frac{J_n}{T v_0^2}\right)\right] - R_0 \sum_{n=0}^{\infty} p_n(\lambda T) \mathbb{E}_{J_n}\left[\frac{e^{J_n+\gamma_n}}{v_0 T}\left(\frac{1}{4} + \frac{1}{v^2 T} - \frac{J_n^2}{v_0^4 T^2}\right)\right]. \tag{6.16}$$

Remark 6.1. When T converges to 0, dynamics of the model are the same as for the Heston model. This is due to the behavior of Poisson processes when $T \downarrow 0$.

6.2. *Derivation of implied volatility approximation for the Bates model*

The Bates model is a particular example of SVJ model of the Heston type. The fact that jumps are log-normal makes the model more tractable. In this section, we will adapt the generic formulas to this particular case. In this model, after each jump, the drift- and volatility-like parameters will change. We define

$$\tilde{v}_0^{(n)} = \sqrt{v_0^2 + n\frac{\sigma_J^2}{T}} \tag{6.17}$$

as the new volatility and

$$\tilde{r}_n = r - \lambda(e^{\mu_J + \frac{1}{2}\sigma_J^2} - 1) + n\frac{\mu_J + \frac{1}{2}\sigma_J^2}{T} \tag{6.18}$$

as the new drift. The parameter n is the number of realized jumps, μ_J and σ_J are the jump-size parameters and λ is the jump intensity. For simplicity, we denote:

$$c_n := -\lambda(e^{\mu_J + \frac{1}{2}\sigma_J^2} - 1) + n\frac{\mu_J + \frac{1}{2}\sigma_J^2}{T}. \tag{6.19}$$

As a consequence, we have that

$$d_\pm(x, \tilde{r}_n, \tilde{v}_0^{(n)}) = \frac{x - \ln K + \tilde{r}_n T}{\tilde{v}_0^{(n)}\sqrt{T}} \pm \frac{\tilde{v}_0^{(n)}\sqrt{T}}{2}. \tag{6.20}$$

Following the steps done in the generic formula, we can define the variables

$$D_{B,1}(x, \tilde{r}_n, \tilde{v}_0^{(n)}, T) = \frac{e^{\gamma_n}}{\tilde{v}_0^{(n)} T}\left(1 - \frac{d_+(x, \tilde{r}_n, \tilde{v}_0^{(n)})}{\tilde{v}_0^{(n)}\sqrt{T}}\right), \tag{6.21}$$

$$D_{B,2}(x, \tilde{r}_n, \tilde{v}_0^{(n)}, T) = \frac{e^{\gamma_n}}{(\tilde{v}_0^{(n)})^3 T^2}(d_+^2(x, \tilde{r}_n, \tilde{v}_0^{(n)}) - \tilde{v}_0^{(n)} d_+(x, \tilde{r}_n, \tilde{v}_0^{(n)})\sqrt{T} - 1). \tag{6.22}$$

It follows that

$$\hat{I}_{B,1}(T, K) = \rho\nu I_{B,1}(T, K) = U_0 \sum_{n=0}^{\infty} p_n(\lambda T) D_{B,1}(x, \tilde{r}_n, \tilde{v}_0^{(n)}, T), \tag{6.23}$$

$$\hat{I}_{B,2}(T, K) = \nu^2 I_{B,2}(T, K) = R_0 \sum_{n=0}^{\infty} p_n(\lambda T) D_{B,2}(x, \tilde{r}_n, \tilde{v}_0^{(n)}, T). \tag{6.24}$$

The approximation of the implied volatility surface has the following shape:

$$\begin{aligned}\hat{I}_B(T, K) = \hat{v}_0 &+ U_0 \sum_{n=0}^{\infty} p_n(\lambda T)\frac{e^{\gamma_n}}{\tilde{v}_0^{(n)} T}\left(1 - \frac{d_+(x, \tilde{r}_n, \tilde{v}_0^{(n)})}{\tilde{v}_0^{(n)}\sqrt{T}}\right) \\ &+ R_0 \sum_{n=0}^{\infty} p_n(\lambda T)\frac{e^{\gamma_n}}{\tilde{v}_0^{(n)} T}\left(\frac{d_+^2(x, \tilde{r}_n, \tilde{v}_0^{(n)}) - \tilde{v}_0^{(n)} d_+(x, \tilde{r}_n, \tilde{v}_0^{(n)})\sqrt{T} - 1}{(\tilde{v}_0^{(n)})^2 T}\right).\end{aligned} \tag{6.25}$$

In particular, the ATM implied volatility curve under the studied model takes the form:

$$\begin{aligned}\hat{I}_B^{\text{ATM}}(T) = \hat{v}_0 &+ U_0 \sum_{n=0}^{\infty} p_n(\lambda T)\frac{e^{\gamma_n^{\text{ATM Bates}}}}{\tilde{v}_0^{(n)} T}\left(\frac{1}{2} - \frac{c_n}{(\tilde{v}_0^{(n)})^2}\right) \\ &- R_0 \sum_{n=0}^{\infty} p_n(\lambda T)\frac{e^{\gamma_n^{\text{ATM Bates}}}}{\tilde{v}_0^{(n)} T}\left(\frac{1}{4} + \frac{1}{(\tilde{v}_0^{(n)})^2 T} - \frac{c_n^2}{(\tilde{v}_0^{(n)})^4}\right),\end{aligned} \tag{6.26}$$

where

$$\gamma_n^{\text{ATM Bates}} = -\frac{1}{2}\left(c_n T + \frac{c_n^2 T}{(\tilde{v}_0^{(n)})^2}\right). \tag{6.27}$$

6.3. *Numerical analysis of the implied volatility approximation for the Bates model*

In the previous section, we have compared the approximation and semi-closed form formulas for option prices under Bates (1996) model. For this model, we also illustrate the approximation quality in terms of implied volatilities.

Because there is no exact closed formula for implied volatilities under the studied model, we take as a reference price the one obtained by means of the complex Fourier transform (Baustian *et al.* 2017). Once we have computed the prices we use a numerical inversion to obtain the desired implied volatilities.

As previously, we start by comparing implied volatilities for well-suited parameter sets. The illustration in Fig. 4 is obtained by setting $\rho = -0.1$, $\nu = 5\%$ and other parameters as in Sec. 5.2. Typically, for a well-suited parameter set, the absolute approximation errors stay within the range 10^{-5}–10^{-7}.

Even for not entirely well-suited parameters we are able to obtain reasonable errors especially for ATM options, see Figs. 5 and 6. In the mode of high volatility

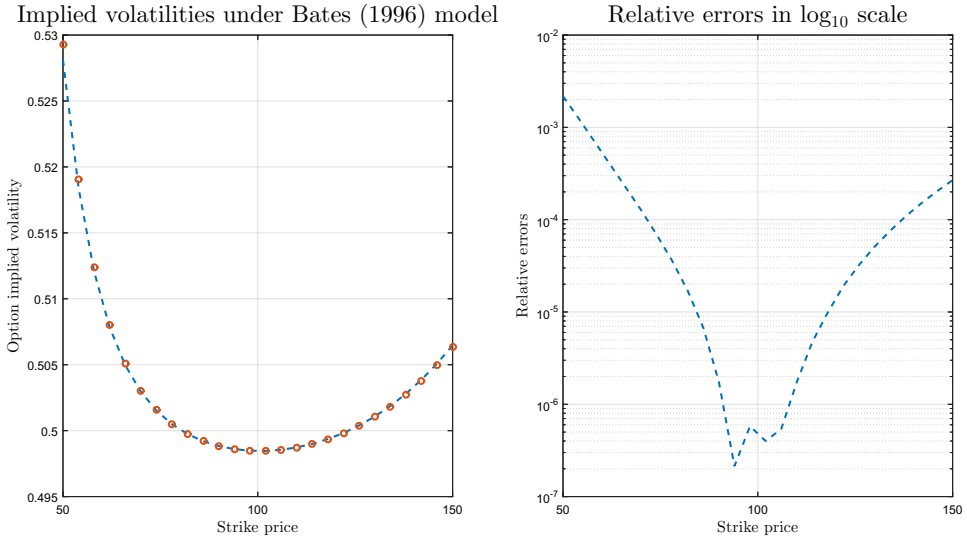

Fig. 4. On the left plot, there is a comparison of approximation and reference implied volatilities. The x- and y-axes represent the implied options volatilities and the options strikes, respectively. On the right plot, there is the relative error of the model. The x- and y-axes represent the relative error and the options strikes, respectively. The parameters are $\rho = -0.2$, $\nu = 5\%$, $\tau = 0.3$, $S_0 = 100$; $r = 0.001$; $\tau = 0.3$; $v_0 = 0.25$; $\kappa = 1.5$; $\theta = 0.2$; $\lambda = 0.05$; $\mu_J = -0.05$; and $\sigma_J = 0.5$.

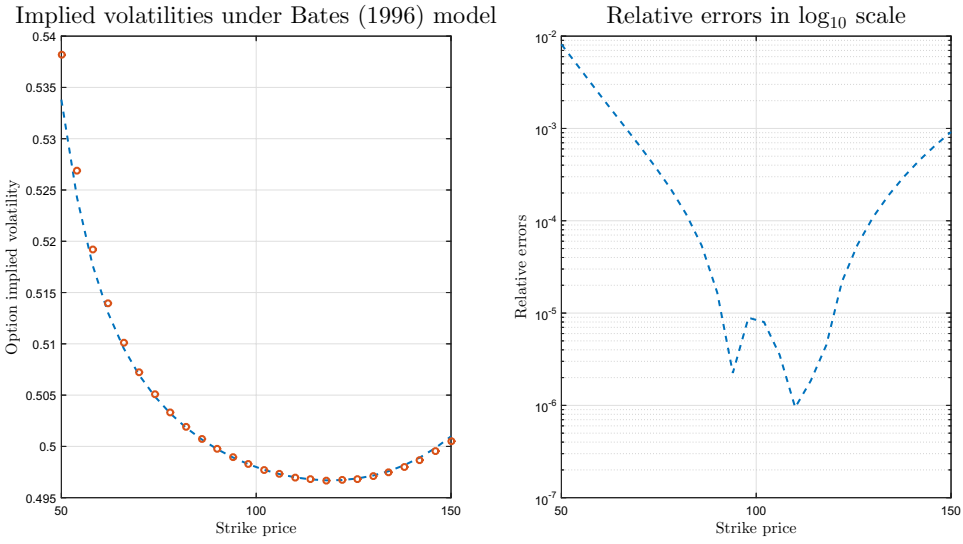

Fig. 5. On the left plot, there is a comparison of approximation and reference implied volatilities. The x- and y-axes represent the implied options volatilities and the options strikes, respectively. On the right plot, there is the relative error of the model. The x- and y-axes represent the relative error and the options strikes, respectively. The parameters are $\rho = -0.8$, $\nu = 5\%$, $\tau = 0.3$, $S_0 = 100$; $r = 0.001$; $\tau = 0.3$; $v_0 = 0.25$; $\kappa = 1.5$; $\theta = 0.2$; $\lambda = 0.05$; $\mu_J = -0.05$; and $\sigma_J = 0.5$.

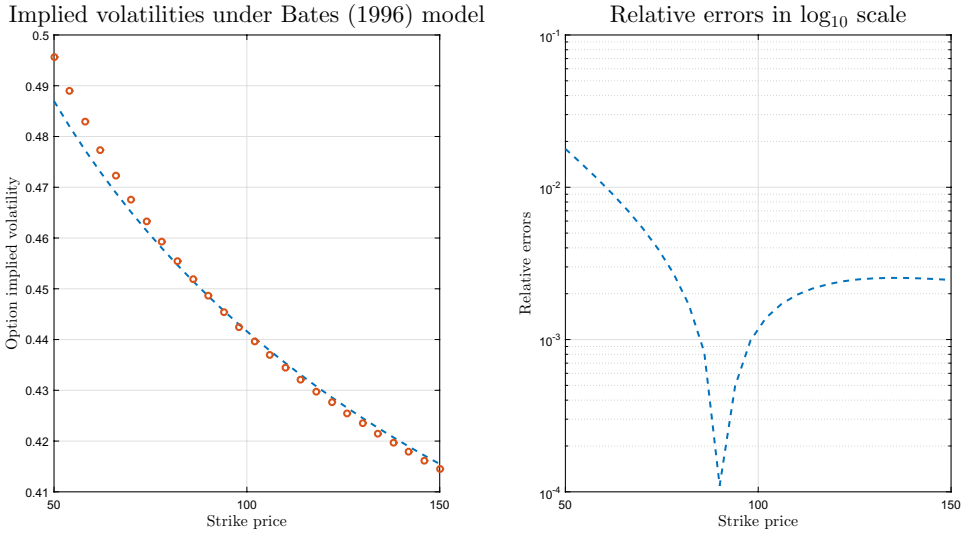

Fig. 6. On the left plot, there is a comparison of approximation and reference implied volatilities. The x- and y-axes represent the implied options volatilities and the options strikes, respectively. On the right plot, there is the relative error of the model. The x- and y-axes represent the relative error and the options strikes, respectively. The parameters are $\rho = -0.8$, $\nu = 50\%$, $\tau = 3$, $S_0 = 100$; $r = 0.001$; $\tau = 0.3$; $v_0 = 0.25$; $\kappa = 1.5$; $\theta = 0.2$; $\lambda = 0.05$; $\mu_J = -0.05$; and $\sigma_J = 0.5$.

ν of the variance process and high absolute value of the instantaneous correlation ρ, the curvature of the smile is not fully captured. However, the errors are typically well below 10^{-2} even in this adverse setting.

7. Conclusion

The aim of the paper has been to derive a generic decomposition formula for SVJ option pricing models with finite activity jumps. In Sec. 4, we had derived this decomposition by extending the results obtained by Alòs (2012) for Heston (1993) SV model. Newly obtained decomposition is rather versatile since it does not need to specify the underlying volatility process and only common integrability and specific sample path properties are required.

Particular approximation formulas for several SVJ models had been presented in Sec. 5 together with the numerical comparison for the Bates (1996) model for which we had showed that the newly proposed approximation is typically three times faster compared to the classical two integral semi-closed pricing formula. Moreover, its computational time does not depend on the model parameters nor on market data. The biggest advantage of the proposed pricing approximation therefore lies in its computational efficiency, which is advantageous for many tasks in quantitative finance such as calibration to real market data that can lead to an extensive number of formula evaluations for SVJ models. On the other hand, general decomposition formula have allowed us to understand the key terms contributing to the option fair value under specific models and hence this theoretical result has also its practical impact.

In Sec. 6, we have obtained an approximative representation for volatility surfaces with respect to the class of SVJ models and we provided its boundary case simplification for ATM options. In particular, we have studied the approximation in the Bates (1996) model case. A numerical comparison of this approximation have been also presented.

Although the generic approach covers various interesting SVJ models, there are other models that do not fit into the general structure described in Sec. 2. For these models, such as Barndorff-Nielsen & Shephard (2001) model or infinite activity jumps models, we still might be able to derive a similar decomposition that was beyond the scope of the present paper. Newly obtained results therefore give suggestions on how to derive approximation formulas for other models.

Acknowledgments

This work was partially supported by the GACR Grant GA18-16680S Rough models of fractional stochastic volatility. Computational resources were provided by the CESNET LM2015042 and the CERIT Scientific Cloud LM2015085, provided under the programme "Projects of Large Research, Development, and Innovations Infrastructures". The work of Josep Vives is partially supported by Spanish grant MEC MTM 2016-76420-P.

Appendix A

In the following appendices, we obtain the error terms of the decomposition in Theorem 4.1 (Appendix A.1), the same formulas for the SVJ model of the Heston type (Appendix A.2) and upper bounds for those terms using Corollary 5.1 (Appendix A.3).

A.1. *Decomposition formulas in the general model*

In this section, we obtain the error terms for a general model.

A.1.1. *Decomposition of the term* (I_n)

The term I can be decomposed by

$$\begin{aligned}
&\frac{1}{8}\mathbb{E}\left[\int_0^T e^{-ru}\Gamma^2 G_n(u,\tilde{X}_u,v_u)d[M,M]_u\right] - \Gamma^2 G_n(0,\tilde{X}_0,v_0)R_0 \\
&\quad = \frac{1}{8}\mathbb{E}\left[\int_0^T e^{-ru}\Gamma^4 G_n(u,\tilde{X}_u,v_u)R_u d[M,M]_u\right] \\
&\qquad + \frac{\rho}{2}\mathbb{E}\left[\int_0^T e^{-ru}\Lambda\Gamma^3 G_n(u,\tilde{X}_u,v_u)R_u\sigma_u d[W,M]_u\right] \\
&\qquad + \rho\mathbb{E}\left[\int_0^T e^{-ru}\Lambda\Gamma^2 G_n(u,\tilde{X}_u,v_u)\sigma_u d[W,R]_u\right] \\
&\qquad + \frac{1}{2}\mathbb{E}\left[\int_0^T e^{-ru}\Gamma^3 G_n(u,\tilde{X}_u,v_u)d[M,R]_u\right]. \qquad \text{(A.1)}
\end{aligned}$$

A.1.2. *Decomposition of the term* (II_n)

The term II can be decomposed by

$$\begin{aligned}
&\frac{\rho}{2}\mathbb{E}\left[\int_0^T e^{-ru}\Lambda\Gamma G_n(u,\tilde{X}_u,v_u)\sigma_u d[W,M]_u\right] - \Lambda\Gamma G_n(0,\tilde{X}_0,v_0)U_0 \\
&\quad = \frac{1}{8}\mathbb{E}\left[\int_0^T e^{-ru}\Lambda\Gamma^3 G_n(u,\tilde{X}_u,v_u)U_u d[M,M]_u\right] \\
&\qquad + \frac{\rho}{2}\mathbb{E}\left[\int_0^T e^{-ru}\Lambda^2\Gamma^2 G_n(u,\tilde{X}_u,v_u)U_u\sigma_u d[W,M]_u\right]
\end{aligned}$$

$$+\rho\mathbb{E}\left[\int_0^T e^{-ru}\Lambda^2\Gamma G_n(u,\tilde{X}_u,v_u)\sigma_u d[W,U]_u\right]$$

$$+\frac{1}{2}\mathbb{E}\left[\int_0^T e^{-ru}\Lambda\Gamma^2 G_n(u,\tilde{X}_u,v_u)d[M,U]_u\right]. \tag{A.2}$$

A.2. *Decomposition formulas in the general model for the SVJ models of the Heston type*

In this section, we obtain the error terms for the SVJ models of the Heston type.

A.2.1. *Decomposition of the term (I_n) in the SVJ models of the Heston type*

The term I can be decomposed by

$$\begin{aligned}
&\frac{1}{8}\mathbb{E}\left[\int_0^T e^{-ru}\Gamma^2 G_n(u,\tilde{X}_u,v_u)d[M,M]_u\right]\\
&\quad-\frac{\nu^2}{8}\Gamma^2 G_n(0,\tilde{X}_0,v_0)\left(\int_0^T \mathbb{E}(\sigma_s^2)\varphi(s)^2 ds\right)\\
&=\frac{\nu^4}{64}\mathbb{E}\left[\int_0^T e^{-ru}\Gamma^4 G_n(u,\tilde{X}_u,v_u)\left(\int_u^T \mathbb{E}_u(\sigma_s^2)\varphi(s)^2 ds\right)\sigma_u^2\varphi^2(u)du\right]\\
&\quad+\frac{\rho\nu^3}{16}\mathbb{E}\left[\int_0^T e^{-ru}\Lambda\Gamma^3 G_n(u,\tilde{X}_u,v_u)\left(\int_u^T \mathbb{E}_u(\sigma_s^2)\varphi(s)^2 ds\right)\sigma_u^2\varphi(u)du\right]\\
&\quad+\frac{\rho\nu^3}{8}\mathbb{E}\left[\int_0^T e^{-ru}\Lambda\Gamma^2 G_n(u,\tilde{X}_u,v_u)\left(\int_u^T e^{-\kappa(z-u)}\varphi(z)^2 dz\right)\sigma_u^2 du\right]\\
&\quad+\frac{\nu^4}{16}\mathbb{E}\left[\int_0^T e^{-ru}\Gamma^3 G_n(u,\tilde{X}_u,v_u)\left(\int_u^T e^{-\kappa(z-u)}\varphi(z)^2 dz\right)\varphi(u)\sigma_u^2 du\right].
\end{aligned} \tag{A.3}$$

A.2.2. *Decomposition of the term (II_n) in the SVJ models of the Heston type*

The term II can be decomposed by

$$\begin{aligned}
&\frac{\rho}{2}\mathbb{E}\left[\int_0^T e^{-ru}\Lambda\Gamma G_n(u,\tilde{X}_u,v_u)\sigma_u d[W,M]_u\right]\\
&\quad-\frac{\rho\nu}{2}\Lambda\Gamma G_n(0,\tilde{X}_0,v_0)\left(\int_0^T \mathbb{E}(\sigma_s^2)\varphi(s)ds\right)
\end{aligned}$$

$$
\begin{aligned}
&= \frac{\rho\nu^3}{16}\mathbb{E}\left[\int_0^T e^{-ru}\Lambda\Gamma^3 G_n(u,\tilde{X}_u,v_u)\left(\int_u^T \mathbb{E}_u(\sigma_s^2)\varphi(s)ds\right)\sigma_u^2\varphi(u)^2du\right]\\
&\quad+\frac{\rho^2\nu^2}{4}\mathbb{E}\left[\int_0^T e^{-ru}\Lambda^2\Gamma^2 G_n(u,\tilde{X}_u,v_u)\left(\int_u^T \mathbb{E}_u(\sigma_s^2)\varphi(s)ds\right)\sigma_u^2\varphi(u)du\right]\\
&\quad+\frac{\rho^2\nu^2}{2}\mathbb{E}\left[\int_0^T e^{-ru}\Lambda^2\Gamma G_n(u,\tilde{X}_u,v_u)\left(\int_u^T e^{-\kappa(z-u)}\varphi(z)dz\right)\sigma_u^2du\right]\\
&\quad+\frac{\rho\nu^3}{4}\mathbb{E}\left[\int_0^T e^{-ru}\Lambda\Gamma^2 G_n(u,\tilde{X}_u,v_u)\left(\int_u^T e^{-\kappa(z-u)}\varphi(z)dz\right)\sigma_u^2\varphi(u)du\right].
\end{aligned}
\tag{A.4}
$$

A.3. *Upper-Bound of decomposition formulas in the SVJ models of the Heston type*

In this section, we obtain the upper-bounds for the SVJ models of the Heston type.

A.3.1. *Upper-Bound of the term (I_n) in the SVJ models of the Heston type*

We can re-write the decomposition formula as

$$
\begin{aligned}
&\frac{1}{8}\mathbb{E}\left[\int_0^T e^{-r(u-t)}\Gamma^2 G_n(u,\tilde{X}_u,v_u)d[M,M]_u\right]\\
&\qquad-\frac{\nu^2}{8}\Gamma^2 G_n(0,\tilde{X}_0,v_0)\left(\int_0^T E(\sigma_s^2)\varphi(s)^2ds\right)\\
&\qquad=\frac{\nu^4}{64}\mathbb{E}\left[\int_0^T e^{-ru}(\partial_x^6-3\partial_x^5+3\partial_x^4-\partial_x^3)\Gamma G_n(u,\tilde{X}_u,v_u)\right.\\
&\qquad\left.\times\left(\int_u^T \mathbb{E}_u(\sigma_s^2)\varphi(s)^2ds\right)\sigma_u^2\varphi^2(u)du\right]\\
&\qquad+\frac{\rho\nu^3}{16}\mathbb{E}\left[\int_0^T e^{-ru}\left(\partial_x^5-2\partial_x^4+\partial_x^3\right)\Gamma G_n(u,\tilde{X}_u,v_u)\right.\\
&\qquad\left.\times\left(\int_u^T \mathbb{E}_u(\sigma_s^2)\varphi^2(s)ds\right)\sigma_u^2\varphi(u)du\right]\\
&\qquad+\frac{\rho\nu^3}{8}\mathbb{E}\left[\int_0^T e^{-ru}(\partial_x^3-\partial_x^2)\Gamma G_n(u,\tilde{X}_u,v_u)\right.
\end{aligned}
$$

$$\times \left(\int_u^T e^{-\kappa(z-u)} \varphi(z)^2 dz \right) \sigma_u^2 du \Bigg]$$
$$+ \frac{\nu^4}{16} \mathbb{E} \left[\int_0^T e^{-ru} (\partial_x^4 - 2\partial_x^3 + \partial_x^2) \Gamma G_n(u, \tilde{X}_u, v_u) \right.$$
$$\left. \times \left(\int_u^T e^{-\kappa(z-u)} \varphi(z)^2 dz \right) \varphi(u) \sigma_u^2 du \right]. \tag{A.5}$$

Applying Lemma 4.1 and defining $a_u := v_u \sqrt{T-u}$, we obtain

$$\left| \frac{1}{8} \mathbb{E} \left[\int_0^T e^{-ru} \Gamma^2 G_n(u, \tilde{X}_u, v_u) d[M, M]_u \right] \right.$$
$$\left. - \frac{\nu^2}{8} \Gamma^2 G_n(0, \tilde{X}_0, v_0) \left(\int_0^T \mathbb{E}(\sigma_s^2) \varphi(s)^2 ds \right) \right|$$
$$\leq C \frac{\nu^4}{64} \mathbb{E} \left[\int_0^T e^{-ru} \left(\frac{1}{a_u^7} + \frac{3}{a_u^6} + \frac{3}{a_u^5} + \frac{1}{a_u^4} \right) v_u^2 (T-u) \varphi(u)^4 \sigma_u^2 du \right]$$
$$+ C \frac{|\rho| \nu^3}{16} \mathbb{E} \left[\int_0^T e^{-ru} \left(\frac{1}{a_u^6} + \frac{2}{a_u^5} + \frac{1}{a_u^4} \right) v_u^2 (T-u) \varphi(u)^3 \sigma_u^2 du \right]$$
$$+ C \frac{|\rho| \nu^3}{8} \mathbb{E} \left[\int_0^T e^{-ru} \left(\frac{1}{a_u^4} + \frac{1}{a_u^3} \right) \sigma_u^2 \varphi(u)^3 du \right]$$
$$+ C \frac{\nu^4}{16} \mathbb{E} \left[\int_0^T e^{-ru} \left(\frac{1}{a_u^5} + \frac{2}{a_u^4} + \frac{1}{a_u^3} \right) \varphi(u)^4 \sigma_u^2 du \right]. \tag{A.6}$$

Now, using Lemma 5.2(ii), we have

$$\left| \frac{1}{8} \mathbb{E} \left[\int_0^T e^{-ru} \Gamma^2 G_n(u, \tilde{X}_u, v_u) d[M, M]_u \right] \right.$$
$$\left. - \frac{\nu^2}{8} \Gamma^2 G_n(0, \tilde{X}_0, v_0) \left(\int_0^T \mathbb{E}(\sigma_s^2) \varphi^2(s) ds \right) \right|$$
$$\leq C \frac{\nu^4}{64} \mathbb{E} \left[\int_0^T e^{-ru} \left(\frac{1}{a_u^7} + \frac{3}{a_u^6} + \frac{3}{a_u^5} + \frac{1}{a_u^4} \right) v_u^4 (T-u)^2 \varphi(u)^3 du \right]$$
$$+ C \frac{|\rho| \nu^3}{16} \mathbb{E} \left[\int_0^T e^{-ru} \left(\frac{1}{a_u^6} + \frac{2}{a_u^5} + \frac{1}{a_u^4} \right) v_u^4 (T-u)^2 \varphi(u)^2 du \right]$$

$$+C\frac{|\rho|\nu^3}{8}\mathbb{E}\left[\int_0^T e^{-ru}\left(\frac{1}{a_u^4}+\frac{1}{a_u^3}\right)v_u^2(T-u)\varphi(u)^2du\right]$$
$$+C\frac{\nu^4}{16}\mathbb{E}\left[\int_0^T e^{-ru}\left(\frac{1}{a_u^5}+\frac{2}{a_u^4}+\frac{1}{a_u^3}\right)\varphi(u)^3v_u^2(T-u)du\right]. \tag{A.7}$$

Finally, applying Lemma 5.2(i), we find that

$$\left|\frac{1}{8}\mathbb{E}\left[\int_0^T e^{-ru}\Gamma^2G_n(u,\tilde{X}_u,v_u)d[M,M]_u\right]\right.$$
$$\left.-\frac{\nu^2}{8}\Gamma^2G_n(0,\tilde{X}_0,v_0)\left(\int_0^T\mathbb{E}(\sigma_s^2)\varphi(s)^2ds\right)\right|$$
$$\leq C\frac{\nu^4}{64}\mathbb{E}\left[\int_0^T e^{-ru}\left(\frac{2\sqrt{2}}{\theta\kappa\sqrt{\theta\kappa}}+\frac{6}{\theta\kappa^2}+\frac{3\sqrt{2}}{\kappa^2\sqrt{\theta\kappa}}+\frac{1}{\kappa^3}\right)du\right]$$
$$+C\frac{|\rho|\nu^3}{16}\mathbb{E}\left[\int_0^T e^{-ru}\left(\frac{2}{\theta\kappa}+\frac{2\sqrt{2}}{\kappa\sqrt{\theta\kappa}}+\frac{1}{\kappa^2}\right)du\right]$$
$$+C\frac{|\rho|\nu^3}{8}\mathbb{E}\left[\int_0^T e^{-ru}\left(\frac{2}{\theta\kappa}+\frac{\sqrt{2}}{\kappa\sqrt{\theta\kappa}}\right)du\right]$$
$$+C\frac{\nu^4}{16}\mathbb{E}\left[\int_0^T e^{-ru}\left(\frac{2\sqrt{2}}{\theta\kappa\sqrt{\theta\kappa}}+\frac{4}{\theta\kappa^2}+\frac{\sqrt{2}}{\kappa^2\sqrt{\theta\kappa}}\right)du\right]. \tag{A.8}$$

Then we have that

$$\left|\frac{1}{8}\mathbb{E}\left[\int_0^T e^{-ru}\Gamma^2G_n(u,\tilde{X}_u,v_u)d[M,M]_u\right]\right.$$
$$\left.-\frac{\nu^2}{8}\Gamma^2G_n(0,\tilde{X}_0,v_0)\left(\int_0^T\mathbb{E}(\sigma_s^2)\varphi(s)^2ds\right)\right|$$
$$\leq C\frac{\nu^4}{64}\left(\frac{2\sqrt{2}}{\theta\kappa\sqrt{\theta\kappa}}+\frac{6}{\theta\kappa^2}+\frac{3\sqrt{2}}{\kappa^2\sqrt{\theta\kappa}}+\frac{1}{\kappa^3}\right)\left(\int_0^T e^{-ru}du\right)$$
$$+C\frac{|\rho|\nu^3}{16}\left(\frac{2}{\theta\kappa}+\frac{2\sqrt{2}}{\kappa\sqrt{\theta\kappa}}+\frac{1}{\kappa^2}\right)\left(\int_0^T e^{-ru}du\right)$$
$$+C\frac{|\rho|\nu^3}{8}\left(\frac{2}{\theta\kappa}+\frac{\sqrt{2}}{\kappa\sqrt{\theta\kappa}}\right)\left(\int_0^T e^{-ru}du\right)$$
$$+C\frac{\nu^4}{16}\left(\frac{2\sqrt{2}}{\theta\kappa\sqrt{\theta\kappa}}+\frac{4}{\theta\kappa^2}+\frac{\sqrt{2}}{\kappa^2\sqrt{\theta\kappa}}\right)\left(\int_0^T e^{-ru}du\right). \tag{A.9}$$

Using the fact that $\int_t^T e^{-ru}ds \leq \frac{1}{r} \wedge T$, we conclude that

$$\begin{aligned}
&\left| \frac{1}{8}\mathbb{E}\left[\int_0^T e^{-ru}\Gamma^2 G_n(u, \tilde{X}_u, v_u) d[M, M]_u \right] \right. \\
&\qquad \left. - \frac{\nu^2}{8}\Gamma^2 G_n(0, \tilde{X}_0, v_0) \left(\int_0^T \mathbb{E}(\sigma_s^2)\varphi(s)^2 ds \right) \right| \\
&\qquad \leq \nu^3(|\rho| + \nu) \left(\frac{1}{r} \wedge T \right) \Pi_1(\kappa, \theta), \qquad \text{(A.10)}
\end{aligned}$$

where Π_1 is a positive function.

A.3.2. *Upper-Bound of the term (II_n) in the SVJ models of the Heston type*

We can re-write the decomposition formula as

$$\begin{aligned}
&\frac{\rho}{2}\mathbb{E}\left[\int_0^T e^{-ru}\Lambda\Gamma G_n(u, \tilde{X}_u, v_u)\sigma_u d[W, M]_u \right] \\
&\quad - \frac{\rho\nu}{2}\Lambda\Gamma G_n(0, \tilde{X}_0, v_0) \left(\int_0^T \mathbb{E}(\sigma_s^2)\varphi(s) ds \right) \\
&= \frac{\rho\nu^3}{16}\mathbb{E}\left[\int_0^T e^{-ru}(\partial_x^5 - 2\partial_x^4 + \partial_x^3)\Gamma G_n(u, \tilde{X}_u, v_u) \right. \\
&\quad \left. \times \left(\int_u^T \mathbb{E}_u(\sigma_s^2)\varphi(s) ds \right) \sigma_u^2 \varphi^2(u) du \right] \\
&\quad + \frac{\rho^2\nu^2}{4}\mathbb{E}\left[\int_0^T e^{-ru}(\partial_x^4 - \partial_x^3)\Gamma G_n(u, \tilde{X}_u, v_u) \right. \\
&\quad \left. \times \left(\int_u^T \mathbb{E}_u(\sigma_s^2)\varphi(s) ds \right) \sigma_u^2 \varphi(u) du \right] \\
&\quad + \frac{\rho^2\nu^2}{2}\mathbb{E}\left[\int_0^T e^{-ru}\partial_x^2\Gamma G_n(u, \tilde{X}_u, v_u) \left(\int_u^T e^{-\kappa(z-u)}\varphi(z) dz \right) \sigma_u^2 du \right] \\
&\quad + \frac{\rho\nu^3}{4}\mathbb{E}\left[\int_0^T e^{-ru}(\partial_x^3 - \partial_x^2)\Gamma G_n(u, \tilde{X}_u, v_u) \right. \\
&\quad \left. \times \left(\int_u^T e^{-\kappa(z-u)}\varphi(z) dz \right) \sigma_u^2 \varphi(u) du \right]. \qquad \text{(A.11)}
\end{aligned}$$

Applying Lemma 4.1 and defining $a_u := v_u\sqrt{T-u}$, we obtain

$$\begin{aligned}
&\left|\frac{\rho}{2}\mathbb{E}\left[\int_0^T e^{-ru}\Lambda\Gamma G_n(u,\tilde{X}_u,v_u)\sigma_u d[W,M]_u\right]\right.\\
&\qquad\left.-\frac{\rho\nu}{2}\Lambda\Gamma G_n(0,\tilde{X}_0,v_0)\left(\int_0^T \mathbb{E}(\sigma_s^2)\varphi(s)ds\right)\right|\\
&\leq C\frac{|\rho|\nu^3}{16}\mathbb{E}\left[\int_0^T e^{-ru}\left(\frac{1}{a_u^6}+\frac{2}{a_u^5}+\frac{1}{a_u^4}\right)\left(\int_u^T \mathbb{E}_u(\sigma_s^2)\varphi(s)ds\right)\sigma_u^2\varphi(u)^2du\right]\\
&\quad+C\frac{\rho^2\nu^2}{4}\mathbb{E}\left[\int_0^T e^{-ru}\left(\frac{1}{a_u^5}+\frac{1}{a_u^4}\right)\left(\int_u^T \mathbb{E}_u(\sigma_s^2)\varphi(s)ds\right)\sigma_u^2\varphi(u)du\right]\\
&\quad+C\frac{\rho^2\nu^2}{2}\mathbb{E}\left[\int_0^T e^{-ru}\frac{1}{a_u^3}\left(\int_u^T e^{-\kappa(z-u)}\varphi(z)dz\right)\sigma_u^2du\right]\\
&\quad+C\frac{|\rho|\nu^3}{4}\mathbb{E}\left[\int_0^T e^{-ru}\left(\frac{1}{a_u^4}+\frac{1}{a_u^3}\right)\left(\int_u^T e^{-\kappa(z-u)}\varphi(z)dz\right)\sigma_u^2\varphi(u)du\right].
\end{aligned}\tag{A.12}$$

Using Lemma 5.2(ii), then

$$\begin{aligned}
&\left|\frac{\rho}{2}\mathbb{E}\left[\int_0^T e^{-ru}\Lambda\Gamma G_n(u,\tilde{X}_u,v_u)\sigma_u d[W,M]_u\right]\right.\\
&\qquad\left.-\frac{\rho\nu}{2}\Lambda\Gamma G_n(0,\tilde{X}_0,v_0)\left(\int_0^T \mathbb{E}(\sigma_s^2)\varphi(s)ds\right)\right|\\
&\leq C\frac{|\rho|\nu^3}{16}\mathbb{E}\left[\int_0^T e^{-ru}\left(\frac{1}{a_u^6}+\frac{2}{a_u^5}+\frac{1}{a_u^4}\right)v_u^4(T-u)^2\varphi(u)^2du\right]\\
&\quad+C\frac{\rho^2\nu^2}{4}\mathbb{E}\left[\int_0^T e^{-ru}\left(\frac{1}{a_u^5}+\frac{1}{a_u^4}\right)v_u^4(T-u)^2\varphi(u)du\right]\\
&\quad+C\frac{\rho^2\nu^2}{2}\mathbb{E}\left[\int_0^T e^{-ru}\frac{1}{a_u^3}\varphi(u)v_u^2(T-u)du\right]\\
&\quad+C\frac{|\rho|\nu^3}{4}\mathbb{E}\left[\int_0^T e^{-ru}\left(\frac{1}{a_u^4}+\frac{1}{a_u^3}\right)\varphi(u)^2v_u^2(T-u)du\right].
\end{aligned}\tag{A.13}$$

Finally, applying Lemma 5.2(i), we find that

$$\begin{aligned}
&\left|\frac{\rho}{2}\mathbb{E}\left[\int_0^T e^{-ru}\Lambda\Gamma G_n(u,\tilde{X}_u,v_u)\sigma_u d[W,M]_u^c\right]\right.\\
&\qquad\left.-\frac{\rho\nu}{2}\Lambda\Gamma G_n(0,\tilde{X}_0,v_0)\left(\int_0^T\mathbb{E}(\sigma_s^2)\varphi(s)ds\right)\right|\\
&\leq C\frac{|\rho|\nu^3}{16}\mathbb{E}\left[\int_0^T e^{-ru}\left(\frac{2}{\theta\kappa}+\frac{2\sqrt{2}}{\kappa\sqrt{\theta\kappa}}+\frac{1}{\kappa^2}\right)du\right]\\
&\quad+C\frac{\rho^2\nu^2}{4}\mathbb{E}\left[\int_0^T e^{-ru}\left(\frac{\sqrt{2}}{\sqrt{\theta\kappa}}+\frac{1}{\kappa}\right)du\right]+C\frac{\rho^2\nu^2}{2}\mathbb{E}\left[\int_0^T e^{-ru}\frac{\sqrt{2}}{\sqrt{\theta\kappa}}du\right]\\
&\quad+C\frac{|\rho|\nu^3}{4}\mathbb{E}\left[\int_0^T e^{-ru}\left(\frac{2}{\theta\kappa}+\frac{\sqrt{2}}{\kappa\sqrt{\theta\kappa}}\right)du\right]. \qquad \text{(A.14)}
\end{aligned}$$

Then we have that

$$\begin{aligned}
&\left|\frac{\rho}{2}\mathbb{E}\left[\int_0^T e^{-ru}\Lambda\Gamma G_n(u,\tilde{X}_u,v_u)\sigma_u d[W,M]_u^c\right]\right.\\
&\qquad\left.-\frac{\rho\nu}{2}\Lambda\Gamma G_n(0,\tilde{X}_0,v_0)\left(\int_0^T\mathbb{E}(\sigma_s^2)\varphi(s)ds\right)\right|\\
&\leq C\frac{|\rho|\nu^3}{16}\left(\frac{2}{\theta\kappa}+\frac{2\sqrt{2}}{\kappa\sqrt{\theta\kappa}}+\frac{1}{\kappa^2}\right)\left(\int_0^T e^{-ru}du\right)\\
&\quad+C\frac{\rho^2\nu^2}{4}\left(\frac{\sqrt{2}}{\sqrt{\theta\kappa}}+\frac{1}{\kappa}\right)\left(\int_0^T e^{-ru}du\right)+C\frac{\rho^2\nu^2}{2}\frac{\sqrt{2}}{\sqrt{\theta\kappa}}\left(\int_0^T e^{-ru}du\right)\\
&\quad+C\frac{|\rho|\nu^3}{4}\left(\frac{2}{\theta\kappa}+\frac{\sqrt{2}}{\kappa\sqrt{\theta\kappa}}\right)\left(\int_0^T e^{-ru}du\right). \qquad \text{(A.15)}
\end{aligned}$$

Using the fact that $\int_t^T e^{-ru}ds \leq \frac{1}{r}\wedge T$, we conclude that

$$\begin{aligned}
&\left|\frac{\rho}{2}\mathbb{E}\left[\int_0^T e^{-ru}\Lambda\Gamma G_n(u,\tilde{X}_u,v_u)\sigma_u d[W,M]_u^c\right]\right.\\
&\qquad\left.-\frac{\rho\nu}{2}\Lambda\Gamma G_n(0,\tilde{X}_0,v_0)\left(\int_0^T\mathbb{E}(\sigma_s^2)\varphi(s)ds\right)\right|\\
&\leq|\rho|\nu^2(|\rho|+\nu)\left(\frac{1}{r}\wedge T\right)\Pi_2(\kappa,\theta), \qquad \text{(A.16)}
\end{aligned}$$

where Π_2 is a positive function.

A.3.3. *Upper-Bound for the terms* (I_n) *and* (II_n) *in the SVJ models of the Heston type*

We have that

$$\begin{aligned}
&\left|\frac{1}{8}\mathbb{E}\left[\int_0^T e^{-ru}\Gamma^2 G_n(u,\tilde{X}_u,v_u)d[M,M]_u\right]\right.\\
&\qquad\left.-\frac{\nu^2}{8}\Gamma^2 G_n(0,\tilde{X}_0,v_0)\left(\int_0^T \mathbb{E}(\sigma_s^2)\varphi(s)^2 ds\right)\right|\\
&\qquad+\left|\frac{\rho}{2}\mathbb{E}\left[\int_0^T e^{-ru}\Lambda\Gamma G_n(u,\tilde{X}_u,v_u)\sigma_u d[W,M]_u^c\right]\right.\\
&\qquad\left.-\frac{\rho\nu}{2}\Lambda\Gamma G_n(0,\tilde{X}_0,v_0)\left(\int_0^T \mathbb{E}(\sigma_s^2)\varphi(s)ds\right)\right|\\
&\leq \nu^3(|\rho|+\nu)\left(\frac{1}{r}\wedge T\right)\Pi_1(\kappa,\theta)+|\rho|\nu^2(|\rho|+\nu)\left(\frac{1}{r}\wedge T\right)\Pi_2(\kappa,\theta)\\
&\leq \nu^2(|\rho|+\nu)^2\left(\frac{1}{r}\wedge T\right)\Pi(\kappa,\theta), \qquad \text{(A.17)}
\end{aligned}$$

where function Π is the maximum of functions Π_1 and Π_2.

References

H. Albrecher, P. Mayer, W. Schoutens & J. Tistaert (2007) The little Heston trap, *Wilmott Magazine* **2007** (January/February), 83–92.

E. Alòs (2006) A generalization of the Hull and White formula with applications to option pricing approximation, *Finance and Stochastics* **10** (3), 353–365, doi:10.1007/s00780-006-0013-5.

E. Alòs (2012) A decomposition formula for option prices in the Heston model and applications to option pricing approximation, *Finance and Stochastics* **16** (3), 403–422, doi:10.1007/s00780-012-0177-0.

E. Alòs, R. de Santiago & J. Vives (2015) Calibration of stochastic volatility models via second-order approximation: The Heston case, *International Journal of Theoretical and Applied Finance* **18** (6), 1–31, doi:10.1142/S0219024915500363.

E. Alòs, J. A. León, M. Pontier & J. Vives (2008) A Hull and White formula for a general stochastic volatility jump-diffusion model with applications to the study of the short-time behavior of the implied volatility, *Journal of Applied Mathematics and Stochastic Analysis*, 17, 359142, doi:10.1155/2008/359142.

E. Alòs, J. A. León & J. Vives (2007) On the short-time behavior of the implied volatility for jump-diffusion models with stochastic volatility, *Finance and Stochastics* **11** (4), 571–589, doi:10.1007/s00780-007-0049-1.

C. A. Ball & A. Roma (1994) Stochastic volatility option pricing, *Journal of Financial and Quantitative Analysis* **29** (4), 589–607, doi:10.2307/2331111.

O. E. Barndorff-Nielsen & N. Shephard (2001), Non-Gaussian Ornstein–Uhlenbeck-based models and some of their uses in financial economics, *Journal of the Royal Statistical Society Series B. Statistical Methodology* **63** (2), 167–241, doi:10.1111/1467-9868.00282.

D. S. Bates (1996), Jumps and stochastic volatility: Exchange rate processes implicit in Deutsche mark options, *The Review of Financial Studies* **9** (1), 69–107, doi:10.1093/rfs/9.1.69.

F. Baustian, M. Mrázek, J. Pospíšil & T. Sobotka (2017) Unifying pricing formula for several stochastic volatility models with jumps, *Applied Stoccastic Models in Business and Industry* **33** (4), 422–442, doi:10.1002/asmb.2248.

C. Bayer, P. Friz & J. Gatheral (2016) Pricing under rough volatility, *Quantitative Finance* **16** (6), 887–904, doi:10.1080/14697688.2015.1099717.

E. Benhamou, E. Gobet & M. Miri (2010) Time dependent Heston model, *SIAM Journal on Financial Mathematics* **1** (1), 289–325, doi:10.1137/090753814.

J. C. Cox, J. E. Ingersoll & S. A. Ross (1985) A theory of the term structure of interest rates, *Econometrica* **53** (2), 385–407, doi:10.2307/1911242.

D. Duffie, J. Pan & K. Singleton (2000) Transform analysis and asset pricing for affine jump-diffusions, *Econometrica* **68** (6), 1343–1376, doi:10.1111/1468-0262.00164.

A. Elices (2008) Models with time-dependent parameters using transform methods: Application to Heston's model, available at arXiv: https://arxiv.org/abs/0708.2020.

J.-P. Fouque, G. Papanicolaou & K. R. Sircar (2000) *Derivatives in Financial Markets with Stochastic Volatility*. Cambridge, U.K.: Cambridge University Press.

J.-P. Fouque, G. Papanicolaou, R. Sircar & K. Solna (2003) Multiscale stochastic volatility asymptotics, *Multiscale Modeling and Simulation* **2** (1), 22–42, doi:10.1137/030600291.

J. Gatheral (2006) *The Volatility Surface*: *A Practitioner's Guide*, Wiley Finance. Hoboken, New Jersey: John Wiley & Sons.

A. Gulisashvili & J. Vives (2012) Two-sided estimates for distribution densities in models with jumps, In: *Stochastic Differential Equations and Processes*, eds. M. Zili and D. V. Filatova, 239–254. Berlin, Heidelberg: Springer, https://www.springer.com/la/book/9783642223679.

F. B. Hanson (2007) *Applied Stochastic Processes and Control for Jump-Diffusions*, *Advances in Design and Control*, Vol. 13. Philadelphia, PA: SIAM.

S. L. Heston (1993) A closed-form solution for options with stochastic volatility with applications to bond and currency options, *The Review of Financial Studies* **6** (2), 327–343, doi:10.1093/rfs/6.2.327.

J. C. Hull & A. D. White (1987) The pricing of options on assets with stochastic volatilities, *The Journal of Finance* **42** (2), 281–300, doi:10.1111/j.1540-6261.1987.tb02568.x.

H. Jafari & J. Vives (2013) A Hull and White formula for a stochastic volatility Lévy model with infinite activity, *Communications on Stochastic Analysis* **7** (2), 321–336.

F. Killmann & E. von Collani (2001) A note on the convolution of the uniform and related distributions and their use in quality control, *Economic Quality Control* **16** (1), 17–41, doi:10.1515/EQC.2001.17.

S. G. Kou (2002) A jump-diffusion model for option pricing, *Management Science* **48** (8), 1086–1101, doi:10.1287/mnsc.48.8.1086.166.

A. L. Lewis (2000) *Option Valuation Under Stochastic Volatility*: *With Mathematica Code*. Newport Beach, CA: Finance Press.

R. Merino & J. Vives (2015) A generic decomposition formula for pricing vanilla options under stochastic volatility models, *International Journal of Stochastic Analysis*, 11, 103647, doi:10.1155/2015/103647.

R. Merino & J. Vives (2017) Option price decomposition in spot-dependent volatility models and some applications, *International Journal of Stochastic Analysis*, 16, 8019498, doi:10.1155/2017/8019498.

R. C. Merton (1976) Option pricing when underlying stock returns are discontinuous, *Journal of Financial Economics* **3** (1–2), 125–144, doi:10.1016/0304-405X(76)90022-2.

S. Mikhailov & U. Nögel (2003) Heston's stochastic volatility model — Implementation, calibration and some extensions, *Wilmott Magazine* **2003** (July), 74–79.

M. Mrázek, J. Pospíšil & T. Sobotka (2016) On calibration of stochastic and fractional stochastic volatility models, *European Journal of Operational Research* **254** (3), 1036–1046, doi:10.1016/j.ejor.2016.04.033.

J. Pospíšil & T. Sobotka (2016) Market calibration under a long memory stochastic volatility model, *Applied Mathematical Finance* **23** (5), 323–343, doi:10.1080/1350486X.2017.1279977.

L. O. Scott (1987) Option pricing when the variance changes randomly: Theory, estimation, and an application, *Journal of Financial Quantitative Analysis* **22** (4), 419–438, doi:10.2307/2330793.

L. O. Scott (1997) Pricing stock options in a jump-diffusion model with stochastic volatility and interest rates: Applications of fourier inversion methods, *Mathematical Finance* **7** (4), 413–426, doi:10.1111/1467-9965.00039.

J. Stein & E. Stein (1991) Stock price distributions with stochastic volatility: An analytic approach, *The Review of Financial Studies* **4** (4), 727–752, doi:10.1093/rfs/4.4.727.

J. Vives (2016) Decomposition of the pricing formula for stochastic volatility models based on malliavin-skorohod type calculus, In: *Statistical Methods and Applications in Insurance and Finance*: *CIMPA School*, *Marrakech and El Kelaa M'gouna*, *Morocco*, *April 2013* (M. Eddahbi, E. H. Essaky & J. Vives, eds.), 103–123. Cham: Springer, doi:10.1007/978-3-319-30417-5_4.

G. Yan & F. B. Hanson (2006) Option pricing for a stochastic-volatility jump-diffusion model with log-uniform jump-amplitude, In: *Proceedings of American Control Conference*, 2989–2994. Piscataway, NJ: IEEE, doi:10.1109/acc.2006.1657175.

Empirical Economics (2019) 57:1935–1958
https://doi.org/10.1007/s00181-018-1535-3

Robustness and sensitivity analyses for stochastic volatility models under uncertain data structure

Jan Pospíšil[1] · **Tomáš Sobotka**[1] · **Philipp Ziegler**[2]

Received: 6 March 2017 / Accepted: 26 June 2018 / Published online: 31 July 2018

Abstract
In this paper, we perform robustness and sensitivity analysis of several continuous-time stochastic volatility (SV) models with respect to the process of market calibration. The analyses should validate the hypothesis on importance of the jump part in the underlying model dynamics. Also an impact of the long memory parameter is measured for the approximative fractional SV model (FSV). For the first time, the robustness of calibrated models is measured using bootstrapping methods on market data and Monte Carlo filtering techniques. In contrast to several other sensitivity analysis approaches for SV models, the newly proposed methodology does not require independence of calibrated parameters—an assumption that is typically not satisfied in practice. Empirical study is performed on a data set of Apple Inc. equity options traded in four different days in April and May 2015. In particular, the results for Heston, Bates and approximative FSV models are provided.

Keywords Robustness analysis · Sensitivity analysis · Stochastic volatility models · Bootstrapping · Monte Carlo filtering

Mathematics Subject Classification 62F35 · 62F40 · 91G20 · 91G70

JEL Classification C52 · C58 · C12 · G12

1 Introduction

Stochastic volatility (SV) models are common tools for retrieving fair values of financial derivatives and are of the interest of both academics and practitioners. For practical

✉ Jan Pospíšil
honik@ntis.zcu.cz

[1] NTIS - New Technologies for the Information Society, Faculty of Applied Sciences, University of West Bohemia, Univerzitní 8, 306 14 Plzeň, Czech Republic

[2] Department of Mathematics, University of Rostock, Ulmenstraße 69, 18057 Rostock, Germany

applicability, one needs to estimate model parameters first. This is typically done by means of calibration or by using filtering estimation techniques, e.g., as in Creel and Kristensen (2015). We consider a classical calibration routine—we focus on calibration to vanilla European options, as they are widely traded and sufficiently liquid. From a variety of introduced SV models, one has to choose an appropriate candidate for pricing tasks. The main assumption of any option pricing model is the structure of modelled dynamics of the underlying. Several empirical studies of various price processes have been analysed in the literature.

Authors Carr and Wu (2003) found the presence of both continuous and jump components of modelled market dynamics for the S&P 500 index data. This was done by analysing out-of-the-money and at-the-money options' decays in the price for time to maturity reaching zero. As in our case, the authors did not examine prices of the underlying directly which would require extremely high-frequency data that could be affected by market microstucture [for time-series tests see, e.g., Barndorff-Nielsen and Shephard (2006), Hwang and Shin (2014)]. In Campolongo et al. (2006) the use of stochastic volatility models with jumps was recommended because the uncertainty in the estimated option prices mostly came from jump parameters of the considered model. This statement was derived from a study with fictional data and model parameters. We test the hypotheses of Carr and Wu (2003), Campolongo et al. (2006) in the case of real market data, and we also show that Campolongo et al. (2006) method is not suitable for practice (at least for our data sets). A different approach, where a model robustness to varying data structures plays a crucial role, is proposed and applied to real market data sets including Apple Inc. equity options traded in April and May 2015. The data set choice is justified in Sect. 3.

In this paper, three subclasses of SV models are considered—they are represented by a standard diffusion Heston (1993) model, jump-diffusion Bates (1996) model and so-called approximative fractional jump-diffusion (FSV) model. The latter approach outperformed the Heston (1993) model in terms of in-sample calibration errors in the study by (Pospíšil and Sobotka 2016). Unlike the case of Bayer et al. (2016) and many other very recent manuscripts, the FSV model is considered only in the long-memory regime ($H > 0.5$). This is due to restrictions on the pricing solution and also in this case we can use the same unifying pricing approach for all three models (Baustian et al. 2017); hence, our comparison is not affected by a noise coming from differences in various numerical implementations of pricing routines. Some comments on the rough volatility regime are to be found in the conclusion.

The considered approaches are tested under uncertainty in the option price structure and are compared with sensitivity and uncertainty analysis tools. Saltelli et al. (2004) defined sensitivity analysis as "the study of how uncertainty in the output of a model (numerical or otherwise) can be apportioned to different sources of uncertainty in the model input". We want to know how sensitive calibration errors are with respect to the changing data structure and also how the calibrated parameters are affected. This is done by performing an uncertainty analysis. According to Saltelli et al. (2008), "uncertainty and sensitivity analyses should be run in tandem, with uncertainty analysis preceding in current practice". The method of Sobol indices is the most common approach for global sensitivity analysis. An application of Sobol indices in option pricing can be found in the paper of Bianchetti et al. (2015), where the impact of

uncertainty in prices and greeks is measured. However, for real market data one cannot assume independence of the input parameter values for calculating Sobol indices. In this paper, we use different global sensitivity analysis methods which are discussed, e.g., in Saltelli et al. (2008): **I.** First of all, on bootstrapped data structures we visualize a dependence of calibrated parameter values by scatterplots; **II.** Secondly, hypotheses of the jump term importance and of a long-memory persistence are assessed by Monte Carlo filtering techniques.

Considered models are calibrated from markets (or bootstrapped data) comprising vanilla European call options. A European call is a contract that gives the buyer a right to buy a share of the underlying asset for a fixed (strike) price K at some future time T. If the buyer observes a stock price at maturity lower than K, he or she doesn't utilize her right to buy the asset for K. Vice versa, the buyer is exercising the right as long as $S_T \geq K$. This translates into the following pay-off function,

$$P(x) = \max(x - K, 0), \quad \text{where } x = S_T.$$

To answer the question—what is the fair value of this contract—one has to build up a set of assumptions on the market that drives $(S_t)_{0<t\leq T}$. Since the Nobel prize winning Black and Scholes (1973) model, one usually considers the stock market to be a stochastic process and the fair value is then obtained using arbitrage-free arguments.[1] Main differences between the considered models are comprised in the process that drives evolution of the stock prices. All approaches in this paper not only assume that the stock price process is of random nature, but also it is assumed that the variance thereof is a stochastic process itself. Hence, a stochastic volatility model can be viewed as a natural extension to the Black–Scholes paradigm.

Purpose of this article is to help practitioners in the daily calibration process of option pricing models. For quantitative tasks beyond the Black–Scholes model, one might face a decision call of choosing a suitable model for particular situation. Different criteria have to be considered, for example, the *in-sample/out-of-sample errors*, the ability to model the *volatility smile*. We compare the *robustness* of different models with respect to a given option structure. This is important, because the equity options traded on different days can vary in several aspects, as, e.g., amount of traded instruments, marked strike prices and expiration times, market ask–bid spreads. Hence, the structure of a daily option market snapshot to which the models are calibrated is another source of uncertainty for the model choice—models might perform differently with respect to different market structures. We show how to analyse this uncertainty, measure its impact on the predicted option fair values, and we provide a hint on how to use this as a criterion for choosing a suitable option pricing model. In doing so, we use bootstrapping of the option data and we also introduce several measures of robustness.

The structure of the paper is as follows. In Sect. 2 we introduce the studied stochastic volatility models and the process of calibration of these models to real market data. In Sect. 3 we describe the methodology, in particular the bootstrapping of option prices, as well as we detail the uncertainty and sensitivity analyses. In Sect. 4 we present

[1] For more details on the arbitrage pricing see, for instance, Shreve (2004).

obtained results by comparing all models in terms of variation in model parameters and in bootstrapped option prices. We also provide the results of the Monte Carlo filtering trials, showing us the importance of the jump intensity for the Bates model and the importance of the long-memory parameter for the approximative fractional model. We conclude all obtained results in Sect. 5.

2 Stochastic volatility models

In this paper, we focus on a class of stochastic volatility models. These modelling approaches are not restricted by the constant volatility assumption (unlike the Black–Scholes model, binomial trees etc.), nor they assume a deterministic structure of the asset volatility process (unlike local volatility models). The models are usually tractable for a wide range of applications including the market calibration task described at the end of this section.

We consider a risk-neutral jump-diffusion setting corresponding to the stochastic basis denoted by $(\Omega, \mathcal{F}, (\mathcal{F}_t)_{t\geq 0}, \mathbb{Q})$. The modelled stock price S_t evolves in time according to the following Itô stochastic differential equations

$$dS_t = rS_t dt + \sqrt{v_t} S_t d\widetilde{W}_t^S + S_{t-} dJ_t, \tag{1}$$

$$dv_t = p(v_t)dt + q(v_t)d\widetilde{W}_t^v, \tag{2}$$

$$d\widetilde{W}_t^S d\widetilde{W}_t^v = \rho\, dt, \quad S_0,\ v_0 \in \mathbb{R}^+, \tag{3}$$

where $p, q \in C^\infty(0,\infty)$ are general coefficient functions for the volatility process and ρ is the correlation between $\mathbb{Q}$-Wiener processes $\widetilde{W}_t^S$ and $\widetilde{W}_t^v$.

To get market dynamics postulated by Heston (1993) we specify $dJ_t \equiv 0$, $p(v_t) = \kappa(\theta - v_t)$ and $q(v_t) = \sigma\sqrt{v_t}$. The set of model parameters Θ^H is then defined as $\Theta^H := \{v_0,\ \kappa,\ \theta,\ \sigma,\ \rho\}$.

For the Bates (1996) model, functions p, q remain the same as in the previous case and dJ_t corresponds to the compensated compound Poisson process with log-normal jump sizes—jumps occur with intensity λ and their sizes are log-normal with parameters μ_J and σ_J. The set of parameters, in the Bates model case, consists of $\Theta^B := \{v_0,\ \kappa,\ \theta,\ \sigma,\ \rho,\ \lambda,\ \mu_J,\ \sigma_J\}$. Due to more degrees of freedom, the model should provide a better market fit and as was shown in Duffie et al. (2000) adding a second jump process to (2) might not improve the fit any more.

Instead of considering a stochastic volatility model with jumps in both underlying and variance dynamics, we use an approximative fractional process as described in Baustian et al. (2017), Pospíšil and Sobotka (2016). Under the approximative fractional model one assumes the same type of jumps as in the Bates model case, but $p(v_t) = \left[(H-1/2)\psi_t\sigma\sqrt{v} + \kappa(\theta - v_t)\right]$ and $q(v_t) = \varepsilon^{H-1/2}\sigma\sqrt{v}$, where $\varepsilon > 0$ is an approximating factor and ψ_t is an Itô integral:

$$\psi_t = \int_0^t (t-s+\varepsilon)^{H-3/2} dW_s^\psi.$$

The set of parameters $\Theta^F := \{v_0, \kappa, \theta, \sigma, \rho, \lambda, \mu_J, \sigma_J, H\}$ also includes the Hurst exponent H. As was shown by Lewis (2000) and Baustian et al. (2017), respectively, all three models attain a semi-closed form solution not only for plain European options, but also for other non-path-dependant payoffs—this is crucial for our experiments; a single trial will involve 200 calibrations of each model to different data sets. We also did not perform analyses of models with time-dependent parameters which were studied by Mikhailov and Nögel (2003), Osajima (2007), Elices (2008), Benhamou et al. (2010) etc. As mentioned in Bayer et al. (2016), the general overall shape of the volatility surface, at least in case of equity markets, does not change in time significantly and hence one should model instantaneous variance as a time-homogeneous stochastic process.

To use the aforementioned models in practice, one has to calibrate them to a given market beforehand.[2] The calibration process can be viewed as an optimization problem of finding the best fit to the given option price surface. Let the surface consist of N options, each with a different strike price (K) and time to maturity (T) combination. A standard market practice is to use a weighted least-square utility function,

$$\begin{aligned} \widehat{\Theta} &= \arg\inf_{\Theta} G(\Theta), \\ G(\Theta) &= \sum_{j=1}^{N} w_j \left(C_j^{\Theta}(T_j, K_j) - C_j^* \right)^2, \end{aligned} \tag{4}$$

where $C_j^{\Theta}(T_j, K_j)$ is a model price calculated using the parameter set Θ and C_j^* represents the jth quoted option price. Weights w_j are commonly represented as a function of the ask–bid price spread. Although various weight functions were tested[3], due to similarities in results we focus on the best performing weights from Mrázek et al. (2016), i.e.,

$$w_j = \frac{1}{\left(C_j^{\text{ask}} - C_j^{\text{bid}} \right)^2} \tag{5}$$

for $j = 1, 2, \ldots, N$.

2.1 Test data sets

For the analyses we utilize data sets that include all traded European call options on Apple Inc. stock on particular testing days. These options are fairly liquid and hence the data sets from slightly different time periods (1/4/2015, 15/4/2015, 1/5/2015 and 15/5/2015.) are deemed to be representative of the equity vanilla option markets for stocks. The structure of the newest data set is depicted in Fig. 1. It is worth to mention that we do not restrict our trials to only specific time-to-maturities nor to a specific moneyness range.

[2] Alternatively one can estimate the parameters from time-series data.

[3] The weight functions introduced by Mrázek et al. (2016) were considered.

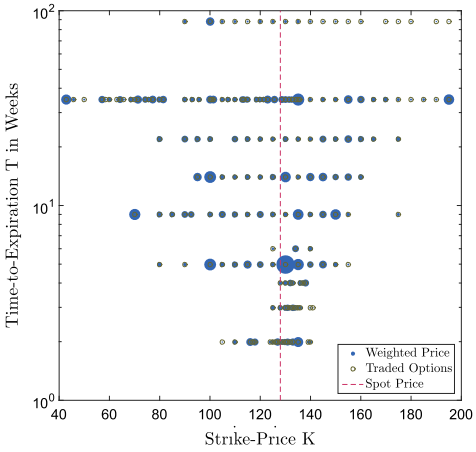

(a)

	Lower bound	Upper bound
v_0	0	1
κ	0	100
θ	0	1
σ	0	4
ρ	-1	1
λ	0	100
μ_J	-10	5
σ_J	0	4
H	0.5	1

(b)

Fig. 1 Data structure and bounds for calibrated parameters. On the left, we depict weighted call prices $w_j C_j^*$ by a ball centred in the $K - T$ plane. The diameter of each filled ball relates to the weighted call price and its centre corresponds to the pair K_j, T_j. **a** Structure of the Apple Inc. call options (15/5/2015). **b** Parameter bounds for all considered calibration trials

3 Methodology

In this section we introduce a methodology to analyse a model robustness with respect to uncertain option price structures. This is done by using bootstrapping techniques to estimate unobserved samples of the data structure. Also we introduce several measures of robustness that will be later used to compare the models.

In what follows, we detail on the sensitivity analysis techniques used in this paper. In particular, our goal is to analyse whether calibrated values of the jump-intensity parameter λ (for the Bates model) and of the Hurst exponent H (for the FSV model) can significantly affect the quality of the market fit. As for the measures of robustness, we take advantage of the bootstrapped samples and we use a Monte Carlo filtering technique to quantify the importance of the mentioned parameters. Both λ and H have important consequences for a model selection choice—by setting $\lambda = 0$ and $H = 0.5$ we obtain the standard Heston (1993) model.

3.1 Bootstrapping option prices

The daily option prices are given as a set of ask- and bid-prices with different strike price K and time to maturity T. These data are new for every day, as the behaviour and the value of the underlying stock, the reference value for the option prices change, and it is not statistical in the sense that we only have one dataset for every time instance. Although the option prices usually have some similarities with prices of former days, the focus of traders can change to different options and therefore not all $K \times T$ combinations have to be the same as well as ask- and bid-prices can differ strongly. This can significantly impact calibration results. Therefore we focus on uncertainty

in the options structure $K \times T$. Let X be a random variable representing the pair (K, T). Then currently observed strike prices and maturities (K_j, T_j), $j = 1, \ldots, N$, as mentioned in (4), are samples of X and to each pair we can attach the quoted market option price C_j^*.

To measure the impact of the uncertain option structure on the model calibration, common methods for uncertainty analysis need statistical data which are not available in practice. In fact, option pricing models are typically recalibrated daily and only to current available and suitable data sets [see, e.g., Mikhailov and Nögel (2003), Yekutieli (2004)]. In the following, we will apply the bootstrapping method to our data set. Since the original paper by Efron (1979) and especially his monograph (Efron 1982), research activities on the bootstrap method grew dramatically and we refer the reader for example to the book by Chernick (2008) and the comprehensive literature review therein. In what follows we apply the standard nonparametric i.i.d. bootstrap method.

We will perform bootstrapping on the set of observed structure (K_j, T_j), $j = 1, \ldots, N$, i.e., we obtain a new set $\mathbf{X}^\dagger$ by sampling N times with replacement.[4] Obviously, for each element of $\mathbf{X}^\dagger$ we can assign a market option price that corresponds to the strike and maturity combination. This provides us with the bootstrap option prices $\mathbf{C}^\dagger = (C_j^\dagger)_{j=1}^N$. This bootstrap procedure is then repeated M times, and hence we get M bootstrapped samples $\mathbf{C}^{\dagger,1}, \mathbf{C}^{\dagger,2}, \ldots \mathbf{C}^{\dagger,M}$, each of size N.

Let $\Theta^{\dagger,i}$ denote the outcome of the calibration procedure (4) applied to the $i-$th bootstrapped sample. The bootstrap estimate of the mean of the bootstrap replications is

$$\bar{\Theta} = \frac{1}{M} \sum_{i=1}^{M} \Theta^{\dagger,i}. \tag{6}$$

3.2 Model comparison

With the bootstrap method, we estimate the calibration parameters M times. As we want to compare different models based on their robustness, we want to analyse

- …variation of the bootstrap replications $\Theta^{\dagger,i}$ and the following
- …variation of the predicted option prices $C^{\Theta^{\dagger,i}}$, based on the bootstrap replications.

Comparison of the three SVJD models is widely supported by diagrams for exploring their inner structure of calibrated parameters and their performance. We analyse the bootstrapped calibration parameters with two different diagrams: For the variation in the bootstrapped calibration parameters Θ_i we use *scatterplot matrices*. For the analysis of variation in option prices, we visualize the errors and variations of $C^{\Theta^{\dagger,i}}$ in the $K \times T$-plane.

[4] For instance, if $N = 6$ one might obtain $\mathbf{X}^\dagger = (X_2, X_1, X_4, X_4, X_3, X_2)$ where $X_j = (K_j, T_j)$.

Variation in $\Theta^{\dagger,i}$

To study the calibration parameters variation, one can use a variety of methods. First of all, we want to analyse the variation in the bootstrap replications $\Theta^{\dagger,i}$ to derive information about the model—e.g., if one really can state that the volatility is strongly mean-reverting. Additionally, we want to study connections between individual calibrated parameters—e.g., if the strength of mean reversion varies for different correlations between the Wiener processes. To gather the information, we analyse the variation in $\Theta^{\dagger,i}$ with the help of scatterplot matrices, square matrices with size equal to the number of model parameters. On the diagonal, histograms of the individual calibration parameters are plotted, while the other entries are occupied by scatterplots.

If one further wants to analyse $\Theta^{\dagger,i}$ with statistical methods, normality of the bootstrapped calibration parameters is an important property—e.g., if we want to calculate confidence intervals for the bootstrap estimate $\bar{\Theta}$ of the calibration parameters. To support such analyses, quantile–quantile plots with respect to the normal distribution are suitable visualization tools.

Variation in $C^{\dagger,i}$

The bootstrapped calibration parameters $\Theta^{\dagger,i}$ contain the uncertainty of the option pricing model with respect to the available options in the input data. As the bootstrapping was motived by the option pricing structure, vice versa it is helpful to know how this uncertainty affects the model price predictions $C^{\Theta^{\dagger,i}}(K_j, T_j)$ for an individual option C_j^*. For this purpose, two measures are introduced:

Firstly, the *bootstrap relative error* for the j-th option with market price C_j^* is calculated by:

$$BRE_j = \frac{|\bar{C}_j - C_j^*|}{C_j^*}, \tag{7}$$

for $j = 1, \ldots, N$, where $\bar{C}_j$ is defined as

$$\bar{C}_j = \frac{1}{M} \sum_{i=1}^{M} C^{\Theta^{\dagger,i}}(K_j, T_j).$$

The measure indicates an individual price prediction error of the bootstrap estimation $\bar{C}$ normalized with the market option price. Using bootstrap relative errors, we should be able to detect systematic prediction errors, which can come from the specific option pricing structure.

We are also interested in the variance of prediction error $|C^{\Theta^{\dagger,i}}(K_j, T_j) - C_j^*|$ for the bootstrapped parameters $\Theta^{\dagger,i}$ with respect to bootstrap trials $i = 1, \ldots, M$. To be able to compare variances of predictions for options with different prices C_j^*, we use

relative errors as before to get the variance error measure V_j for the j-th option:

$$V_j = \mathrm{Var}\left(\frac{|C^{\Theta^{\dagger,i}}(K_j, T_j) - C_j^*|}{C_j^*}\right), \tag{8}$$

This measure is evaluated for all traded options $j = 1, \ldots, N$.

The error and variance measures are visualized with diagrams in the $K \times T$ plane. Each traded option is marked with a circle which is centred according to (K, T) of the contract. For a clear arrangement, the T-axis is in logarithmic scale, because there are many traded options with short but slightly different time to maturity. Current asset price, the reference for the option prices, is plotted as a dashed line. Finally, the average relative error and the variance of the bootstrapped prices are visualized as balls, where each ball area is scaled with the error or variance measure.

3.3 Sensitivity analysis

According to Saltelli et al. (2008), the scatterplots can be used as a tool for sensitivity analysis to measure the impact of input parameters on model outputs. Additionally, in this paper we would like to inspect, if fractionality of stochastic volatility and jumps are important for the robustness of option market calibration. Fractionality is represented by the Hurst parameter $H > 0.5$, while jumps are represented by the intensity parameter λ (which is linked to the parameters σ_J and μ_J). Therefore, the importance of jumps and fractionality can be translated into the question, if H and λ have an impact on the quality of the calibration result. This question will be addressed by the Monte Carlo filtering technique, which analyses if a distribution of values of a chosen parameter affects significantly some specific quality measure.

In our context, we have chosen the following Monte Carlo filtering technique:[5] To each set of calibrated model parameters, obtained from the bootstrapped data, we assign average absolute relative error (AARE) with respect to the whole set of traded options as a quality measure for the parameter set. This enables us to divide the sets of parameters into a behavioural (well fitting) group and a non-behavioural (poor fitting) group with respect to the AARE measure. As a behavioural set of parameters, we consider parameters for which AARE is in the lower 3/8 quantile. Those parameters lead to market fits that are comparable to the best fits of non-bootstrapped data sets. A non-behavioural set, on the other hand, consists of parameters that lead to the worst 37.5% of the AARE values (upper 3/8 quantile). The rest (1/4 of the results) is consider as a "grey zone" and is not taken into account for the comparison.[6] For the behavioural/non-behavioural sets, we perform a two-sample Kolmogorov–Smirnov (KS) test to verify the null hypothesis whether both sets are sampled from the same (continuous) distribution. According to Saltelli et al. (2008), by rejecting the null

[5] For more details on Monte Carlo filtering approaches see, for instance Saltelli et al. (2008).

[6] In this case, we will not be able to decide whether the parameters lead to a good or bad description of the modelled market.

hypothesis at a reasonable level of significance[7] we show that the parameters are important with respect to the calibration procedure. However, if we are not able to reject the hypothesis then we cannot judge the importance of the selected parameter.

The KS test seems suitable in contrast to other tests, especially the Chi-square goodness of fit test. According to Senger and Celik (2013) the two-sided Kolmogorov–Smirnov test has two major advantages:

- It still performs well for small sample sizes, where the Chi-square test could fail.
- For arbitrary sample sizes it is often more powerful than the Chi-square test.

The equal size of behavioural and non-behavioural dataset is chosen due to the fact, that otherwise the two-sided KS test can perform very poorly, as shown in Kim (1976). To assess the null hypothesis we use asymptotic p values. As a rule of thumb for using asymptotic values (as opposed to simulated values) is recommended the following criterion:[8]

$$\frac{n_1 n_2}{n_1 + n_2} \geq 4,$$

where n_1, n_2 are sizes of the tested samples. In our case ($n_1 = n_2 = 200 \times 3/8 = 75$) the left-hand side of the criterion takes 35.7; hence we are expecting to get reliable outcomes from asymptotic p values. Moreover, we also add plots illustrating empirical cumulative distribution functions of both sets to visually assess differences between the behavioural and non-behavioural parameter values. Since our samples are of a finite size, we could use also the non-asymptotic p values as described, for example, by Hájek et al. (1999). However, they are computationally more demanding than their asymptotic counterparts. In our case, most of the conclusions drawn are not sensitive to small perturbations of p values (see Sect. 4), hence we use the standard asymptotic p values.

For the Bates model we would like to answer whether the jumps are worth implementing to fit the observed market or if one should stay within the Heston model framework ($\lambda > 0$). We also judge the importance of the Hurst parameter in the fractional stochastic volatility case ($H > 0.5$).

4 Results

In our trials, the bootstrap calibration was performed $M = 200$ times. In the following text we discuss the results based on the four data sets mentioned above.[9] For example the data set from 15 May consists of 197 options and the most weight is typically assigned to the at-the-money contracts allocated near spot price in Fig. 1. Apart from that, the weights are almost evenly distributed in the $K \times T$ plane.

We start the model comparison by examining the overall calibration errors of all three models as seen in Table 1. We note that the additional model features of the Bates model (jumps) and the FSV model (jumps and approximative fractional Brownian

[7] For all trials we use "standard" $\alpha = 5\%$ level of significance. In most of the trials we could have even lower α and still we would reject the null hypothesis.

[8] See, e.g., www.mathworks.com/help/stats/kstest2.html.

[9] All results and data are available in supplementary materials.

Table 1 Overall calibration errors of the three models for Apple Inc. stock on all four datasets

Trading day	1/4/2015 (%)	15/4/2015 (%)	1/5/2015 (%)	15/5/2015 (%)
Heston model	5.15	3.79	6.58	3.39
Bates model	3.73	3.57	5.77	3.41
FSV model	2.21	2.16	5.89	3.20

motion) usually lead to a better market fit. The best average relative errors were obtained on the 15/4/2015 data set (FSV model reached 2.16% error) and the worst market fit in terms of the consider measure was w.r.t. 1/5/2015 data and the Heston model (6.58%). We conclude that using the Heston model we were able to retrieve similar error measures to the Bates and FSV model only for the data set from 15/5/2015.

Variation in ^{†,i}

In Figs. 2 and 3, the scatterplot matrices of the parameters $\Theta^{\dagger,i}_{\text{Bates}}$ and $\Theta^{\dagger,i}_{\text{FSV}}$ are depicted (the results for $\Theta^{\dagger,i}_{\text{Heston}}$ are similar to the ones for the Bates model, we discuss them shortly at the end of the section). First and foremost, we inspect if we reached the lower and upper bounds for the calibration parameters (the bounds are listed in Fig. 1b). This can indicate

- …for a zero bound (e.g., $\kappa \geq 0$), that a model parameter (e.g., mean reversion κ) could be dropped,
- …for nonzero bounds (e.g., $\kappa \leq 100$), that they should be reselected if it is not in contradiction with the parameter interpretation and if it does not breach model restrictions.

For correlation ρ, the natural limits at -1 and 1 indicate that only one Brownian motion can model both, the random movement of the asset price and its volatility. Additionally, ρ and μ_J include zero in the interior of their calibration range, which should be considered during the exploration of scatterplots. e.g., for the uncorrelated Heston model De Marco and Martini (2012) showed an explicit formula which not even needs numerical integration and, possibly, even the other models might be simplified. On the contrary, the value $\mu_J = 0$ has no model reducing consequences, e.g., the model is not simplified for this particular value. Last but not least, a dependence structure between the calibration parameters can be obtained from a single scatterplot and we are able to compare the bootstrap mean $\bar{\Theta}$ (red star) and the parameters Θ from the overall calibration (black cross).

Starting with the Bates model and the last criteria, one cannot observe a significant accumulation of ρ and μ_J at zero in the histograms at the diagonal of Fig. 2. Further on, the histograms show that the parameters $v_0, \kappa, \theta, \sigma, \rho$ and μ_J have no concentration at their limits. However, the small values of λ (mostly between 10^{-3} and 10^{-4}) and the accumulation of σ_J at zero are noticeable. Moreover, if one looks at the scatterplot between λ and μ_J, λ and σ_J, one observes that *either* λ is nearly zero *or* σ_J and μ_J are close to zero. For the model this means, we have two possible cases: either the

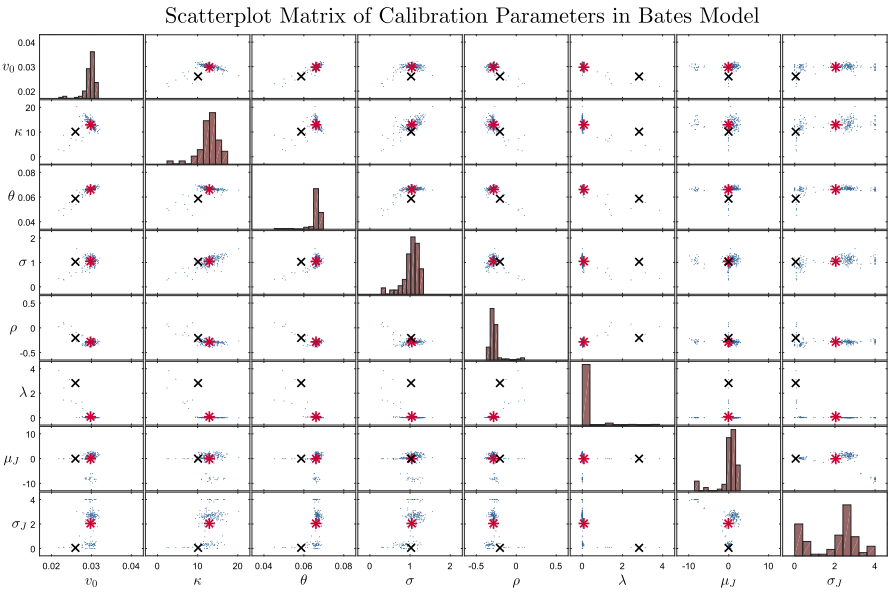

Fig. 2 Scatterplot matrix for the Bates model (15/5/2015, for results on other data sets see the supplementary materials). Diagonal elements depict histograms of parameter values obtained by bootstrap calibrations (e.g., the fist histogram corresponds to the values of v_0). Off-diagonal elements illustrate a dependence structure for each parameter pair. In those figures, a black cross represents the reference value of the specific parameter (obtained from calibration to the whole data set) and by a red star we depict the bootstrap estimate of the value—the closer the two are, the better

Bates model imposes very rare jumps, or it produces frequent jumps of small sizes. If the jump-frequency λ tends to zero, then the average jumps sizes μ_J are almost for all calibrations negative. This statistical connection between λ, μ_J and σ_J should be considered at the calibration by a general modelling decision. One option would be to fix the jump-intensity parameter λ beforehand.

Furthermore, the scatterplots depict that from all parameters κ is the one with the strongest correlation structure. One can see from the scatterplots that the stronger the mean reversion is,

– …the higher is the volatility of volatility σ,
– …the lower is the initial volatility v_0 and the long-run volatility θ,
– …the more negative the correlation ρ between the two Brownian motions is.

The difference between $\bar{\Theta}_{\text{Bates}}$ and Θ_{Bates} for most parameters is not very large, apart from λ and σ_J: the overall calibration resulted in a model with many small jumps of the same size, while the bootstrap resulted in the mean in a model with rare jumps of different size.

In Figs. 2 and 3 we can see that the histograms of FSV and Bates model are quite similar for $v_0, \theta, \rho, \lambda, \mu_J$ and σ_J. The rate of mean-reversion κ in FSV model is slightly different to Bates model, as in some of the trials we can get a fast mean-reversion rate,

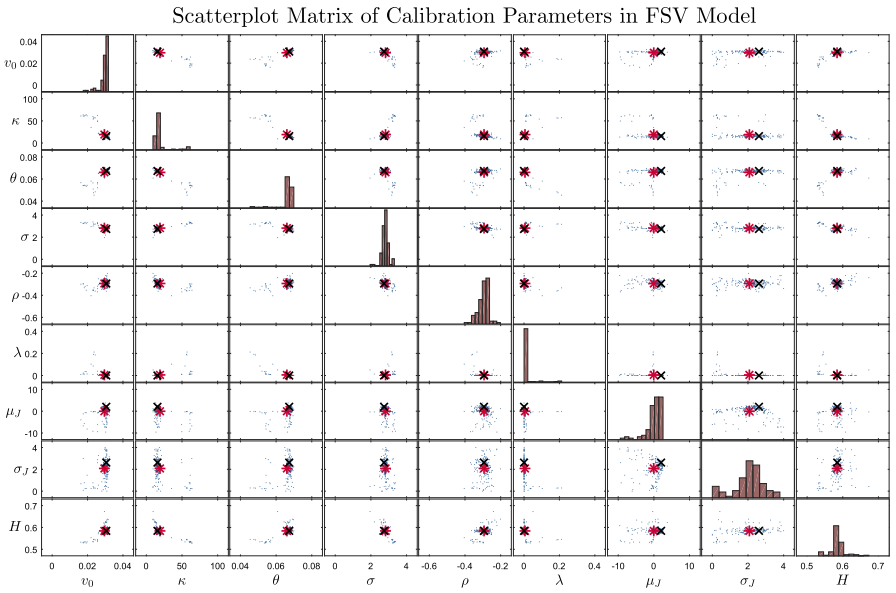

Fig. 3 Scatterplot matrix for the FSV model (15/5/2015, for results on other data sets see the supplementary materials). Diagonal elements depict histograms of parameter values obtained by bootstrap calibrations (e.g., the fist histogram corresponds to the values of v_0). Off-diagonal elements illustrate a dependence structure for each parameter pair. In those figures, a black cross represents the reference value of the specific parameter (obtained from calibration to the whole data set) and by a red star we depict the bootstrap estimate of the value—the closer the two are, the better

$\kappa \gtrapprox 50$. Furthermore, σ in FSV model is significantly higher than in Bates model. This can be explained by the scaling with $\varepsilon^{H-1/2}$ [see Eq. (2) and the definition of $q(v_t)$]. The Hurst parameter H is positively correlated with v_0, θ and ρ and negatively with κ and σ. In Tables 2 and 3 we provide pairwise correlation coefficients for both models. Note that these are all stochastic volatility parameters, a connection of the Hurst parameter with the jump parameters is not obvious in the scatterplots, see also Table 3. Finally, in FSV model $\bar{\Theta}_{\text{FSV}}$ and Θ_{FSV} are very close together which is a desirable result.

For the Heston model, the scatterplot matrix showed similar results as the upper left 5×5 submatrix of Fig. 2. There were no accumulations of $\Theta^{\dagger,i}_{\text{Heston}}$ at the bounds and the correlation seemed nearly linear. Independence of the calibration parameters, necessary for the sensitivity analysis method proposed in Campolongo et al. (2006), cannot be assumed for any of the models. Thus, this method is not suitable in our context.

One can notice from the Q–N plots in Fig. 4 that normality of the bootstrapped parameters and of the resulting calibration error can be assumed for the Heston model—for Bates and FSV this was not the case. Therefore, statistical techniques which assume normality of the data could be used to further analyse the Heston model, but not for comparison of all three models.

Table 2 Pairwise correlation coefficients of calibrated parameters for the Bates model and the data from 15/5/2015

	v_0	κ	θ	σ	ρ	λ	μ_J	σ_J
λ	− 0.7456	− 0.0356	− 0.7940	− 0.5483	0.7235	–	0.0012	− 0.2984
μ_J	0.0866	− 0.0356	0.0938	0.0526	− 0.1065	0.0012	–	− 0.3553
σ_j	0.2647	0.3807	0.3726	0.5504	− 0.0207	− 0.2984	− 0.3553	–

Table 3 Pairwise correlation coefficients of calibrated parameters for the FSV model and the data from 15/5/2015

	v_0	κ	θ	σ	ρ	λ	μ_J	σ_J	H
λ	− 0.4622	0.5778	− 0.7648	0.3080	− 0.3574	–	− 0.0637	− 0.3983	− 0.3600
μ_J	0.3347	− 0.3603	0.3055	− 0.3131	− 0.0725	− 0.0637	–	− 0.1080	0.2063
σ_j	0.4027	− 0.3974	0.4286	− 0.1420	0.0986	− 0.3983	− 0.1080	–	0.2894
H	0.7134	− 0.7859	0.6600	− 0.6059	0.4673	− 0.3600	0.2063	0.2894	–

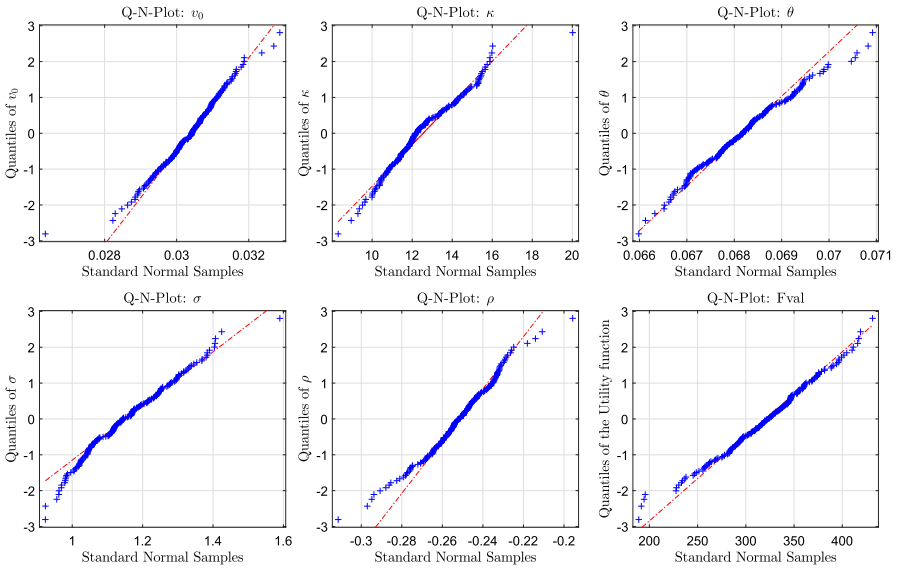

Fig. 4 Q–N plots for Heston model parameters ($v_0, \kappa, \theta, \sigma, \rho$) and corresponding values *Fval* of the calibration utility function (15/5/2015)

Variation in $C^{\dagger,i}$

In Fig. 5, the bootstrap relative errors (7) and the bootstrap variances (8) for every call option are shown. The structure of the errors appears similar for all three models—a result that fits very good to the overall calibration errors for the considered data set. The highest errors appear for all three models for the OTM options, especially if the strike price is grater than 150 USD. For all data sets the lowest values of the bootstrap relative error were obtained by the FSV model.

The variance error measure V_j shows for all three models the same structure in the $K \times T$ plane, but values differ strongly. In the data set from 1/4/2015, the measured variances were the lowest for the FSV model again, whereas the Bates model provided us with the worst values. Surprisingly, Bates model was clearly outperformed for all considered data sets. On the other hand results for Heston and FSV slightly differed for the other data sets. We refer a reader to the corresponding figures in supplementary materials.

4.1 Sensitivity analysis

In this section we would like to inspect model reducing possibilities due to specific values of parameters for the Bates and the FSV model. We check whether the jump-intensity λ plays a crucial role in obtaining good error measures for the Bates model calibration. If we fix $\lambda = 0$, we would obtain the standard Heston model. Similarly we proceed with the FSV model, where we inspect if we can profit from setting $H > 0.5$, unlike formally fixing $H = 0.5$ to obtain the Bates model.

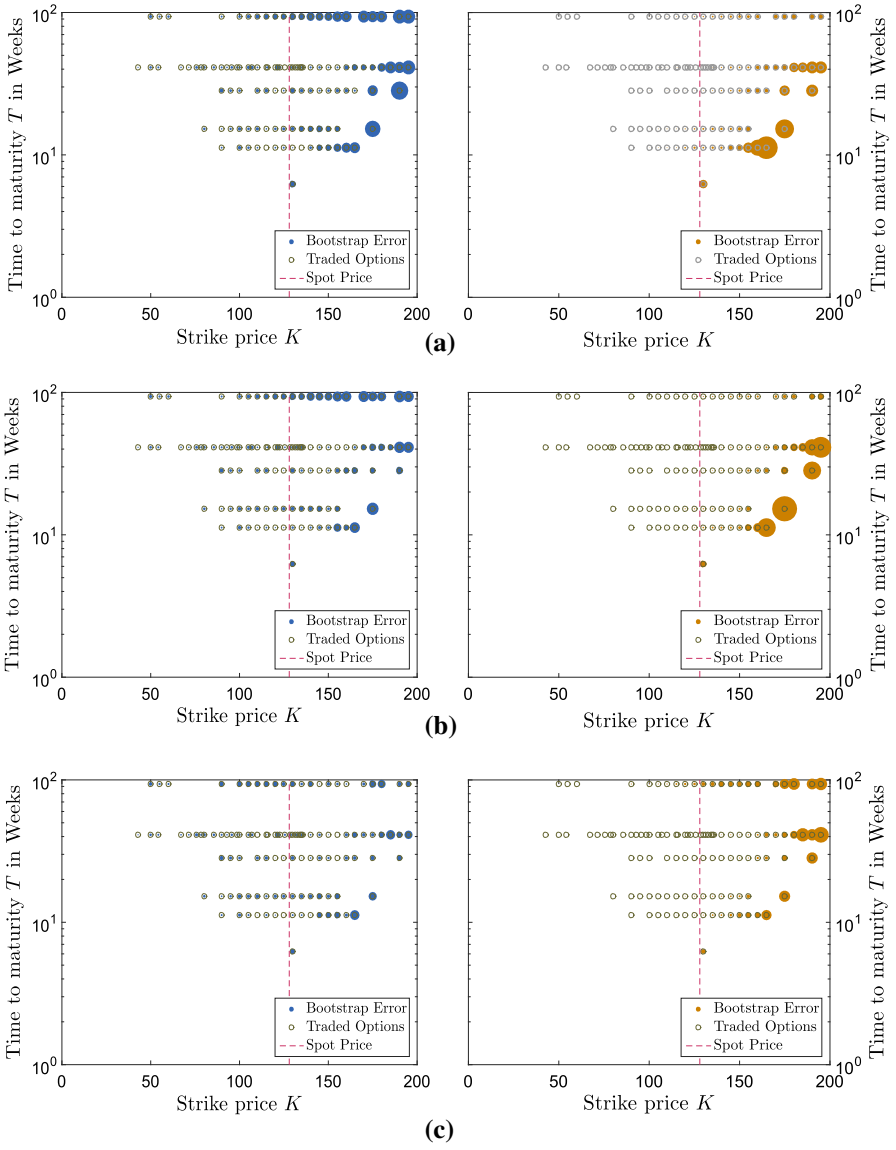

Fig. 5 Calibration errors and variance of the obtained option price surface in $K \times T$ plane. On the left, we depict bootstrap relative errors BRE_j for all bootstrap calibrations w.r.t. 1/4/2015 data set by filled circles with diameter proportionate to the error. On the right, the variance V_j of each option price is illustrated—as before, a diameter of a specific filled circle is proportionate to the option price variance. For results on other data sets see the supplementary materials. **a** Heston model, **b** Bates model and **c** FSV model

Table 4 Importance of λ for calibrations Apple Inc. stock on all four datasets

Data sets	1/4/2015	15/4/2015	1/5/2015	15/5/2015
Hypothesis	1	1	1	1
p value	1.30%	0.43%	8.45e−12%	3.56%

Hypothesis 0 denotes we were unable to reject the null hypothesis and vice versa for 1

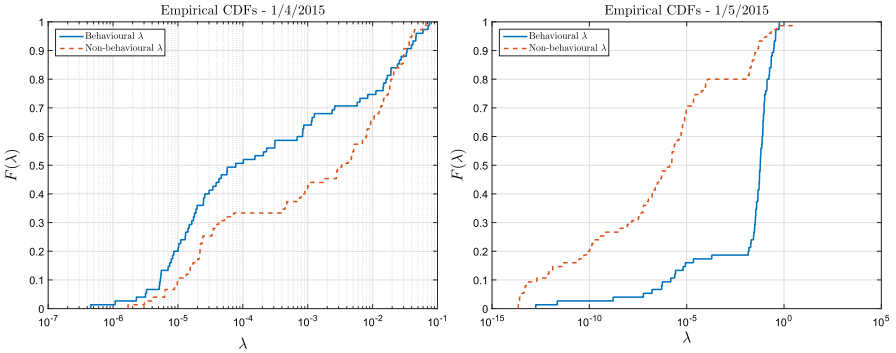

Fig. 6 Empirical cumulative distribution functions of behavioural and non-behavioural sets for the Bates model and jump parameter λ

Importance of jumps

For all available datasets we managed to reject the null hypothesis that both the behavioural and non-behavioural sets of λ are from the same distribution with 5% level of significance. In Table 4 we also display the p values obtained from the 2-sample Kolmogorov–Smirnov test. These are the maximal levels of significance that would lead to not rejecting the null hypothesis. Hence, we are able to conclude the similar result as in Campolongo et al. (2006)—the jump term is of significant help for calibration trials (Fig. 6). In our case the conclusion is drawn from the real market data and using the Monte Carlo filtering technique introduced in Sect. 3. However, it is worth mentioning that this technique identifies input parameters which influence extremes in the output (quality of calibration fit) and hence slightly differs from the classical variance-based sensitivity analysis.

We observe that the calibrated λ's can take quite small values, but as was shown in Campolongo et al. (2006), even in that case, the jumps might effect option prices significantly, especially for out-of-the-money contracts.

Sensitivity of the calibration with respect to the Hurst parameter

Following the procedure of Monte Carlo filtering for jump intensity λ we are interested in the importance of the Hurst parameter. Since for $H = 0.5$ one gets a standard stochastic volatility model with jumps, if we are able to conclude that calibration of H is crucial to obtain a good market fit, then we get a justification of the approxima-

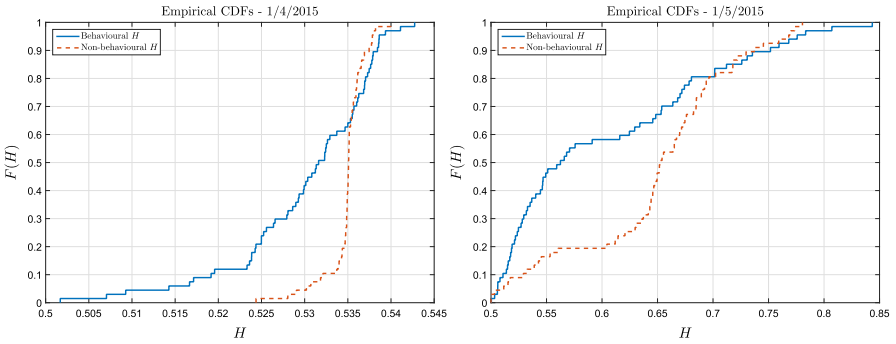

Fig. 7 Empirical cumulative distribution functions of behavioural and non-behavioural sets for the FSV model and fractionality parameter H

Table 5 Importance of H for calibrations Apple Inc. stock on all four datasets

Data sets	1/4/2015	15/4/2015	1/5/2015	15/5/2015
Hypothesis	1	0	1	1
p value	2.78e−10%	30.00%	5.08e−03%	2.17%

Hypothesis 0 denotes we were unable to reject the null hypothesis and vice versa for 1

tive fractional model which is in-line with the long-memory phenomenon of realized volatility time series.

We were able to reject the null hypothesis for data sets from 1 April and May and also from 15 May. p values were quite small (see Table 5) for these data sets, unlike for the data from 15 April (Fig. 7). In this case, we were not able to reject the null hypothesis at any reasonable level of significance and hence we cannot make any conclusion regarding this data set.

Test trials for various weight functions

In this section we focus on a sensitivity of the obtained results with respect to changes in the calibration procedure. In particular, we analyse if we are able to obtain qualitatively similar results for different weight functions in the utility function (4). The bootstrap calibration trials are evaluated for the following weight functions (using notation from Sect. 2):

$$w_j^A = \frac{1}{\left|C_j^{\text{ask}} - C_j^{\text{bid}}\right|}, \qquad w_j^B = \frac{1}{\left(C_j^{\text{ask}} - C_j^{\text{bid}}\right)^2},$$

$$w_j^C = \frac{1}{\sqrt{C_j^{\text{ask}} - C_j^{\text{bid}}}}, \qquad w_j^D = \frac{1}{N_T\, N_{K,T_j}},$$

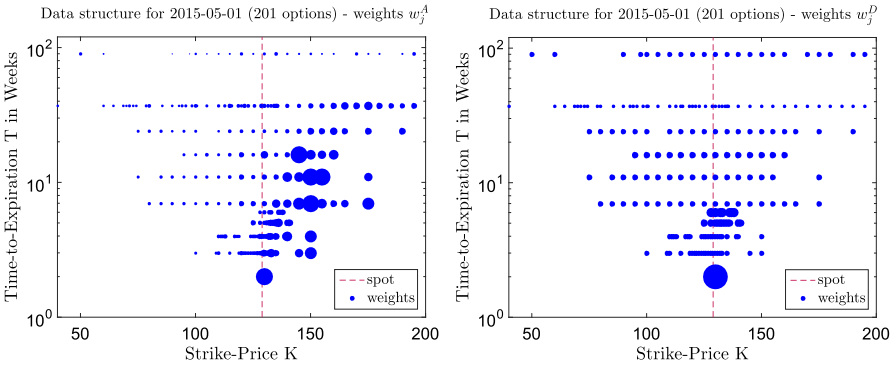

Fig. 8 Data structure for 2015-05-01 (201 traded options) with weights w_j^A and w_j^D. The diameter of each filled ball relates to the weight value for each traded option and the centre of the ball corresponds to its pair K_j, T_j

where N_T, N_{K,T_j} is the number of (distinct) maturities of the corresponding traded options (C_j) and the number of distinct strikes for a specific maturity T_j, respectively. This weigh function was used for example by Detlefsen and Härdle (2007) and for the calibration this would mean that we assign equal weights within a single maturity, but two options across different maturities might be weighted differently (Fig. 8). Moreover, weights of all traded options for each maturity sum up to $1/N_T$.

Several other weight functions could be considered, e.g., a function of the number of traded contracts with the same (K, T) pair, or a function of the Black–Scholes Vega greek. We did not consider those choices in this paper. For the first choice, we lack the number of total traded contracts for particular dates in our data set. On the other hand, the Black–Scholes Vega weights are typically used as a backbone calibration weights only—they serve as a first-order approximation of errors in terms of implied volatilities (Christoffersen et al. 2009). Hence, those weights are not suitable for our purposes.

We also note that $w_j^B \equiv w_j$, i.e., these weights were used for all computations in the previous trials. In this section, we comment on qualitative differences between different calibration set-ups only. All obtained results (4 weights, 3 models, 4 dates) are provided as supplementary materials.

We conclude that for weights which are functions of the ask-bid spread, i.e., $w_j^A - w_j^C$, we retrieved fairly similar results for most of the trials, see for example Fig. 9 or similar figures in the supplementary materials. However, with respect to the overall calibration errors we typically retrieved slightly inferior results compared to weights w_j^B, cf. Tables 1 and 6.

The results obtained by w_j^D differed significantly from the other results. This is caused not only by less pronounced weight distribution for maturities with more traded options, but also by an overemphasis on a single option in particular maturities for short-term contracts, compare left and right hand side of Fig. 8. Overall calibration error measures are greater than the ones obtained using ask–bid spreads. For w_j^D we also observed more extreme behaviour of the bootstrap calibration—depending if the

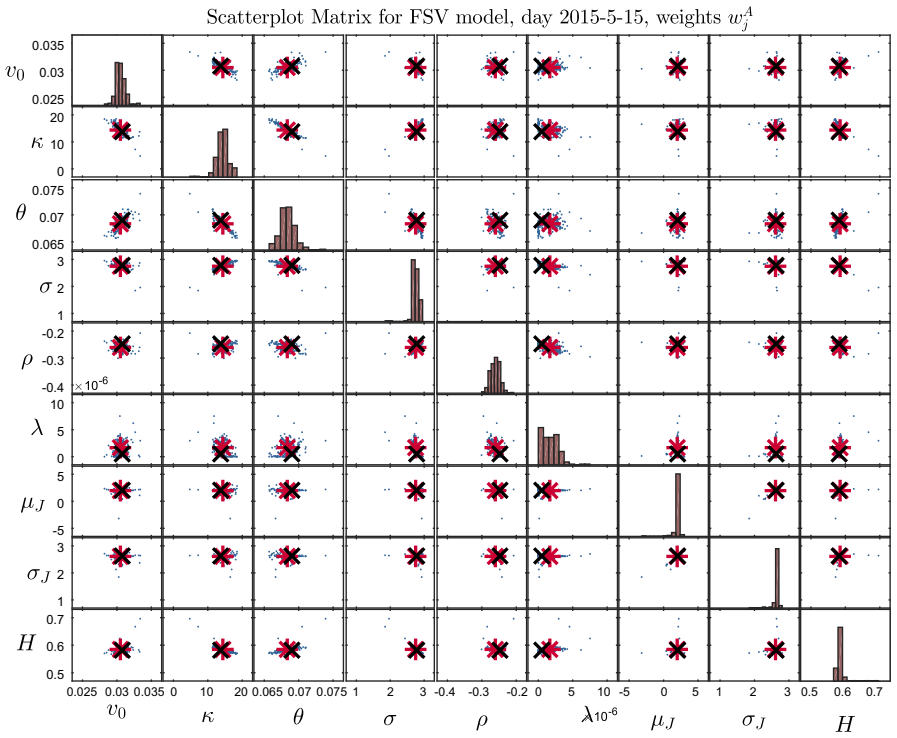

Fig. 9 Scatterplot matrix for the FSV model, weights w_j^A, 15/5/2015 (for results on other data sets see the supplementary materials). Diagonal elements depict histograms of parameter values obtained by bootstrap calibrations. Off-diagonal elements illustrate a dependence structure for each parameter pair. In those figures, a black cross represents the reference value of the specific parameter (obtained from calibration to the whole data set) and by a red star we depict the bootstrap estimate of the value—the closer the two are, the better

Table 6 Overall calibration errors of the three models on all four datasets, calibration weights w_j^A

	2015-04-01 (%)	2015-04-15 (%)	2015-05-01 (%)	2015-05-15 (%)
Heston	5.18	4.44	6.67	3.96
Bates	5.14	4.87	6.62	4.88
FSV	3.48	2.78	5.69	4.13

most weighted option was in the bootstrap sample or not. Overall calibration errors could reach up to 9.49% in this case, which is significantly worse than for the weights that were used in previous tests (w_j^B), but also thus obtained errors are inferior to any other tested weights. Hence, we conclude that weights w_j^D are not very suitable for the calibration of SV models, unless the structure of traded options is similar for each maturity.

5 Conclusion

In this paper, we have performed the robustness and sensitivity analysis of several continuous-time stochastic volatility models (Heston, Bates and FSV model) with respect to market calibration. Using the bootstrap method we calibrated the model parameters 200 times and we compared all three models with respect to the variation in model parameters and in bootstrapped option prices.

The bootstrap relative errors of all three models (Fig. 5, data from 1/4/2015) are qualitatively similar—the best errors are achieved by FSV model and the worst results by Heston model for all data sets. One can observe higher errors for OTM options ($K > S_0$). As for the bootstrap variances, the structure remains similar for all three models, but absolute levels differ significantly. Option prices (and hence market errors) obtained by Bates model have the largest variance with respect to the changing data structure. Therefore, the Bates model appears to be the least robust. For 1/4/2015 data set, we retrieved the best bootstrap errors and lowest variances by the FSV model. The Heston model can achieve lower variances (e.g., 15/5/2015), but bootstrap errors were greater compared to the FSV approach. From scatterplot matrices depicted in Figs. 2 and 3 we can observe that the histograms of Bates and FSV model differ especially for parameters κ and σ. It is worth to mention that considering different parameter bounds (cf. Fig. 1b) may lead to different calibration results, with values of some of the calibrated parameters close to the boundary. Since κ is the parameter with the strongest correlation structure, we performed all the tests with relatively high upper bound ($\kappa \leq 100$). In the scatterplot matrices one can further see non-statistical connections of jump parameters, especially for the Bates model. To avoid this, one could fix one jump parameter for the calibration process (e.g., λ).

In Fig. 4 we can observe that the calibrated parameters for the Heston model are almost normally distributed unlike for the other models. For the other models, one should be careful with normality assumptions of Θ. Additionally the calibrated parameters cannot be modelled as independent random variables (see Figs. 2, 3), therefore standard sensitivity analysis tests are not suitable in this context. For this reason we used the Monte Carlo filtering technique to show the importance of the jumps intensity λ in the Bates model and the importance of long-memory parameter H in the FSV model. As for the jumps, in all four considered data sets we were able to conclude that considering jumps (nonzero λ) in a model plays a significant role in calibration to real market data. Even small values of λ can effect the call prices, especially for the out-of-the-money contracts. We could say that calibration of the fractionality parameter H is important only in three cases out of four.

Recently, Mrázek et al. (2016) studied the calibration task for FSV model and compared it to the Heston case with respect to in- and out-of-sample errors on equity index data sets. Our study confirms that the approximative fractional model can outperform other studied SV models (see Table 1). Moreover, we have shown that this approach is more robust with respect to the uncertainty in the data structure, especially when compared to the other jump-diffusion model. However, it is surprising that an additional parameter (Hurst parameter H) leads to smaller bootstrap variance. Hence, we are also able to draw the conclusion that jumps can also lead to decreased robustness

(Bates model), so the importance of jump terms discussed in Campolongo et al. (2006) can affect model performance in a negative manner as well.

5.1 Further research

As mentioned in the introduction, we have considered only a long-memory regime ($H > 0.5$) of the FSV model, due to technical restrictions of the pricing solution. Bayer et al. (2016) have shown that a simple rough paths volatility model can perform surprisingly well even for short maturities, unlike the standard diffusion volatility models without jumps. This observation was also supported by Fukasawa (2011), who has shown a jump-like behaviour of the rough volatility model. Incorporating a rough volatility regime ($H < 0.5$) could also improve robustness of the model in terms of criteria introduced in this paper. Verification of this hypothesis is still due to a further research. In fact, the proposed methodology can be successfully applied to a rough volatility model as soon as one has an efficient pricing solution.

Acknowledgements This work was supported by the GACR Grant 14-11559S Analysis of Fractional Stochastic Volatility Models and their Grid Implementation. Computational resources were provided by the CESNET LM2015042 and the CERIT Scientific Cloud LM2015085, provided under the programme "Projects of Large Research, Development, and Innovations Infrastructures".

Compliance with ethical standards

Conflict of interest The authors declare that they have no conflict of interest.

Ethical approval This article does not contain any studies with human participants or animals performed by any of the authors.

References

Barndorff-Nielsen OE, Shephard N (2006) Econometrics of testing for jumps in financial economics using bipower variation. J Financ Econom 4(1):1–30. https://doi.org/10.1093/jjfinec/nbi022

Bates DS (1996) Jumps and stochastic volatility: exchange rate processes implicit in Deutsche mark options. Rev Financ Stud 9(1):69–107. https://doi.org/10.1093/rfs/9.1.69

Baustian F, Mrázek M, Pospíšil J, Sobotka T (2017) Unifying pricing formula for several stochastic volatility models with jumps. Appl Stoch Models Bus Ind 33(4):422–442. https://doi.org/10.1002/asmb.2248

Bayer C, Friz P, Gatheral J (2016) Pricing under rough volatility. Quant Finance 16(6):887–904. https://doi.org/10.1080/14697688.2015.1099717

Benhamou E, Gobet E, Miri M (2010) Time dependent Heston model. SIAM J Financ Math 1(1):289–325. https://doi.org/10.1137/090753814

Bianchetti M, Kucherenko S, Scoleri S (2015) Pricing and risk management with high-dimensional quasi Monte Carlo and global sensitivity analysis. Wilmott 2015(78):46–70. https://doi.org/10.1002/wilm.10434

Black FS, Scholes MS (1973) The pricing of options and corporate liabilities. J Polit Econ 81(3):637–654. https://doi.org/10.1086/260062

Campolongo F, Cariboni J, Schoutens W (2006) The importance of jumps in pricing European options. Reliab Eng Syst Saf 91(10):1148–1154. https://doi.org/10.1016/j.ress.2005.11.016

Carr P, Wu L (2003) What type of process underlies options? A simple robust test. J Finance 58(6):2581–2610. https://doi.org/10.1046/j.1540-6261.2003.00616.x

Chernick MR (2008) Bootstrap methods: a guide for practitioners and researchers, 2nd edn. Wiley series in probability and statistics. Wiley, Hoboken
Christoffersen P, Heston S, Jacobs K (2009) The shape and term structure of the index option smirk: why multifactor stochastic volatility models work so well. Manag Sci 55(12):1914–1932. https://doi.org/10.1287/mnsc.1090.1065
Creel M, Kristensen D (2015) ABC of SV: Limited information likelihood inference in stochastic volatility jump-diffusion models. J Empir Finance 31:85–108. https://doi.org/10.1016/j.jempfin.2015.01.002
De Marco S, Martini C (2012) The term structure of implied volatility in symmetric models with applications to Heston. Int J Theor Appl Finance 15(04):1250,026. https://doi.org/10.1142/S0219024912500264
Detlefsen K, Härdle WK (2007) Calibration risk for exotic options. J Deriv 14(4):47–63. https://doi.org/10.3905/jod.2007.686422
Duffie D, Pan J, Singleton K (2000) Transform analysis and asset pricing for affine jump-diffusions. Econometrica 68(6):1343–1376. https://doi.org/10.1111/1468-0262.00164
Efron B (1979) Bootstrap methods: another look at the jackknife. Ann Stat 7(1):1–26
Efron B (1982) The jackknife, the bootstrap and other resampling plans, CBMS-NSF Regional Conference Series in Applied Mathematics, vol **38**. Society for Industrial and Applied Mathematics (SIAM), Philadelphia, PA
Elices A (2008) Models with time-dependent parameters using transform methods: application to Heston's model. arXiv:0708.2020
Fukasawa M (2011) Asymptotic analysis for stochastic volatility: martingale expansion. Finance Stoch 15(4):635–654. https://doi.org/10.1007/s00780-010-0136-6
Hájek J, Šidák Z, Sen PK (1999) Theory of rank tests, 2nd edn. Probability and mathematical statistics. Academic Press Inc., San Diego
Heston SL (1993) A closed-form solution for options with stochastic volatility with applications to bond and currency options. Rev Financ Stud 6(2):327–343. https://doi.org/10.1093/rfs/6.2.327
Hwang E, Shin DW (2014) A bootstrap test for jumps in financial economics. Econom Lett 125(1):74–78. https://doi.org/10.1016/j.econlet.2014.08.024
Kim PJ (1976) The smirnov distribution. Ann Inst Stat Math 28(1):267–275. https://doi.org/10.1007/BF02504745
Lewis AL (2000) Option valuation under stochastic volatility: with mathematica code. Finance Press, Newport Beach
Mikhailov S, Nögel U (2003) Heston's stochastic volatility model—implementation, calibration and some extensions. Wilmott Mag 2003(July):74–79
Mrázek M, Pospíšil J, Sobotka T (2016) On calibration of stochastic and fractional stochastic volatility models. Eur J Oper Res 254(3):1036–1046. https://doi.org/10.1016/j.ejor.2016.04.033
Osajima Y (2007) The asymptotic expansion formula of implied volatility for dynamic SABR model and FX hybrid model. https://doi.org/10.2139/ssrn.965265
Pospíšil J, Sobotka T (2016) Market calibration under a long memory stochastic volatility model. Appl Math Finance 23(5):323–343. https://doi.org/10.1080/1350486X.2017.1279977
Saltelli A, Tarantola S, Campolongo F, Ratto M (2004) Sensitivity analysis in practice: a guide to assessing scientific models. Wiley, Chichester
Saltelli A, Ratto M, Andres T, Campolongo F, Cariboni J, Gatelli D, Saisana M, Tarantola S (2008) Global sensitivity analysis: the primer. Wiley, Chichester
Senger O, Celik AK (2013) A Monte Carlo simulation study for Kolmogorov–Smirnov two-sample test under the precondition of heterogeneity: upon the changes on the probabilities of statistical power and type I error rates with respect to skewness measure. J Stat Econom Methods 2(4):1–16
Shreve SE (2004) Stochastic calculus for finance. Springer Finance. Springer, New York
Yekutieli I (2004) Implementation of the Heston model for the pricing of FX options. Tech. rep, Bloomberg LP